



Stevenson, Richard P. (2014) *Investigating the role of fascin in murine models of inflammatory bowel disease and tumourigenesis*. PhD thesis.

<https://theses.gla.ac.uk/5107/>

Copyright and moral rights for this work are retained by the author

A copy can be downloaded for personal non-commercial research or study, without prior permission or charge

This work cannot be reproduced or quoted extensively from without first obtaining permission in writing from the author

The content must not be changed in any way or sold commercially in any format or medium without the formal permission of the author

When referring to this work, full bibliographic details including the author, title, awarding institution and date of the thesis must be given

Enlighten: Theses

<https://theses.gla.ac.uk/>
research-enlighten@glasgow.ac.uk

**Investigating the role of fascin in murine models of
inflammatory bowel disease and tumourigenesis**

Mr. Richard P Stevenson MBChB MRCS(Ed)

**The Beatson Institute for Cancer Research
University of Glasgow**

Faculty of Medicine

**A Thesis submitted for the Degree of Doctor of
Philosophy January 2014**

Abstract

Recent evidence suggests that stem cells are important for cancer metastasis and that the epithelial-to-mesenchymal transition also involves a transition toward stemness. Current thinking suggests that Lgr5, a 7-transmembrane spanning G-protein, also marks a certain population of stem cells capable of regenerating an intestinal crypt and that the specialised immune secretory paneth cell, is important for maintenance of the stem cell niche. We implicate fascin in regulating the balance of Lgr5 stem cells during acute small intestinal and colonic inflammation and in regenerating small intestinal and colonic tissue.

Fascin is an actin bundling protein that drives the assembly of filopodia through the cross-linking of actin filaments into straight bundles. Conserved from amoebas to man, fascin was originally purified from extracts of sea urchin oocytes and coelomocytes and later found in *Drosophila* as the *singed* gene product. It is involved in the invasion and metastasis of multiple epithelial cancer types through stabilisation of actin in invadopodia, finger like protrusions used by cancer cells to invade into and degrade the extra-cellular matrix. Fascin, whilst normally low or absent from epithelia, localises to the leading edges of migratory cells and is over-expressed in many cancers of the same epithelial origin including lung, colorectal, pancreatic and liver. Fascin has also recently been shown to increase during inflammatory bowel disease (IBD) conditions such as diverticulitis, Crohn's disease and ulcerative colitis. In this thesis I have investigated the role of fascin in murine models of IBD and have demonstrated that fascin is required for the haematopoietic production of leucocytes, in response to inflammation and that the loss of fascin, in the presence of high Wnt levels, results in enhanced proliferation of small intestinal and colonic epithelial cells.

One of the serious consequences of IBD is the increased lifetime risk of the patient developing an intestinal malignancy secondary to the disease. The exact mechanism underlying the increase in malignancies has not yet been fully established, however it is postulated that chronic inflammation and the effect this has on the major molecular pathways involved in carcinogenesis underlies the transformation from benign to malignant disease. Highest fascin expression has been shown in the dysplastic, pre-malignant cells in human IBD tissues

indicating an important role of fascin in the transformation of benign to malignant cells. In this thesis, I have demonstrated that loss of fascin impairs tumour initiation in inflammatory driven and sporadic intestinal tumourigenesis models, which is likely, in part, to be as a consequence of reduced leucocytes, in particular neutrophils, which may be CXCL2 mediated.

Declaration

I declare that all work contained within this thesis, unless otherwise stated, was undertaken by myself. No part of this work has been submitted for consideration as part of any other degree or award.

Acknowledgements

I would like to thank my supervisor, Professor Laura Machesky, for giving me the opportunity to work in her lab and for the guidance and support which has brought me to the culmination of this thesis.

I would like to thank my wife, Jo Stevenson, for her love and support throughout this fellowship and our two wonderful children, Emily and Sebastian who continually provide a respite to the world of science.

My parents, Howard and Dianne Stevenson, have given me the platform in life to achieve the position I am in today, and for that I will be forever grateful. My hope is that I can provide the same for our children.

The Beatson Institute has been a fantastic place to study and I would like to thank all the members of R2 & R6, BAIR, histology and the BSU for all the help they have given throughout my time here.

Cancer Research UK and the Royal College of Surgeons, Edinburgh, have funded my work.

Publications arising from the work included within this thesis

Stevenson RP, Veltman D, Machesky LM. Actin-bundling proteins in cancer progression at a glance. *J Cell Sci* 125: 1073-9, 2012

Yafeng Ma, Louise E. Reynolds, Ang Li, **Richard P. Stevenson**, Kairbaan M. Hodivala-Dilke, Shigeko Yamashiro and Laura M. Machesky. Fascin 1 is dispensable for developmental and tumour angiogenesis. *Biology Open*. doi: 10.1242/bio.20136031

Li A, Morton JP, Ma Y, Karim SA, Zhou Y, Faller WJ, Woodham EF, Morris HT, **Stevenson RP**, Juin A, Jamieson NB, MacKay CJ, Carter CR, Leung HY, Yamashiro S, Blyth K, Sansom OJ, Machesky LM, Fascin is Regulated by Slug, Promotes Progression of Pancreatic Cancer in Mice, and is Associated with Patient Outcome, *Gastroenterology* (2014), doi: 10.1053/ j.gastro.2014.01.046.

Definitions/Abbreviations

AhR	Aryl hydrocarbon receptor
AOM	Azoxymethane
APC	Adenomatous Polyposis Coli
Ascl2	Achaete-scute complex homolog 2
ATP	Adenosine Tri-Phosphate
Axin2	Axis inhibition protein 2
bHLH	Basic helix-loop-helix
Bmi1	Bmi1 polycomb ring finger oncogene
BrdU	Bromodeoxyuridine
BSA	Bovine serum albumin
CAC	Colitis associated carcinogenesis
CBC	Crypt based columnar
CCM	Crypt culture media
CD	Crohn's disease
CO ₂	Carbon dioxide
cDNA	Complement DNA
CK1 α	Casein kinase 1 α
Cobl	Cordon bleu
CRC	Colorectal cancers
CREB	cAMP response element-binding protein
CRUK	Cancer Research United Kingdom
Cxcl1	Chemokine (C-X-C motif) ligand 1
Cxcl2	Chemokine (C-X-C motif) ligand 2
Cxcl5	Chemokine (C-X-C motif) ligand 5
Cxcr2	Chemokine (C-X-C motif) receptor 2)
D14Ert449e	DNA segment, Chr 14, ERATO Doi 449, expressed
Ddx3y	DEAD (Asp-Glu-Ala-Asp) box polypeptide 3, Y-linked
DMEM	Dulbecco's modified eagle medium
DMH	1,2-dimethylhydrazine
DMSO	Dimethyl sulfoxide

DNA	Deoxyribonucleic acid
Dsh	Dishevelled
DSS	Dextran sodium sulphate
DTT	DL- dithiothreitol
ECM	Extracellular matrix
EDTA	Ethylenediaminetetraacetic acid
EGF	Epidermal growth factor
Eif2s3y	Eukaryotic translation initiation factor 2, subunit 3, structural gene Y-linked
ELISA	Enzyme-linked immunosorbent assay
EMT	Epithelial-to-mesenchymal transition
Ephb3	Ephrin type-B receptor 3
ERDR1	Erythroid differentiation regulator 1
Ets2	v-ets avian erythroblastosis virus E26 oncogene homolog 2
F-actin	Filamentous actin
FACS	Fluorescence-activated cell sorting
FAK	Focal adhesion kinase
FAP	Familial Adenomatous Polyposis
FAPC	Fascin ^{-/-} APC ^{fl/fl} p53 ^{fl/fl} /p53 ^{R172H} Ah-cre
FBC	Full blood count
FBS	Fetal Bovine Serum
FKC	Fascin ^{-/-} , KRas ^{G12D} Pdx1-Cre
FOV	Field of view
Fscn1	Fascin1
GAPDH	Glyceraldehyde 3-phosphate dehydrogenase
GI	Gastro-intestinal
GSK3	Glycogen synthase kinase
H ₂ O	Water
HCl	Hydrochloric acid
Hes	Hairy/enhancer of split
Het	Heterozygous

HNPCC	Hereditary non-polyposis colorectal cancer
IBD	Inflammatory bowel disease
IEC	Intestinal epithelial cell
IF	Immunofluorescence
IHC	Immunohistochemistry
IKK	I κ B kinase
IL-11	Interleukin-11
IL-11b	Interleukin-11b
IL-6	Interleukin-6
IP	Intra-peritoneal
ISC	Intestinal stem cell
I κ B α	Nuclear factor of kappa light polypeptide gene enhancer in B-cells inhibitor alpha
JAK-STAT	Janus kinase/signal transducers and activators of transcription
Jak1	Janus Kinase1
Jak2	Janus Kinase2
Jak3	Janus Kinase3
KCl	Potassium chloride
KO	Knockout
KPC	KRas ^{G12D} p53 ^{R172H} Pdx1-Cre
LEF1	Lymphoid enhancer-binding factor-1
Lgr5	Leucine-rich repeat-containing G-protein coupled receptor 5
LRP	Lipoprotein receptor-related protein
Ly6e	Lymphocyte antigen 6 complex, locus E
Min	Multiple intestinal neoplasia
MMP	Matrix metalloproteinase
MPO	Myeloperoxidase
MRC-T	Medical Research Council Technology
mRNA	Messenger ribose nucleic acid
NaCl	Sodium chloride

NaHCO ₃	Sodium bicarbonate
NaOH	Sodium hydroxide
NBF	Neutral buffered formalin
NF-κB	Nuclear factor kappa-light-chain-enhancer of activated B cells
Nrn1	Neuritin 1
Olfm4	Olfactomedin 4
OSM	Oncostatin M
Paip1	Polyadenylate binding protein-interacting protein 1
PAK	p21 activated kinases
PanIN	Pancreatic intra-epithelial neoplasia
PBS	Phosphate buffered saline
PBT	Phosphate buffered saline tween
Pen-Strep	Penicillin-streptomycin
PFA	Paraformaldehyde
PI	Propidium iodide
PKC	Protein kinase C
PMN	Polymorphonuclear neutrophils
PP2A	Protein phosphatase 2A
PVDF	Polyvinylidene difluoride
qRT-PCR	Quantitative real-time polymerase chain reaction
Rac	Ras-related C3 botulinum toxin substrate 1
RBC	Red blood cell
Rgmb	RGM domain family, member B
RIPA	Radioimmunoprecipitation assay
ROS	Reactive oxygen species
RPM	Revolutions per minute
S39	Serine 39
shRNA	Short hairpin RNA
SI	Small intestine
Slc14a1	Solute carrier family 14 (urea transporter), member 1

Sox9	SRY (sex determining region Y)-box 9
Stat3	Signal transducer and activator of transcription 3
TA	Transit amplifying
TCF	T cell factor
TGF- β	Transforming growth factor- β
TIMP	Tissue inhibitor of matrix metalloproteinase
TJL	The Jackson Laboratory
Tnfrsf19	Tumor necrosis factor receptor superfamily, member 19
TNF α	Tumour Necrosis Factor alpha
TSP	Thrombospondin-1
UC	Ulcerative colitis
WASP	Wiskott-Aldrich syndrome family protein
WB	Western blot
WBC	White blood cell
Wnt3a	Wingless-type MMTV integration site family, member 3A
WT	Wild-type
Xist	X specific transcripts
Zfp68	Zinc finger protein 68

Table of Contents

Title.....	1
Abstract	2
Declaration	4
Acknowledgements	5
Publications arising from the work included within this thesis.....	6
Definitions/Abbreviations	7
List of Tables	15
List of Figures	16
1 Chapter 1 - Introduction.....	18
1.1 The Gastro-Intestinal (GI) Tract	19
1.2 Fascin	23
1.2.1 Introduction to fascin	23
1.2.2 Structure of fascin	24
1.2.3 Regulation of fascin.....	25
1.3 Inflammatory Bowel Disease (IBD).....	27
1.3.2 Small Intestine and colorectal cancer	37
1.3.3 Genetic modification of mice	40
1.4 Actin bundling proteins and cancer	42
1.4.1 Actin bundling proteins in tumourigenesis and cancer progression .	42
1.4.2 The actin cytoskeleton is regulated by multiple actin-binding proteins.....	45
1.4.3 A role for actin bundling proteins in metastasis	45
1.4.4 Actin bundle-containing structures in normal and cancer cells.....	48
1.4.5 Concluding remarks and future perspectives	56
1.5 Thesis aims	56
References.....	57
2 Chapter 2 - Materials and Methods	69
2.1 Materials.....	70
2.1.1 Reagents and Solutions.....	70
2.1.2 Antibodies and Dyes	74
2.1.3 Primers.....	75
2.1.4 Enzymes and kits	77
2.2 Methods	78
2.2.1 Cell culture	78
2.2.2 Crypt and adenoma culture	79
2.2.3 Protein Immunoblotting.....	80
2.2.4 Immunofluorescence (IF)	82
2.2.5 Histology and staining of tissue	82
2.2.6 Paraffin embedding of organoids	83
2.2.7 Testing of the fascin antibody	83
2.2.8 Anti-neutrophil antibodies.....	84
2.2.9 Generation, maintenance and treatment of mouse colonies	84
2.2.10 Mouse Models.....	85
2.2.11 Blood counts.....	88
2.2.12 Epithelial cell extraction	88
2.2.13 Flow cytometry	88

	13
2.2.14	Clonogenicity assay..... 89
2.2.15	Cell adhesion assay..... 89
2.2.16	Quantitative Real-Time Polymerase Chain Reaction (qRT-PCR).... 90
2.2.17	Gene expression microarray 91
2.2.18	Organotypic invasion model..... 92
References 93
3	Chapter 3 - Fascin regulates small intestine regeneration and neutrophil recruitment in response to injury..... 95
3.1	Summary..... 96
3.2	Introduction 96
3.3	Results 97
3.3.1	Characterisation of fascin KO small intestine with respect to WT .. 97
3.3.2	Fascin expression in untreated and regenerating small intestine .. 102
3.3.3	Loss of fascin results in a mild increase in histological damage in small intestinal time course post irradiation 103
3.3.4	Loss of fascin results in enhanced proliferation after irradiation .. 106
3.3.5	Loss of fascin results in impaired neutrophil recruitment in regenerating small intestines post irradiation..... 109
3.3.6	Fascin KO crypts have impaired proliferation <i>in-vitro</i> in standard medium 110
3.3.7	Fascin KO crypts have enhanced proliferation upon addition of Wnt3a 113
3.3.8	Clonogenicity assay 117
3.3.9	Gene expression microarray WT vs. fascin KO crypts 118
3.4	Discussion..... 124
3.4.1	Fascin is not required to maintain normal homeostatic small intestinal architecture 124
3.4.2	Loss of fascin results in a mild increase in histological damage in a small intestinal time course post irradiation 126
3.4.3	The absence of fascin allows enhanced small intestinal proliferation in the presence of high levels of Wnt ligand..... 126
3.4.4	Fascin is required for optimal neutrophil recruitment..... 127
3.4.5	Crypt gene expression microarray changes 128
References 130
4	Chapter 4 - Fascin regulates colonic regeneration and neutrophil recruitment in response to injury 132
4.1	Summary..... 133
4.2	Introduction 133
4.3	Results 134
4.3.1	Characterisation of untreated fascin KO colon with respect to WT 134
4.3.2	No difference in histological damage between WT and fascin KO colons in response to DSS 137
4.3.3	Loss of fascin results in enhanced crypt proliferation in regenerating colons 139
4.3.4	Fascin expression in untreated and regenerating colons 145
4.3.5	Loss of fascin results in impaired neutrophil production and recruitment in regenerating colons 146
4.4	Discussion..... 149
4.4.1	Fascin is not required to maintain normal homeostatic colonic architecture..... 149
4.4.2	Fascin KO mice have greater clinical deterioration 149

4.4.3	Fascin KO have enhanced crypt proliferation in the DSS model	150
4.4.4	Loss of fascin results in impaired neutrophil production and recruitment in regenerating colons	151
	References.....	152
5	Chapter 5 - Loss of fascin results in an impaired inflammatory response and reduced tumourigenesis	153
5.1	Summary.....	154
5.2	Introduction	154
5.3	Results	155
5.3.1	Colitis associated carcinogenesis (CAC) model	155
5.3.2	The role of fascin in sporadic and inducible tumourigenesis models ..	159
5.4	Discussion.....	168
5.4.1	Loss of fascin results in an impaired immune response and reduced tumourigenesis in the colitis associated carcinogenesis (CAC) model	168
5.4.2	Loss of fascin results in reduced tumourigenesis in the inducible Fascin ^{-/-} APC ^{fl/fl} p53 ^{fl/fl} and Fascin ^{-/-} APC ^{fl/fl} p53 ^{R172H} Ah-cre mice	169
5.4.3	The regulation of fascin expression in benign and malignant tumours is unclear	170
	References.....	171
6	Chapter 6 - Conclusions and Future Directions	174
6.1	Summary.....	175
6.2	Future Directions.....	180
6.3	Conclusion.....	181
	References.....	182
	Appendices	183
	Appendix A: Fascin1 is dispensable for developmental and tumour angiogenesis	184
	Appendix B: Fascin is regulated by Slug, promotes progression of pancreatic cancer in mice, and is associated with patient outcome.....	192

List of Tables

Table 1-1 Clinical correlation between actin bundling proteins and cancer	54
Table 2-1 Reagents and Solutions	74
Table 2-2 Antibodies and Dyes	75
Table 2-3 Primers.....	77
Table 2-4 Enzymes and kits	78
Table 3-1 Crypt gene expression microarray showing the top 10 genes with the highest fold change	119
Table 3-2 Top 5 associated networks and network functions derived from small intestinal crypt gene expression array.....	119

List of Figures

Figure 1-1 Anatomy of the gastro-intestinal (GI) tract	20
Figure 1-2 Murine small Intestine and colonic epithelium	22
Figure 1-3 Structure of fascin	25
Figure 1-4 Regulation of fascin	26
Figure 1-5 Comparison of ulcerative colitis and Crohn's disease and the expression of fascin in human samples	28
Figure 1-6 The Wnt signalling pathway.....	34
Figure 1-7 Small Intestine and colonic crypt architecture	35
Figure 1-8 Functional classification of genes derived from the Lgr5 stem cell signature.....	37
Figure 1-9 The role of inflammation and cancer	40
Figure 1-10 Cre-lox recombination	41
Figure 1-11 Structure and functions of filopodia, invadopodia and stress fibres	44
Figure 1-12 The roles of actin bundling proteins in cell:cell junctions and microvilli	47
Figure 1-13 Actin bundling proteins and the cell cortex	49
Figure 2-1 A regenerating small intestinal crypt	86
Figure 3-1 Characterisation of untreated fascin KO small intestine with respect to WT.....	99
Figure 3-2 qRT-PCR data of untreated whole tissue extraction comparing WT and fascin KO small intestines.....	101
Figure 3-3 Fascin expression in untreated and irradiated small intestine	103
Figure 3-4 Small intestine irradiation time course	105
Figure 3-5 Enhanced small intestinal crypt proliferation in the fascin KO in response to irradiation	108
Figure 3-6 Impaired neutrophil recruitment in the fascin KO is likely chemokine mediated	110
Figure 3-7 Fascin KO small intestinal crypts have impaired proliferation and reduced crypt fission in standard medium	112
Figure 3-8 Fascin KO crypts have impaired proliferation <i>in-vitro</i> in standard medium	113
Figure 3-9 Fascin KO crypts have enhanced proliferation upon addition of Wnt3a	115
Figure 3-10 No detectable fascin expression in small intestinal crypts on WB .	116
Figure 3-11 Clonogenicity assay	118
Figure 3-12 Cell Death, Cell Cycle, Cellular Growth and Proliferation	120
Figure 3-13 Cellular Development, Cellular Growth and Proliferation, Reproductive System Development and Function.....	121
Figure 3-14 Gene expression, Organ Morphology, Vitamin and Mineral Metabolism	122
Figure 3-15 Inflammatory Response, Cellular compromise, Drug Metabolism ..	123
Figure 3-16 Amino Acid Metabolism, Endocrine System Development and Function, Molecular Transport	124
Figure 3-17 Schematic diagram demonstrating crypt architecture	125
Figure 4-1 Characterisation of fascin KO colon with respect to WT	135
Figure 4-2 qRT-PCR data of untreated whole tissue extraction comparing WT and fascin KO colons.....	137
Figure 4-3 Fascin KO mice deteriorate clinically to a greater degree in response to DSS (compared with WT), however there is no difference in histological damage	139

Figure 4-4 BrdU analysis shows that loss of fascin results in enhanced crypt proliferation in regenerating crypts.....	140
Figure 4-5 Enhanced levels of proliferation, stem cell and NF- κ B markers in the fascin KO regenerating colons post DSS	142
Figure 4-6 TNF α blocker has no demonstrable effect on the expression of fascin, proliferation of crypts or recruitment of neutrophils/macrophages in the colitis model	144
Figure 4-7 Fascin expression in untreated and regenerating colons.....	145
Figure 4-8 Loss of fascin results in impaired neutrophil production and recruitment in regenerating colons	148
Figure 5-1 Fascin KO mice have reduced colonic tumour number and burden in the colitis associated carcinogenesis model	156
Figure 5-2 Fascin KO mice have reduced numbers of circulating leucocytes and recruited neutrophils to the tumour microenvironment.....	158
Figure 5-3 Fascin expression in sporadic and inducible murine intestinal tumourigenesis models.....	160
Figure 5-4 Fascin is not a Wnt target, nor is its expression regulated by Il-11 or Stat3	162
Figure 5-5 Reduced tumour number and burden in the inducible FAPC model .	163
Figure 5-6 Organotypic invasion model	165
Figure 5-7 Orthotopic caecal model and cell adhesion assay.....	167
Figure 6-1 Proposed model of mechanism - the role of fascin in influencing gene expression changes	176
Figure 6-2 Proposed mechanism - reduced tumour initiation in CAC model	178
Figure 6-3 Proposed mechanism - reduced tumour initiation in FAPC mouse model	179

1 Chapter 1 – Introduction

1.1 The Gastro-Intestinal (GI) Tract

The gastro-intestinal (GI) tract, also known as the alimentary canal, is a hollow muscular tube that extends from the mouth to the anus (Fig. 1-1). The intestinal tract extends from the duodenum to the rectum and is anatomically divided into the small and large intestine (or colon). The small intestine can be further subdivided into the duodenum, jejunum and ileum, whilst the colon can also be subdivided into three parts namely the caecum, colon and rectum (Fig. 1-1). The principal role of the GI tract is the breakdown of foodstuffs, extraction of nutrients and the excretion of waste products. Given that it is essentially a hollow tube passing through our bodies, it also has an important immune role and barrier function preventing pathogens within the lumen entering the blood and lymph. The two processes are effectively dealt with by the epithelial cells, which form a selectively permeable membrane, and the gut mucosa, which creates a barrier whilst also participating in host defence through activation of the mucosal immune system (Shen 2009).

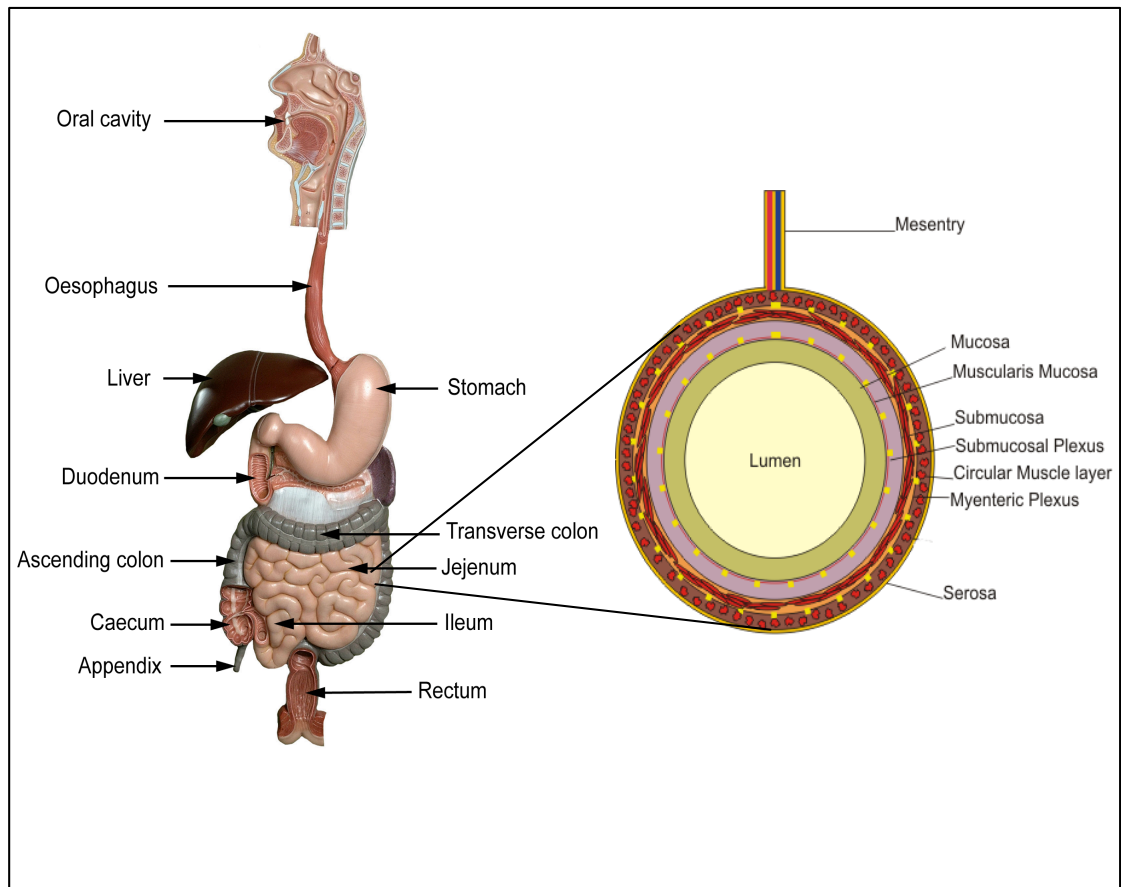


Figure 1-1 Anatomy of the gastro-intestinal (GI) tract

The GI tract starts at the mouth and extends to the anus. The small intestine is divided into the duodenum, jejunum and ileum. The colon is divided into the caecum, colon and rectum. There are 4 layers to the small intestine and colon namely the mucosa, submucosa, muscularis mucosa and serosa. Images shown with permission from Anatomisty.com and wikibooks.org.

The small intestine and colon share many characteristics, but also differ significantly in some aspects. Microscopically, both have four layers in their wall: mucosa, submucosa, muscularis and adventitia (or serosa) (Fig. 1-1). The mucosa, composed of glandular epithelium, lamina propria and the muscularis mucosa, lines the intestinal lumen and is the innermost layer. Absent from the colon, but present in the small intestine, vaginations of the mucosa form villus structures which radically increase the surface area of the small intestine and thereby the absorptive capacity. The colon, in contrast has a flat epithelium. Common to both small intestine and colon, are invaginations of the mucosa (specifically the glandular epithelium), which form structures termed the Crypts of Lieberkühn wherein lie the proliferative cells of the small intestine. Pluripotent stem cells have long been established as the driving force behind the proliferative capacity of the self-renewing intestinal epithelium (Bjerknes and

Cheng 2006), which renews faster than any other tissue in the mammalian body (Crosnier, Stamatakis et al. 2006). Located at the base of the crypts in the stem cell compartment, the stem cells undergo division and the resultant daughter cells exit the stem cell compartment into the adjacent transit-amplifying (TA) compartment (Munoz, Stange et al. 2012). Whilst in the TA, the cells undergo up to 5 divisions whilst moving up the crypt-villus axis whereby they subsequently terminally differentiate into 4 cell types: paneth cells, goblet cells, entero-endocrine cells and enterocytes (Fig. 1-2). Goblet cells, entero-endocrine cells and enterocytes migrate upwards towards the tip of the villus where they undergo apoptosis and are shed into the intestinal lumen. In contrast, paneth cells migrate downwards where they reside, interspersed by crypt based columnar (CBC) cells at the base of the crypt for up to 8 weeks. CBCs were first identified almost 40 years ago (Cheng and Leblond 1974) and have recently been renamed as “small cycling cells” (Munoz, Stange et al. 2012). They are readily distinguishable through their expression of the *Lgr5* gene (Barker, van Es et al. 2007), an orphan G protein-coupled receptor (McDonald, Wang et al. 1998), lineage tracing of which has determined that these small cycling cells are capable of generating all differentiated intestinal epithelial cells (Blanpain and Simons 2013).

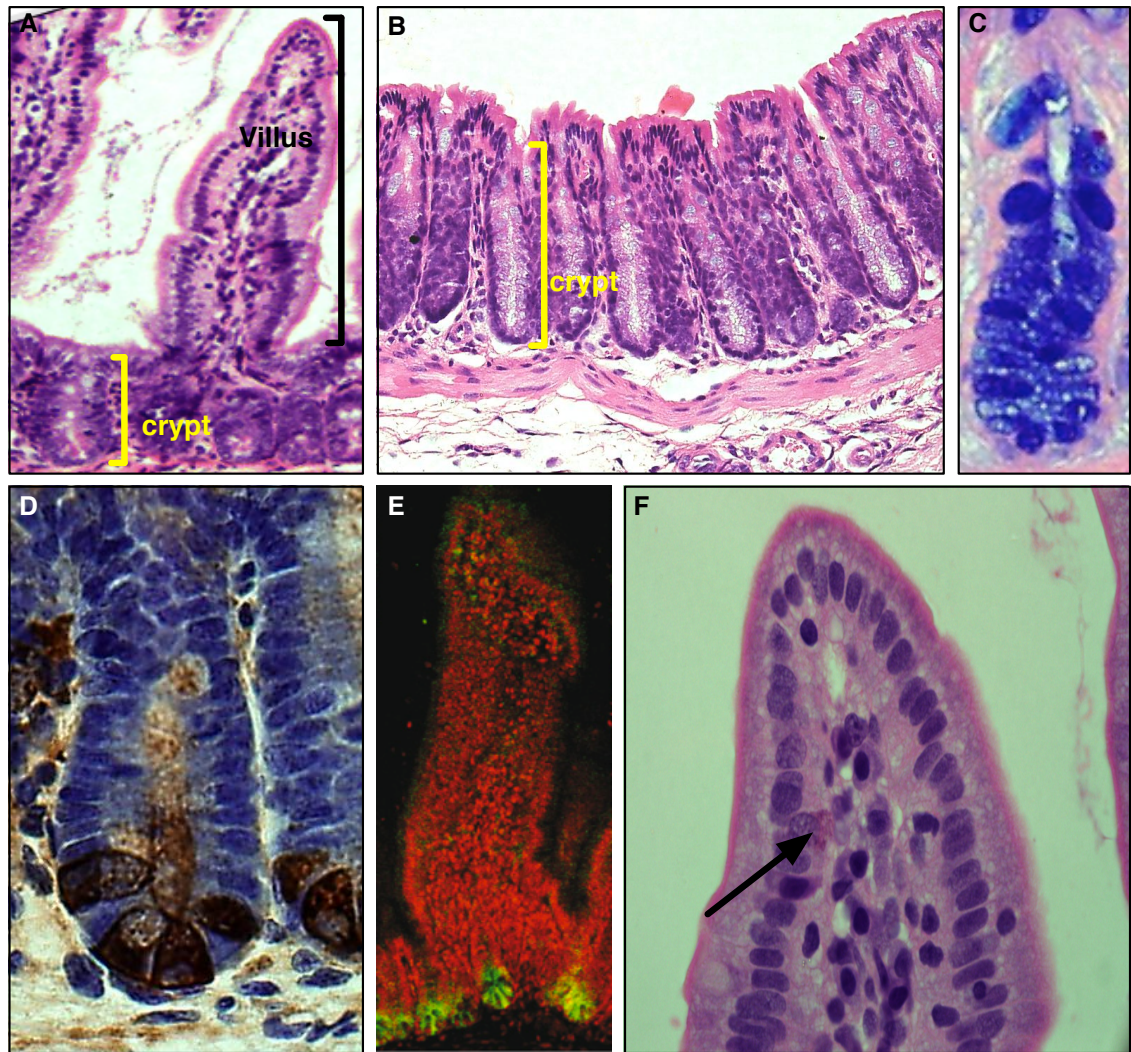


Figure 1-2 Murine small Intestine and colonic epithelium

Haematoxylin and eosin (H&E) staining of mouse small intestine (A) shows characteristic mucosal vaginations of the mucosa termed villi with mucosal invaginations, termed crypts also labelled. The colonic epithelium differs in the absence of villi and harbours a flat epithelium (B). Alcian Blue staining of colonic goblet cells (C) which are mucin secreting. Lysosyme staining (brown) of small intestinal paneth cells with haematoxylin (blue) counterstain (D). Lgr5 stem cells (GFP labelled, green with DNA dye ToPro-3 (red)) at the base of a small intestinal crypt mark the small cycling cells capable of generating all intestinal epithelial cell types, (image adapted and reprinted by permission from Macmillan Publishers Ltd: Nature (Barker, van Es et al. 2007), copyright 2007). H&E staining of a small intestinal entero-endocrine cell (F).

The function of each of the differentiated epithelial cell types is distinct: paneth cells, through their secretion of antimicrobial peptides are important in intestinal host defence (Wehkamp, Fellermann et al. 2005). It is interesting that paneth cells are present in the developing colon up to gestational age of 13.5 weeks, after which time they are largely absent from the colon, but persist in the small intestine (Bevins and Salzman 2011). Exceptions to this exist, particularly in some chronic inflammatory disease states such as inflammatory bowel disease (IBD) and, under such circumstances, are termed metaplastic

paneth cells (Cunliffe, Rose et al. 2001). Goblet cells secrete mucin which forms a protective blanket throughout the intestine (Specian and Oliver 1991), enterocytes are involved in digestion and also have a barrier function (Snoeck, Goddeeris et al. 2005) whilst entero-endocrine cells have a hormone/peptide secretory role in response to intestinal contents (Krause, Yamada et al. 1985).

The dynamic nature of epithelial cell motility is driven by the actin cytoskeleton, but it is also thought to be involved in regulating cell polarity, molecular signalling at cell:cell adhesion complexes and in the mechanisms underlying cellular proliferation and differentiation (Heath 1996). Fascin is a key actin bundling protein and is important for the regulation of cytoskeletal structures, motility and cellular signalling (Adams 2004a; Hashimoto, Skacel et al. 2005). The dynamic changes in motility, mediated by the actin cytoskeleton and governed by actin bundling proteins such as fascin, which cells undergo in wound healing, resemble in many respects those changes seen in invading tumour cells. The role of fascin with regard actin and cell motility has been well characterised, however the role of fascin in cellular signalling and proliferation is poorly understood. In this thesis, I aim to investigate the role of fascin in the molecular processes underlying epithelial cell proliferation and the transformation from benign inflammatory disease to a malignant process.

1.2 Fascin

1.2.1 Introduction to fascin

Fascin is an evolutionarily conserved 55kDa actin-bundling protein that drives the assembly of filopodia through the cross-linking of actin filaments into straight bundles (Chen, Yang et al. 2010). Conserved from amoebas to man, fascin was originally purified from extracts of sea urchin oocytes and coelomocytes and later found in *Drosophila* as the *singed* gene product (Otto, Kane et al. 1979). It is involved in the invasion and metastasis of multiple epithelial cancer types through stabilisation of actin in invadopodia, finger like protrusions used by cancer cells to invade into and degrade the extra-cellular matrix (Li, Dawson et al. 2010). Fascin, whilst normally low or absent from

epithelia (Hashimoto, Skacel et al. 2006), localises to the leading edges of migratory cells and is over-expressed in many cancers of the same epithelial origin including lung, colorectal, pancreatic and liver (Qualtrough, Singh et al. 2009). Fascin is expressed by fibroblasts and dendritic cells (Banchereau, Briere et al. 2000) and expression levels were recently shown to increase during inflammatory bowel conditions such as diverticulitis, Crohn's disease and ulcerative colitis (Qualtrough, Smallwood et al. 2011).

1.2.2 Structure of fascin

In mammals, three isoforms of fascin exist: fascin 1 (studied in this thesis and from hereon described as "fascin") is widely expressed throughout embryogenesis in neural and mesenchymal tissues, however in adults is confined to certain tissues such as brain, endothelium and testes (Machesky and Li 2010). Fascin 2 is only found in the retina and hair-cell stereocilia, whilst fascin 3 is testes specific (Wada, Abe et al. 2001; Tubb, Mulholland et al. 2002; Wada, Abe et al. 2003). The structure of fascin is composed of four β -trefoil domains and both N- and C- terminal residues are needed to preserve actin-bundling function (Fig. 1-3) (Yang, Huang et al. 2013).

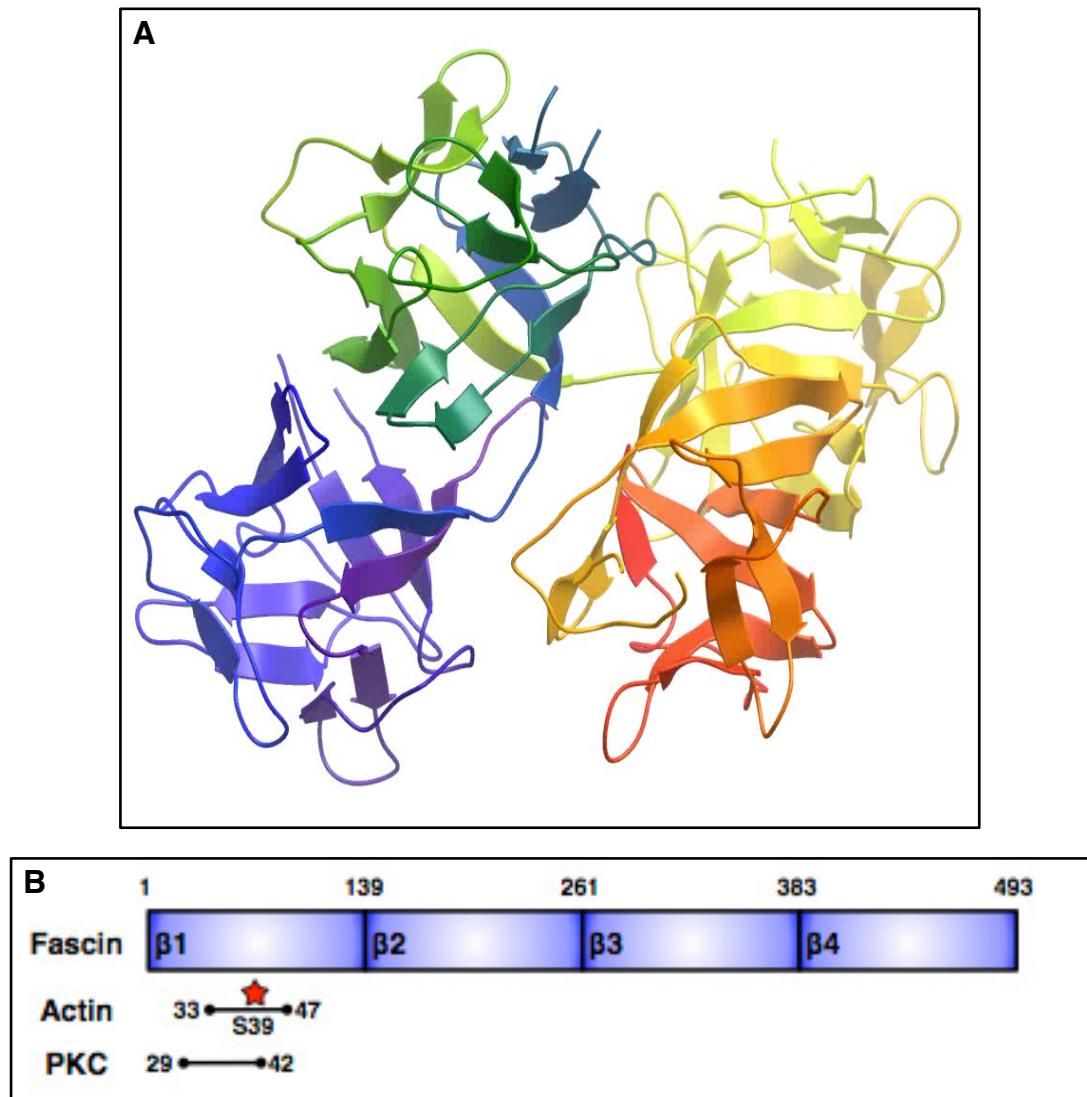


Figure 1-3 Structure of fascin

(A) Crystal structure of fascin demonstrating four β -trefoil domains (image courtesy of Andrew Pannifer, Beatson Drug Discovery). (B) Schematic representation of fascin again demonstrating four β -trefoil domains and selected binding partners. Red star asterisk indicates mutations on residues resulting in the loss of binding with each partner (image adapted from Dr. A Li).

1.2.3 Regulation of fascin

Fascin has previously been implicated, in colon cancer, as a potential target of β -catenin TCF signalling with expression levels often correlating with those of fascin, particularly at the invasive front of tumours (Vignjevic, Schoumacher et al. 2007). This, however, remains controversial and a recent paper, using comparative genomics to analyse the fascin promoter region demonstrated that the regulation of fascin is controlled by CREB (cAMP response element-binding protein) and AhR (aryl hydrocarbon receptor) transcription factors, with no

evidence to support the role of β -catenin in the regulation of fascin in human carcinoma cells (Hashimoto, Loftis et al. 2009).

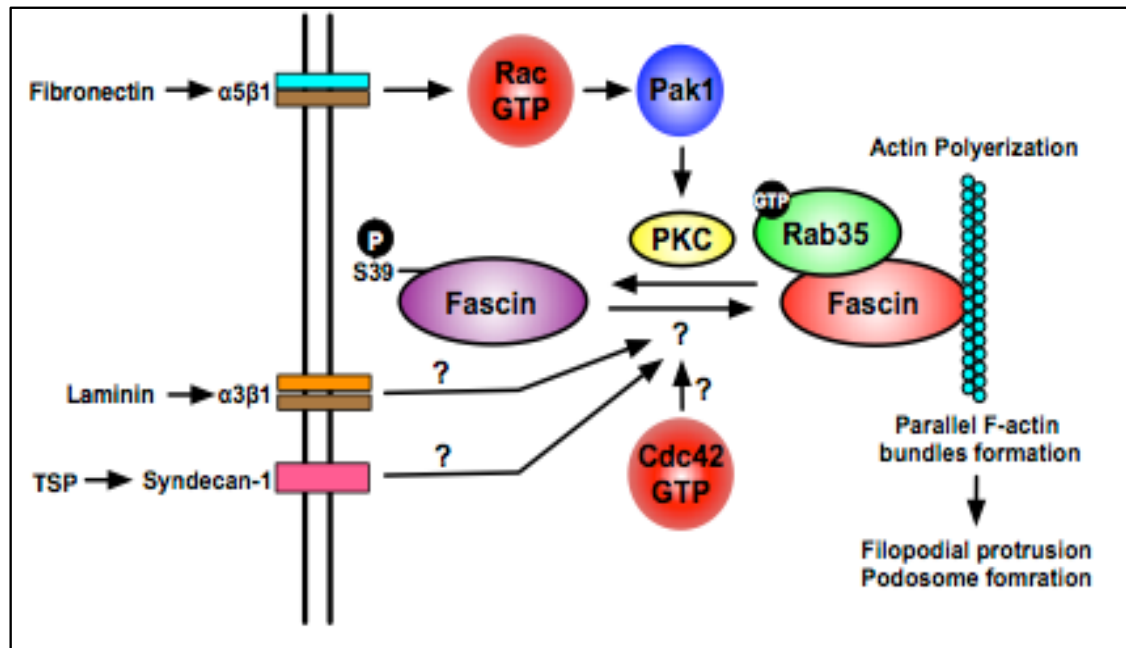


Figure 1-4 Regulation of fascin

Schematic representation of the regulation of fascin. Extra-cellular membrane (ECM) components Thrombospondin-1 (TSP) and laminin are important for the organisation of the actin cytoskeleton through the integrins Syndecan-1 and $\alpha 3\beta 1$ which are important for the bundling of Filamentous-actin by fascin. Rab35 controls actin bundling through the recruitment of fascin as an effector protein. Ligation of the integrin $\alpha 5\beta 1$ by fibronectin activates Rac and, through the effector Pak1 regulates the formation of PKC/fascin complexes. Image adapted from Dr. A Li.

Many proteins which bind actin can be negatively regulated by phosphorylation for example, phosphorylation of fascin at S39 (serine 39), near the N-terminus, can negatively regulate the actin bundling activity (Ono, Yamakita et al. 1997). It is thought that the formation of PKC/fascin complexes is under the control of the G protein Rac (Ras-related C3 botulinum toxin substrate 1) via Pak (Parsons and Adams 2008), although whether this is a direct or indirect regulation is unclear (Fig. 1-4). In *Drosophila* Ras-related protein Rab35 controls actin bundling through the recruitment of fascin as an effector protein (Zhang, Fonovic et al. 2009). In addition to PKC phosphorylation of S39, there may be other phosphorylation sites which are important for the regulation of fascin: there are 7 new sites listed on the Phosida database which may prove important, although currently our understanding of these is minimal. Lastly, components of the extra-cellular matrix (ECM) and certain extracellular signals have been

shown to regulate the phosphorylation status of fascin (and hence it's actin binding/bundling activity) (Kureishy, Sapountzi et al. 2002; Adams 2004b).

1.3 Inflammatory Bowel Disease (IBD)

1.3.1.1 Overview

Inflammatory Bowel Disease (IBD) is a term that encompasses autoimmune inflammatory conditions affecting the small intestine and colon (Baumgart and Carding 2007). Cases of IBD were first described by Italian anatomist Giovanni Battista Morgagni (1682-1771) and Scottish Physician Sir T. Kennedy Dalziel (1861-1924) (Kirsner 1988). Ulcerative colitis (UC) and Crohn's disease (CD) are the two principle IBD conditions. Several other atypical forms also fall under the colitis umbrella, principally ischaemic colitis, indeterminate colitis, collagenous colitis, lymphocytic colitis, diversion colitis and Behçet's disease, however these are not related to an underlying inflammatory pathogenesis. Whilst the morbidity associated with IBD is clearly adverse to a patient's quality of life, one of the serious consequences is the increased lifetime risk of the patient developing an intestinal malignancy secondary to the disease. It is widely accepted that patients with IBD are at a significantly higher risk of developing an intestinal malignancy with figures often quoted of a 10-12 fold increased risk of small bowel adenocarcinoma in CD patients (Solem, Harmsen et al. 2004) and up to 20 fold risk of colon cancer in UC patients (Xie and Itzkowitz 2008). Furthermore, IBD patients develop these tumours at an earlier age (Munkholm, Loftus et al. 2006) than the general population. It is unsurprising, then, that patients with IBD are offered enhanced surveillance in an attempt to identify and treat tumours at an early stage (Cairns, Scholefield et al. 2010). The exact mechanism underlying the increase in malignancies has not been established. Genetic factors have been postulated, but not proven, and instead it is thought that oxidative stress, consequent to the chronic inflammation and the effect this has on the major molecular pathways involved in carcinogenesis (Itzkowitz and Yio 2004) underlies the transformation from benign to malignant disease.

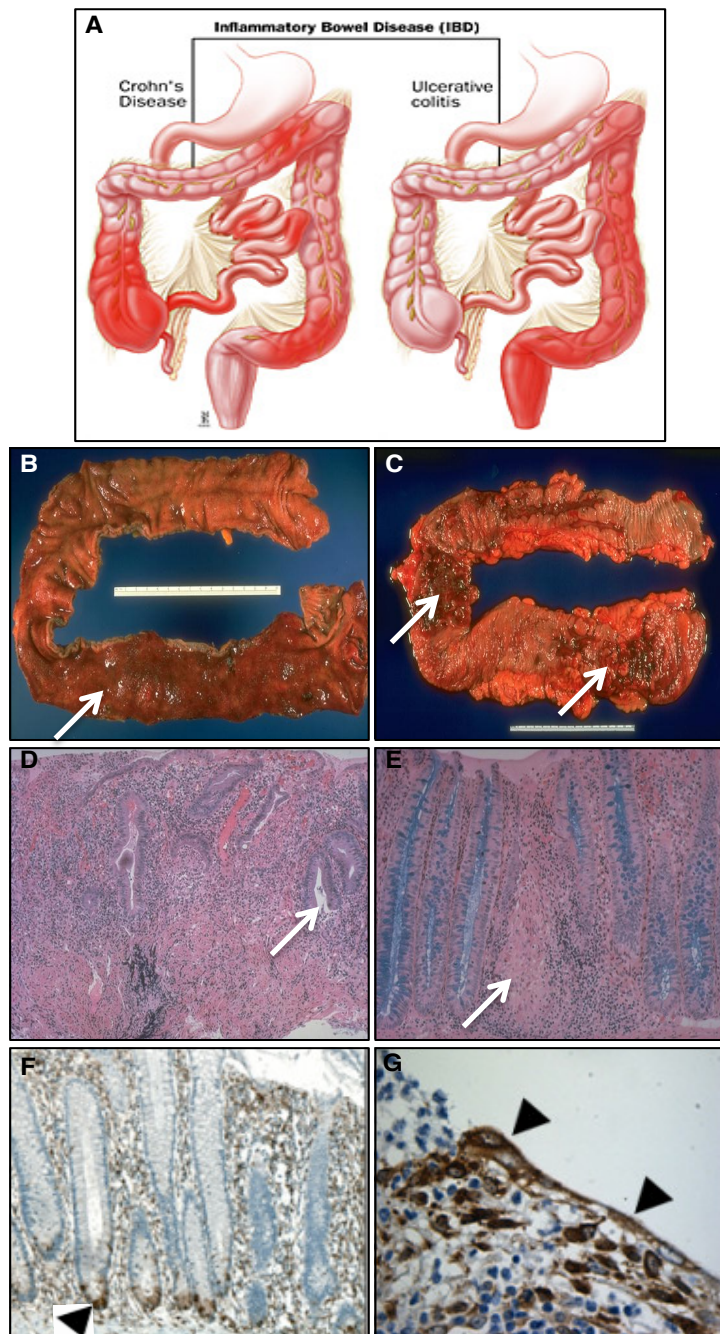


Figure 1-5 Comparison of ulcerative colitis and Crohn's disease and the expression of fascin in human samples

(A) CD is typically asymmetrical with 'skip lesions' and ileal involvement. In contrast UC typically shows continuous involvement most commonly affecting the distal colon (Illustration by Michael Linkinholer, used with permission, © Copyright 2013, Johns Hopkins Medicine, All rights reserved.). UC specimen (B) showing characteristic appearance with diffuse mucosal involvement (arrow indicates continuous area of ulceration) and CD colonic specimen (C) demonstrating serpiginous ulcers with macroscopically normal mucosa in-between ulcerated areas (arrows indicate the ulcerated areas in different sections of the specimen separated by areas of normal mucosa). Histological sample of UC (D) demonstrating distortion of the normal crypt architecture with chronic inflammatory changes seen in the lamina propria (arrowed). Histological sample of CD (E) demonstrating appearance of granulomas (arrowed). Images B,C,D,E printed with permission, copyright "University of Washington 2004". Fascin has recently been shown to be expressed in human tissue samples of IBD with expression seen both in the base of regenerating crypts (F) and also at the leading edge of the ulcers (G) where changes in cell shape, mediated by the actin cytoskeleton are thought to be important in wound healing. Images F,G taken with permission from (Qualtrough, Smallwood et al. 2011).

1.3.1.2 Crohn's disease

The name, Crohn's disease (CD) originated when first described in 1932 by an American Gastroenterologist, Burrill Bernard Crohn, who published a case series of fourteen patients with terminal ileitis (Crohn, Ginzburg et al. 2000). CD is a chronic relapsing, remitting disease affecting any part of the GI tract from mouth to anus (Fig. 1-5). Whilst the classical presentation is of a patient in the second or third decade of life with clinical symptoms of abdominal pain, altered bowel habit (often bloody) and concurrent weight loss (Lichtenstein, Hanauer et al. 2009), many patients display a heterogeneous pattern of localised and systemic symptoms. Histologically, it is characterised by focal, transmural inflammation with approximately 50% of patients demonstrating the diagnostic granulomatous formation (Lichtenstein, Hanauer et al. 2009). The precise aetiology is unknown, although lifestyle, dietary and genetic factors are thought to play an important role (Braat, Peppelenbosch et al. 2006).

1.3.1.3 Ulcerative colitis

Ulcerative colitis (UC) is an idiopathic chronic relapsing inflammatory disease affecting the colon and rectum (Fig. 1-5). First described as a clinical condition in 1859 (Sir Samuel Wilks, a British Physician) (Lukas, Bortlik et al. 2006), the aetiology of the condition remains unclear. Whilst a genetic component (Baumgart and Carding 2007) and an abnormality of the innate immune response to gut bacteria (Ardizzone and Porro 2002) are almost certainly pre-requisites for the condition, multiple environmental triggers have also been described. The clinical presentation of UC is similar to CD in that patients classically present in the second and third decade of life (Stange, Travis et al. 2008) with abdominal pain and altered bowel habit (bloody diarrhoea). Histologically, distinguishing UC from CD can be difficult (Seldenrijk, Morson et al. 1991). Whereas CD is transmural, UC is largely confined to the mucosa with features of gland distortion and the absence of granuloma (Feakins 2013).

1.3.1.4 Intestinal restitution and regeneration in IBD

A feature common to both UC and CD is the infiltration of leucocytes to the gut mucosa with resultant damage to epithelial cells. Macrophages, neutrophils, dendritic cells and T-lymphocytes, once migrated into the gut mucosa form

reactive oxygen species (ROS) which modulate the inflammation and resultant tissue damage (Xavier and Podolsky 2007). Mucosal surfaces, lined by epithelial cells, act as a barrier to pathogens and damage to this leads to a defect in the barrier function (Turner 2009). It is therefore important in patients with IBD that this barrier is restored in order that gut function and the immune response is optimised. Failure to do so may result in a 'leaky barrier', which may result in a chronic cycle of further immune cell infiltration, release of cytokines and consequent chronic impairment of barrier function (Clayburgh, Shen et al. 2004). The repair of the mucosa is classified in two phases, namely restitution and regeneration (Okamoto and Watanabe 2005). Restitution involves the migration of epithelial cells into the damaged mucosa where they de-differentiate, form similar structures to pseudopods through the re-organisation of their actin cytoskeleton then, upon closure of the barrier, re-differentiate to their original form (Sturm and Dignass 2008). Whereby restitution does not involve cellular proliferation (Taupin and Podolsky 2003), regeneration involves the rapid proliferation of epithelial cells and the formation of typical intestinal crypt structures (Qualtrough, Smallwood et al. 2011). Both restitution and regeneration are key steps in the physiological repair of the intestine and the transition from relapse to remission. The cellular and molecular processes responsible for these processes are as yet, not fully understood (Okamoto and Watanabe 2005) and further understanding of these is crucial in developing therapies for patients with IBD. Fascin, an actin bundling protein, has recently been shown to be expressed in human tissue specimens of UC and Crohn's colitis with expression correlating with disease severity (Qualtrough, Smallwood et al. 2011). Fascin was seen to be expressed both at the leading edge of the ulcerated area (where restitution takes place) and also at the base of the regenerating crypts. Furthermore, highest fascin expression was seen in the dysplastic, pre-malignant cells indicating potentially multiple roles for fascin in the repair of IBD damaged tissue, proliferation of epithelial cells and also in the transformation of benign to malignant cells (Qualtrough, Smallwood et al. 2011). Given this exciting data, we wished to take advantage of the fascin knockout (KO) mouse, which we have at the Beatson Institute (through our collaboration with Dr. Shigeko Yamashiro, Rutgers NY) in order to further explore the role of fascin in IBD and the transformation from benign to malignant cells.

1.3.1.5 Animal models of IBD

Animal models recapitulating small intestinal and colonic inflammation have been in practise for some time (Elson, Sartor et al. 1995). Whilst these animal models do not replicate the heterogenous nature of human IBD, nor do they replace studies on human samples, they have greatly advanced our understanding of many of the mechanisms underlying the pathogenesis of the disease in humans and potential therapeutic targets.

The models broadly fall into four categories namely, (1) spontaneous models such as C3H/HeJBir mice (Sundberg, Elson et al. 1994) which develop spontaneous CD4⁺T-cell induced transmural colitis at around 3 weeks of age in response to antigens of commensal gut bacteria. (2) Inducible models are mediated through mechanical or chemical disruption of the mucosa leading to activation of the mucosal immune system (i.e. Dextran Sodium Sulphate (DSS), which is administered orally, and radiation induced small intestinal inflammation). (3) Genetically engineered models include transgenic mice which constitutively express TL1A (a TNF superfamily member and mediator of gut inflammation (Shih, Barrett et al. 2011)) and targeted gene deletions (such as Il-2, Il-10 and TGF- β (Podolsky 1997)). (4) Adoptive transfer models such as T-cell transfer (Ostanin, Bao et al. 2009) involves the transfer of specific cells to animals which are immunocompromised (Wirtz and Neurath 2007) (Wirtz and Neurath 2000).

In this thesis, I have made use of chemically induced models such as DSS and gamma irradiation in mice to induce acute colitis and small intestinal inflammation respectively. DSS is a non-genotoxic sulphated polysaccharide (Okayasu, Hatakeyama et al. 1990) which causes elevated levels of ROS, termed oxidative stress. Under normal circumstances, cells are able to defend themselves against ROS damage with various enzymes and antioxidants playing an important role. However, when the level of ROS exceeds the body's capacity to neutralise it, harmful effects occur, notably DNA damage (Cooke, Evans et al. 2003). The small intestinal stem cells, which reside at the base of the crypts, are thought to be more susceptible to high levels of oxidative stress than the other more differentiated cells in the crypt as a result of increased oxidized DNA pyrimidines (Oberreuther-Moschner, Rechkemmer et al. 2005) resulting in a

reduction in self-renewal and differentiation (Wang, Zhang et al. 2013). DSS functions in two distinct methods, first the colonic mucosa is damaged thereby disrupting the barrier function and secondly through the consequent localised inflammatory response and chemokine stimulation by epithelial cells (Ohtsuka and Sanderson 2003) (Laroui, Ingersoll et al. 2012). Clinically, rodents treated with DSS demonstrate features of UC namely bloody diarrhoea and weight loss, whilst the pathological features also show similar features to that of UC (Okayasu, Hatakeyama et al. 1990) with evidence of mucosal ulceration and colonic shortening (Erichsen, Milde et al. 2005).

DSS specifically affects the colon, therefore, in order to investigate regeneration in the small intestine, we employed alternative methods. The use of whole body gamma (Y) radiation in animal models does not recapitulate small intestinal inflammation as accurately as DSS does the colon, however it is an effective tool to investigate the mechanisms relevant to small intestinal regeneration. Rapidly cycling stem cells at the base of crypts are responsible for the proliferation and regeneration of epithelial cells and are sensitive to damaging genotoxic stimuli such as Y-radiation, which results in stress-induced apoptosis (Watson and Pritchard 2000). Global apoptosis of a crypt cell population results in the disappearance of a crypt within 2 days, however if a single clonogenic cell within a crypt survives, it is able to repopulate the entire crypt within 3-4 days (Ottewell, Duckworth et al. 2006). 3-5 days following irradiation is the recognised time frame to examine regenerating crypts (Martin, Potten et al. 1998). In this thesis, we used the 3 day time point, unless otherwise stated.

1.3.1.6 Physiology behind intestinal regeneration

The ability of crypt cells to survive inflammatory insults, proliferate, differentiate and regenerate the intestine are evidently key features. Various growth factors have been shown to be important for crypt survival and proliferation such as transforming growth factor- β (TGF- β) and Il-11 (both improve crypt survival (Potten 1995)), and keratinocyte growth factor (both protective and enhances epithelial cell proliferation (Potten, O'Shea et al. 2001)).

The Wnt signalling pathway (Fig. 1-6) is important for the differentiation of pluripotent stem cells during intestinal embryogenesis (Gregorieff and Clevers 2005) and is an essential regulator of intestinal homeostasis through downstream gene transcription effects (Gregorieff and Clevers 2005). The canonical Wnt signalling pathway begins with one of the Wnt proteins binding Frizzled receptor (Rao and Kuhl 2010), facilitated by other co-receptors such as LRP (lipoprotein receptor-related protein). Following this, a signal is passed through an interaction between LRP and Dsh (phosphoprotein Dishevelled) and Axin is recruited from the destruction complex. The destruction complex comprises Axin, PP2A (protein phosphatase 2A), GSK3 (glycogen synthase kinase), CK1 α (casein kinase 1 α) and Wnt signalling inhibitor APC (Adenomatous polyposis coli). Under physiological conditions, β -catenin undergoes proteosomal degradation by the destruction complex, however when Wnt signalling is activated and Axin is recruited, the destruction complex is inactivated. β -catenin subsequently accumulates in the cytoplasm before translocating to the nucleus and binding T cell factor (TCF) transcription factors with consequent activation of Wnt target genes such as Lgr5 (Leucine-rich repeat-containing G protein-coupled receptor 5) and c-Myc (Gregorieff and Clevers 2005).

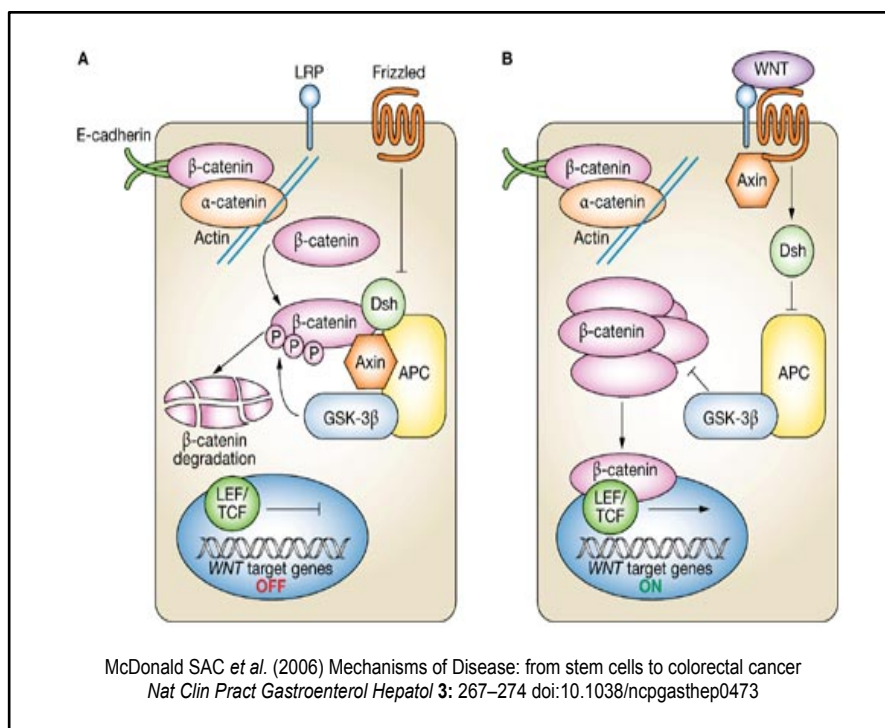


Figure 1-6 The Wnt signalling pathway

The Wnt pathway is an essential regulator of intestinal homeostasis with inactivating mutations in the Wnt signaling inhibitor, APC accounting for 80% of colorectal cancers (CRCs). (A), when Wnt is not activated, the APC destruction complex degrades β -catenin, however when Wnt is activated, it binds the LRP receptor, Axin is removed from the destruction complex allowing β -catenin to translocate to the nucleus where it binds to transcription factors and activates Wnt target genes such as Lgr5. Whilst the precise role of the Wnt pathway is unclear in intestinal regeneration, we know that high levels of β -catenin and the Wnt target gene c-Myc accumulate in regenerating intestinal crypts and that c-Myc is required to induce intestinal regeneration in the mouse. It has been suggested that, in CRCs, fascin is a target of β -catenin (as they are frequently expressed in the same locations with expression levels correlating), however its precise role remains unclear. Image reprinted by permission from Macmillan Publishers Ltd: *Nature Clinical Practice Gastroenterology & Hepatology* (McDonald, Preston et al. 2006), copyright 2006.

1.3.1.7 Intestinal stem cells

Intestinal epithelial cells (IECs) fall into two broad categories, namely secretory (paneth, goblet and entero-endocrine cells) and absorptive (enterocytes). The eventual outcome of an IEC exiting the transit-amplifying compartment is dependant upon the process of how each intestinal stem cell (ISC) differentiates and the various pathways involved regulating this at each step (Fig. 1-7). The Notch signalling pathway has a key role in regulating whether an ISC

differentiates into a secretory or absorptive lineage (van Es, van Gijn et al. 2005). Specifically, it has been shown that active Notch signalling leads to transcription of Hes (Hairy/Enhancer of Split) genes which in turn code Hes repressors (Stanger, Datar et al. 2005) which have been shown to inhibit Math1 (a basic helix-loop-helix (bHLH) transcription factor) thought to be expressed by a common progenitor required for the differentiation of the secretory cell lineage (Fig. 1-7) (Yang, Bermingham et al. 2001).

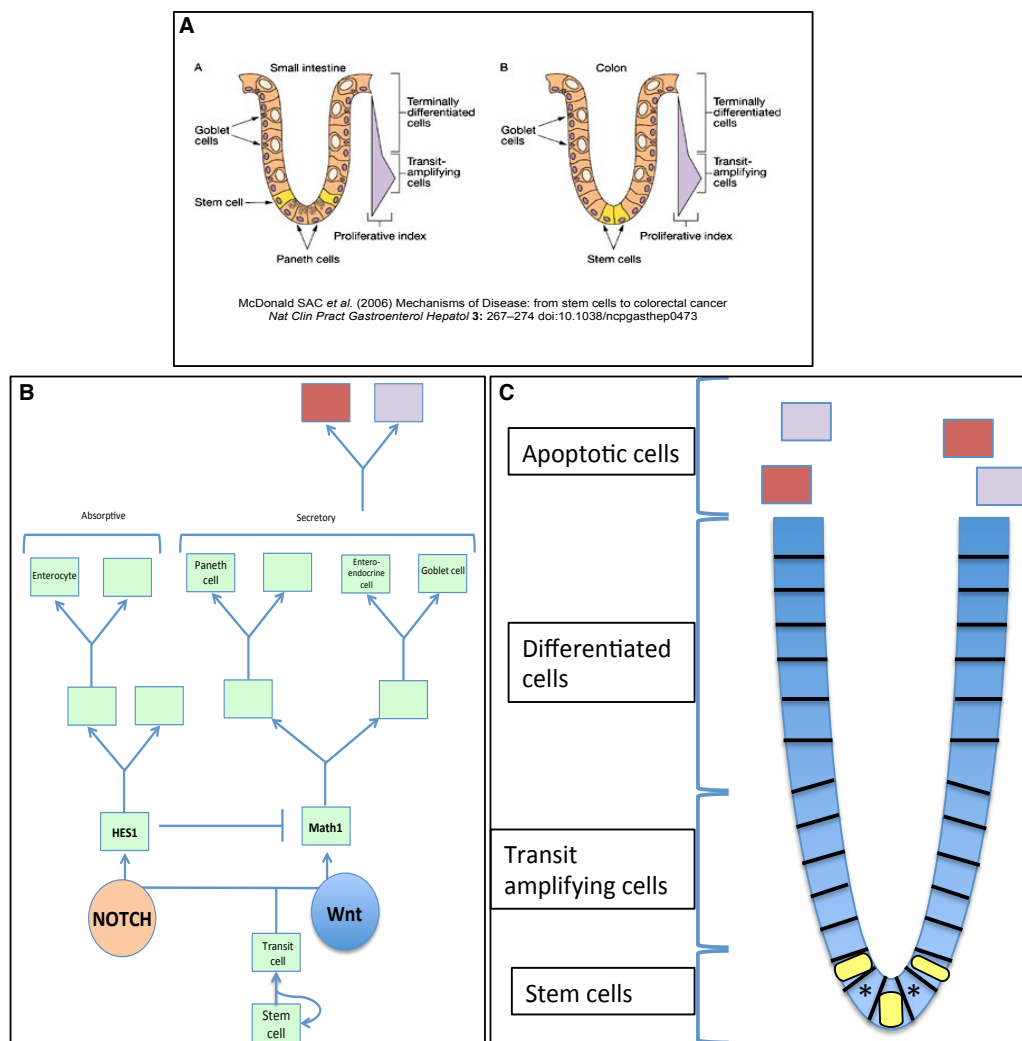


Figure 1-7 Small Intestine and colonic crypt architecture

(A) Schematic representation of small intestine and colonic crypts with stem cells located in the base of the crypts (image reprinted by permission from Macmillan Publishers Ltd: *Nature Clinical Practice Gastroenterology & Hepatology* (McDonald, Preston et al. 2006), copyright 2006. (B,C) Schematic representation of the asymmetric differentiation of Lgr5 small cycling stem cells (marked with yellow rectangles in (C)): towards the base of the crypts, the stem cells divide to give one daughter transit cell capable of differentiation and one daughter stem cell. The transit cells divide several times after which they undergo terminal differentiation into one of the four epithelial cell types. The Wnt and NOTCH signaling pathways are key in the determination of the cell fate. (B,C) images adapted with permission from Integrative Biology.

Inactivating mutations of the Wnt signalling inhibitor APC result in the formation of adenomas originating from the Lgr5 stem cells indicating that these small cycling cells not only function as the principal stem cell of the intestine, but also act as the origin of sporadic intestinal cancers (Barker, Ridgway et al. 2009). A technique used in this thesis whereby single Lgr5 cells can be isolated and cultured *in-vitro* to form organoids possessing all differentiated epithelial cell types is a novel method of investigating molecular mechanisms important in intestinal regeneration (Sato, Vries et al. 2009). A single Lgr5 stem cell can form an indefinite, self-renewing "minigut" in culture growing in a polarised sphere with their apical surfaces pointing into the lumen. This process works even more efficiently if a paneth cell and an Lgr5 cells are co-cultured to reconstitute a crypt (Sato, Vries et al. 2009). As previously mentioned, lineage tracing (a method which analyses the genetic component of marker proteins in stem cells and their progeny (Blanpain and Simons 2013)) has been used to determine 510 signature genes isolated from the Lgr5 cells (Fig. 1-8) (Munoz, Stange et al. 2012) which function as specific intestinal stem cell markers (for example, neuritin 1 (Nrn1) and olfactomedin 4 (Olfm4)).

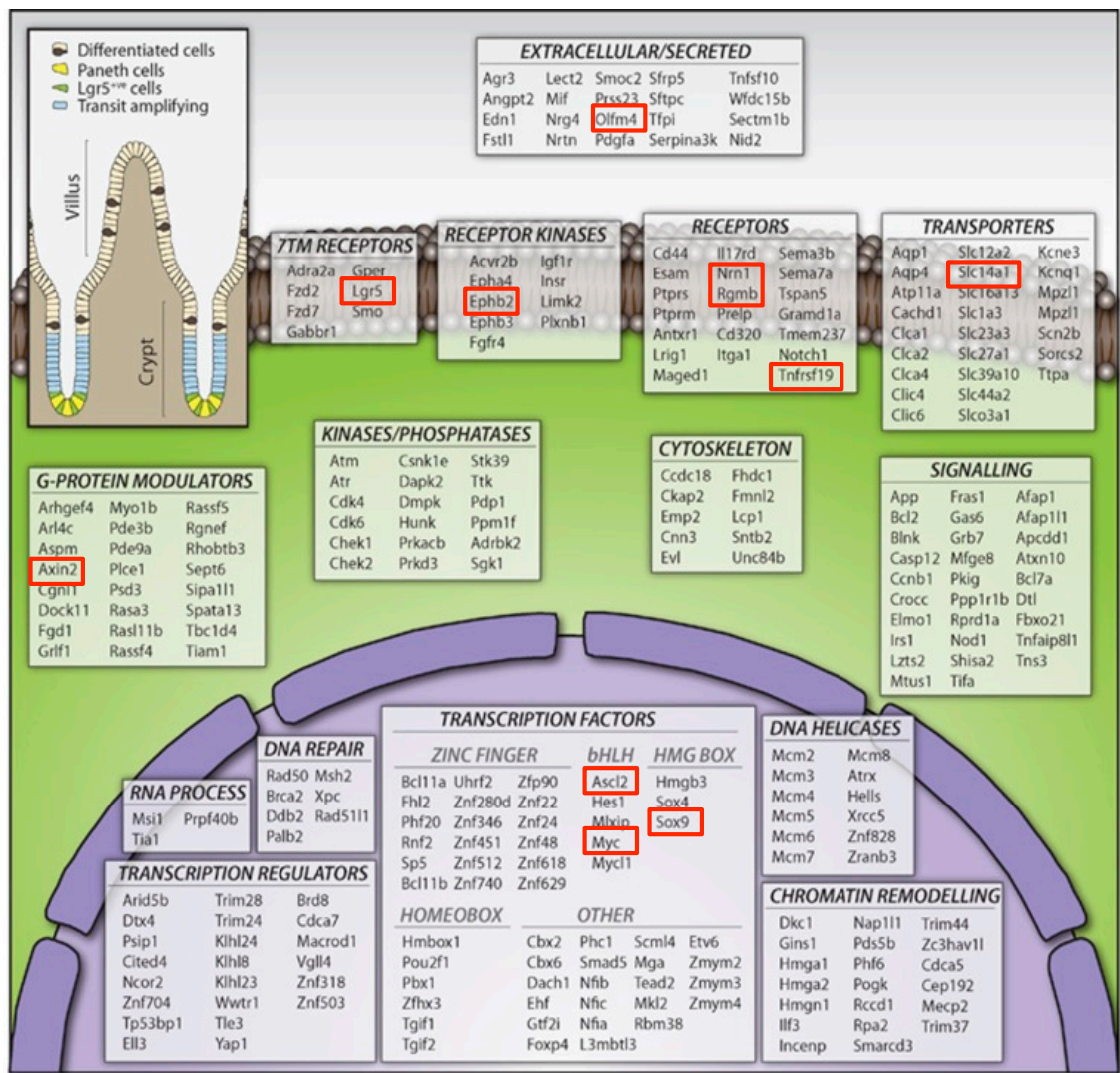


Figure 1-8 Functional classification of genes derived from the Lgr5 stem cell signature

A selection of genes separated into functional classes derived from the Lgr5 intestinal stem cell signature. A selection of genes highlighted in red were analysed, using qRT-PCR in this thesis and will be discussed in later chapters. Figure adapted and reprinted by permission from Macmillan Publishers Ltd: The EMBO Journal (Munoz, Stange et al. 2012), copyright 2012.

1.3.2 Small Intestine and colorectal cancer

Malignant tumours arising within the GI tract can be divided into those arising in the small intestine and those arising in the colon and rectum. Small intestinal cancers are relatively rare with approximately 1200 new cases/year in the UK. 40% are adenocarcinomas, 30% neuroendocrine, 10% sarcoma and the remainder lymphomas. Patients with Crohn's disease, familial adenomatous polyposis (FAP), hereditary non-polyposis colorectal cancer (HNPCC) and Peutz-Jeghers syndrome are at an increased risk. Colorectal cancers (CRC), in contrast are the 3rd commonest cancer in the UK with approximately 41,000 new cases/year in

the UK. The vast majority are adenocarcinomas with the remainder either squamous, neuroendocrine, lymphomas or sarcomas (statistics taken from Cancer Research UK website: <http://www.cancerresearchuk.org>). Patients with IBD, FAP, HNPCC are all at significantly higher risk of developing CRC.

Malignancies arising from the GI tract can be further categorised into sporadic (through genetic alterations (Kinzler and Vogelstein 1996)) and inflammation induced ((Coussens and Werb 2002)). Sporadic tumours themselves will also have an intrinsic inflammatory component and indeed have been shown to control aspects of the inflammatory response to enhance their progression (Coussens, Raymond et al. 1999).

The Wnt signalling pathway, whilst essential for normal intestinal homeostasis, was first discovered for its role in CRC. Inactivating mutations in the Wnt signalling inhibitors APC (Powell, Zilz et al. 1992) and Axin2 (Liu, Dong et al. 2000) or oncogenic mutations in β -catenin (Morin, Sparks et al. 1997) are responsible for the vast majority of CRCs (Fodde and Brabletz 2007). Loss of APC or Axin2 or oncogenic mutation of β -catenin results in nuclear accumulation of β -catenin whereby, through the eventual dis-regulated activation of TCF target genes, the dynamic interplay that exists between epithelial cells proliferating and differentiating is disrupted and the process of tumourigenesis is initiated (van de Wetering, Sancho et al. 2002).

The importance of inflammation and cancer was first hypothesised by Rudolf Virchow in 1863 when he noted the presence of leucocytes in tumour samples (Balkwill and Mantovani 2001). The molecular pathways, which link inflammation and cancer are complex with various mechanisms postulated. Inflammatory mediators, through ROS production, damage cellular DNA whilst also being involved in the suppression of key pathways involved in DNA repair (Fig. 1-9) (Colotta, Allavena et al. 2009). Tumour necrosis factor alpha (TNF α) is an important cytokine and mediator of the inflammatory response (Locksley, Killeen et al. 2001). Produced primarily by macrophages (Olszewski, Groot et al. 2007), TNF α is responsible for co-ordinating the acute phase of the inflammatory response through activation of NF- κ B (nuclear factor kappa-light-chain-enhancer of activated B cells) (Fitzgerald, Meade et al. 2007). NF- κ B is a transcription factor involved in the regulation of many different key immune system responses

(Ghosh, May et al. 1998), which are clinically significant with respect to both cancer (Rayet and Gelinas 1999) and inflammation (Tak and Firestein 2001). There are two recognised pathways involved in the activation of NF- κ B, the canonical (classical) and non-canonical (alternative) (Karin 1999). In the canonical pathway, NF- κ B in the inactivated state is bound to I κ B α (nuclear factor of kappa light polypeptide gene enhancer in B-cells inhibitor alpha). Phosphorylation of I κ B α (initiated by extra-cellular signals such as pro-inflammatory cytokines) results in the activation of the enzyme IKK (I κ B kinase), which phosphorylates I κ B α resulting in its eventual degradation and subsequent activation of NF- κ B. Once activated, NF- κ B translocates to the nucleus where, either alone or in combination with other transcription factors (such as members of the JAK-STAT signalling pathway) it activates target genes and in doing so modulates cell function. The Janus kinase/signal transducers and activators of transcription (JAK-STAT) pathway is a key pathway in mammals and is involved in cellular processes such as proliferation, differentiation, apoptosis and migration (Rawlings, Rosler et al. 2004). STAT3 (signal transducer and activator of transcription 3) and NF- κ B have been muted as one of the key links between inflammation and cancer (Bollrath and Greten 2009). STAT3 and NF- κ B can interact with each other and in doing so affect their respective transcriptional functions (Yu, Zhang et al. 2002). Their co-operative binding can also induce certain target genes (Yang, Liao et al. 2007) and furthermore, they have been shown to co-operatively enhance tumourigenesis through the activation of certain genes involved in angiogenesis, apoptosis and transcription of immunosuppressive and pro-inflammatory cytokines (Fan, Mao et al. 2013). Fascin has been shown to be a potential target of both NF- κ B (Kress, Kalmer et al. 2011) and STAT3 (Snyder, Huang et al. 2011). Given the recent published data showing the expression of fascin in human tissue samples of IBD (Qualtrough, Smallwood et al. 2011) and the well recognised roles of fascin in tumours (Gao and Wu 2008), we sought to investigate the role of fascin in murine models of IBD and intestinal tumourigenesis.

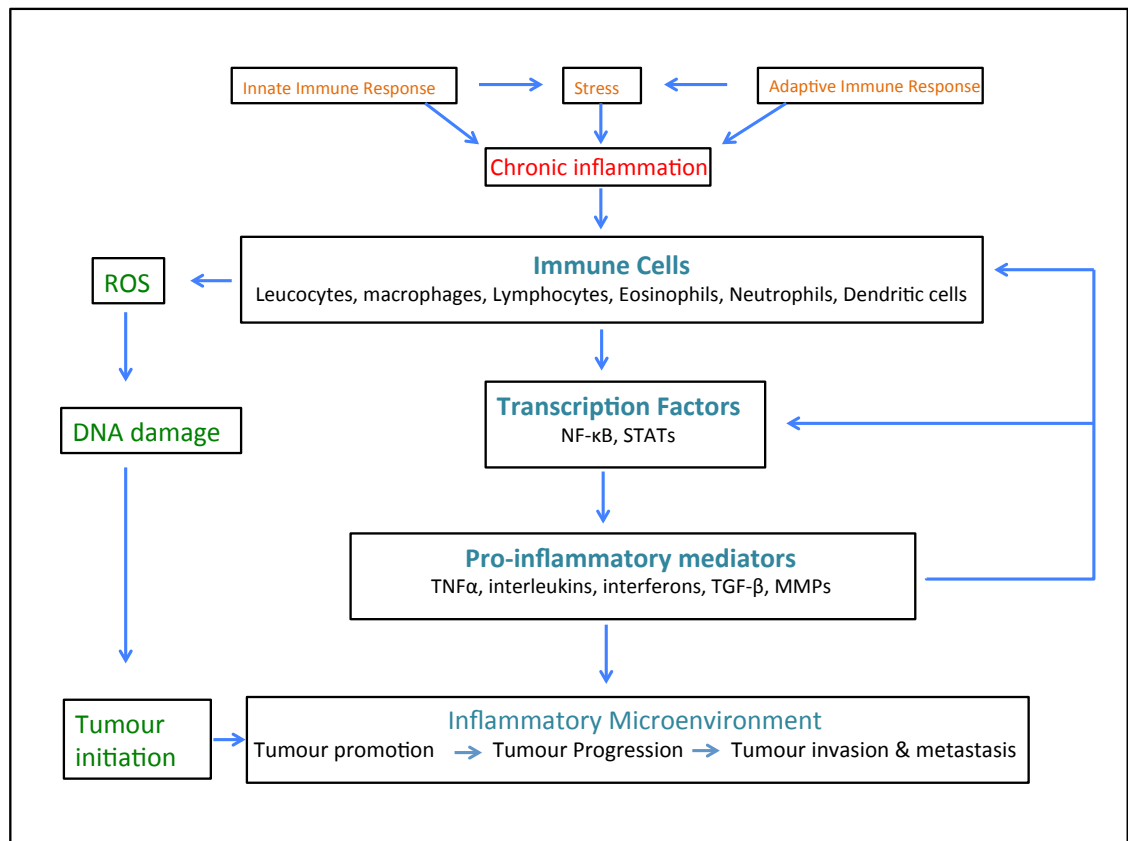


Figure 1-9 The role of inflammation and cancer

In the majority of chronic inflammatory conditions (such as IBD), the accumulation of inflammatory and immune cells results in localised tissue damage through the production of ROS. Pro-inflammatory mediators such as $\text{TNF}\alpha$ are regulated through a complicated positive and negative loop feedback by transcription factors such as $\text{NF-}\kappa\text{B}$ and members of the JAK-STAT pathway. Figure adapted with permission from IBWF website.

1.3.3 Genetic modification of mice

Experimental methods involving the genetic manipulation of mice, in isolation or in combination with chemicals have proven useful in developing models to study cancers arising in the GI tract. Whilst they do not replace studies on human cancers, they are valuable tools to replicate mechanisms key to the development of human cancers and provide a platform to both further our understanding of the mechanisms involved and to enable the testing of disease modifying drugs, which ultimately may be beneficial for use in humans.

There are different techniques to produce genetic modifications in mice. One such technique, resulting in a transgenic mouse, involves the incorporation of a segment of foreign DNA into the host genome, using techniques such as pronuclear injection (Gordon, Scangos et al. 1980) and retroviral vectors.

Another technique (used to generate the fascin knockout mouse used in this thesis), involves inducing genetic disruptions into embryonic stem cells through the use of DNA constructs. These cells are then injected into mice blastocysts (Thomas and Capecchi 1987) and the resultant progeny are bred with either a disrupted or deleted gene (termed “knockout” KO) or if it is inserted it is termed “knockin”.

The introduction of the Cre/lox system (Fig. 1-10) heralded a new era in genetic mouse modelling whereby it was possible to (in)activate any gene in any tissue at any time (Sauer 1998). Constitutive models refer to the permanent disruption of a target gene in every cell of the body whereas conditional models can be either tissue specific or inducible (Bockamp, Sprengel et al. 2008). In the intestine, two Cre lines: Ahcre and villin-Cre-ER are commonly used for conditional recombination. Ahcre expression is mediated, in response to lipophilic xenobiotics such as β -naphthoflavone, via the cytochrome P450 promoter (Ireland, Kemp et al. 2004) whereas the villin-Cre-ER line is tamoxifen dependant.

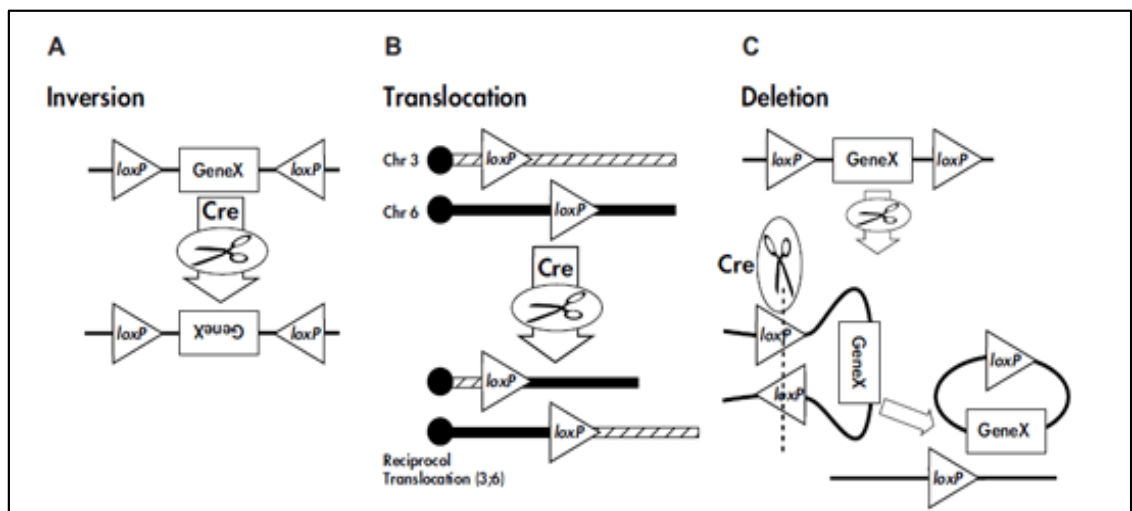


Figure 1-10 Cre-lox recombination

Depending on the orientation and position of the flanking loxP sites, the final outcome of the floxed segment will be determined. (A) When loxP sites face each other, recombination results in Inversion. (B) When the loxP sites are on different chromosomes, recombination results in a chromosomal translocation whilst in (C), the loxP sites are aligned in the same direction on the one chromosome and recombination results in the deletion of the floxed segment. Figure courtesy of the Jackson Laboratory.

1.3.3.1 Murine models of small intestine and colorectal tumourigenesis

Inactivating mutations in the APC gene leading to activation of the Wnt signalling pathway have been shown to result in the formation of multiple sporadic small intestinal adenomas in mice (Moser, Pitot et al. 1990). The Min (multiple intestinal neoplasia) mouse which harboured a heterozygous mutation in the APC gene was the first genetic mouse model which replicated the equivalent human hereditary disease Familial Adenomatous Polyposis (FAP) (Su, Kinzler et al. 1992) characterised by germline mutations of the APC gene. Further inducible models of APC loss in mice have since been developed (Sansom, Reed et al. 2004) using the technique of conditional targeting of APC (Shibata, Toyama et al. 1997). p53 is a crucial tumour suppressor gene, frequently mutated in multiple human tumours (Olive, Tuveson et al. 2004). p53 loss of function in murine models can be achieved through a variety of models (Broz and Attardi 2010) such as the use of tissue specific conditional p53 knockout (KO) mice whereby the p53 sequences are floxed on either side by 2 LoxP sites (Broz and Attardi 2010).

Chemically induced models of colonic tumourigenesis have been developed, for example using the genotoxic carcinogen Azoxymethane (AOM). AOM is a metabolite of 1,2-dimethylhydrazine (DMH) and causes mutations of β -catenin thereby activating Wnt signalling. It is a reproducible, highly potent chemical and has been used widely in rodents, in combination with DSS to induce multiple colonic tumours (De Robertis, Massi et al. 2011).

1.4 Actin bundling proteins and cancer

The following section is adapted from a review article we published in 2012 (Stevenson, Veltman et al. 2012).

1.4.1 Actin bundling proteins in tumourigenesis and cancer progression

Cells use their cytoskeletons to move, polarise, divide and maintain organisation within multicellular tissues. Actin is a highly conserved essential building block of the cytoskeleton that forms cables and struts, which are constantly

remodelled by more than 100 different actin-binding proteins. The initiation of new actin filaments and their subsequent organization is a key step in the development of specialised cellular structures, such as filopodia (spikes), lamellipodia (sheet-like protrusions), stress fibres (elastic contractile bundles), microvilli (finger-like surface protrusions) and invadopodia (invasive cell feet) (see Table 1 for a more complete list). Whilst the cytoskeleton is important in normal cellular function, it is also often subverted in cancer cells and contributes to changes in cell growth, stiffness, movement and invasiveness (Fig. 1-11). We hereby give an overview of the role of actin filament crosslinking or bundling in normal cellular structures and discuss how alterations in the activity or expression patterns of actin bundling proteins could be linked to cancer progression.

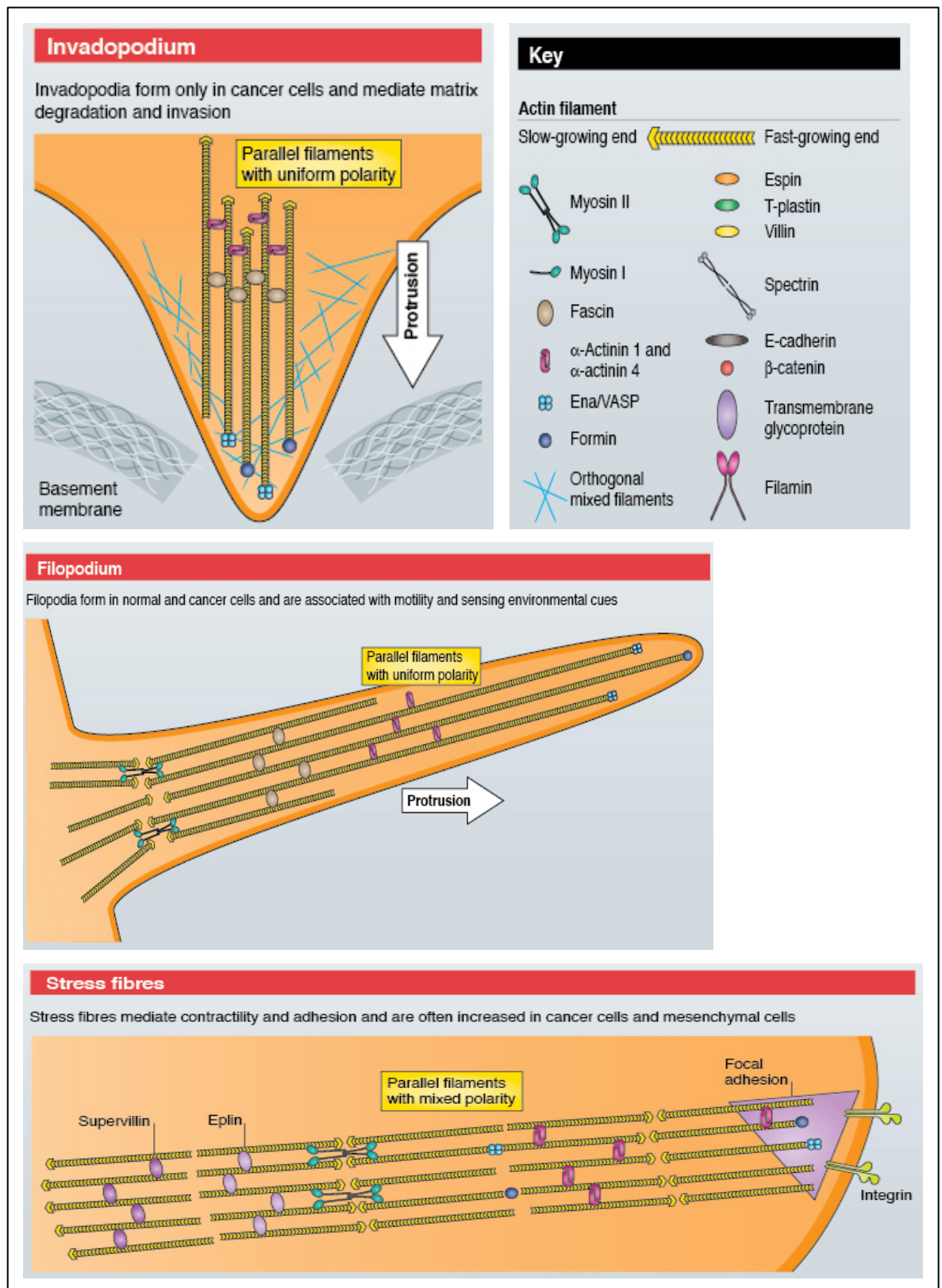


Figure 1-11 Structure and functions of filopodia, invadopodia and stress fibres

Invadopodia are dynamic actin-rich membrane protrusions found only in invasive cancer cells, uniquely able to degrade the extracellular matrix (ECM) through proteolysis of its constituents. Filopodia are cytoplasmic spiky projections containing tight bundles of long actin filaments that sometimes originate within lamellipodia, as well as in cell-to-cell communication and cell positioning within tissues. Defined by their protrusive behaviour, they function in cell migration and contribute to cancer cell invasion at least *in-vitro*. Stress fibres are elastic contractile bundles often found to be increased in cancer and mesenchymal cells. Reproduced with permission (Stevenson, Veltman et al. 2012).

1.4.2 The actin cytoskeleton is regulated by multiple actin-binding proteins

Actin is one of the most abundant proteins in mammalian cells and underpins the compartmentalisation of cellular contents and cell motile behaviour.

Spontaneous nucleation or initiation of new filaments is crucial to cellular dynamics, so it is highly regulated. The main regulators are nucleation promoting proteins, such as the Arp2/3 complex and Wiskott-Aldrich syndrome family protein (WASP)-family proteins (Suetsugu, Miki et al. 2002) as well as WASP-homology containing proteins, such as protein spire homolog (Spire) and cordon bleu (Cobl) (Dominguez 2009). Nucleation of actin filaments generally takes place adjacent to a lipid bilayer, such as just underneath the plasma membrane or on internal endocytic vesicles, with the new ATP-bound actin subunits being added closest to the membrane surface.

Filaments can be assembled into superstructures by various actin filament cross-linking proteins and, depending on the relative concentrations of the crosslinker and the filament will either form bundles or gels. In general, crosslinking proteins have two actin binding sites, often because they dimerise, and the location of actin-binding sites determines the filament arrangement and subsequently the type of crosslinked structure formed. Actin bundles can be of either mixed or uniform polarity, depending on whether they are contractile, orthogonal or parallel.

1.4.3 A role for actin bundling proteins in metastasis

Cancer cells face many challenges for successful metastasis. They must break away from the primary tumour and invade through the surrounding tissue, which usually includes a basement membrane and extracellular stroma and sometimes also muscle. Metastatic cells then typically invade through the lymphatic or vascular endothelium including through their basement membrane, and into the circulation. They exit the lymphatic or vascular system and make their way into a new niche where they seed a new tumour, often after lying dormant for months or years. During this time, cells adapt their motility and adhesive capacity to suit their environment, much in the same way as embryonic cells do

during morphogenesis [recently reviewed in (Hanahan and Weinberg 2011; Roussos, Condeelis et al. 2011)].

The actin cytoskeleton serves many crucial functions for the metastatic cell, including acting as a scaffold for signalling, a connection with the extracellular environment, a mechanosensor and a regulator of the mechanical properties of the cell. Therefore, actin-bundling proteins, which modulate where and how cells form actin filament structures of varying geometries, can be hijacked by cancer cells as they face new challenges. However, there is no general rule whether actin bundling promotes or inhibits cancer metastasis; rather, cells can adjust the extent of actin bundling to alter their signalling, growth, or adhesion and mechanical properties and thus be selected for survival during tumour progression and metastatic spread. Typically, mechanical stiffness and increased contractility of a cancer cell is positively correlated with its ability to invade and metastasise (Narumiya, Tanji et al. 2009), but some studies suggest that exceptions exist (Swaminathan, Mythreya et al. 2011).

As mentioned above, the actin cytoskeleton also maintains the compartmentalisation of cellular contents and thus is a major determinant of cell polarity. Polarity is essential for normal tissue homeostasis and when disrupted can lead to tumour promotion through the breakdown of cell-cell junctions and to epithelial-to-mesenchymal transition (EMT) (Royer and Lu 2011). Cell divisions are also polarised within tissues, so if polarity is lost, tissue integrity can be compromised resulting in overgrowth, aberrant invasive behaviour and promotion of tumours. Actin bundling contributes to the polarity of epithelial cells by maintaining cell-cell adherens junctions, tight junctions, and microvilli, and to polarised trafficking of endosomal and exocytic components (Fig. 1.12). However, the picture of how exactly cells subvert actin bundling to succeed in metastasis is still very much emerging and represents an exciting area of future research for metastasis prevention.

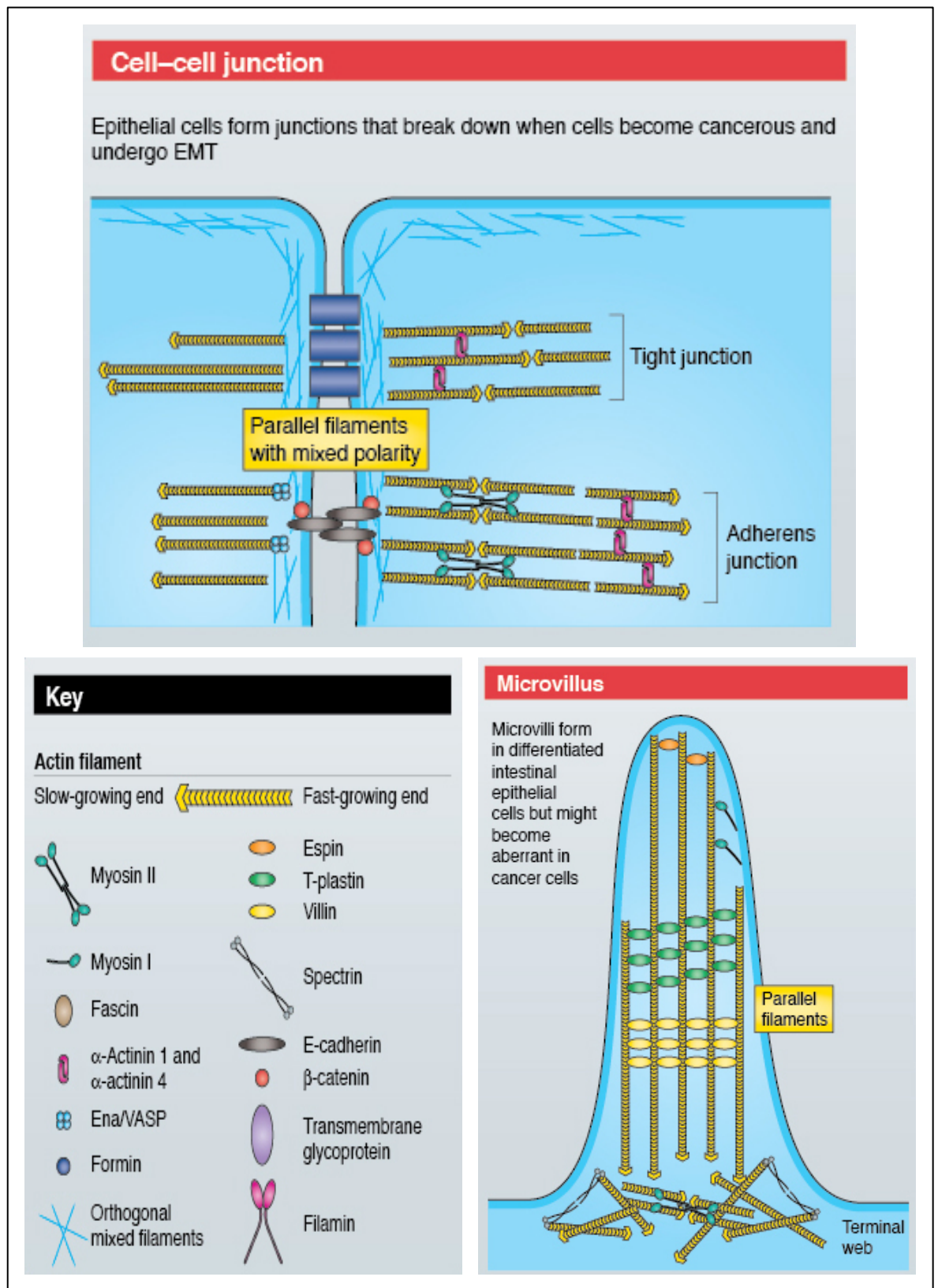


Figure 1-12 The roles of actin bundling proteins in cell:cell junctions and microvilli

Epithelial cells form junctions which break down when cells become cancerous and undergo EMT. Microvilli are finger-like projections of the plasma membrane that increase the surface area of cells to enhance absorption and secretion. Reproduced with permission (Stevenson, Veltman et al. 2012).

1.4.4 Actin bundle-containing structures in normal and cancer cells

1.4.4.1 Cell Cortex

Underneath the plasma membrane lies a meshwork of actin filaments and crosslinking proteins termed the cortex that links the cytoskeleton to the plasma membrane (Fig. 1.13). A strong cortical attachment to the plasma membrane promotes protrusive motility, which is often referred to as ‘mesenchymal’. In contrast, a weak attachment of the cytoskeleton to the cortex coupled with increased contractility promotes blebs, which are detachments between the cortex and membrane, leading to a different type of motility sometimes called “bleb-based” (Friedl and Wolf 2010). Modulation of cortical stiffness thus changes how cells move in different environments. The cortex also provides a scaffold for the organisation of transmembrane receptors and glycoproteins into networks for effective signal transduction and coupling of mechanical stresses to signals.

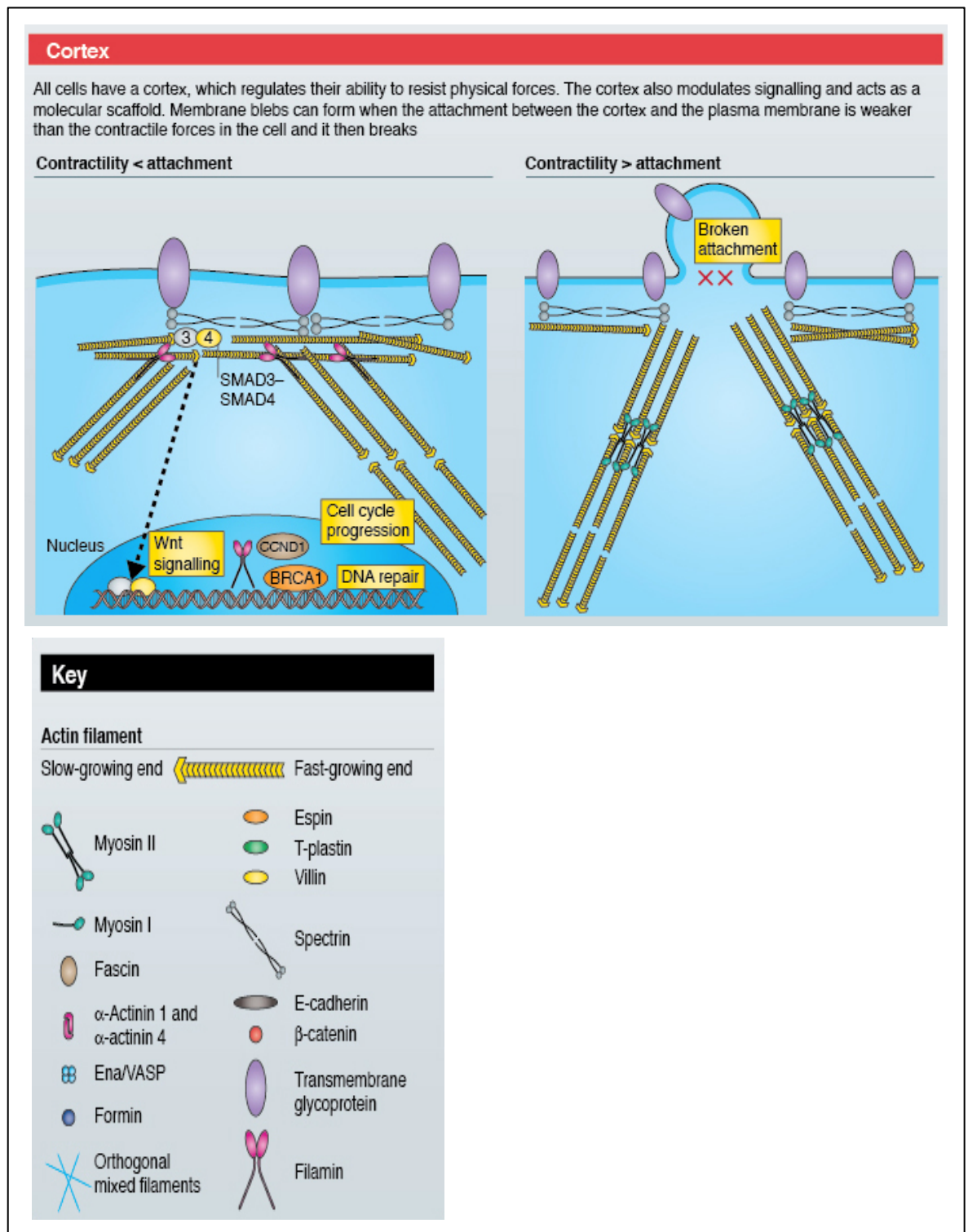


Figure 1-13 Actin bundling proteins and the cell cortex

The cell cortex regulates the ability of the cell to resist physical forces whilst also acting as a molecular scaffold and signal modulator. Reproduced with permission (Stevenson, Veltman et al. 2012).

Non-muscle myosin-IIa and -IIb are the main actin-based contractile myosin motors that crosslink actin filaments of the cell cortex and regulate cell stiffness. Phosphorylation of the myosin-II light chain triggers the contractile

activity of myosin-II and this increased contractility is associated with increased cancer cell invasion. When cells switch from a protrusive to a bleb-based motility, they increase their myosin-II activity and the added force is used for squeezing through tight spaces in the extracellular matrix (Friedl and Wolf 2010). Not only do tumour cells increase their own contractility sometimes, but they can also influence the contractile properties of stromal cells, such as fibroblasts (Wyckoff, Pinner et al. 2006; Gaggioli, Hooper et al. 2007; Sanz-Moreno, Gadea et al. 2008). Consequentially, as contractility increases, matrix stiffness also increases and this has tumour promoting properties (Samuel, Lopez et al. 2011). A stiff matrix can promote cancer cell growth through increased assembly of signalling platforms resulting from stronger contacts between integrins and the matrix, which leads to the activation of growth promoting signalling pathways such as via focal adhesion kinase (FAK) (Frame, Patel et al. 2010).

Spectrins are another class of important actin crosslinkers of the cell cortex and signalling scaffolds. In erythrocytes, they are crucial for the maintenance of integrity and shear forces in the blood, but non-erythroid spectrins have gained increased attention recently. In colorectal and pancreatic cancers, β 2-spectrin sequesters transcriptional activators and its loss inappropriately activates Wnt signalling and promotes tumourigenesis by releasing components of the transforming growth factor beta (TGFB) signalling pathway (i.e. Smad3 and Smad4) (Thenappan, Li et al. 2009; Jiang, Gillen et al. 2010). Embryonic spectrin (also called embryonic liver fodrin, ELF) shows altered expression in many cancer types (Table 1) and its loss causes deregulation of Cyclin D1 and aberrant cell cycle progression (Kitisin, Ganesan et al. 2007). Spectrin and the spectrin-like fodrin proteins are also important for the establishment or maintenance of cell polarity, so their role in cancer may be tumour or tissue type dependent.

1.4.4.2 Cell-cell contacts

Epithelia are held together by adherens junctions, which contain transmembrane cadherin receptors that interact extra-cellularly with the cadherins of neighbouring cells and intra-cellularly with the actin cytoskeleton (Schock and Perrimon 2002). Apical to adherens junctions are tight junctions, which regulate permeability of epithelia and maintain a separation between

luminal structures and the external space. Adherens junctions connect to the cell cortex and to actin filament bundles that are held in place by proteins, such as α -actinin and myosin-II. When epithelial cells become cancerous, adherens junctions break down, which releases β -catenin that then enters the nucleus to stimulate growth and also promote EMT via the canonical Wnt signalling pathway. Junctional breakdown also physically releases tumour cells, allowing them to escape from the primary tumour and migrate and invade the surrounding tissue (Fig. 1.11).

1.4.4.3 Microvilli

Microvilli are finger-like projections of the plasma membrane that increase the surface area of cells to enhance absorption and secretion. Small Intestinal brush-border microvilli contain a parallel actin bundle core made up of about 40 actin filaments of uniform polarity that are cross-linked by at least three different actin-bundling proteins: T-plastin (also named T-fimbrin), villin and small espin (Bartles, Zheng et al. 1998; Loomis, Zheng et al. 2003). T-plastin is a monomeric protein, specifically expressed at high levels in the small intestine, that crosslinks F-actin into straight bundles (Delanote, Vandekerckhove et al. 2005; Brown and McKnight 2010). T-plastin (Table 1) expression is enhanced in some cancer cell lines that are resistant to treatment with the chemotherapeutic drug cisplatin (Delanote, Vandekerckhove et al. 2005). Villin has a role in the bundling, nucleation, capping and severing of actin filaments in a Ca^{2+} dependent manner, and was found to be highly expressed in a multitude of adenocarcinomas originating from epithelial cells of the small intestinal tract that bear brush border microvilli (Grone, Weber et al. 1986; Moll, Robine et al. 1987; Suh, Yang et al. 2005). Small espin contributes to elongation of microvilli from the barbed end of the actin bundle, but has not yet been implicated in cancer. In malignant cells, an increased number of microvilli with irregular morphology correlate with metastatic status (Ren 1990; Ren 1991). This finding remains unexplained, but may in part reflect the increased metabolic activity of malignant cells and downstream effects on tumour growth (Zhang and Takenaka 1995). Microvilli disorganization may also occur as a result of partial loss of differentiation and polarity and lead to aberrant cytoskeletal assemblies that contribute to invasive capacity.

1.4.4.4 Filopodia

Filopodia are cytoplasmic spiky projections containing tight bundles of long actin filaments that sometimes originate within lamellipodia (Borisy and Svitkina 2000). Defined by their protrusive behaviour, they function in cell migration and contribute to cancer cell invasion at least *in-vitro* (Nurnberg, Kitzing et al. 2011), as well as in cell-to-cell communication and cell positioning within tissues (Mattila and Lappalainen 2008). Fascin is found in filopodia, but is normally expressed in mesenchymally and neurally derived cells rather than epithelia (Adams 2004a; Adams 2004b; Hashimoto, Kim et al. 2011). Upon transformation, fascin expression is often up-regulated, leading to increased cell motility and invasive potential (Machesky and Li 2010). Fascin forms parallel crosslinks between individual actin filaments located along the filopodial shaft and thus promotes filopodial protrusions (Fig. 1.11). Bundle formation strengthens filaments and increases the lifetime of both filopodia and invasive protrusions. Interestingly, fascin is highly expressed at the invasive front of tumours, at which the actively invading cells are located, and *in-vitro* reduction of fascin causes reduced motility and invasion (Hashimoto, Skacel et al. 2005; Hashimoto, Parsons et al. 2007; Li, Dawson et al. 2010; Schoumacher, Goldman et al. 2010).

1.4.4.5 Invadopodia and podosomes

Invadopodia are dynamic actin-rich membrane protrusions found only in invasive cancer cells (Weaver 2006). They contain a mixture of bundled and branched actin (Schoumacher, Goldman et al. 2010), but are uniquely able to degrade the extracellular matrix (ECM) through proteolysis of its constituents, such as fibronectin, laminin and collagen. Podosomes are similar structures also found in hematopoietic cells, endothelial cells and src-transformed fibroblasts (Murphy and Courtneidge 2011). Matrix degradation by podosomes and invadopodia is achieved through the secretion and membrane presentation of proteases such as the matrix metalloproteinases (MMPs), which are regulated by nitric oxide (increasing their activity) and by tissue inhibitor of matrix metalloproteinases (TIMPs) (inhibitory). The ability to migrate through the ECM is fundamental for the ability of cancer cells to invade adjacent tissues and subsequently metastasise to distant sites within the body. Invadopodia contain a number of actin bundling proteins, including fascin, which stabilises them and increases

their lifetime (Li, Dawson et al. 2010; Schoumacher, Goldman et al. 2010), α -actinin, formin and Ena/VASP proteins (Fig. 1.11).

Table 1-1 Clinical correlation between actin bundling proteins and cancer

Protein	Structures and cells	Function	Role in cancer	References
T-plastin/ T-fimbrin	Microvilli of epithelial & mesenchymal cells	Crosslinks F-actin into straight bundles	T-plastin expression is enhanced in cisplatin-resistant human cancer cell lines	(Hisano, Ono et al. 1996)
L-plastin/ L-Fimbrin	Microvilli of haematopoietic cells and malignant human cells of non-haematopoietic origin ¹	Crosslinks F-actin into straight bundles	68% of epithelial carcinomas investigated and 53% of non-epithelial mesenchymal tumours examined expressed L-plastin. L-plastin expression correlates positively with colorectal cancer stage and severity.	(Delanote, Vandekerckhove et al. 2005; Foran, McWilliam et al. 2006; Yuan, Zhao et al. 2010)
Villin	Epithelial cells of the gastrointestinal tract that possess brush border microvilli	Crosslinks filaments in low Ca ²⁺ and severs filaments at high Ca ²⁺	Expression altered in Barrett's esophagus, bladder cancer, colorectal and small intestinal cancer.	(Younes, Harris et al. 1989; Sampson, Yeh et al. 2001; Zhang, Lin et al. 2007; Shi, Bhagwandeem et al. 2008)
Fascin	Neurons, dendritic cells, endothelial cells and cancer cells. Mainly in filopodia and invadopodia, but also at cell-cell contacts.	Crosslinks actin into parallel bundles. Thought to be a monomer with two actin binding sites.	Significant independent prognostic indicator of poor outcome in cancers of the liver, ovary, lung, pancreas, colon, head & neck squamous cell carcinoma and brain.	Reviewed in (Machesky and Li 2010)
Alpha-actinin-1 and -4	Cellular protrusions, stress fibres, lamellipodia microvilli, invadopodia of multiple cell types.	Crosslinks actin into parallel bundles by forming dimers head-to-tail	Expression in breast, ovary, pancreas, lung, astrocytoma cancers. Associated with poor prognosis and tumour chemoresistance (ovary)	(Honda, Yamada et al. 2004; Menez, Le Maux Chansac et al. 2004; Honda, Yamada et al. 2005; Fu, Qin et al. 2007; Yamamoto, Tsuda et al. 2007; Kikuchi, Honda et al. 2008; Welsch, Keleg et al. 2009; Yamamoto, Tsuda et al. 2009; Hirooka, Akashi et al. 2011)
Myosin-I	Microvilli of small intestinal epithelial cells and cortex of many cell types.	Motor protein that connects membranes and actin and mediates transport of intracellular cargo vesicles as well as attaching actin filaments in microvilli to the plasma membrane.	No clinical studies	n/a
Myosin-II	Microvilli terminal web of small intestinal epithelia and stress fibres of multiple cell types.	Actin-based motor that also bundles actin. Generates/maintains cortical tension, assembly of contractile structures. Cell body translocation and retraction of the posterior of the cell during migration.	Interacts with S100A4 (also known as metastasin), which is heavily associated with cancer invasion and metastasis. Significant positive correlation between expression levels of myosin light chain kinase (which activates myosin II) and likelihood of non-small cell lung cancer recurrence and metastasis.	(Minamiya, Nakagawa et al. 2005) (Oslejskova, Grigorian et al. 2008)
Myosin-X	Localises to filopodia in multiple cell types.	Unconventional myosin motor – transports cargo to filopodial tip	No clinical studies.	n/a
Spectrin (Fodrin)	Microvilli and terminal web of small intestinal epithelial cells and cell cortex of many cell types.	Crosslinks actin into orthogonal networks by forming tetramers. Forms a scaffold for signalling complexes	Reduced expression of spectrin associated with poor prognosis in pancreatic cancer and progression in	(Jiang, Gillen et al. ; Younes, Harris et al. 1989; Simpson and Page 1992; Sormunen, Paakko et al. 1994;

		and keeps Smad3/4 inhibited. Possible tumour suppressor and regulates cell polarity. Has also been proposed to be a differentiation marker in colonic neoplasia.	hepatocellular cancer. Spectrin contributes to platinum chemotherapy resistance.	Tuominen, Sormunen et al. 1996; Sormunen, Leong et al. 1999; Kitisin, Ganesan et al. 2007; Thenappan, Li et al. 2009; Baek, Pishvaian et al. 2011; Maeda, Shibata et al. 2011)
Filamin-A	Cell cortex, filopodia of many cell types.	Crosslinks into orthogonal gels	Prostate cancer metastasis correlates with low nuclear and high cytoplasmic filamin-A. Aberrant association of filamin-A with the prion protein PrPA correlates with worse prognosis in pancreatic cancer. A secreted variant of filamin-A in the blood correlates with high grade astrocytomas and metastatic breast cancer.	(Anilkumar, Rajasekaran et al. 2003; Loy, Sim et al. 2003; Smith, Oxford et al. 2007; Kwon, Hanna et al. 2008; Alper, Stetler-Stevenson et al. 2009; Bedolla, Wang et al. 2009; Li, Yu et al. 2009; Burton, Gaffar et al. 2010; Li, Xin et al. 2010; Li, Yu et al. 2010; Sy, Li et al. 2010; Uramoto, Akyurek et al. 2010; Ai, Huang et al. 2011; Castoria, D'Amato et al. 2011; Zhou, Toyly et al. 2011)
Mena	Filopodia of many cell types and invadopodia of cancer cells.	Related to VASP tetramerizes and bundles actin filaments while promoting elongation. Occurs in several splice forms and some (i.e. Mena(INV) and Mena1a) increase cellular invasion.	Mena is overexpressed in breast cancers that show anti-tumour immune response. Expressed in colorectal polyps with high dysplasia and in 80% of colorectal lesions (n=36).	(Di Modugno, Bronzi et al. 2004; Gurzu, Jung et al. 2008)
Eplin	Stress fibres of multiple cell types.	Actin filament bundling and side-binding	Eplin downregulation correlates with progression and metastasis in prostate cancer and eplin may be anti-angiogenic. Potential tumour suppressor in breast cancer.	(Jiang, Martin et al. 2008; Sanders, Ye et al. 2010; Zhang, Wang et al. 2010; Sanders, Martin et al. 2011)
Lim domain proteins LMO2, LMO4, LMO7	Found in stress fibres, focal adhesions and cell-cell junctions of multiple cell types. Nuclear transcription co-factor.	May sequester transcription machinery and nuclear proteins in the cytoplasm. May regulate communication between the nucleus and cytoplasm/cytoskeleton.	Correlated in multiple studies with cancer either as predictors of poor or better prognosis.	(Visvader, Venter et al. 2001; Mizunuma, Miyazawa et al. 2003; Wang, Kudryavtseva et al. 2004; Sum, Segara et al. 2005a; Sum, Shackleton et al. 2005b; Ma, Guan et al. 2007; Wang, Lin et al. 2007; Yu, Ohuchida et al. 2008; Nakata, Ohuchida et al. 2009; Krcmery, Camarata et al. 2010; Kwong, Scarlett et al. 2010)7(Hu, Guo et al. 2011)
Formins	Stress fibres and filopodia of multiple cell types.	Actin nucleation and parallel bundling. Also interacts with microtubules.	Downregulation of formin-like 2 correlates with a poor prognosis in hepatocellular carcinoma. Higher expression correlates with tumour differentiation.	(Liang, Guan et al. 2010)
Supervillin	Stress fibres and focal adhesions of multiple cell types. Implicated in nuclear architecture.	Actin bundling into parallel bundles.	Androgen receptor co-regulator that may be important in androgen dependent prostate cancer.	(Wulfskuhle, Donina et al. 1999; Sampson, Yeh et al. 2001)

1.4.5 Concluding remarks and future perspectives

As we find out more about how tumours evolve, we are also humbled by the staggering complexity of cancer and of the body. The actin cytoskeleton represents a major network of proteins that impinge on motility, invasion, polarity, survival and growth of normal cells, and as such is often subverted by tumour cells. We are just starting to understand how tumours manipulate the cytoskeleton to gain advantage and to uncover those key proteins that may be future targets against invasion and metastasis. It seems unlikely that one particular actin-binding protein will ever rise above the rest as the most important target in metastasis, but rather, like signal transduction networks, we will find those hub proteins or key pathways that can promote tumour progression and develop therapies aimed at those. Actin bundling represents perhaps one of those hubs, but we still need to understand the contributions of mechanical regulation of cell stiffness, transcriptional control and maintenance of the cells ability to contact its neighbours and the matrix, before we are able to exploit it for therapeutic benefits.

1.5 Thesis aims

Actin bundling proteins are crucial in regulating the actin cytoskeleton, but are increasingly thought to be involved in molecular signalling and mechanisms involving cellular proliferation and differentiation. Fascin in particular, has recently been shown to have an as yet undetermined role in IBD. Fascin is also known to be expressed in tumours arising from the gastro-intestinal tract and, given the established link between inflammation and cancer, we hypothesised that fascin has a multi-faceted role in the immune response to inflammation, intestinal regeneration and promotion of tumourigenesis. We set out to achieve this with the following aims:

- 1) To investigate the potential role of fascin in small intestinal and colonic epithelial regeneration.

- 2) To investigate the potential immunological role of fascin in response to small intestinal and colonic inflammation.
- 3) To investigate the potential role of fascin in the transformation from benign to malignant disease in murine models of IBD.
- 4) To investigate the potential role of fascin in sporadic murine models of tumourigenesis arising from the small intestine and colon.

References

- Adams, J. C. (2004)a. "Fascin protrusions in cell interactions." Trends Cardiovasc Med **14**(6): 221-226.
- Adams, J. C. (2004)b. "Roles of fascin in cell adhesion and motility." Curr Opin Cell Biol **16**(5): 590-596.
- Ai, J., H. Huang, et al. (2011). "FLNA and PGK1 are two potential markers for progression in hepatocellular carcinoma." Cell Physiol Biochem **27**(3-4): 207-216.
- Alper, O., W. G. Stetler-Stevenson, et al. (2009). "Novel anti-filamin-A antibody detects a secreted variant of filamin-A in plasma from patients with breast carcinoma and high-grade astrocytoma." Cancer Sci **100**(9): 1748-1756.
- Anilkumar, G., S. A. Rajasekaran, et al. (2003). "Prostate-specific membrane antigen association with filamin A modulates its internalization and NAALADase activity." Cancer Res **63**(10): 2645-2648.
- Ardizzone, S. and G. B. Porro (2002). "Inflammatory bowel disease: new insights into pathogenesis and treatment." Journal of Internal Medicine **252**(6): 475-496.
- Baek, H. J., M. J. Pishvaian, et al. (2011). "Transforming growth factor-beta adaptor, beta2-spectrin, modulates cyclin dependent kinase 4 to reduce development of hepatocellular cancer." Hepatology **53**(5): 1676-1684.
- Balkwill, F. and A. Mantovani (2001). "Inflammation and cancer: back to Virchow?" Lancet **357**(9255): 539-545.
- Banchereau, J., F. Briere, et al. (2000). "Immunobiology of dendritic cells." Annu Rev Immunol **18**: 767-+.
- Barker, N., R. A. Ridgway, et al. (2009). "Crypt stem cells as the cells-of-origin of intestinal cancer." Nature **457**(7229): 608-U119.
- Barker, N., J. H. van Es, et al. (2007). "Identification of stem cells in small intestine and colon by marker gene Lgr5." Nature **449**(7165): 1003-U1001.
- Bartles, J. R., L. Zheng, et al. (1998). "Small espin: a third actin-bundling protein and potential forked protein ortholog in brush border microvilli." J Cell Biol **143**(1): 107-119.
- Baumgart, D. C. and S. R. Carding (2007). "Inflammatory bowel disease: cause and immunobiology." Lancet **369**(9573): 1627-1640.
- Bedolla, R. G., Y. Wang, et al. (2009). "Nuclear versus cytoplasmic localization of filamin A in prostate cancer: immunohistochemical correlation with metastases." Clin Cancer Res **15**(3): 788-796.

- Bevins, C. L. and N. H. Salzman (2011). "Paneth cells, antimicrobial peptides and maintenance of intestinal homeostasis." *Nat Rev Microbiol* **9**(5): 356-368.
- Bjerknes, M. and H. Cheng (2006). "Intestinal epithelial stem cells and progenitors." *Adult Stem Cells* **419**: 337-383.
- Blanpain, C. and B. D. Simons (2013). "Unravelling stem cell dynamics by lineage tracing." *Nature Reviews Molecular Cell Biology* **14**(8): 489-502.
- Bockcamp, E., R. Sprengel et al. (2008). "Conditional transgenic mouse models: from the basics to genome-wide sets of knockouts and current studies of tissue regeneration." *Regen Med* **3**(2), 217-235
- Bollrath, J. and F. R. Greten (2009). "IKK/NF-kappaB and STAT3 pathways: central signalling hubs in inflammation-mediated tumour promotion and metastasis." *EMBO Rep* **10**(12): 1314-1319.
- Borisy, G. G. and T. M. Svitkina (2000). "Actin machinery: pushing the envelope." *Curr Opin Cell Biol* **12**(1): 104-112.
- Braat, H., M. P. Peppelenbosch, et al. (2006). "Immunology of Crohn's disease." *Ann N Y Acad Sci* **1072**: 135-154.
- Brown, J. W. and C. J. McKnight (2010). "Molecular model of the microvillar cytoskeleton and organization of the brush border." *PLoS One* **5**(2): e9406.
- Broz, D. K. and L. D. Attardi (2010). "In vivo analysis of p53 tumor suppressor function using genetically engineered mouse models." *Carcinogenesis* **31**(8): 1311-1318.
- Burton, E. R., A. Gaffar, et al. (2010). "Downregulation of Filamin A Interacting Protein 1-Like is Associated with Promoter Methylation and Induces an Invasive Phenotype in Ovarian Cancer." *Mol Cancer Res*.
- Cairns, S. R., J. H. Scholefield, et al. (2010). "Guidelines for colorectal cancer screening and surveillance in moderate and high risk groups (update from 2002)." *Gut* **59**(5): 666-689.
- Castoria, G., L. D'Amato, et al. (2011). "Androgen-induced cell migration: role of androgen receptor/filamin A association." *PLoS One* **6**(2): e17218.
- Chen, L., S. Yang, et al. (2010). "Migrastatin analogues target fascin to block tumour metastasis." *Nature* **464**(7291): 1062-1066.
- Cheng, H. and C. P. Leblond (1974). "Origin, differentiation and renewal of the four main epithelial cell types in the mouse small intestine. V. Unitarian Theory of the origin of the four epithelial cell types." *Am J Anat* **141**(4): 537-561.
- Clayburgh, D. R., L. Shen, et al. (2004). "A porous defense: the leaky epithelial barrier in intestinal disease." *Lab Invest* **84**(3): 282-291.
- Colotta, F., P. Allavena, et al. (2009). "Cancer-related inflammation, the seventh hallmark of cancer: links to genetic instability." *Carcinogenesis* **30**(7): 1073-1081.
- Cooke, M. S., M. D. Evans, et al. (2003). "Oxidative DNA damage: mechanisms, mutation, and disease." *Faseb Journal* **17**(10): 1195-1214.
- Coussens, L. M., W. W. Raymond, et al. (1999). "Inflammatory mast cells up-regulate angiogenesis during squamous epithelial carcinogenesis." *Genes & Development* **13**(11): 1382-1397.
- Coussens, L. M. and Z. Werb (2002). "Inflammation and cancer." *Nature* **420**(6917): 860-867.
- Crohn, B. B., L. Ginzburg, et al. (2000). "Regional ileitis: a pathologic and clinical entity. 1932." *Mount Sinai Journal of Medicine* **67**(3): 263-268.
- Crosnier, C., D. Stamataki, et al. (2006). "Organizing cell renewal in the intestine: stem cells, signals and combinatorial control." *Nature Reviews Genetics* **7**(5): 349-359.

- Cunliffe, R. N., F. R. A. J. Rose, et al. (2001). "Human defensin 5 is stored in precursor form in normal Paneth cells and is expressed by some villous epithelial cells and by metaplastic Paneth cells in the colon in inflammatory bowel disease." *Gut* **48**(2): 176-185.
- De Robertis, M., E. Massi, et al. (2011). "The AOM/DSS murine model for the study of colon carcinogenesis: From pathways to diagnosis and therapy studies." *J Carcinog* **10**: 9.
- Delanote, V., J. Vandekerckhove, et al. (2005). "Plastins: versatile modulators of actin organization in (patho)physiological cellular processes." *Acta Pharmacol Sin* **26**(7): 769-779.
- Di Modugno, F., G. Bronzi, et al. (2004). "Human Mena protein, a serex-defined antigen overexpressed in breast cancer eliciting both humoral and CD8+ T-cell immune response." *Int J Cancer* **109**(6): 909-918.
- Dominguez, R. (2009). "Actin filament nucleation and elongation factors--structure-function relationships." *Crit Rev Biochem Mol Biol* **44**(6): 351-366.
- Elson, C. O., R. B. Sartor, et al. (1995). "Experimental-Models of Inflammatory Bowel-Disease." *Gastroenterology* **109**(4): 1344-1367.
- Erichsen, K., A. M. Milde, et al. (2005). "Low-dose oral ferrous fumarate aggravated intestinal inflammation in rats with DSS-induced colitis." *Inflamm Bowel Dis* **11**(8): 744-748.
- Fan, Y. H., R. F. Mao, et al. (2013). "NF-kappa B and STAT3 signaling pathways collaboratively link inflammation to cancer." *Protein & Cell* **4**(3): 176-185.
- Feakins, R. M. (2013). "Inflammatory bowel disease biopsies: updated British Society of Gastroenterology reporting guidelines." *J Clin Pathol*.
- Fitzgerald, D. C., K. G. Meade, et al. (2007). "Tumour necrosis factor-alpha (TNF-alpha) increases nuclear factor kappaB (NFkappaB) activity in and interleukin-8 (IL-8) release from bovine mammary epithelial cells." *Vet Immunol Immunopathol* **116**(1-2): 59-68.
- Fodde, R. and T. Brabletz (2007). "Wnt/beta-catenin signaling in cancer stemness and malignant behavior." *Curr Opin Cell Biol* **19**(2): 150-158.
- Foran, E., P. McWilliam, et al. (2006). "The leukocyte protein L-plastin induces proliferation, invasion and loss of E-cadherin expression in colon cancer cells." *Int J Cancer* **118**(8): 2098-2104.
- Frame, M. C., H. Patel, et al. (2010). "The FERM domain: organizing the structure and function of FAK." *Nat Rev Mol Cell Biol* **11**(11): 802-814.
- Friedl, P. and K. Wolf (2010). "Plasticity of cell migration: a multiscale tuning model." *J Cell Biol* **188**(1): 11-19.
- Fu, L., Y. R. Qin, et al. (2007). "Identification of alpha-actinin 4 and 67 kDa laminin receptor as stage-specific markers in esophageal cancer via proteomic approaches." *Cancer* **110**(12): 2672-2681.
- Gaggioli, C., S. Hooper, et al. (2007). "Fibroblast-led collective invasion of carcinoma cells with differing roles for RhoGTPases in leading and following cells." *Nat Cell Biol* **9**(12): 1392-1400.
- Gao, X. and D. H. Wu (2008). "[Fascin expression in human epithelial tumors and its clinical significance]." *Nan Fang Yi Ke Da Xue Xue Bao* **28**(6): 953-955.
- Ghosh, S., M. J. May, et al. (1998). "NF-kappa B and Rel proteins: evolutionarily conserved mediators of immune responses." *Annu Rev Immunol* **16**: 225-260.
- Gordon, J. W., G. A. Scangos, et al. (1980). "Genetic transformation of mouse embryos by microinjection of purified DNA." *Proc Natl Acad Sci U S A* **77**(12): 7380-7384.

- Gregorieff, A. and H. Clevers (2005). "Wnt signaling in the intestinal epithelium: from endoderm to cancer." Genes & Development **19**(8): 877-890.
- Grone, H. J., K. Weber, et al. (1986). "Villin--a marker of brush border differentiation and cellular origin in human renal cell carcinoma." Am J Pathol **124**(2): 294-302.
- Gurzu, S., I. Jung, et al. (2008). "The expression of cytoskeleton regulatory protein Mena in colorectal lesions." Rom J Morphol Embryol **49**(3): 345-349.
- Hanahan, D. and R. A. Weinberg (2011). "Hallmarks of cancer: the next generation." Cell **144**(5): 646-674.
- Hashimoto, Y., D. J. Kim, et al. (2011). "The roles of fascins in health and disease." J Pathol **224**(3): 289-300.
- Hashimoto, Y., D. W. Loftis, et al. (2009). "Fascin-1 Promoter Activity Is Regulated by CREB and the Aryl Hydrocarbon Receptor in Human Carcinoma Cells." Plos One **4**(4).
- Hashimoto, Y., M. Parsons, et al. (2007). "Dual actin-bundling and protein kinase C-binding activities of fascin regulate carcinoma cell migration downstream of Rac and contribute to metastasis." Mol Biol Cell **18**(11): 4591-4602.
- Hashimoto, Y., M. Skacel, et al. (2005). "Roles of fascin in human carcinoma motility and signaling: Prospects for a novel biomarker?" International Journal of Biochemistry & Cell Biology **37**(9): 1787-1804.
- Hashimoto, Y., M. Skacel, et al. (2006). "Prognostic significance of fascin expression in advanced colorectal cancer: an immunohistochemical study of colorectal adenomas and adenocarcinomas." Bmc Cancer **6**: 241.
- Heath, J. P. (1996). "Epithelial cell migration in the intestine." Cell Biology International **20**(2): 139-146.
- Hirooka, S., T. Akashi, et al. (2011). "Localization of the invadopodia-related proteins actinin-1 and cortactin to matrix-contact-side cytoplasm of cancer cells in surgically resected lung adenocarcinomas." Pathobiology **78**(1): 10-23.
- Hisano, T., M. Ono, et al. (1996). "Increased expression of T-plastin gene in cisplatin-resistant human cancer cells: identification by mRNA differential display." FEBS Lett **397**(1): 101-107.
- Honda, K., T. Yamada, et al. (2005). "Actinin-4 increases cell motility and promotes lymph node metastasis of colorectal cancer." Gastroenterology **128**(1): 51-62.
- Honda, K., T. Yamada, et al. (2004). "Alternative splice variant of actinin-4 in small cell lung cancer." Oncogene **23**(30): 5257-5262.
- Hu, Q., C. Guo, et al. (2011). "LMO7 Mediates Cell-Specific Activation of the Rho-Myocardin-Related Transcription Factor-Serum Response Factor Pathway and Plays an Important Role in Breast Cancer Cell Migration." Mol Cell Biol **31**(16): 3223-3240.
- Ireland, H., R. Kemp, et al. (2004). "Inducible Cre-mediated control of gene expression in the murine gastrointestinal tract: Effect of loss of beta-catenin." Gastroenterology **126**(5): 1236-1246.
- Itzkowitz, S. H. and X. Yio (2004). "Inflammation and cancer IV. Colorectal cancer in inflammatory bowel disease: the role of inflammation." Am J Physiol Gastrointest Liver Physiol **287**(1): G7-17.
- Jiang, W. G., T. A. Martin, et al. (2008). "Epln-alpha expression in human breast cancer, the impact on cellular migration and clinical outcome." Mol Cancer **7**: 71.

- Jiang, X., S. Gillen, et al. (2010). "Reduced expression of the membrane skeleton protein beta1-spectrin (SPTBN1) is associated with worsened prognosis in pancreatic cancer." *Histol Histopathol* **25**(12): 1497-1506.
- Karin, M. (1999). "How NF-kappaB is activated: the role of the I-kappaB kinase (IKK) complex." *Oncogene* **18**(49): 6867-6874.
- Kikuchi, S., K. Honda, et al. (2008). "Expression and gene amplification of actinin-4 in invasive ductal carcinoma of the pancreas." *Clin Cancer Res* **14**(17): 5348-5356.
- Kinzler, K. W. and B. Vogelstein (1996). "Lessons from hereditary colorectal cancer." *Cell* **87**(2): 159-170.
- Kirsner, J. B. (1988). "Historical aspects of inflammatory bowel disease." *J Clin Gastroenterol* **10**(3): 286-297.
- Kitisin, K., N. Ganesan, et al. (2007). "Disruption of transforming growth factor-beta signaling through beta-spectrin ELF leads to hepatocellular cancer through cyclin D1 activation." *Oncogene* **26**(50): 7103-7110.
- Krause, W. J., J. Yamada, et al. (1985). "Quantitative Distribution of Enteroendocrine Cells in the Gastrointestinal-Tract of the Adult Opossum, *Didelphis-Virginiana*." *Journal of Anatomy* **140**(Jun): 591-605.
- Krcmery, J., T. Camarata, et al. (2010). "Nucleocytoplasmic functions of the PDZ-LIM protein family: new insights into organ development." *Bioessays* **32**(2): 100-108.
- Kress, A. K., M. Kalmer, et al. (2011). "The tumor marker Fascin is strongly induced by the Tax oncoprotein of HTLV-1 through NF-kappa B signals." *Blood* **117**(13): 3609-3612.
- Kureishy, N., V. Sapountzi, et al. (2002). "Fascin, and their roles in cell structure and function." *BioEssays* **24**(4): 350-361.
- Kwon, M., E. Hanna, et al. (2008). "Functional characterization of filamin a interacting protein 1-like, a novel candidate for antivascular cancer therapy." *Cancer Res* **68**(18): 7332-7341.
- Kwong, R. A., C. J. Scarlett, et al. (2010). "LMO4 expression in squamous cell carcinoma of the anterior tongue." *Histopathology* **58**(3): 477-480.
- Laroui, H., S. A. Ingersoll, et al. (2012). "Dextran Sodium Sulfate (DSS) Induces Colitis in Mice by Forming Nano-Lipocomplexes with Medium-Chain-Length Fatty Acids in the Colon." *Plos One* **7**(3).
- Li, A., J. C. Dawson, et al. (2010). "The actin-bundling protein fascin stabilizes actin in invadopodia and potentiates protrusive invasion." *Curr Biol* **20**(4): 339-345.
- Li, C., W. Xin, et al. (2010). "Binding of pro-prion to filamin A: by design or an unfortunate blunder." *Oncogene* **29**(39): 5329-5345.
- Li, C., S. Yu, et al. (2010). "Pro-prion binds filamin A, facilitating its interaction with integrin beta1, and contributes to melanomagenesis." *J Biol Chem* **285**(39): 30328-30339.
- Li, C., S. Yu, et al. (2009). "Binding of pro-prion to filamin A disrupts cytoskeleton and correlates with poor prognosis in pancreatic cancer." *J Clin Invest* **119**(9): 2725-2736.
- Liang, L., J. Guan, et al. (2010). "Down-regulation of formin-like 2 predicts poor prognosis in hepatocellular carcinoma." *Hum Pathol*.
- Lichtenstein, G. R., S. B. Hanauer, et al. (2009). "Management of Crohn's disease in adults." *Am J Gastroenterol* **104**(2): 465-483; quiz 464, 484.
- Liu, W., X. Dong, et al. (2000). "Mutations in AXIN2 cause colorectal cancer with defective mismatch repair by activating beta-catenin/TCF signalling." *Nature Genetics* **26**(2): 146-147.

- Locksley, R. M., N. Killeen, et al. (2001). "The TNF and TNF receptor superfamilies: integrating mammalian biology." Cell **104**(4): 487-501.
- Loomis, P. A., L. Zheng, et al. (2003). "Espin cross-links cause the elongation of microvillus-type parallel actin bundles in vivo." The Journal of cell biology **163**(5): 1045-1055.
- Loy, C. J., K. S. Sim, et al. (2003). "Filamin-A fragment localizes to the nucleus to regulate androgen receptor and coactivator functions." Proc Natl Acad Sci U S A **100**(8): 4562-4567.
- Lukas, M., M. Bortlik, et al. (2006). "What is the origin of ulcerative colitis? Still more questions than answers." Postgrad Med J **82**(972): 620-625.
- Ma, S., X. Y. Guan, et al. (2007). "The significance of LMO2 expression in the progression of prostate cancer." J Pathol **211**(3): 278-285.
- Machesky, L. M. and A. Li (2010). "Fascin: Invasive filopodia promoting metastasis." Commun Integr Biol **3**(3): 263-270.
- Maeda, O., K. Shibata, et al. (2011). "Spectrin alphall and betall tetramers contribute to platinum anticancer drug resistance in ovarian serous adenocarcinoma." Int J Cancer.
- Martin, K., C. S. Potten, et al. (1998). "Altered stem cell regeneration in irradiated intestinal crypts of senescent mice." Journal of Cell Science **111 (Pt 16)**: 2297-2303.
- Mattila, P. K. and P. Lappalainen (2008). "Filopodia: molecular architecture and cellular functions." Nat Rev Mol Cell Biol **9**(6): 446-454.
- McDonald, S. A. C., S. L. Preston, et al. (2006). "Mechanisms of disease: from stem cells to colorectal cancer." Nature Clinical Practice Gastroenterology & Hepatology **3**(5): 267-274.
- McDonald, T., R. P. Wang, et al. (1998). "Identification and cloning of an orphan G protein-coupled receptor of the glycoprotein hormone receptor subfamily." Biochemical and Biophysical Research Communications **247**(2): 266-270.
- Menez, J., B. Le Maux Chansac, et al. (2004). "Mutant alpha-actinin-4 promotes tumorigenicity and regulates cell motility of a human lung carcinoma." Oncogene **23**(15): 2630-2639.
- Minamiya, Y., T. Nakagawa, et al. (2005). "Increased expression of myosin light chain kinase mRNA is related to metastasis in non-small cell lung cancer." Tumour Biol **26**(3): 153-157.
- Mizunuma, H., J. Miyazawa, et al. (2003). "The LIM-only protein, LMO4, and the LIM domain-binding protein, LDB1, expression in squamous cell carcinomas of the oral cavity." Br J Cancer **88**(10): 1543-1548.
- Moll, R., S. Robine, et al. (1987). "Villin: a cytoskeletal protein and a differentiation marker expressed in some human adenocarcinomas." Virchows Arch B Cell Pathol Incl Mol Pathol **54**(3): 155-169.
- Morin, P. J., A. B. Sparks, et al. (1997). "Activation of beta-catenin-Tcf signaling in colon cancer by mutations in beta-catenin or APC." Science **275**(5307): 1787-1790.
- Moser, A. R., H. C. Pitot, et al. (1990). "A Dominant Mutation That Predisposes to Multiple Intestinal Neoplasia in the Mouse." Science **247**(4940): 322-324.
- Munkholm, P., E. V. Loftus, Jr., et al. (2006). "Prevention of colorectal cancer in inflammatory bowel disease: value of screening and 5-aminosalicylates." Digestion **73**(1): 11-19.
- Munoz, J., D. E. Stange, et al. (2012). "The Lgr5 intestinal stem cell signature: robust expression of proposed quiescent '+4' cell markers." Embo Journal **31**(14): 3079-3091.

- Murphy, D. A. and S. A. Courtneidge (2011). "The 'ins' and 'outs' of podosomes and invadopodia: characteristics, formation and function." Nat Rev Mol Cell Biol **12**(7): 413-426.
- Nakata, K., K. Ohuchida, et al. (2009). "LMO2 is a novel predictive marker for a better prognosis in pancreatic cancer." Neoplasia **11**(7): 712-719.
- Narumiya, S., M. Tanji, et al. (2009). "Rho signaling, ROCK and mDia1, in transformation, metastasis and invasion." Cancer Metastasis Rev **28**(1-2): 65-76.
- Nurnberg, A., T. Kitzing, et al. (2011). "Nucleating actin for invasion." Nat Rev Cancer **11**(3): 177-187.
- Oberreuther-Moschner, D. L., G. Rechkemmer, et al. (2005). "Basal colon crypt cells are more sensitive than surface cells toward hydrogen peroxide, a factor of oxidative stress." Toxicology Letters **159**(3): 212-218.
- Ohtsuka, Y. and I. R. Sanderson (2003). "Dextran sulfate sodium-induced inflammation is enhanced by intestinal epithelial cell chemokine expression in mice." Pediatric Research **53**(1): 143-147.
- Okamoto, R. and M. Watanabe (2005). "Cellular and molecular mechanisms of the epithelial repair in IBD." Dig Dis Sci **50** Suppl 1: S34-38.
- Okayasu, I., S. Hatakeyama, et al. (1990). "A Novel Method in the Induction of Reliable Experimental Acute and Chronic Ulcerative-Colitis in Mice." Gastroenterology **98**(3): 694-702.
- Olive, K. P., D. A. Tuveson, et al. (2004). "Mutant p53 gain of function in two mouse models of Li-Fraumeni syndrome." Cell **119**(6): 847-860.
- Olszewski, M. B., A. J. Groot, et al. (2007). "TNF trafficking to human mast cell granules: mature chain-dependent endocytosis." J Immunol **178**(9): 5701-5709.
- Ono, S., Y. Yamakita, et al. (1997). "Identification of an Actin Binding Region and a Protein Kinase C Phosphorylation Site on Human Fascin." Journal of Biological Chemistry **272**(4): 2527-2533.
- Oslejskova, L., M. Grigorian, et al. (2008). "The metastasis associated protein S100A4: a potential novel link to inflammation and consequent aggressive behaviour of rheumatoid arthritis synovial fibroblasts." Ann Rheum Dis **67**(11): 1499-1504.
- Ostanin, D. V., J. X. Bao, et al. (2009). "T cell transfer model of chronic colitis: concepts, considerations, and tricks of the trade." American Journal of Physiology-Gastrointestinal and Liver Physiology **296**(2): G135-G146.
- Ottewell, P. D., C. A. Duckworth, et al. (2006). "Gastrin increases murine intestinal crypt regeneration following injury." Gastroenterology **130**(4): 1169-1180.
- Otto, J. J., R. E. Kane, et al. (1979). "Formation of filopodia in coelomocytes: localization of fascin, a 58,000 dalton actin cross-linking protein." Cell **17**(2): 285-293.
- Parsons, M. and J. C. Adams (2008). "Rac regulates the interaction of fascin with protein kinase C in cell migration." J Cell Sci **121**(17): 2805-2813.
- Podolsky, D. K. (1997). "Lessons from genetic models of inflammatory bowel disease." Acta Gastro-Enterologica Belgica **60**(2): 163-165.
- Potten, C. S. (1995). "Interleukin-11 Protects the Clonogenic Stem-Cells in Murine Small-Intestinal Crypts from Impairment of Their Reproductive Capacity by Radiation." International Journal of Cancer **62**(3): 356-361.
- Potten, C. S., J. A. O'Shea, et al. (2001). "The effects of repeated doses of keratinocyte growth factor on cell proliferation in the cellular hierarchy

- of the crypts of the murine small intestine." Cell Growth & Differentiation **12**(5): 265-275.
- Powell, S. M., N. Zilz, et al. (1992). "Apc Mutations Occur Early during Colorectal Tumorigenesis." Nature **359**(6392): 235-237.
- Qualtrough, D., K. Singh, et al. (2009). "The actin-bundling protein fascin is overexpressed in colorectal adenomas and promotes motility in adenoma cells in vitro." British Journal of Cancer **101**(7): 1124-1129.
- Qualtrough, D., K. Smallwood, et al. (2011). "The actin-bundling protein Fascin is overexpressed in inflammatory bowel disease and may be important in tissue repair." BMC Gastroenterol **11**.
- Rao, T. P. and M. Kuhl (2010). "An Updated Overview on Wnt Signaling Pathways A Prelude for More." Circ Res **106**(12): 1798-1806.
- Rawlings, J. S., K. M. Rosler, et al. (2004). "The JAK/STAT signaling pathway." Journal of Cell Science **117**(Pt 8): 1281-1283.
- Rayet, B. and C. Gelinas (1999). "Aberrant rel/nfkb genes and activity in human cancer." Oncogene **18**(49): 6938-6947.
- Ren, J. (1991). "Relationship between development of microvilli on tumor cells and growth or metastatic potential of tumor cells." Hokkaido Igaku Zasshi **66**(2): 187-200.
- Ren, J., Hamada, J.-i., Okada, F., Takeichi, N., Morikawa, K., Hosokawa, M. and Kobayashi, H. (1990). "Correlation between the Presence of Microvilli and the Growth or Metastatic Potential of Tumor Cells." Cancer Science **81**: 920-926.
- Roussos, E. T., J. S. Condeelis, et al. (2011). "Chemotaxis in cancer." Nat Rev Cancer **11**(8): 573-587.
- Royer, C. and X. Lu (2011). "Epithelial cell polarity: a major gatekeeper against cancer?" Cell Death Differ **18**(9): 1470-1477.
- Sampson, E. R., S. Y. Yeh, et al. (2001). "Identification and characterization of androgen receptor associated coregulators in prostate cancer cells." J Biol Regul Homeost Agents **15**(2): 123-129.
- Samuel, M. S., J. I. Lopez, et al. (2011). "Actomyosin-mediated cellular tension drives increased tissue stiffness and beta-catenin activation to induce epidermal hyperplasia and tumor growth." Cancer Cell **19**(6): 776-791.
- Sanders, A. J., T. A. Martin, et al. (2011). "EPLIN is a negative regulator of prostate cancer growth and invasion." J Urol **186**(1): 295-301.
- Sanders, A. J., L. Ye, et al. (2010). "The impact of EPLINalpha (Epithelial protein lost in neoplasm) on endothelial cells, angiogenesis and tumorigenesis." Angiogenesis **13**(4): 317-326.
- Sansom, O. J., K. R. Reed, et al. (2004). "Loss of Apc in vivo immediately perturbs Wnt signaling, differentiation, and migration." Genes & Development **18**(12): 1385-1390.
- Sanz-Moreno, V., G. Gadea, et al. (2008). "Rac activation and inactivation control plasticity of tumor cell movement." Cell **135**(3): 510-523.
- Sato, T., R. G. Vries, et al. (2009). "Single Lgr5 stem cells build crypt-villus structures in vitro without a mesenchymal niche." Nature **459**(7244): 262-U147.
- Sauer, B. (1998). "Inducible gene targeting in mice using the Cre/lox system." Methods-a Companion to Methods in Enzymology **14**(4): 381-392.
- Schock, F. and N. Perrimon (2002). "Molecular mechanisms of epithelial morphogenesis." Annual review of cell and developmental biology **18**: 463-493.

- Schoumacher, M., R. D. Goldman, et al. (2010). "Actin, microtubules, and vimentin intermediate filaments cooperate for elongation of invadopodia." *J Cell Biol* **189**(3): 541-556.
- Seldenrijk, C. A., B. C. Morson, et al. (1991). "Histopathological Evaluation of Colonic Mucosal Biopsy Specimens in Chronic Inflammatory Bowel-Disease - Diagnostic Implications." *Gut* **32**(12): 1514-1520.
- Shen, L. (2009). "Functional morphology of the gastrointestinal tract." *Curr Top Microbiol Immunol* **337**: 1-35.
- Shi, X. Y., B. Bhagwandeem, et al. (2008). "CDX2 and villin are useful markers of intestinal metaplasia in the diagnosis of Barrett esophagus." *Am J Clin Pathol* **129**(4): 571-577.
- Shibata, H., K. Toyama, et al. (1997). "Rapid colorectal adenoma formation initiated by conditional targeting of the APC gene." *Science* **278**(5335): 120-123.
- Shih, D. Q., R. Barrett, et al. (2011). "Constitutive TL1A (TNFSF15) Expression on Lymphoid or Myeloid Cells Leads to Mild Intestinal Inflammation and Fibrosis." *Plos One* **6**(1).
- Simpson, J. F. and D. L. Page (1992). "Altered expression of a structural protein (fodrin) within epithelial proliferative disease of the breast." *Am J Pathol* **141**(2): 285-289.
- Smith, S. C., G. Oxford, et al. (2007). "Expression of ral GTPases, their effectors, and activators in human bladder cancer." *Clin Cancer Res* **13**(13): 3803-3813.
- Snoeck, V., B. Goddeeris, et al. (2005). "The role of enterocytes in the intestinal barrier function and antigen uptake." *Microbes and Infection* **7**(7-8): 997-1004.
- Snyder, M., X. Y. Huang, et al. (2011). "Signal Transducers and Activators of Transcription 3 (STAT3) Directly Regulates Cytokine-induced Fascin Expression and Is Required for Breast Cancer Cell Migration." *Journal of Biological Chemistry* **286**(45): 38886-38893.
- Solem, C. A., W. S. Harmsen, et al. (2004). "Small intestinal adenocarcinoma in Crohn's disease: a case-control study." *Inflamm Bowel Dis* **10**(1): 32-35.
- Sormunen, R., P. Paakko, et al. (1994). "Fodrin and actin in the normal, metaplastic, and dysplastic respiratory epithelium and in lung carcinoma." *Am J Respir Cell Mol Biol* **11**(1): 75-84.
- Sormunen, R. T., A. S. Leong, et al. (1999). "Immunolocalization of the fodrin, E-cadherin, and beta-catenin adhesion complex in infiltrating ductal carcinoma of the breast-comparison with an in vitro model." *J Pathol* **187**(4): 416-423.
- Specian, R. D. and M. G. Oliver (1991). "Functional Biology of Intestinal Goblet Cells." *American Journal of Physiology* **260**(2): C183-C193.
- Stange, E. F., S. P. L. Travis, et al. (2008). "European evidence-based Consensus on the diagnosis and management of ulcerative colitis: Definitions and diagnosis." *Journal of Crohns & Colitis* **2**(1): 1-23.
- Stanger, B. Z., R. Datar, et al. (2005). "Direct regulation of intestinal fate by Notch." *Proc Natl Acad Sci U S A* **102**(35): 12443-12448.
- Stevenson, R. P., D. Veltman, et al. (2012). "Actin-bundling proteins in cancer progression at a glance." *Journal of Cell Science* **125**(5): 1073-1079.
- Sturm, A. and A. U. Dignass (2008). "Epithelial restitution and wound healing in inflammatory bowel disease." *World J Gastroenterol* **14**(3): 348-353.

- Su, L. K., K. W. Kinzler, et al. (1992). "Multiple Intestinal Neoplasia Caused by a Mutation in the Murine Homolog of the Apc Gene." *Science* **256**(5057): 668-670.
- Suetsugu, S., H. Miki, et al. (2002). "Spatial and temporal regulation of actin polymerization for cytoskeleton formation through Arp2/3 complex and WASP/WAVE proteins." *Cell motility and the cytoskeleton* **51**(3): 113-122.
- Suh, N., X. J. Yang, et al. (2005). "Value of CDX2, villin, and alpha-methylacyl coenzyme A racemase immunostains in the distinction between primary adenocarcinoma of the bladder and secondary colorectal adenocarcinoma." *Mod Pathol* **18**(9): 1217-1222.
- Sum, E. Y., D. Segara, et al. (2005)a. "Overexpression of LMO4 induces mammary hyperplasia, promotes cell invasion, and is a predictor of poor outcome in breast cancer." *Proc Natl Acad Sci U S A* **102**(21): 7659-7664.
- Sum, E. Y., M. Shackleton, et al. (2005)b. "Loss of the LIM domain protein Lmo4 in the mammary gland during pregnancy impedes lobuloalveolar development." *Oncogene* **24**(30): 4820-4828.
- Sundberg, J. P., C. O. Elson, et al. (1994). "Spontaneous, Heritable Colitis in a New Substrain of C3h/HeJ Mice." *Gastroenterology* **107**(6): 1726-1735.
- Swaminathan, V., K. Mythreye, et al. (2011). "Mechanical stiffness grades metastatic potential in patient tumor cells and in cancer cell lines." *Cancer Res* **71**(15): 5075-5080.
- Sy, M. S., C. Li, et al. (2010). "The fatal attraction between pro-prion and filamin A: prion as a marker in human cancers." *Biomark Med* **4**(3): 453-464.
- Tak, P. P. and G. S. Firestein (2001). "NF-kappaB: a key role in inflammatory diseases." *J Clin Invest* **107**(1): 7-11.
- Taupin, D. and D. K. Podolsky (2003). "Trefoil factors: initiators of mucosal healing." *Nat Rev Mol Cell Biol* **4**(9): 721-732.
- Thenappan, A., Y. Li, et al. (2009). "New Therapeutics Targeting Colon Cancer Stem Cells." *Curr Colorectal Cancer Rep* **5**(4): 209.
- Thomas, K. R. and M. R. Capecchi (1987). "Site-Directed Mutagenesis by Gene Targeting in Mouse Embryo-Derived Stem-Cells." *Cell* **51**(3): 503-512.
- Tubb, B., D. J. Mulholland, et al. (2002). "Testis Fascin (FSCN3): A Novel Paralog of the Actin-Bundling Protein Fascin Expressed Specifically in the Elongate Spermatid Head." *Experimental Cell Research* **275**(1): 92-109.
- Tuominen, H., R. Sormunen, et al. (1996). "Non-erythroid spectrin (fodrin) in cutaneous tumours: diminished in cell membranes, increased in the cytoplasm." *Br J Dermatol* **135**(4): 576-580.
- Turner, J. R. (2009). "Intestinal mucosal barrier function in health and disease." *Nat Rev Immunol* **9**(11): 799-809.
- Uramoto, H., L. M. Akyurek, et al. (2010). "A positive relationship between filamin and VEGF in patients with lung cancer." *Anticancer Res* **30**(10): 3939-3944.
- van de Wetering, M., E. Sancho, et al. (2002). "The beta-catenin/TCF-4 complex imposes a crypt progenitor phenotype on colorectal cancer cells." *Cell* **111**(2): 241-250.
- van Es, J. H., M. E. van Gijn, et al. (2005). "Notch/gamma-secretase inhibition turns proliferative cells in intestinal crypts and adenomas into goblet cells." *Nature* **435**(7044): 959-963.
- Vignjevic, D., M. Schoumacher, et al. (2007). "Fascin, a Novel Target of B-Catenin-TCF Signaling, Is Expressed at the Invasive Front of Human Colon Cancer." *Cancer Research* **67**(14): 6844-6853.

- Visvader, J. E., D. Venter, et al. (2001). "The LIM domain gene LMO4 inhibits differentiation of mammary epithelial cells in vitro and is overexpressed in breast cancer." Proc Natl Acad Sci U S A **98**(25): 14452-14457.
- Wada, Y., T. Abe, et al. (2003). "Autosomal Dominant Macular Degeneration Associated With 208delG Mutation in the FSCN2 Gene." Arch Ophthalmol **121**(11): 1613-1620.
- Wada, Y., T. Abe, et al. (2001). "Mutation of Human Retinal Fascin Gene (FSCN2) Causes Autosomal Dominant Retinitis Pigmentosa." Investigative Ophthalmology & Visual Science **42**(10): 2395-2400.
- Wang, K., T. Zhang, et al. (2013). "Redox homeostasis: the linchpin in stem cell self-renewal and differentiation." Cell Death & Disease **4**.
- Wang, N., E. Kudryavtseva, et al. (2004). "Expression of an engrailed-LMO4 fusion protein in mammary epithelial cells inhibits mammary gland development in mice." Oncogene **23**(8): 1507-1513.
- Wang, N., K. K. Lin, et al. (2007). "The LIM-only factor LMO4 regulates expression of the BMP7 gene through an HDAC2-dependent mechanism, and controls cell proliferation and apoptosis of mammary epithelial cells." Oncogene **26**(44): 6431-6441.
- Watson, A. J. M. and D. M. Pritchard (2000). "Lessons from genetically engineered animal models VII. Apoptosis in intestinal epithelium: lessons from transgenic and knockout mice." American Journal of Physiology-Gastrointestinal and Liver Physiology **278**(1): G1-G5.
- Weaver, A. (2006). "Invadopodia: specialized cell structures for cancer invasion." Clin Exp Metastasis **23**: 97-105.
- Wehkamp, J., M. Fellermann, et al. (2005). "Mechanisms of disease: defensins in gastrointestinal diseases." Nature Clinical Practice Gastroenterology & Hepatology **2**(9): 406-415.
- Welsch, T., S. Keleg, et al. (2009). "Actinin-4 expression in primary and metastasized pancreatic ductal adenocarcinoma." Pancreas **38**(8): 968-976.
- Wirtz, S. and M. F. Neurath (2000). "Animal models of intestinal inflammation: new insights into the molecular pathogenesis and immunotherapy of inflammatory bowel disease." Int J Colorectal Dis **15**(3): 144-160.
- Wirtz, S. and M. F. Neurath (2007). "Mouse models of inflammatory bowel disease." Advanced Drug Delivery Reviews **59**(11): 1073-1083.
- Wulfkuhle, J. D., I. E. Donina, et al. (1999). "Domain analysis of supervillin, an F-actin bundling plasma membrane protein with functional nuclear localization signals." J Cell Sci **112** (Pt 13): 2125-2136.
- Wyckoff, J. B., S. E. Pinner, et al. (2006). "ROCK- and myosin-dependent matrix deformation enables protease-independent tumor-cell invasion in vivo." Curr Biol **16**(15): 1515-1523.
- Xavier, R. J. and D. K. Podolsky (2007). "Unravelling the pathogenesis of inflammatory bowel disease." Nature **448**(7152): 427-434.
- Xie, J. L. and S. H. Itzkowitz (2008). "Cancer in inflammatory bowel disease." World Journal of Gastroenterology **14**(3): 378-389.
- Yamamoto, S., H. Tsuda, et al. (2007). "Actinin-4 expression in ovarian cancer: a novel prognostic indicator independent of clinical stage and histological type." Mod Pathol **20**(12): 1278-1285.
- Yamamoto, S., H. Tsuda, et al. (2009). "Actinin-4 gene amplification in ovarian cancer: a candidate oncogene associated with poor patient prognosis and tumor chemoresistance." Mod Pathol **22**(4): 499-507.

- Yang, J., X. Liao, et al. (2007). "Unphosphorylated STAT3 accumulates in response to IL-6 and activates transcription by binding to NFkappaB." Genes Dev **21**(11): 1396-1408.
- Yang, Q., N. A. Bermingham, et al. (2001). "Requirement of Math1 for secretory cell lineage commitment in the mouse intestine." Science **294**(5549): 2155-2158.
- Yang, S., F. K. Huang, et al. (2013). "Molecular mechanism of fascin function in filopodial formation." Journal of Biological Chemistry **288**(1): 274-284.
- Younes, M., A. S. Harris, et al. (1989). "Fodrin as a differentiation marker. Redistributions in colonic neoplasia." Am J Pathol **135**(6): 1197-1212.
- Yu, J., K. Ohuchida, et al. (2008). "LIM only 4 is overexpressed in late stage pancreas cancer." Mol Cancer **7**: 93.
- Yu, Z., W. Zhang, et al. (2002). "Signal transducers and activators of transcription 3 (STAT3) inhibits transcription of the inducible nitric oxide synthase gene by interacting with nuclear factor kappaB." Biochemical Journal **367**(Pt 1): 97-105.
- Yuan, C. B., R. Zhao, et al. (2010). "[Significance of plasmic L-plastin levels in the diagnosis of colorectal cancer]." Zhonghua wei chang wai ke za zhi = Chinese journal of gastrointestinal surgery **13**(9): 687-690.
- Zhang, J., M. Fonovic, et al. (2009). "Rab35 Controls Actin Bundling by Recruiting Fascin as an Effector Protein." Science **325**(5945): 1250-1254.
- Zhang, M. Q., F. Lin, et al. (2007). "Expression of mucins, SIMA, villin, and CDX2 in small-intestinal adenocarcinoma." Am J Clin Pathol **128**(5): 808-816.
- Zhang, S., X. Wang, et al. (2010). "EPLIN downregulation promotes epithelial-mesenchymal transition in prostate cancer cells and correlates with clinical lymph node metastasis." Oncogene.
- Zhang, X. and I. Takenaka (1995). "Morphological changes of microvilli on different surfaces of epithelial cells in the rat bladder treated with N-butyl-N-(4-hydroxybutyl) nitrosamine." Urol Res **23**(6): 371-376.
- Zhou, A. X., A. Toyly, et al. (2011). "Filamin A mediates HGF/c-MET signaling in tumor cell migration." Int J Cancer **128**(4): 839-846.

2 Chapter 2 – Materials and Methods

2.1 Materials

2.1.1 Reagents and Solutions

Compounds/Reagents	Type	Manufacturer
10X Modified Eagle Medium (MEM)		BD Biosciences
4-Hydroxytamoxifen		Sigma
4.0 vicryl sutures		Ethicon
6xDNA loading dye		New England Biolabs
Acetic Acid		Fisher Scientific
Acetone		Fisher Scientific
Actin		In house
Adenoma culture media	ADF supplemented with Glutamine 1:100, Hepes 10mM, Pen/strep 1:100, N2 supplement 1:100, B27 supplement 1:50, murine recombinant EGF (50ng/ml), murine recombinant noggin (100ng/ml).	In house
Advanced Dulbecco's Modified Eagle Medium (DMEM)/f12 (ADF)		Invitrogen
Agarose		Melford
Antibody Diluent		Dako
Azoxymethane (AOM)		Sigma
B-naphthoflavone		Sigma
b27	Serum supplement	Invitrogen
BrdU (Bromodeoxyuridine) solution		Sigma
BSA (Bovine Serum Albumin)		Sigma
Caerulein		Sigma

Chloroform		Fisher Scientific
Citrate buffer, pH 6.4		Dako
Crypt Culture Media (CCM)	ADF supplemented with Glutamine 1:100, Hepes 10mM, Pen/strep 1:100, N2 supplement 1:100, B27 supplement 1:50, murine recombinant EGF (50ng/ml), murine recombinant noggin (100ng/ml), human recombinant R-spondin1 (500ng/ml)	In house
Dextran sodium Sulphate (DSS)		MP Biochemicals
Dimethyl Sulfoxide (DMSO)		Sigma
DL- dithiothreitol (DTT)		Sigma
DMEM		Invitrogen
DNA Ladders	1kb	Invitrogen
DNase I recombinant		Roche
EGF (Epidermal Growth Factor)		Peprtech
Etanercept		Pfizer
Ethanol		VWR chemicals
Ethidium bromide		Invitrogen
Ethylenediaminetetraacetic acid (EDTA)		Sigma
Extraction buffer	0.5M KCl, 0.1M K ₂ HPO ₄ .	In house
Fetal Bovine Serum (FBS)		PAA Cell Culture Company
Fibroblasts (Human)		Dr. P Timpson
Fibronectin		BD Biosciences
Gelatin		Sigma

Glycine		Sigma
Goat serum		Sigma
Halt phosphatase inhibitor cocktail		Pierce
Hepes	Buffer	PAA Cell Culture Company
Hydrochloric Acid (HCl)		Fisher Scientific
Il-11 (Interleukin-11)		Ass. Professor Mathias Ernst (The Walter and Eliza Hall Institute of Medical Research)
L-Glutamine		Invitrogen
LDS sample buffer		Life Technologies
Matrigel (Growth factor reduced, phenol red free) 10ml		BD Bioscience
Methacarn	60% Absolute Methanol 30% Chloroform 10% Glacial Acetic Acid	In house
Methanol		Sigma
n2	Supplement	Invitrogen
Neutral Buffered Formalin (NBF)		Leica
Nicotinamide		Sigma
NuPAGE MOPS SDS Running Buffer		Invitrogen
NuPAGE Novex Bis-Tris Mini Gels	10%, 12% and 4-12% gel	Invitrogen
NuPAGE Sample Buffer (4X)		Invitrogen
NuPAGE Sample Reducing Agent (10X)		Invitrogen
NuPAGE Transfer Buffer		Invitrogen
Paraformaldehyde (PFA)		EMS
PBS (Phosphate Buffered	170mM NaCl, 3.3mM	Beatson Institute

Saline)	KCl, 1.8mM Na ₂ HPO ₄ , 10.6mM H ₂ PO ₄	Central Services
PBT (Phosphate Buffered Saline Tween)	PBS, 0.5% BSA, 0.1% Tween20	In house
Penicillin-Streptomycin (Pen/Strep)		Gibco
Potassium Chloride (KCl)		Sigma
Prolong Gold Antifade reagent with DAPI		Invitrogen
Propidium Iodide (PI)		Sigma
Protease inhibitor cocktail		Pierce
R-spondin	Wnt agonist	R&D Systems
Rat tail collagen		In house
Recombinant human TNF α		R&D Systems
Recombinant Mouse Oncostatin M (OSM)		R&D Systems
Recombinant Murine Noggin	Growth Factor	Peprotech
RIPA (Radioimmunoprecipitation assay buffer) Buffer	50 mM Tris-HCl, 150 mM NaCl, 1% NP-40 and 0.25% Na-deoxycholate	In house
RNAlater TM	RNA stabilisation reagent	Life Technologies
RNase TM free water		Qiagen
RNase TM ZAP	RNase cleaning reagent	Sigma
SDS (sodium dodecyl sulfate) Blotting buffer	0.03% SDS 25 mM Tris-HCl (pH 7.6) 192 mM glycine 20% methanol	Beatson Institute Central Services
SeeBlue Plus2 Pre-Stained Standard		Invitrogen
Sodium Chloride (NaCl)		Fisher Scientific

Sodium Hydroxide (NaOH)		Fisher Scientific
TAE	40mM Tris, 0.1% glacial acetic acid, 1mM EDTA	Beatson Institute Central Services
TBST	10mM Tris-HCl, pH 7.4, 150mM NaCl	Beatson Institute Central Services
TE	10mM Tris-HCl, pH 8.0, 1mM EDTA	Beatson Institute Central Services
Tris/Borate/EDTA (TBE) buffer	Tris base: 108 g Boric acid: 55 g 0.5M EDTA: 40 mL Distilled H ₂ O to 1L	Beatson Institute Central Services
Triton X-100		Sigma
TrypLE		Life Technologies
TrypLE 1X		Invitrogen
Trypsin		Gibco
Wnt-3a, recombinant mouse		Millipore
y27632 rock inhibitor		Sigma

Table 2-1 Reagents and Solutions

2.1.2 Antibodies and Dyes

Antibody/Dye	Dilution	Manufacturer
Alcian Blue		Cell Path
Anti-mouse IgG HRP linked	WB (Western Blot) - 1:5000	Cell Signalling
Anti-Rabbit IgG HRP linked	WB - 1:5000	Cell Signalling
Calcein	5 μ M	Molecular Probes
Caspase3	IHC (Immunohistochemistry) - 1:50	Cell signalling

Eosin		Beatson Histology Services
F4/80	IHC - 1:200	AbCam
FITC-conjugated anti-mouse		BD Biosciences
Haematoxylin		Cell Path
Mouse anti-BrdU	IF (Immunofluorescence) - 1:100	BD Bioscience
Mouse anti-BrdU	FC (Flow cytometry) - 1:50	Dako
Mouse anti-Fascin	IHC - 1:100	Abcam
Mouse anti-Fascin (55K2)	WB - 1:500	Dako
Myeloperoxidase (MPO)	IHC - 1:200	Dako
NIMP	IHC - 1:50	AbCam
Rabbit anti-Fascin	IHC - 1:200	ATLAS antibodies
Rabbit anti-GAPDH	WB - 1:500	Cell Signalling
Rabbit anti-Ki67 (SP6)	WB - 1:500	Neomarkers
Rhodamine Phalloidin	IF - 1:200	Molecular Probes
Von Willebrand Factor	IHC - 1:400	AbCam

Table 2-2 Antibodies and Dyes

2.1.3 Primers

Primer	Type	Manufacturer
APC (Adenomatous Polyposis Coli)	qRT-PCR QuantiTect	Qiagen
Ascl2 (Achaete-scute complex homolog 2)	qRT-PCR QuantiTect	Qiagen
Axin2 (axis inhibition protein 2)	qRT-PCR QuantiTect	Qiagen
Bmi1 (Bmi1 polycomb ring finger oncogene)	qRT-PCR QuantiTect	Qiagen
c-Myc	qRT-PCR QuantiTect	Qiagen
Caspase 8	qRT-PCR QuantiTect	Qiagen
Caspase 9	qRT-PCR QuantiTect	Qiagen

Cxcl1 (Chemokine (C-X-C motif) ligand 1)	qRT-PCR QuantiTect	Qiagen
Cxcl2 (Chemokine (C-X-C motif) ligand 2)	qRT-PCR QuantiTect	Qiagen
Cxcl5 (Chemokine (C-X-C motif) ligand 5)	qRT-PCR QuantiTect	Qiagen
Cxcr2 (Chemokine (C-X-C motif) receptor 2)	qRT-PCR QuantiTect	Qiagen
Cyclin D1	qRT-PCR QuantiTect	Qiagen
Cyclin D2	qRT-PCR QuantiTect	Qiagen
Ephb3 (Ephrin type-B receptor 3)	qRT-PCR QuantiTect	Qiagen
Ets2 (v-ets avian erythroblastosis virus E26 oncogene homolog 2)	qRT-PCR QuantiTect	Qiagen
Fscn1 (fascin1)	qRT-PCR QuantiTect	Qiagen
GAPDH (Glyceraldehyde 3-phosphate dehydrogenase)	qRT-PCR QuantiTect	Qiagen
Il-11 (Interleukin-11)	qRT-PCR QuantiTect	Qiagen
Il-11b (Interleukin-11b)	qRT-PCR QuantiTect	Qiagen
Il-6 (Interleukin-6)	qRT-PCR QuantiTect	Qiagen
Jak1 (Janus Kinase1)	qRT-PCR QuantiTect	Qiagen
Jak2 (Janus Kinase2)	qRT-PCR QuantiTect	Qiagen
Jak3 (Janus Kinase3)	qRT-PCR QuantiTect	Qiagen
Ki67	qRT-PCR	Invitrogen
LEF1 (Lymphoid enhancer-binding factor-1)	qRT-PCR QuantiTect	Qiagen
Lgr5 (Leucine-rich repeat-containing G-protein coupled receptor 5)	qRT-PCR QuantiTect	Qiagen
lysozyme	qRT-PCR QuantiTect	Qiagen
MPO (Myeloperoxidase)	qRT-PCR QuantiTect	Qiagen
NF- κ B (nuclear factor kappa-light-chain-enhancer of	qRT-PCR QuantiTect	Qiagen

activated B cells)		
Nrn1 (neurtin 1)	qRT-PCR QuantiTect	Qiagen
Olfm4 (olfactomedin 4)	qRT-PCR QuantiTect	Qiagen
Rgmb (RGM domain family, member B)	qRT-PCR QuantiTect	Qiagen
Slc14a1 (solute carrier family 14 (urea transporter), member 1)	qRT-PCR QuantiTect	Qiagen
Sox9 (SRY (sex determining region Y)-box 9)	qRT-PCR QuantiTect	Qiagen
Stat3 (Signal transducer and activator of transcription 3)	qRT-PCR QuantiTect	Qiagen
Tnfrsf19 (Tumor necrosis factor receptor superfamily, member 19)	qRT-PCR QuantiTect	Qiagen
TNF α (Tumour necrosis factor alpha)	qRT-PCR QuantiTect	Qiagen
Wnt3a (wingless-type MMTV integration site family, member 3A)	qRT-PCR QuantiTect	Qiagen
β -catenin	qRT-PCR QuantiTect	Qiagen

Table 2-3 Primers

2.1.4 Enzymes and kits

Kit	Manufacturer
Alexa Fluor 546 protein labelling kit	Invitrogen
Amaxa Nucleofection Kit	Lonza
Click-iT EdU Alexa Fluor 488 Flow Cytometry assay Kit	Invitrogen
DyNAmo SYBR Green 2-Step qRT-PCR Kit	Thermo Scientific

DAKO Envision™ Mouse, Rabbit Detection kit	DAKO
Lipofectamine 2000	Invitrogen
Precision Red Advanced Protein Assay	Cytoskeleton Inc.
RNeasy mini kit	Qiagen
SimplyBlue SafeStain	Invitrogen
SuperSignal West Pico Chemiluminescent Substrate	Thermo Scientific

Table 2-4 Enzymes and kits

2.2 Methods

2.2.1 Cell culture

Origin of cell lines

HCT116 and HT29 cells were obtained from Dr. Ang Li, Beatson Institute for Cancer Research.

Maintenance of cell lines

All cell lines were cultured in sterile 10cm Falcon dishes in 5% CO₂ at 37° C. The cell lines were maintained in DMEM supplemented with 2mM glutamine and 10% Fetal Bovine Serum (FBS). The cells were passaged every 3-4 days or when sub-confluent with a 1:10 ratio. Passage involved aspiration of the medium, washing with PBS buffer then addition of 1ml of PE buffer containing 0.25% trypsin for 5 minutes. The cells were then re-suspended in 10ml DMEM, 1ml of which was added to 20ml fresh DMEM and the suspension added to a new 10cm plate.

Storage of cell lines

Cells were trypsinised as described, pelleted by centrifugation, re-suspended in 50% DMEM, 40% FBS and 10% DMSO and stored in cryotubes initially at -70° C overnight in Mr. Frosty containers before transfer to a liquid nitrogen tank.

Thawing of cell lines involved placing the cryotubes in a 37°C water bath then adding the thawed cells to a pre-warmed 10cm falcon plate containing DMEM. The following day the medium was aspirated and fresh DMEM was added.

2.2.2 Crypt and adenoma culture

2.2.2.1 Establishment of primary mouse small intestinal crypt cell lines

The crypt culture method has previously been described (Sato, Vries et al. 2009). Briefly, 6-8 week old C57Bl/6 mice were culled and the proximal 10cm of the small intestine was dissected and flushed with ice cold PBS. The small intestine was opened longitudinally and the villi were scraped off with a coverslip. The small intestine was then cut into 5mm pieces and transferred to a 50ml Falcon tube containing ice cold PBS. The pieces were washed using a 25ml pipette and, once the supernatant had settled, this was replaced with fresh PBS. The washing was repeated approximately 10 times until the supernatant was clear. The small intestine was then incubated with 25ml PBS containing 2mM EDTA at 4°C for 30 minutes on a roller bank. The EDTA supernatant was discarded and the small intestine was washed with PBS to remove any traces of EDTA. The small intestine was again suspended in 10ml PBS and vigorously pipetted 10-15 times with the crypt rich supernatant removed and kept. This was repeated a further 3 times resulting in 4 crypt enriched fractions. The 3 fractions containing the most crypts were then combined and diluted with Advanced DMEM/F12 (ADF) to 50ml and centrifuged at 1200rpm for 5 minutes. The pellets were re-suspended in 10ml ADF and passed through a 70µm cell strainer. A further 5ml ADF was then passed through the filter to ensure all crypts were collected. The tube was then centrifuged at 600rpm for 2 minutes. The ADF wash step was then repeated until no single cells could be seen. During this time, the number of crypts was counted and the number required determined. After further centrifugation, the pellet was re-suspended in growth factor reduced Matrigel at approximately 1000 crypts/ml. 50µl of Matrigel was seeded per well in a 24 well falcon plate and incubated at 37°C in 5% CO₂ for 5 minutes until the Matrigel had solidified. The plate was then removed and 500µl crypt culture medium (CCM) added.

The medium was replaced every second day and the crypts were passaged at 7-10 days. Crypts could be frozen and thawed as described.

In some experiments exogenous Wnt3a and Oncostatin M (OSM) were added to the medium for the stated length of time at concentrations of 100ng/ml and 50ng/ml respectively.

2.2.2.2 Establishment of primary mouse intestinal tumour cell lines

The adenoma culture method has been described previously (Sato, Stange et al. 2011). Briefly, the adenoma is cut from the intestine and then, using scissors cut into small pieces and washed 3-5 times in ice cold PBS to remove any debris. The adenoma was then incubated in ice cold PBS containing 5mM EDTA for 10 minutes on a roller bank at 4°C. The EDTA supernatant was aspirated and the adenoma was then washed in PBS a further 3 times to remove any EDTA. The adenoma was next incubated in 5ml 10x Trypsin (5mg/ml) with 0.8µg DNase for 30 minutes at 37°C. Following this, the falcon tube was shaken vigorously and the supernatant was collected in a 50ml falcon tube. The adenoma was then washed a further 3 times with 10ml ADF and the supernatant collected in the falcon tube. The supernatant was next centrifuged at 1200rpm for 5 minutes. The supernatant was removed and the pellet washed twice with ADF to remove any remaining trypsin. The number of cells was next counted and around 100 cells were plated per well. These were re-suspended in Matrigel (50µl per well in a 24 well plate) and incubated at 37°C in 5% CO₂ for 5 minutes before the adenoma culture medium was added. The medium was replaced every second day and the adenomas were passaged at 7-10 days. Adenomas could be frozen and thawed as described.

2.2.3 Protein Immunoblotting

2.2.3.1 Protein extraction from tissues or primary murine cell lines

Freshly extracted tissue (homogenised using the Precellys®24-Dual tissue homogeniser) or cells, which had been cultured *in-vitro*, were washed in PBS and centrifuged at 1200rpm for 5 minutes. The supernatant was removed and the

pellet re-suspended in 300µl RIPA buffer supplemented with 10µl protease inhibitor cocktail and 10µl Halt phosphatase inhibitor cocktail for 10 minutes on ice. The solution was then centrifuged at 13000rpm for 5 minutes at 4°C and the supernatant aspirated and stored at -20°C. The pellet was discarded. The protein concentration was determined using Precision Red Advanced Protein Assay reagent.

2.2.3.2 Western Blotting

Proteins, separated using polyacrylamide gel electrophoresis, were transferred from the gel to PVDF membrane between Whatman 3MM paper at 200mA for 75 minutes in 1x SDS blotting buffer. Membranes were blocked in 3% milk in 1XTBST for 1 hour at room temperature and incubated with the primary antibody at the appropriate concentration, for the required duration at the appropriate temperature as determined by the manufacturer. Following this, the membranes were washed in 1X TBST 3 times for 5 minutes and then incubated with the appropriate secondary antibody in 1X TBST for a minimum of 1 hour at room temperature and then again washed in 1X TBST 3 times for 5 minutes. All incubations and washes were performed on a rocking table or roller bank. The proteins were next visualised using supersignal west pico chemiluminescent substrate or supersignal west femto maximum sensitivity substrate. Using the GeneSnap software and Bio-imaging system the images were processed and recorded. Western blots found within this thesis are representative results obtained from at least 3 repeated experiments for each experiment shown, unless otherwise stated.

2.2.3.3 Protein separation using polyacrylamide gel electrophoresis (SDS-PAGE)

Protein samples were diluted with NuPAGE LDS Sample Buffer (4X) and NuPAGE Reducing Agent (10X) resulting in a 1X solution which was heated at 70°C for 10 min. The protein was then resolved on precast NuPAGE Novex Bis-Tris Mini Gels (4-12%) according to molecular weight by electrophoresis in gel tanks with 1X NuPAGE MOPS SDS Running Buffer at 150V for 2 hours. 7µl of SeeBlue Plus2 Pre-stained Standard was used as the molecular weight marker.

2.2.4 Immunofluorescence (IF)

Small intestinal crypts: coverslips were incubated in PBS supplemented with 1% BSA and 0.1% bovine gelatin for 30 minutes at 37°C in 5% CO₂ in a 6 well falcon plate. 400µl of crypt culture medium was then added to each well and incubated for a further 20 minutes at 37°C in 5% CO₂. The crypts were transferred to a 15ml falcon and centrifuged at 1200rpm for 5 minutes. The supernatant was discarded and a drop of the crypts was seeded onto the coverslips and incubated for 1 hour at 37°C in 5% CO₂. The medium was next aspirated and the crypts were next fixed in 4% PFA at room temperature for 20 minutes or in methanol (for the fascin antibody) at -20°C for 20 minutes. They were next washed 3 times in PBS and permeabilised in PBS supplemented with 1% Triton X-100 for 10 minutes. Following this they were incubated for 30 minutes in blocking buffer (PBS supplemented with 1% BSA, 3% goat serum, 0.2% Triton X-100). Next, they were incubated with the primary antibody at the appropriate concentration in working buffer (PBS supplemented with 0.1% BSA, 0.3% goat serum and 0.2% Triton X-100) overnight at 4°C. The following day the samples were washed 3 times with working buffer before being incubated with the secondary antibody at the appropriate concentration in working buffer for 2 hours. They were again washed 3 times in working buffer before being mounted on slides with Prolong Gold Antifade reagent with DAPI. Crypts were then visualised with the Olympus FV1000 inverted laser scanning confocal microscope or the Zeiss Axioskop2 microscope equipped with a digital camera C4742-95 (Hamamatsu).

2.2.5 Histology and staining of tissue

2.2.5.1 Immunohistochemistry (IHC)

Formalin or methacarn fixed paraffin embedded sections were deparaffinised and rehydrated through immersion in xylene and a grade alcohol series before being washed in 1X TBST. Antigen retrieval was achieved through incubation of sections in microwave heated 1X citrate buffer (pH 6.0) in a pressure cooker (600ml water was added to the pressure cooker. A small container with 30ml citrate buffer diluted to 300ml were placed within the pressure cooker and pre-heated on full power for 10 minutes. Slides were then added to the container

and heated on full power for 4 minutes following optimisation of the pressure). Sections were allowed to cool for 20 minutes before washing in 1X TBST for 5 minutes before sections were blocked with Peroxidase (Envision kit) for 5 minutes at room temperature. The sections were next washed 3 times with 1X TBST before they were incubated with the primary antibody at the appropriate concentration for 2 hours. They were again washed 3 times with 1X TBST before the peroxidase labelled polymer was added for 30 minutes. Sections were next washed 3 times with 1X TBST before the Substrate-chromagen was applied for the recommended length of time. Sections were next immersed in deionised water to terminate the reaction and were then counterstained with haematoxylin and mounted. For haematoxylin and eosin staining, standard protocols were followed and performed by C. Nixon and colleagues, Beatson Institute, Histology Services.

2.2.6 Paraffin embedding of organoids

2% Agarose gel (1g Agarose in 50ml 0.5x TBE Buffer) was prepared, added to a 250ml conical flask and incubated at 55°C for a minimum of 30 minutes. The organoids were transferred out of Matrigel to a 15ml falcon tube and spun at 600rpm for 3 minutes. The supernatant was aspirated and discarded and the pellet washed twice with PBS. The pellet was next fixed with 500µl 4% PFA (room temperature) or methanol (-20°C) for 20 minutes. The samples were centrifuged at 600rpm for 5 minutes. The pellet was re-suspended with 100µl of the warmed 2% Agarose and added to a 24 well falcon plate and sent to histology for processing.

2.2.7 Testing of the fascin antibody

Both fascin antibodies (DAKO and Sigma) were optimised and tested by Dr. Ang Li for use in Western blotting (1:500) and Immunohistochemistry (1:200). For both WBs and IHC sections, a positive and negative control was used in each instance to ensure the method worked, unless otherwise stated.

2.2.8 Anti-neutrophil antibodies

Two different anti-neutrophil antibodies were used: NIMP and MPO. The MPO antibody is more specific for neutrophils, whereas the NIMP antibody does detect some other immune cells in addition to neutrophils. Where possible, the MPO antibody was used, however, when the tissue was fixed in methacarn, the NIMP antibody was preferred, as the MPO antibody did not work in these conditions. Quantification of neutrophils was carried out independently and only samples, which were processed and stained in identical fashion, were compared. Reference is made to the type of antibody used in each of the experiments.

2.2.9 Generation, maintenance and treatment of mouse colonies

2.2.9.1 Transgenic mice

All experiments were performed in accordance with UK Home Office regulations. All animals were culled by Schedule 1 methods as per Home Office Guidelines. The fascin1 global knockout mouse (C57BL/6) has previously been described (Yamakita, Matsumura et al. 2009). They have been shown to be both healthy and to have no major developmental defects and, with the exception of a larger lateral ventricle of the brain is anatomically indistinguishable from wild-type (WT).

Regarding the $\underline{\text{Fascin}}^{-/-} \underline{\text{APC}}^{\text{fl/fl}} \underline{\text{p53}}^{\text{fl/fl}}$ and $\underline{\text{Fascin}}^{-/-} \underline{\text{APC}}^{\text{fl/fl}} \underline{\text{p53}}^{\text{R172H}} \underline{\text{Ah-cre}}$ (FAPC) mice, the $\underline{\text{APC}}^{\text{fl}}$ mouse (Shibata, Toyama et al. 1997), $\underline{\text{p53}}^{\text{fl}}$ (Jonkers, Meuwissen et al. 2001), $\underline{\text{p53}}^{\text{R172H}}$ (Olive, Tuveson et al. 2004) and Ah-cre (Ireland, Kemp et al. 2004) have all previously been described. The crossings, maintenance, induction and culling of these mice was performed by Dr. Ee Hong Tan (post-doctoral researcher, Professor Owen Sansom's lab) using schedule 1 methods in accordance with Home Office guidelines. The experimental cohorts were generated by crossing $\underline{\text{AhCre}}^{+} \underline{\text{APC}}^{\text{fl/+}}$ mice with $\underline{\text{p53}}^{\text{fl/+}}$ or $\underline{\text{p53}}^{\text{R172H}}$ mice. The progeny were then interbred to yield the $\underline{\text{APC}}^{\text{fl/+}} \underline{\text{p53}}^{\text{fl/fl}}$, $\underline{\text{APC}}^{\text{fl/+}} \underline{\text{p53}}^{\text{R172H}}$ and $\underline{\text{APC}}^{+/+} \underline{\text{p53}}^{\text{fl/fl}}$, $\underline{\text{APC}}^{+/+} \underline{\text{p53}}^{\text{R172H}}$ cohorts. Mice were then mated to Fascin1 deficient mice. Progeny from these crosses then were interbred to obtain $\underline{\text{Fascin1}}$ homozygous or wild-type $\underline{\text{APC}}^{\text{fl/fl}} \underline{\text{p53}}^{\text{fl/fl}} \underline{\text{Ah-cre}}$ or $\underline{\text{APC}}^{\text{fl/fl}} \underline{\text{p53}}^{\text{R172H}}$ (FAPC).

The mice were genotyped by Transnetyx (Memphis, TN). AhCre expression was induced using 3 intra-peritoneal injections of β -naphthoflavone (80 mg/kg), separated by 8 hours, as has been described previously (Ireland, Kemp et al. 2004). The mice were monitored regularly and upon developing signs of intestinal tumours were culled (using schedule 1 procedures in accordance with Home Office guidelines) and a full necropsy performed. Organs were fixed in either methacarn or 10% neutral buffered formalin (NBF).

2.2.9.2 Genotyping

Genomic DNA was prepared from tail biopsies and genotyping of the transgene was performed as previously described (Serrano, Lee et al. 1996; McClive and Sinclair 2001) by the company Transnetyx (Memphis, Tennessee).

2.2.10 Mouse Models

2.2.10.1 Irradiation model

Prior to the movement to the new Biological Services Unit (BSU) at the Beatson, we used a cobalt source at a dose of 14Gy in 6-12 week old mice. In the new BSU we used the Xstrahl 232 X-Ray irradiator at a dose of 10Gy or 12Gy in 6-12 week old mice. Mice were culled (using a schedule 1 method in accordance with Home Office guidelines) at either 6, 12 or 72 hours post irradiation.

The reduced dose using the Xstrahl 232 X-Ray irradiator was calculated by Rachel Ridgway (Beatson Institute) and was shown to give a similar level of damage to the 14Gy dose using the Cobalt source. She compared small intestine samples taken from WT mice irradiated at varying doses ranging from 10Gy - 16Gy and calculated that the most similar level of damage and subsequent regeneration was caused by 10 - 12Gy. In experimental models, when comparing WT to fascin KO mice, the same source and dose of radiation was used to ensure validity of results. The mice had blood aspirated from the inferior vena cava and transferred to EDTA containing blood tubes. The small intestines were harvested, flushed, opened and fixed in 10% NBF. Prior to fixation, the proximal

5mm of the small intestine was transferred to *RNAlater*TM and stored for future whole tissue extraction use in qRT-PCR.

2.2.10.2 Colitis model

The Dextran Sodium Sulphate (DSS) murine colitis model has previously been described (Okayasu, Hatakeyama et al. 1990). Briefly, 6-12 week old mice were weighed prior to having their standard water bottle replaced with either 2% or 3.5% DSS. Mice were examined daily for clinical signs of sickness and weighed at regular intervals. After 5 days of DSS the drinking bottle was replaced with sterile water for 72 hours. Mice were culled (using a schedule 1 method in accordance with Home Office guidelines) at varying time points up until 72 hours following cessation of DSS. The mice had blood aspirated from the inferior vena cava and the colons were harvested, flushed, opened and fixed in 10% NBF. Prior to fixation, the proximal 5mm of the colon was transferred to *RNAlater*TM and stored for future whole tissue extraction use in qRT-PCR.

2.2.10.3 Regenerating crypts

Both the irradiation and colitis models are useful to investigate small intestinal and colonic regeneration respectively. When quantifying the number of regenerating crypts we only counted crypts which had a minimum of 6 definite cells within the base of the crypt.

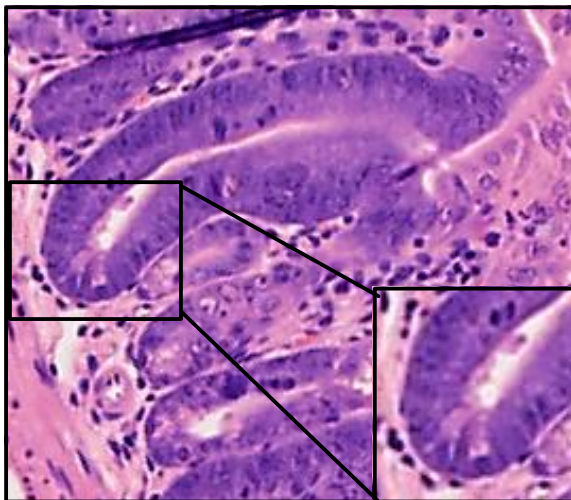


Figure 2-1 A regenerating small intestinal crypt

A WT regenerating small intestinal crypt demonstrating a minimum of 6 definite cells within the base of the crypt.

2.2.10.4 Colitis associated carcinogenesis (CAC) model

The Azoxymethane/Dextran Sodium Sulphate (AOM/DSS) CAC model has previously been described (Greten, Eckmann et al. 2004). Briefly, 6-12 week old mice were weighed prior to AOM injection. Mice received a single intra-peritoneal (IP) injection of 12.5mg/kg AOM on the Wednesday and then commenced their first 5 day 2% DSS course 5 days later on the following Monday. After 5 days of 2% DSS the mice were changed onto sterile drinking water, which they remained on until the Monday that is 21 days after the first cycle of 2% DSS began at which point the 2% DSS cycle was repeated. A third cycle of 2% DSS started 21 days after the second cycle commenced and the mice are then culled (using a schedule 1 method in accordance with Home Office guidelines) 70 days after the initial injection of AOM. The mice had blood aspirated from the inferior vena cava and the colons were harvested, flushed, opened and fixed in either 10% NBF or methacarn. Prior to fixation, tumours were transferred to RNAlater™ and stored for future whole tissue extraction use in qRT-PCR.

2.2.10.5 Orthotopic caecal model

Cell lines generated from the tumours of FAPC mice which were either WT or null for fascin were dissociated to single cells using TryPLE and re-suspended in Matrigel at 4°C. 50 spheres were injected per mouse which, once dissociated yielded approximately 5000 cells. 8-12 week old athymic nude mice (purchased from Charles River Laboratories) were anaesthetised using isofluorane and their abdomen washed with 70% ethanol. A 1-2cm skin incision was made over the caecum, the muscle layer identified and the peritoneum opened. The caecum was exteriorised and 50µl of the Matrigel containing cells was injected in the sub-serosal layer of the caecum. Any Matrigel that was spilt was mopped up using a cotton bud soaked in PBS. The caecum was returned, the peritoneal layer closed with interrupted 4.0 vicryl sutures and the skin closed with skin clips. The mice were culled (using schedule 1 procedures in accordance with Home Office guidelines) when they had lost 10% of their body weight or were showing clinical signs of ill health. After the mice were culled, a full necropsy was performed and the organs fixed in 10% NBF.

2.2.11 Blood counts

Blood aspirated from the inferior vena cava of mice (1ml) was immediately transferred to a blood tube containing EDTA. The Glasgow Veterinary School Haematology laboratory performed analysis.

2.2.12 Epithelial cell extraction

10cm of the proximal small intestine (SI) or the whole colon was dissected, flushed and opened. The SI villi were scraped using a cover glass and discarded. The samples were incubated in 5mM EDTA/PBS (SI) or 25mM EDTA/PBS (colon) for 5 minutes at 4°C on a roller bank before the EDTA/PBS was discarded and the sample washed x1 in PBS to remove any trace of EDTA. 10ml of ice cold PBS was added and the sample vigorously shaken before the supernatant was collected. This was repeated to yield a total of 3 fractions that were combined and centrifuged at 600rpm for 3 minutes prior to storage in *RNAlater*TM or RIPA buffer or fixation in 70% ethanol/30% PBS dependant on the purpose of the extract.

2.2.13 Flow cytometry

Mice received an intra-peritoneal injection of BrdU, two hours prior to culling (using a schedule 1 method in accordance with Home Office guidelines) and the cells were extracted using the whole tissue extraction previously described and fixed in 70% ethanol/30% PBS for 30 minutes at room temperature. The cells were centrifuged at 1200rpm and the ethanol aspirated and discarded. The pellet was washed once in 2ml of PBS to remove any trace of ethanol. The pellet was then re-suspended in 100µl of PBS and vortexed before 100µl of 4M HCl was added and the pellet vortexed and left for 15 minutes at room temperature. The pellet was next centrifuged at 1200rpm for 5 minutes at room temperature before being re-suspended in 1ml PBS and further centrifuged at 1200rpm for 5 minutes. The pellet was next re-suspended in 1ml PBT and again centrifuged at 1200rpm for 5 minutes prior to re-suspension in 100µl anti-BrdU antibody (1:20

dilution in PBT) and incubated for 30 minutes at room temperature. The sample was next centrifuged at 1200rpm for 5 minutes and the supernatant aspirated and discarded. The pellet was re-suspended in PBT and again centrifuged at 1200rpm for 5 minutes. The supernatant was aspirated and discarded and the pellet re-suspended in 100µl FITC-conjugated anti-mouse secondary antibody (1:40 dilution in PBT) and incubated for 30 minutes at room temperature. The sample was centrifuged at 1200rpm for 5 minutes and the supernatant aspirated and discarded and the pellet re-suspended in 1ml PBT. The sample was again centrifuged at 1200rpm for 5 minutes and the pellet re-suspended in 250µl PBS containing 100µg PI and incubated for 30 minutes at room temperature before processing on BD FACS-Calibur (BD Bioscience).

2.2.14 Clonogenicity assay

The cultured small intestinal crypts were centrifuged at 600rpm for 5 minutes and the medium/Matrigel aspirated prior to re-suspension of the pellet in PBS, further centrifugation and aspiration of the supernatant. The pellet was re-suspended in 1ml TryPLE and incubated at 37°C for 3 minutes. 5ml ADF was added to the sample and mixed through pipetting. The sample was centrifuged at 1200rpm for 5 minutes before being re-suspended in Matrigel and plating of the single cells in 6 well falcon plate at 200µl per well. The plate was incubated for 5 minutes at 37°C in 5% CO₂ before the crypt culture medium (+/- exogenous Wnt3a at 100ng/ml) was added to each well. The crypts were photographed on day 5 and day 10 and the number of colonies determined. 3 independent experiments were performed in duplicate for each cell line.

2.2.15 Cell adhesion assay

We trypsinised the FAPC adenoma cell lines (which were either WT or null for fascin), plated them on fibronectin covered 6 well plates for 30 minutes, washed them with PBS 3 times to wash off any non-adherent cells then stained the remaining adherent cells with calcein in order to quantify the number of viable

cells. The number of fluorescent cells was determined per FOV and the results quantified. 3 independent experiments were performed in duplicate for each cell line.

2.2.16 Quantitative Real-Time Polymerase Chain Reaction (qRT-PCR)

2.2.16.1 RNA extraction

For RNA extraction the RNeasyTM kit was used. Whole tissue extraction was performed on the proximal 5mm of the SI or colon or on whole tumours dissected from either the SI or colon which had previously been stored in RNAlaterTM at -80°C. The samples were removed from the RNAlaterTM, transferred to precellys pre-filled beads tubes and 350µl of Buffer RLT was added. The samples were homogenised using the Precellys®24-Dual tissue homogeniser and the resultant lysate aspirated, placed in an RNeasyTM spin column with 300µl of 70% ethanol added and mixed. The sample was centrifuged at 4°C at 10000rpm for 15 seconds and the flow-through discarded. 700µl Buffer RW1 was added to the spin easy column and the sample centrifuged for 15 seconds at 10000rpm, flow through discarded. 500µl Buffer RPE was added to the spin column and centrifuged for 15 seconds at 10000rpm, flow through discarded. 500µl Buffer RPE was added to the spin column and centrifuged for 2 minutes at 10000rpm, flow through discarded. The spin column was placed in a new 1.5ml collection tube and 30µl RNaseTM free water was added directly to the spin column membrane and centrifuged for 1 minute at 10000rpm. The elute from the previous step was again placed in the spin column and centrifuged for a further 1 minute. The resultant concentration of RNA was measured using the nanonvue (GE Healthcare) and stored at -80°C or was immediately used for reverse transcription to complement DNA (cDNA).

2.2.16.2 Reverse transcription of RNA to cDNA

Reverse transcription was performed using the Thermo Scientific DyNAmo SYBR Green 2-Step qRT-PCR Kit. 0.5µg of RNA was combined with 1µl Random Hexamer primer set (300ng/µl), 10µl 2x RT buffer, 2µl M-MuLV RNase H⁺ reverse

transcriptase and RNaseTM free water to a final volume of 20 μ l. The sample was placed in a PCR machine with a cycling protocol of 25 $^{\circ}$ C 10 minutes, 37 $^{\circ}$ C 30 minutes, 85 $^{\circ}$ C 5 minutes then held at 4 $^{\circ}$ C. The resultant cDNA was stored at -80 $^{\circ}$ C or used immediately for qRT-PCR.

2.2.16.3 qRT-PCR

The cDNA was diluted with RNaseTM free water at a dilution of 1:10. 5 μ l cDNA was combined with 10 μ l 2x Master mix, 1 μ l primer mix and 4 μ l RNaseTM free water. The samples were then placed in the Chromo4 (Bio-Rad) real-time PCR Detection System. The cycling protocol is as follows: 95 $^{\circ}$ C 15 minutes, 94 $^{\circ}$ C 10 seconds, X $^{\circ}$ C (5 $^{\circ}$ C below lower primer T_m) 25 seconds, 72 $^{\circ}$ C 30 seconds, 39 cycles, 72-95 $^{\circ}$ C 20 minutes.

The analysis was performed using Opticon Monitoring Software. 3 independent experiments were performed in duplicate for each sample.

2.2.17 Gene expression microarray

1 μ g RNA (n=4 WT, n=4 fascin KO) extracted from cultured small intestinal crypts was sent to Richard Talbot (The Roslin Institute, Edinburgh) for analysis using the Illumina WG6 array. The un-normalised probe level data analysis was performed by Gabriela Kalna, Head of Computational Biology, Beatson Institute. Illumina gene expression data set was analysed in Partek Genomics Suite Software. Log₂ transformation of the data and quantile normalisation was followed by the differential gene expression analysis using t-test. All p-values were corrected for multiple testing using Benjamini & Hochberg step up method that controls the false discovery rate. Finally, the fold change values were considered in ranking genes of interest.

2.2.18 Organotypic invasion model

The organotypic model has previously been described (Timpson, McGhee et al. 2011).

2.2.18.1 Preparation of collagen 1 from rat tails

12-15 juvenile rat-tails were washed in 70% ethanol and the tendons removed using toothed forceps. For every 1g of tendon, 250ml 0.5M acetic acid was added and stirred at 4°C for 48 hours. The solution was centrifuged at 10000rpm for 30 minutes and the pellet discarded. An equal volume of 10% NaCl was added to the supernatant and stirred at 4°C for 60 minutes then centrifuged at 10000rpm for 30 minutes. The supernatant was discarded and the precipitate re-dissolved in 0.25M acetic acid at 1:1 ratio then stirred for 24 hours at 4°C. The collagen solution was next dialysed against 6-8 changes of 6L 17.5mM acetic acid over the next 3 days. The collagen was next centrifuged at 26400rpm for 90 minutes, the supernatant removed and the concentration adjusted to approximately 2mg/ml.

2.2.18.2 Preparation of the 3D matrix

25ml of the collagen was added to 3ml 10x MEM and the pH adjusted to approximately 7.2 with the addition of 0.22M NaOH. 1×10^6 human fibroblasts were trypsinised and centrifuged at 400rpm for 5 minutes. The fibroblasts were re-suspended with 3ml FBS and immediately added to the collagen mixture on ice. 2.5ml was plated onto a sterile 35mm falcon dish and incubated at 37°C in 5% CO₂ for 5 minutes. Once solidified, 1ml of DMEM supplemented with 10% FBS was added and the collagen/fibroblast matrix detached carefully using a pipette. The next day a further 1ml DMEM supplemented with 10% FBS was added and the matrix was allowed to contract over the next 7-10 days with the medium being changed every second day.

2.2.18.3 Seeding of cells on matrix

The adenoma cell line was centrifuged at 600rpm for 5 minutes, washed once in PBS and again centrifuged. The PBS was removed and the pellet re-suspended in 1ml TryPLE and incubated at 37°C for 3 minutes. 5ml ADF was added and the number of cells counted. 1×10^5 cells were re-suspended in the adenoma culture

medium and added to the collagen/fibroblast matrix which had been placed in a 24 well falcon plate and incubated at 37° C in 5% CO₂ for 72 hours.

2.2.18.4 Transfer of matrix to grid

Stainless steel grids were cut using scissors to form a tripod and placed in a sterile 6cm falcon plate. The matrix was transferred onto the grid and adenoma culture medium was added so that the base of the matrix was submerged, but the top was not in order to generate a gradient promoting invasion. The cells were allowed to invade for 14 days with the medium being changed every second day. Once completed, the matrix was removed, cut longitudinally in half using a scalpel, fixed in 4% PFA at room temperature or methanol at -20° C for 30 minutes. They were then transferred to 10% NBF and sent to histology for processing.

References

- Bleich, A., M. Mahler, et al. (2004). "Refined histopathologic scoring system improves power to detect colitis QTL in mice." *Mamm Genome* **15**(11): 865-871.
- Greten, F. R., L. Eckmann, et al. (2004). "IKK beta links inflammation and tumorigenesis in a mouse model of colitis-associated cancer." *Cell* **118**(3): 285-296.
- Hingorani, S. R., E. F. Petricoin, et al. (2003). "Preinvasive and invasive ductal pancreatic cancer and its early detection in the mouse." *Cancer Cell* **4**(6): 437-450.
- Hingorani, S. R., L. F. Wang, et al. (2005). "Trp53(R172H) and KraS(G12D) cooperate to promote chromosomal instability and widely metastatic pancreatic ductal adenocarcinoma in mice." *Cancer Cell* **7**(5): 469-483.
- Ireland, H., R. Kemp, et al. (2004). "Inducible Cre-mediated control of gene expression in the murine gastrointestinal tract: Effect of loss of beta-catenin." *Gastroenterology* **126**(5): 1236-1246.
- Jonkers, J., R. Meuwissen, et al. (2001). "Synergistic tumor suppressor activity of BRCA2 and p53 in a conditional mouse model for breast cancer." *Nature Genetics* **29**(4): 418-425.
- Kielley, W. W. and W. F. Harrington (1960). "A Model for the Myosin Molecule." *Biochimica Et Biophysica Acta* **41**(3): 401-421.
- McClive, P. J. and A. H. Sinclair (2001). "Rapid DNA extraction and PCR-sexing of mouse embryos." *Molecular Reproduction and Development* **60**(2): 225-226.

- Millard, T. H., G. Bompard, et al. (2005). "Structural basis of filopodia formation induced by the IRSp53/MIM homology domain of human IRSp53." EMBO J **24**(2): 240-250.
- Okayasu, I., S. Hatakeyama, et al. (1990). "A Novel Method in the Induction of Reliable Experimental Acute and Chronic Ulcerative-Colitis in Mice." Gastroenterology **98**(3): 694-702.
- Olive, K. P., D. A. Tuveson, et al. (2004). "Mutant p53 gain of function in two mouse models of Li-Fraumeni syndrome." Cell **119**(6): 847-860.
- Pardee, J. D. and J. A. Spudich (1982). "Purification of Muscle Actin." Methods in Enzymology **85**: 164-181.
- Sato, T., D. E. Stange, et al. (2011). "Long-term expansion of epithelial organoids from human colon, adenoma, adenocarcinoma, and Barrett's epithelium." Gastroenterology **141**(5): 1762-1772.
- Sato, T., R. G. Vries, et al. (2009). "Single Lgr5 stem cells build crypt-villus structures in vitro without a mesenchymal niche." Nature **459**(7244): 262-265.
- Serrano, M., H.-W. Lee, et al. (1996). "Role of the INK4a Locus in Tumor Suppression and Cell Mortality." Cell **85**(1): 27-37.
- Shibata, H., K. Toyama, et al. (1997). "Rapid colorectal adenoma formation initiated by conditional targeting of the APC gene." Science **278**(5335): 120-123.
- Spudich, J. A. and S. Watt (1971). "The regulation of rabbit skeletal muscle contraction. I. Biochemical studies of the interaction of the tropomyosin-troponin complex with actin and the proteolytic fragments of myosin." Journal of Biological Chemistry **246**(15): 4866-4871.
- Timpson, P., E. J. McGhee, et al. (2011). "Organotypic collagen I assay: a malleable platform to assess cell behaviour in a 3-dimensional context." J Vis Exp(56): e3089.
- Yamakita, Y., F. Matsumura, et al. (2009). "Fascin1 is Dispensable For Mouse Development But is Favorable for Neonatal Survival." Cell Motility and the Cytoskeleton **66**(8): 524-534.

3 Chapter 3 – Fascin regulates small intestine regeneration and neutrophil recruitment in response to injury

3.1 Summary

Two of the key features in the pathogenesis of inflammatory bowel disease (IBD) are the histological changes to the intestinal epithelial barrier (Khor, Gardet et al. 2011), caused by the inflammation and the regenerative phase which follows. I demonstrate here that under normal homeostatic conditions, loss of fascin from the murine small intestine has no effect on small intestinal epithelial architecture or the number of proliferating cells on the crypt-villus axis. However, following irradiation of the mice, the degree of histological damage is mildly increased in the fascin KO, but also there is an enhanced number of proliferating cells in the crypt axis of the fascin KO regenerating crypts. This was further confirmed using the *in-vitro* crypt culture method, with enhanced expression of the intestinal stem cell gene *Lgr5* shown to drive increased proliferation in the absence of fascin.

Furthermore, there are fewer recruited neutrophils in the irradiated small intestines of the fascin KO mice compared with WT, and reduced levels of chemokines CXCL1 and CXCL2, with impaired dendritic cell function the likely cause.

3.2 Introduction

The expression of fascin in the GI tract appears to be transient, age and health status dependent. Fascin is present in cells of the GI tract during weeks 8-12 of embryogenesis in humans (Zhang, Tao et al. 2008), but absent in later weeks of gestation. Multiple studies have demonstrated either low levels or absence of fascin in normal adult epithelial tissue (Tan, Lewis et al. 2013) and, whilst fascin has been shown to be expressed in human samples of inflammatory conditions affecting the colon (Qualtrough, Smallwood et al. 2011), it is unknown whether fascin is expressed in small intestinal samples of IBD.

One of the pathological hallmarks of IBD is the infiltration of polymorphonuclear neutrophils (PMN) into the inflamed tissue (Larmonier, Midura-Kiela et al. 2011) in both Crohn's disease and ulcerative colitis (UC) specimens. The primary role

for neutrophils in the acute phase of inflammation involves the recognition and ingestion of extracellular pathogens. They are also crucial for the activation and regulation of both the innate and adaptive immune response, in particular the regulation of the immune cells (Mantovani, Cassatella et al. 2011). Fascin is expressed by dendritic cells (Pinkus, Lones et al. 2002), a key orchestrator of the immune response to inflammation through the production of chemokines upon maturation (McColl 2002). In this chapter I will show impaired recruitment of neutrophils in the fascin KO small intestine post irradiation. I hypothesise that this may, in part, be as a result of impaired dendritic cell function and consequent chemokine production.

The Wnt pathway is the principal regulator of intestinal physiology (Fevr, Robine et al. 2007) through β -catenin, which, once translocated to the nucleus, binds and activates transcription factors of the TCF/LEF family. The downstream effect on gene expression stimulates stem cell expansion and subsequent intestinal regeneration. In this chapter I will show that the loss of fascin permits enhanced intestinal proliferation through generic up regulation of Wnt members and targets, in particular the rapid cycling Lgr5 expressing stem cells located at the base of intestinal crypts (Barker, van Es et al. 2007).

3.3 Results

3.3.1 Characterisation of fascin KO small intestine with respect to WT

In our experiments, we have compared fascin expressing “wild type” (WT) and fascin knockout (KO) mice. The fascin KO is a global KO mouse that has been shown to be both healthy and to have no major developmental defects (Yamakita, Matsumura et al. 2009) and, with the exception of a larger lateral ventricle of the brain, is anatomically indistinguishable from WT (Yamakita, Matsumura et al. 2009).

We initially quantified the number and height of the crypts in the untreated small intestines of both WT and fascin KO mice and found no significant difference between the two (Fig. 3-1).

We next quantified the number of BrdU positive cells per crypt and the position of the highest BrdU positive cell in the crypt axis and also found no significant difference (Fig. 3-1).

Lastly, we quantified the number of paneth cells using the lysosyme antibody in order to determine whether loss of fascin affected the number in each crypt. A gene expression microarray (Sato, van Es et al. 2011) of isolated paneth cells (available at <http://www.ncbi.nlm.nih.gov/geo/query/acc.cgi?acc=GSE25109>) demonstrated that paneth cells express fascin, albeit at low levels at a level 3 fold higher than that found in the isolated Lgr5 cells. As such, we wished to determine whether loss of fascin would negatively affect the number of paneth cells in the fascin KO small intestine, however we found no significant difference ($p=0.700$) (Fig. 3.1). This correlated with the qRT-PCR analysis of the whole tissue extract for lysosyme, which also showed no significant difference (not shown).

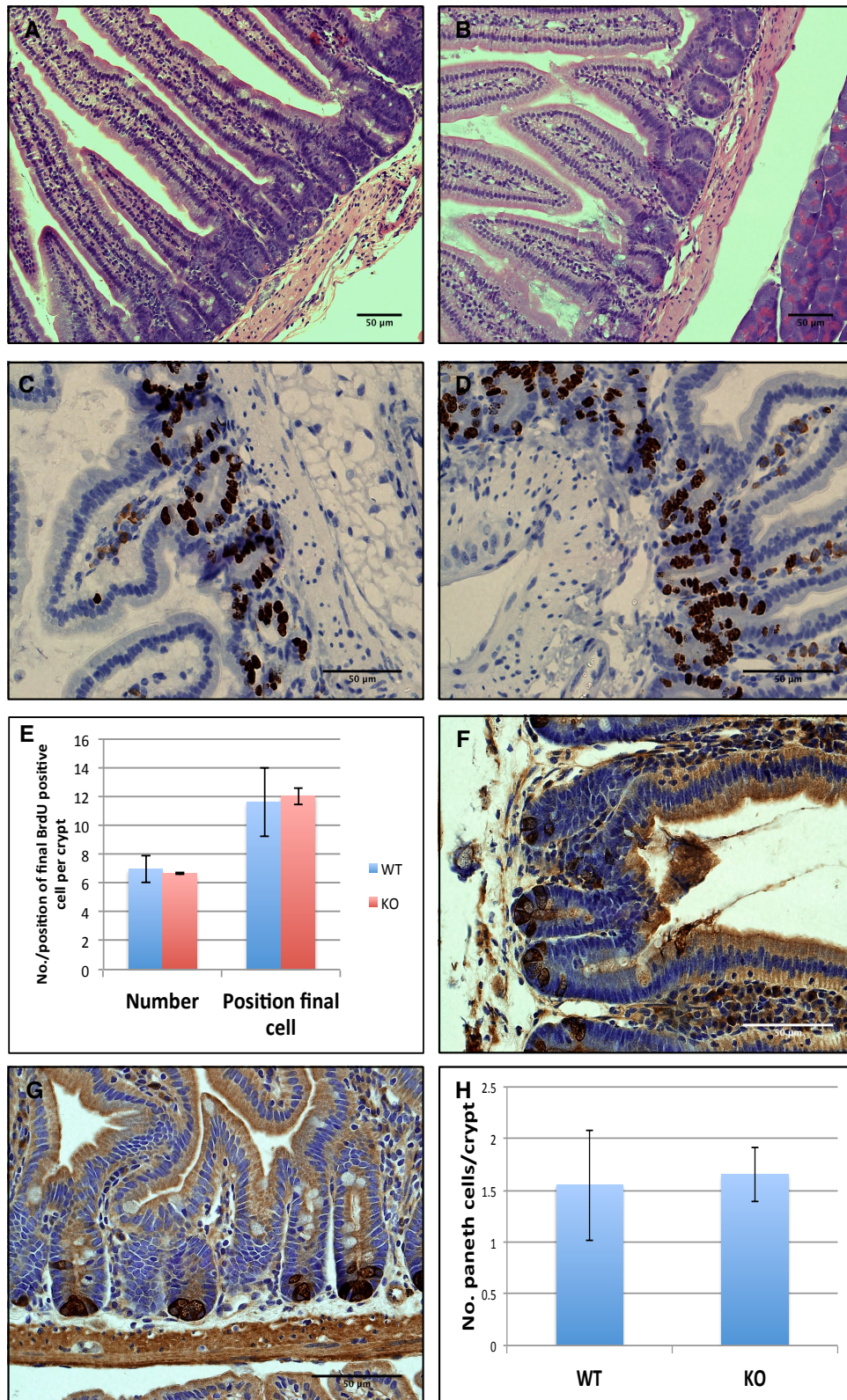


Figure 3-1 Characterisation of untreated fascin KO small intestine with respect to WT

No difference between the number or height of crypts in WT (A) and fascin KO (B) untreated small intestine (H&E stained). WT (C) and fascin KO (D) BrdU stained small intestine demonstrating no difference (E) in the number or position of highest BrdU positive cell on the crypt axis (representative images of n=2 independent experiments with 25 crypts counted independently per sample. Error bars represent standard deviation (SD)). WT (F) and fascin KO (G) small intestines stained with lysosyme antibody demonstrating no significant difference in the number of paneth cells (H) (n=3, p=0.700 Mann-Whitney test. Error bars represent SD).

We first compared the gene expression levels of key genes, using qRT-PCR in the small intestines of untreated fascin KO and WT mice using whole tissue extracted from the mice. Interestingly, despite no microscopic change in the small intestines we found significantly lower levels of the proliferative marker Ki67 in the fascin KO and also significantly lower levels of the intestinal stem cell marker Lgr5 ($p=8.29E-07$) in the fascin KO compared with the WT (Fig. 3-2). Both Ki67 and BrdU are well-recognised proliferative markers, but they differ in key aspects. BrdU is a thymidine analogue and is incorporated into the DNA and typically marks only cells actively synthesising DNA (although it remains incorporated after synthesis and is passed down to the daughter cells). Ki67 is less specific and is a protein-based antibody therefore does not need to be injected into the mouse. It marks dividing cells throughout most of the mitotic process with the exception of the resting phase, G0.

We also checked the levels of Olfm4 and Nrn1, two genes that were found from a mass spectrometry analysis of Lgr5 and their daughter cells (Munoz, Stange et al. 2012), however we found no significant difference (Olfm4 $p=0.489$. Nrn1 $p=0.395$) between WT and fascin KO (Fig. 3-2).

We wished to identify whether the lower levels of Lgr5 mRNA (in the fascin KO) was due to lower Wnt signalling in the fascin KO small intestine so we checked the levels of the Wnt ligand (Wnt3a), other Wnt pathway members Axin2, APC, β -catenin and Wnt targets c-Myc, LEF1, Cyclin D1 and Cyclin D2. β -catenin ($p=0.000138$), APC ($p=0.0134$) and c-Myc ($p=0.0318$) were significantly lower in the fascin KO whereas there was no significant difference with Wnt3a ($p=0.421$), Axin2 ($p=0.113$), LEF1 ($p=0.163$), Cyclin D1 ($p=0.303$) and Cyclin D2 ($p=0.453$) (Fig. 3-2). Given that Lgr5 is a target gene of NF- κ B (Schwitalla, Fingerle et al. 2013), we also looked at the level of NF- κ B and the upstream cytokine TNF α to determine whether these correlated with the observed decrease in Lgr5 in the fascin KO. Both TNF α ($p=0.0138$) and NF- κ B ($p=0.00189$) were significantly lower in the fascin KO (Fig. 3-2). None of the genes we looked at were expressed significantly higher in the untreated fascin KO small intestine. Lastly, we quantified the levels of chemokines CXCL1, CXCL2 and CXCL5 and CXC receptor CXCR2 in the untreated small intestine and found significantly reduced levels of CXCL1 ($p=0.00384$) and CXCL5 ($p=0.0414$) in the fascin KO, no significant

difference in CXCL2 ($p=0.122$) and no significant difference in the chemokine receptor CXCR2 ($p=0.407$) (Fig. 3.2). Thus, we conclude that, in physiological conditions fascin loss resulted in lower levels of basal TNF α and NF- κ B mRNA, as well as lower levels of some CXCL chemokines. This may account for the lower overall proliferation rate and lower Lgr5 mRNA also detected in the fascin KO. However, the changes are complex, requiring further investigation to determine which may be causal of actual phenotype changes.

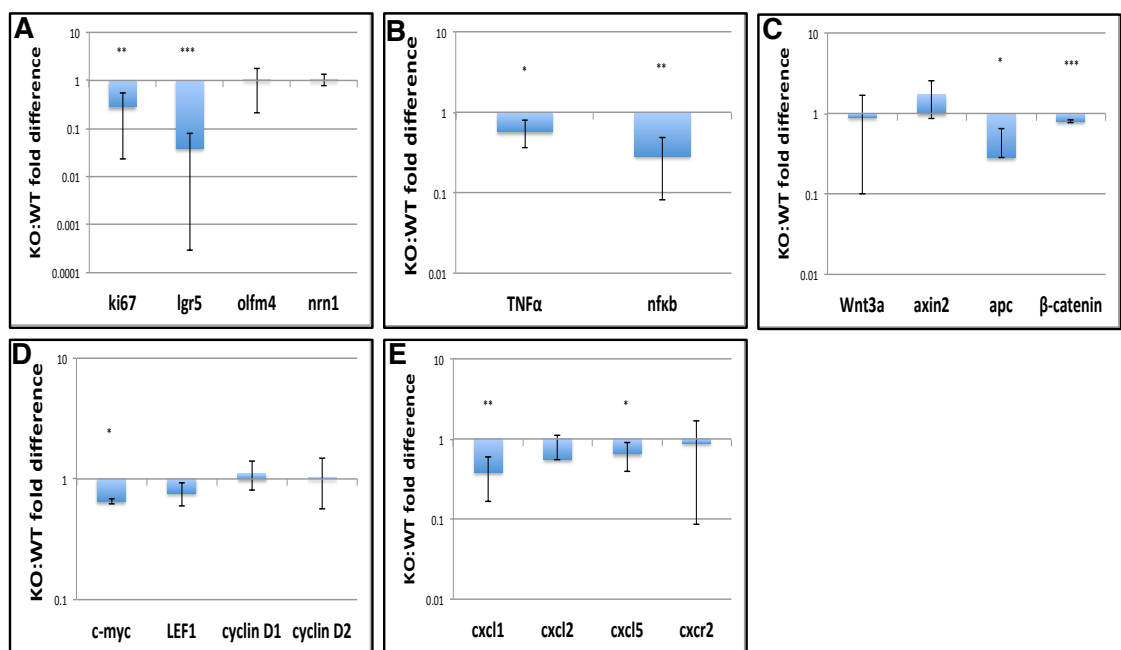


Figure 3-2 qRT-PCR data of untreated whole tissue extraction comparing WT and fascin KO small intestines

Logarithmic scales demonstrating significantly reduced levels of Ki67 ($p=0.00436$), Lgr5 ($p=8.29E-07$) (A), TNF α ($p=0.0138$) and NF- κ B ($p=0.00189$) (B) in the untreated fascin KO small intestine. There was no significant difference between Olfm4 ($p=0.489$) or Nrn1 ($p=0.395$). Examination of Wnt ligand ($p=0.421$) levels demonstrate no significant difference between WT and fascin KO and further analysis of Wnt members shows significantly reduced levels of APC ($p=0.0134$) and β -catenin ($p=0.000138$) in the fascin KO (C). Wnt target c-Myc ($p=0.0318$) was significantly reduced in the fascin KO, whilst there was no significant difference with regards LEF1 ($p=0.163$), Cyclin D1 ($p=0.303$) and Cyclin D2 ($p=0.453$). When we examined the various neutrophil related chemokines CXCL1 ($p=0.00384$) and CXCL5 ($p=0.0414$) were significantly lower in the fascin KO whilst there was no significant difference in CXCL2 ($p=0.122$) or the chemokine receptor CXCR2 ($p=0.407$) (E). Statistical analysis using Student's t-test, $n=3$ for each sample. Error bars represent SD. Significance asterisks: * = <0.05 , ** = <0.01 , *** = <0.001 .

3.3.2 Fascin expression in untreated and regenerating small intestine

Multiple studies have demonstrated low levels or absence of fascin in normal epithelial tissue (Tan, Lewis et al. 2013), so we first characterised the expression of fascin in the small intestines of untreated WT mice using immunohistochemistry (IHC), Western blot (WB) and qRT-PCR. Fascin expression was absent from IHC using the fascin antibody - only non-specific background staining of the villi was seen which was also demonstrated in the fascin KO negative controls. Protein levels of fascin within the tissues were only demonstrable in WB with the use of the Femto substrate (Fig. 3-3). Low levels were also detected using qRT-PCR (Fig. 3-3). 72 hours post irradiation we repeated the qRT-PCR on whole tissue extracted from WT small intestine and found that the level of fascin mRNA had risen by almost 50% compared with untreated small intestine. Protein levels also appeared higher by IHC (Fig. 3.3).

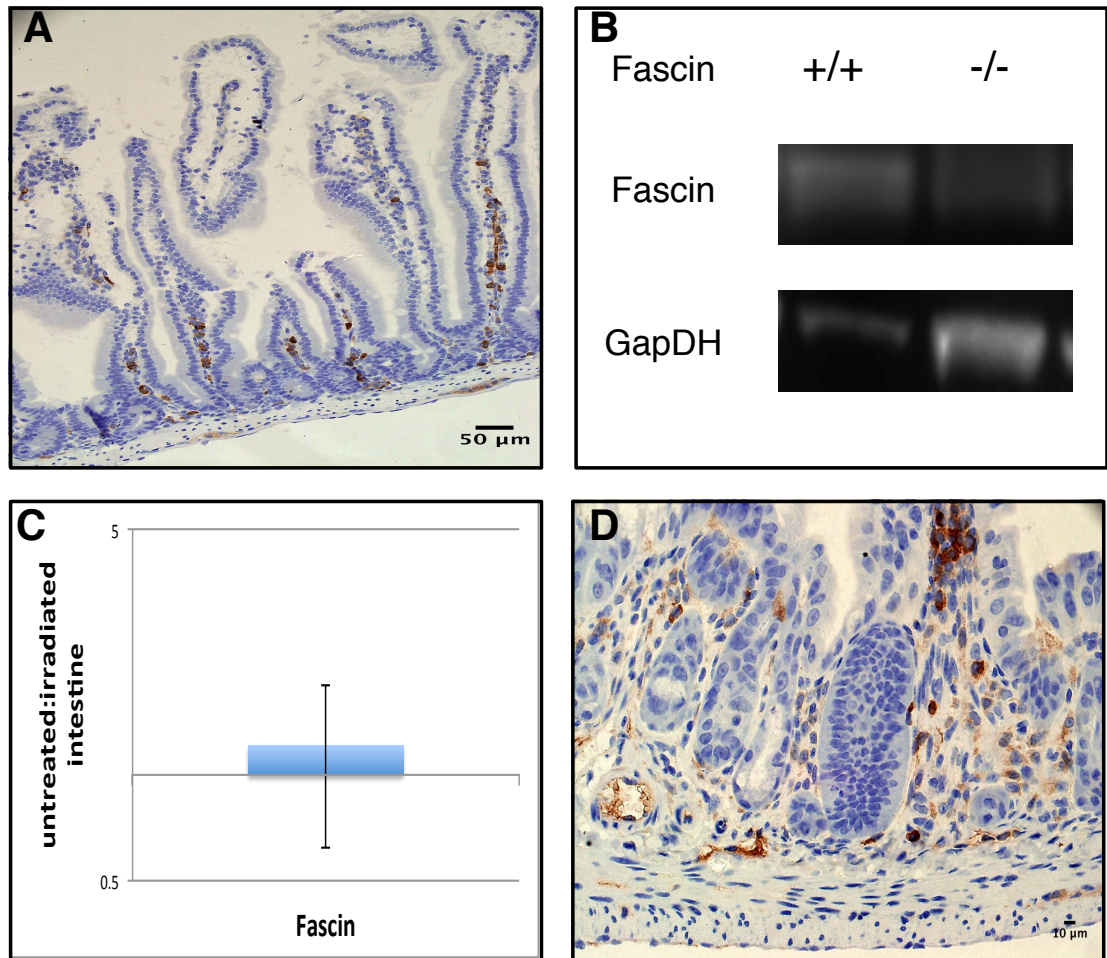


Figure 3-3 Fascin expression in untreated and irradiated small intestine

Only non-specific staining of fascin (brown) was detectable in the untreated WT villi (A) – this was also seen in the negative controls (fascin KO) and was deemed to be not significant. Protein levels of fascin were only detected at low levels in WB using femto substrate (B). Images representative of 3 independent experiments. 72 hours post irradiation in the regenerating small intestine the level of fascin had risen by 50% compared with untreated tissue as demonstrated with qRT-PCR (C) and IHC (D). Error bars represent SD.

3.3.3 Loss of fascin results in a mild increase in histological damage in small intestinal time course post irradiation

In order to determine the effect loss of fascin has on radiation damaged small intestines we set up an irradiation time course whereby we irradiated the mice with 14Gy gamma irradiation (resulting in the ablation of small intestinal crypts and endothelial cells, following which, a small number of surviving small intestinal stem cells (ISCs) differentiate and expand to form regenerating crypts (Potten and Hendry 1975)), then culled the mice (using schedule 1 procedures in accordance with Home Office guidelines) at time points of 6, 24 and 72 hours. The histological damage was assessed, blind, by a pathology trainee using The

Jackson Laboratory (TJL) scoring system developed at the Hannover Medical School (Bleich, Mahler et al. 2004). This incorporated four criteria which were subjectively used, microscopically to assess and compare the histological damage notably (1) severity, (2) degree of hyperplasia, (3) degree of ulceration and (4) percentage of area involved. A score of 0-3 was used (0 being no damage, 3 being maximal) for the four categories and the overall score was determined. At the 6 hour time point both WT and fascin KO scored 4 out of a maximal 16, whereas at the 24 hour time point the fascin KO scored 6/16 and the WT 5/16 indicating marginally increased damage in the fascin KO 24 hours post 12Gy irradiation ($p=0.0791$, Mann Whitney test). At the 72 hour time point both WT and fascin KO were assessed as 6/16 ($n=3$ for each time point) (Fig. 3.4).

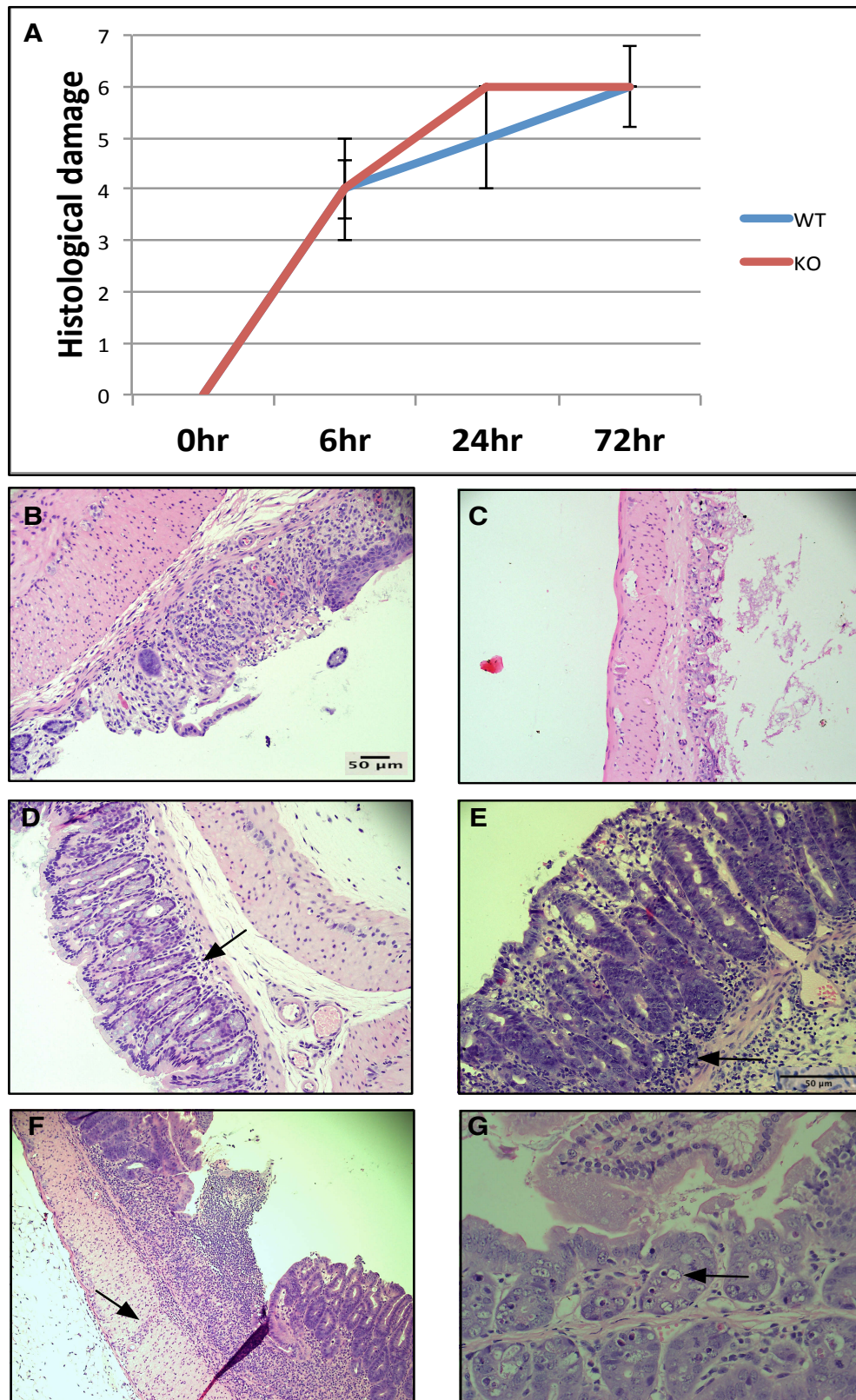


Figure 3-4 Small intestine irradiation time course

A) Histological damage demonstrates a hint of more damage in the fascin KO small intestine at the 24 hour time point ($p=0.791$), compared with WT: $n=3$ per time point. Error bars represent SD. B) Example of severity score of 1 and C) worsening severity scored as 3. D) Evidence (arrowed) of moderate hyperplasia (score of 1) and E) severe hyperplasia (arrowed) with a score of 3. F) Evidence of ulceration (arrowed) with score of 1 and G) vacuolated cell (arrowed) which were commoner in the fascin KO.

3.3.4 Loss of fascin results in enhanced proliferation after irradiation

Given the enhanced levels of Lgr5 stem cells and other Wnt targets in the untreated WT small intestines we wished to determine whether this would positively or negatively affect proliferation in the WT regenerating small intestines in response to the irradiation. We first quantified the number ($p=0.476$) and height ($p=0.264$) of regenerating crypts in the mice 72 hours after irradiation, but found no significant difference between WT and fascin KO (Fig. 3-5). We next quantified the number of and position of the highest BrdU positive cell in the crypt axis to examine any defect in proliferation in the fascin KO. Surprisingly, there were significantly higher numbers ($p=0.0143$) of BrdU positive cells in the KO and also the position ($p=0.0143$) of the highest BrdU positive cell in the crypt axis was significantly higher in the fascin KO indicating enhanced proliferation in the fascin KO (Fig. 3-5). We next wanted to determine whether there were any gene expression changes that might explain the observed phenotype. Using qRT-PCR of whole tissue extracted at the 72 hour time point from the irradiated small intestines, we examined the same gene set as for the untreated small intestines and found that, in contrast to the untreated data (in which there were significantly lower levels of Lgr5 and other Wnt targets in the fascin KO), we found the opposite in that there were significantly elevated levels of β -catenin ($p=0.00904$) and targets Lgr5 ($p=0.00173$) and c-Myc ($p=0.0171$) in the fascin KO (Fig. 3-5). It was notable that the level of Lgr5 was 5 fold higher in the regenerating small intestine of the fascin KO. There was no significant difference in the levels of Wnt3a (not shown), Axin2 ($p=0.262$), Olfm4 ($p=0.293$) or Nrn1 ($p=0.348$). We again looked at the levels of TNF α ($p=0.170$) and NF- κ B ($p=0.343$) however, unlike the untreated small intestines, there was no significant difference in the irradiated small intestines (Fig. 3-5). Lastly we performed FACS cell cycle analysis of crypt cells extracted from small intestines 72 hours following irradiation. This was, however inconsistent with our BrdU quantification data and demonstrated decreased numbers of fascin KO crypt cells in the S phase with more in G1 (Fig. 3.5). We predicted that, given that there were enhanced numbers of BrdU positive cells in the fascin KO regenerating small intestine, this would correlate with higher numbers of fascin KO crypt cells in the S-phase of the cell cycle when DNA is actively replicated. This, however was not the case, although the FACS results were not significant

so definitive conclusions cannot be made. The administered dose and duration from injection of BrdU to culling is very important in ensuring consistency of results. It must be stressed that there was considerable difficulty gaining sufficient cells to perform the FACS analysis. It was necessary to pool crypt extracts from 3 mice and, despite this there were often less than the required optimal number of cells in each phase of the cell cycle thereby affecting the accuracy and reliability of the final analysis. Despite this discrepancy, we conclude that fascin KO small intestines have an enhanced proliferative response following irradiation and show elevated levels of some Wnt signalling and target genes.

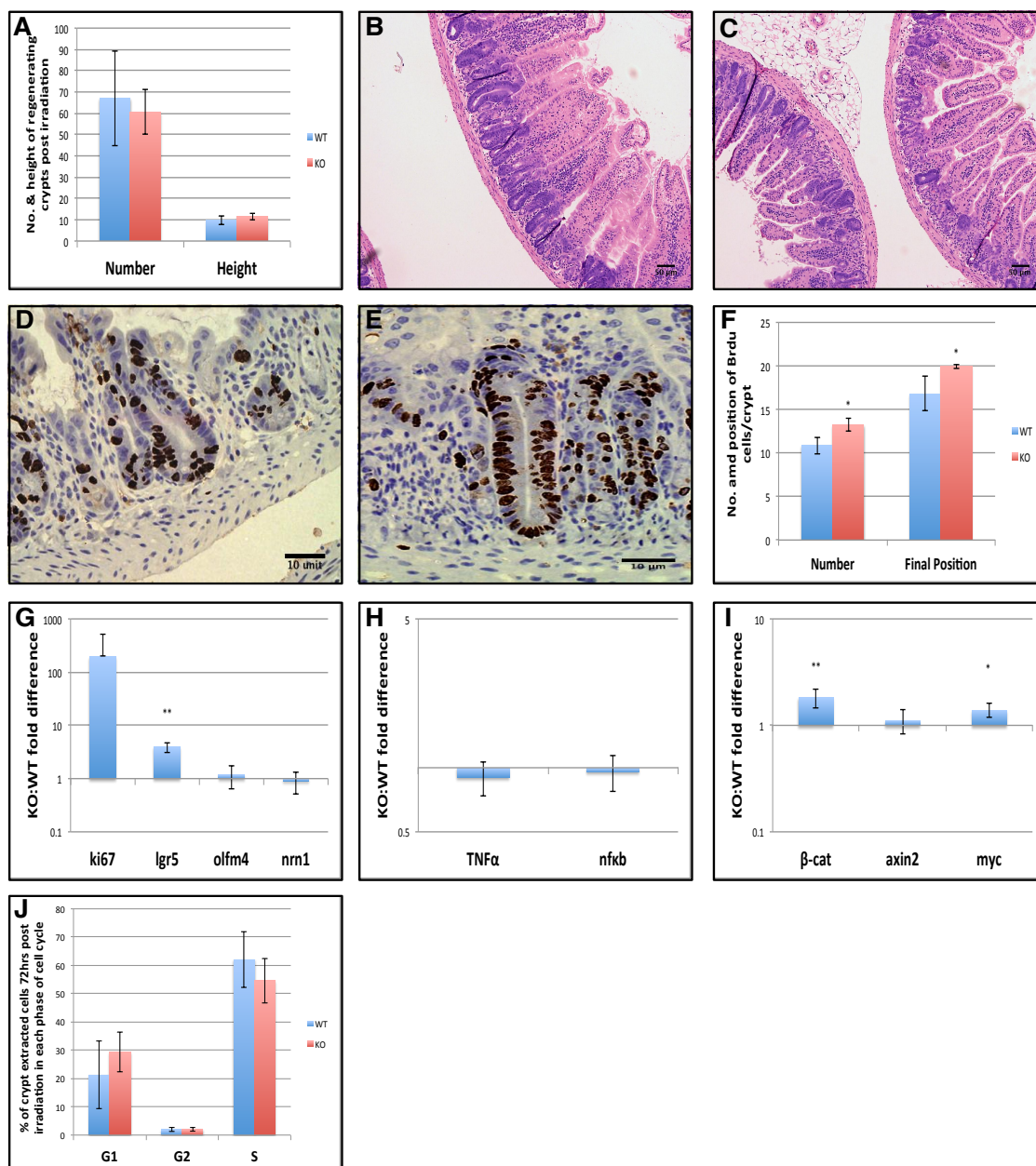


Figure 3-5 Enhanced small intestinal crypt proliferation in the fascin KO in response to irradiation

72 hours post irradiation of the mice, there was no significant difference in either the number ($p=0.476$) or height ($p=0.264$) of regenerating crypts (A) between WT (B) and fascin KO (C). WT (D) and fascin KO (E) small intestines with BrdU staining demonstrating that both the number ($p=0.0143$) and position ($p=0.0143$) of the final BrdU positive cell in the crypt axis was significantly higher in the fascin KO (F) indicating enhanced proliferation in the absence of fascin ($n=4$ with 11-23 crypts independently counted per sample, Mann-Whitney test). Images representative of 4 independent experiments. qRT-PCR analysis of whole tissue extracted from small intestines 72 post irradiation demonstrating a trend, albeit not significant, towards enhanced levels of Ki67 ($p=0.165$) and significantly enhanced levels of Lgr5 ($p=0.00173$) in the fascin KO. There was no significant difference in either Olfm4 ($p=0.293$) or Nrn1 ($p=0.348$) (G). No significant difference in the levels of TNF α ($p=0.170$) or NF- κ B ($p=0.343$) (H), however significantly elevated levels of β -catenin ($p=0.00904$) and c-Myc ($p=0.0171$) in the fascin KO, whilst no significant difference in Axin2 ($p=0.262$) (I). FACS cell cycle analysis demonstrating a trend towards a lower percentage of fascin KO crypt cells in the S phase with higher numbers in G1, although not significant: $n=3$ each sample was made from 2 pooled epithelial extractions in age/sex matched mice. For qRT-PCR statistical analysis, $n=3$, student's t-test. Error bars represent SD. Significance asterisks: * = <0.05 , ** = <0.01 , *** = <0.001 .

3.3.5 Loss of fascin results in impaired neutrophil recruitment in regenerating small intestines post irradiation

The importance of the immune response to inflammation (Brown and Mayer 2007) is well recognised. Dendritic cells are key mediators of this immune response (Banchereau and Steinman 1998) and are well known to express fascin (Pinkus, Pinkus et al. 1997). It was important, therefore to determine the effect that loss of fascin *in-vivo* had on the immune response in the small intestine post irradiation. We initially quantified the number of neutrophils (using the anti-neutrophil antibody NIMP on IHC sections) in the regenerating small intestines of WT and fascin KO mice 72 hours post 12Gy irradiation. We demonstrated significantly reduced numbers of neutrophils in the fascin KO ($p=0.0383$) compared with WT (Fig. 3-6). We attempted on numerous occasions to optimise an anti-dendritic cell antibody for use in our mouse IHC samples, however we were unable to achieve positive staining even with positive controls. Given that dendritic cells express fascin, it would have been useful to double stain the regenerating intestines with an anti-fascin and an anti-dendritic cell antibody to further characterise the cells which express fascin in the tissue, however further work is needed to acquire a reliable anti-dendritic cell antibody. We next performed a Western Blot on isolated neutrophils (supplied by Dr. Philip Hawkins, University of Cambridge) to determine whether they expressed fascin, however no expression was seen (Fig. 3-6). We further wished to understand mechanistically the observed reduction in neutrophil recruitment in the fascin KO so, using qRT-PCR we quantified the levels of the CXCL ligands 1,2 and 5 and the chemokine receptor CXCR2 in whole tissue extracted from the irradiated small intestines at the 72 hour time point. We found significantly reduced levels of CXCL1 ($p=0.0136$) and CXCL2 ($p=0.000879$) and reduced levels of the receptor CXCR2 ($p=0.0591$) in the fascin KO (Fig. 3-6). There was no difference noted in CXCL5 ($p=0.464$) (Fig 3.6). Collectively, these findings indicate the phenotype seen may be in part CXC chemokine mediated. It would be desirable to have a time course of these levels to know whether the fascin KO showed a delayed or fully impaired response, but with the data currently available, we conclude that the neutrophil response is reduced.

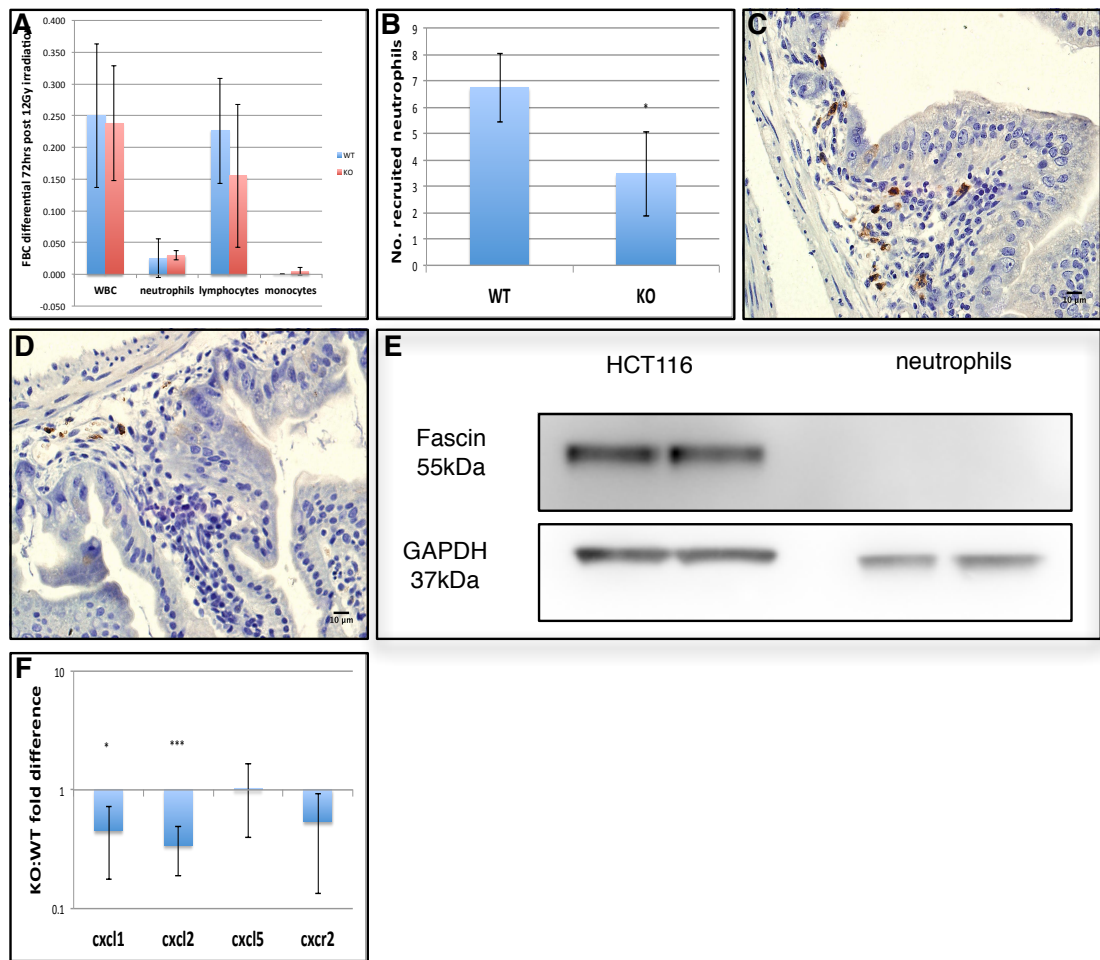


Figure 3-6 Impaired neutrophil recruitment in the fascin KO is likely chemokine mediated

Full blood count analysis of WT and fascin KO 72 hours post irradiation showing as expected global reduction in all blood cells (A) (n=3). We next quantified (B) the number of neutrophils recruited 72 hours post irradiation of WT (C) and fascin KO (D) small intestines and demonstrated a significant reduction of neutrophils in the fascin KO (p=0.0383, n=3 with 5 FOVs independently counted per mouse, Mann Whitney test). Images representative of 3 independent experiments. Western blot (E) showing that neutrophils do not express fascin, Image representative of 3 independent experiments. qRT-PCR analysis (F) of whole tissue extracted from the small intestines of WT and fascin KO mice 72 hours post irradiation demonstrating a significant reduction in the levels of the chemokines CXCL1 (p=0.0136) and CXCL2 (p=0.000879) in the fascin KO. No significant difference in the level of CXCL5 (p=0.464). Reduced levels of CXCR2 (p=0.0591) in the fascin KO. qRT-PCR data statistical analyses, n=3, student's t-test. Error bars represent SD. Significance asterisks: * = <0.05, ** = <0.01, *** = <0.001.

3.3.6 Fascin KO crypts have impaired proliferation *in-vitro* in standard medium

Given the enhanced fascin KO crypt proliferation *in-vivo* post irradiation, we wished to determine whether this could be replicated *in-vitro*. Using the crypt culture technique pioneered by the Clevers lab (Sato, Vries et al. 2009), we initially characterised the growth and the number of crypt fission events of isolated small intestinal crypts in standard medium over an 8 day period. The

growth of the WT crypts was significantly greater ($p=3.26E-07$ day 6) than the fascin KO and they also underwent significantly more fission events ($p=0.00757$ day 4) (Fig. 3-7). It was noted that the difference in growth and fission was most apparent during the initial 6 days of culture. After this time point, the difference was less pronounced (Fig. 3.7). Ki67 staining was performed and this demonstrated an enhanced number of proliferating cells in the WT (Fig. 3-8). We also assessed the levels of stem cell markers and Wnt pathway members and targets in these cultured crypts. Using qRT-PCR, we demonstrated a trend towards lower levels of all stem cell markers in the fascin KO with *Lgr5* ($p=0.0461$) and *Nrn1* ($p=0.00443$) significant (Fig. 3-8). The same Wnt members and targets were analysed as earlier, however there was no significant difference between WT and fascin KO (Fig. 3-8). We next looked at the levels of TNF α , NF- κ B and other members of the jak-stat signalling pathway. Whilst all members showed a trend towards lower levels in the fascin KO, only NF- κ B ($p=0.0215$), Il-11 ($p=0.0279$), Jak1 ($p=0.0195$) and Jak2 ($p=0.0359$) were significant (Fig. 3-8).

FACS cell cycle analysis of the percentage of WT and fascin KO cells in each phase of the cell cycle demonstrated slightly higher numbers of fascin KO cells in the S phase and in G1, although this was not significant (Fig. 3.8).

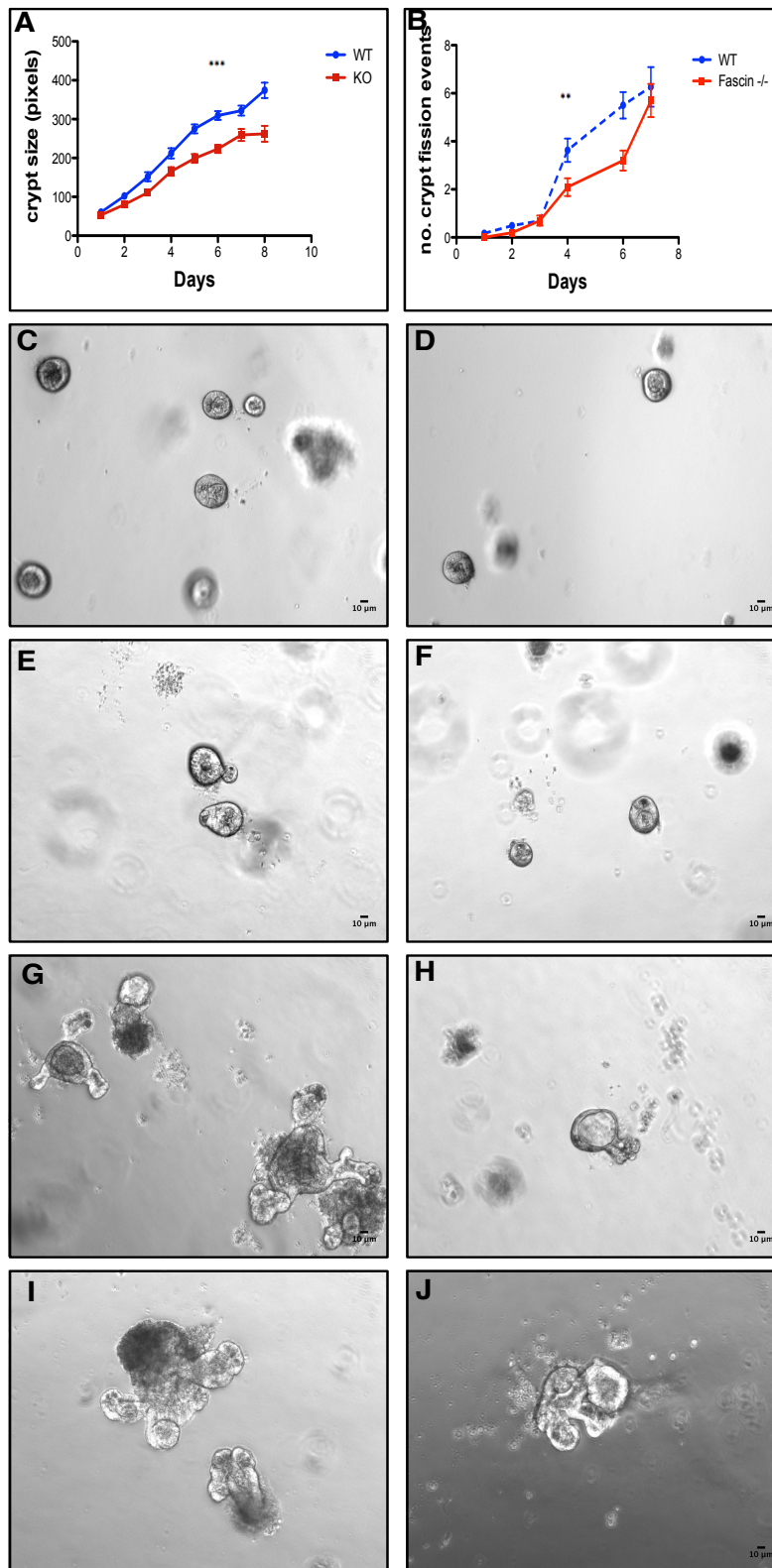


Figure 3-7 Fascin KO small intestinal crypts have impaired proliferation and reduced crypt fission in standard medium

When cultured in standard medium, the fascin KO crypts grew significantly slower ($p=3.26E-07$, day 6 student's t-test) (A) and underwent significantly fewer crypt fission events than WT ($p=0.00757$, day 4, student's t-test) (B). WT (C) and fascin KO (D) crypts day 1. WT (E) and fascin KO (F) day 2. WT (G) and fascin KO (H) day 5. WT (I) and fascin KO (J) day 7. $n=3$ with a minimum of 40 crypts counted per time point. Images representative of 3 independent experiments. Error bars represent SD. Significance asterisks: * = <0.05 , ** = <0.01 , *** = <0.001

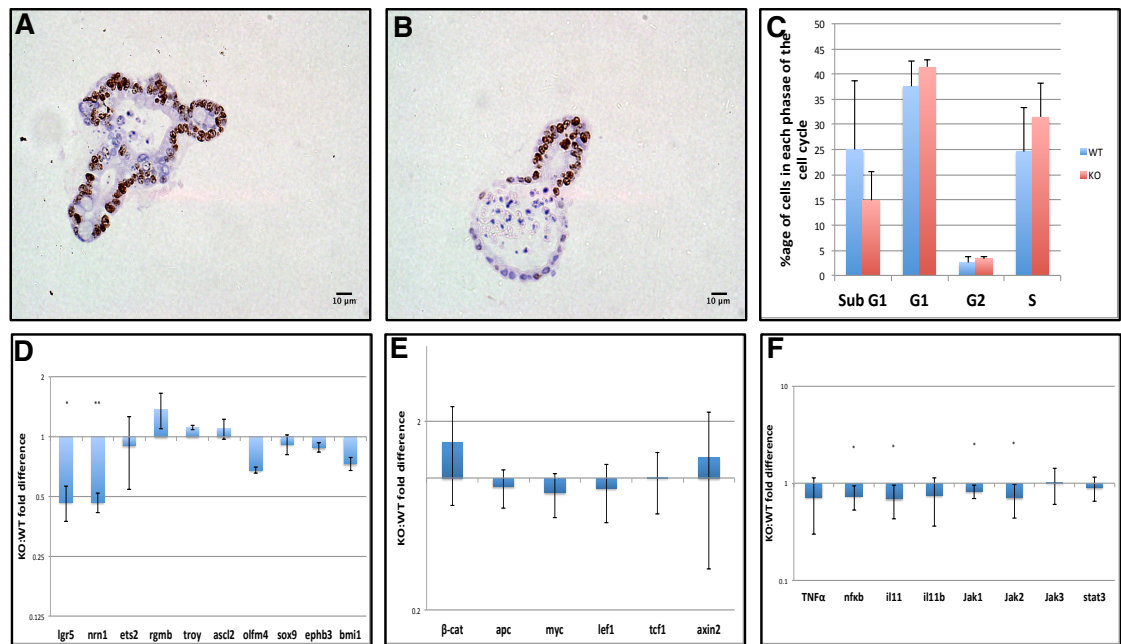


Figure 3-8 Fascin KO crypts have impaired proliferation *in-vitro* in standard medium

Ki67 staining of Agarose embedded WT (A) and fascin KO (B) crypts 4 days after culture demonstrating enhanced proliferation in the WT. Images representative of 3 independent experiments. FACS analysis of cell cycle (C) demonstrating higher numbers of fascin KO cells in the S phase and in G1, although not significant: n=3 independent experiments). qRT-PCR analysis of the WT and fascin KO crypts showing significantly lower levels of Lgr5 (p=0.0461) and Nrn1 (p=0.00443) and lower levels of the majority of the other stem cells in the fascin KO compared with WT (D). qRT-PCR analysis of the Wnt members and targets showing no significant change between WT and fascin KO (E). qRT-PCR analysis of the jak-stat pathway demonstrating, in general, lower levels of the majority of members in the fascin KO with significantly lower levels of NF- κ B (p=0.0216), O(p=0.0279), Jak1 (p=0.0195) and Jak2 (p=0.0359) (F). qRT-PCR data statistical analyses, n=3, student's t-test. Error bars represent SD. Significance asterisks: * = <0.05, ** = <0.01, *** = <0.001.

3.3.7 Fascin KO crypts have enhanced proliferation upon addition of Wnt3a

In order to replicate regeneration *in-vitro*, we added exogenous Wnt3a to the crypt culture medium for 5 days. Both the growth (p=5.45E-06) of the fascin KO crypts and the number of fission events (p=0.0290) was now greater in the fascin KO compared with WT (Fig. 3-9). Ki67 staining also demonstrated an enhanced number of proliferating cells in the fascin KO. We again performed FACS cell cycle analysis of crypts, which had been in standard medium with exogenous Wnt3a for 5 days and this demonstrated higher numbers of fascin KO cells in S phase and in G1, although not significant (Fig. 3-9). We repeated the gene expression analysis using qRT-PCR and demonstrated that the majority of stem cell markers were now higher in the fascin KO with significance being shown in Lgr5 (p=0.0489), Ets2 (p=0.0485), Rgmb (p=0.00872), Tnfrsf19 (p=0.00198) and

Ascl2 ($p=0.0498$) (Fig. 3-9). We further analysed the Wnt members and targets we had looked at previously and this demonstrated a significant increase in the levels of β -catenin ($p=0.0177$) in the fascin KO, whereas APC ($p=0.048$) was significantly lower in the fascin KO (Fig. 3-9). There was no significant difference in the levels of c-Myc ($p=0.152$), LEF1 ($p=0.426$), TCF1 ($p=0.108$) or Axin2 ($p=0.726$) (Fig. 3-9). We again looked at the levels of TNF α , NF- κ B and other members of the jak-stat signalling pathway and this showed a trend, albeit not significant, towards increased levels of all markers in the fascin KO following the addition of Wnt3a to the medium in contrast to the standard medium conditions (Fig 3.9).

We wished to determine whether fascin could be detected in WT crypts in standard medium, however a Western Blot demonstrated no expression (Fig. 3-10). We further wished to examine whether fascin expression could be induced with either Wnt3a or the cytokine Oncostatin M (OSM). OSM has been shown (in breast cancer cells), through activation of Il-6 and Stat3 to directly regulate fascin expression (Snyder, Huang et al. 2011), however neither resulted in expression of fascin in the crypts, as demonstrated by WB (Fig 3.10).

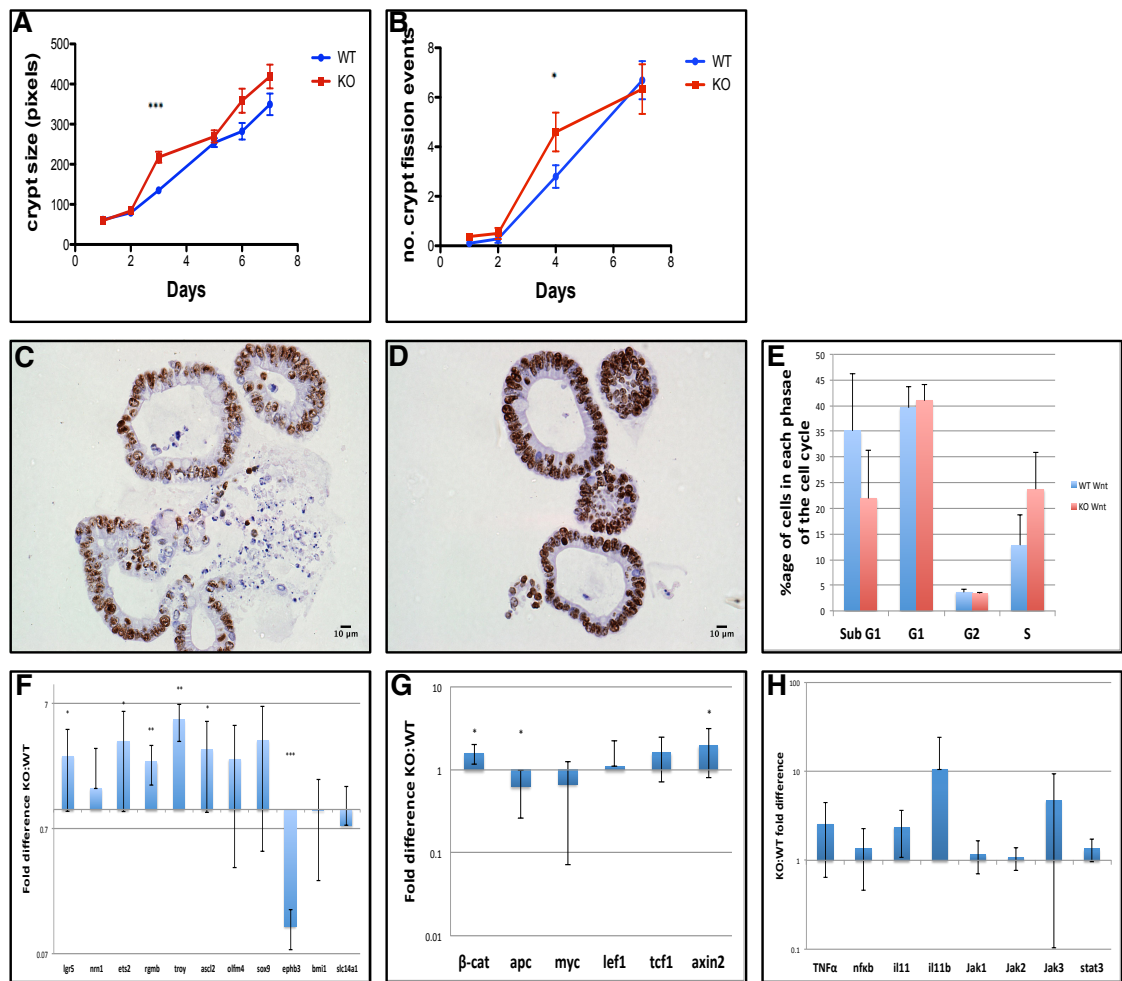


Figure 3-9 Fascin KO crypts have enhanced proliferation upon addition of Wnt3a

In contrast to the standard medium conditions, upon addition of exogenous Wnt3a to the standard crypt medium the fascin KO crypts grew significantly faster ($p=5.45E-06$, day 3, student's t-test) (A) and undergo significantly more fission events ($p=0.0290$, day 4, student's t-test) (B) compared with WT ($n=3$ independent experiments per time point). Ki67 staining of Agarose embedded WT (C) and fascin KO (D) crypts indicates enhanced proliferation in the fascin KO: images representative of 3 independent experiments. FACS analysis of cell cycle (E) of crypts in Wnt3a conditioned medium demonstrating a higher percentage of fascin KO cells in S phase, although not significant, $n=3$ independent experiments. qRT-PCR analysis of the crypts following 5 days of Wnt3a demonstrates that the majority of stem cell markers are now higher in the fascin KO crypts (F) with significance seen in *Lgr5* ($p=0.0489$), *Ets2* ($p=0.0485$), *Rgmb* ($p=0.00872$), *Tnfrsf19* ($p=0.00198$) and *Ascl2* ($p=0.0498$). Wnt members analysis (G) shows a significant increase in the levels of β -catenin ($p=0.0177$) and Axin2 ($p=0.0726$) in the fascin KO, whereas APC ($p=0.0484$) was significantly lower in the fascin KO. Finally, analysis of the members of the jak-stat pathway shows increased levels of all markers in the fascin KO (H) following the addition of Wnt3a to the medium in contrast to the standard medium conditions, albeit not significant. Error bars represent SD. Significance asterisks: * = <0.05 , ** = <0.01 , *** = <0.001 .

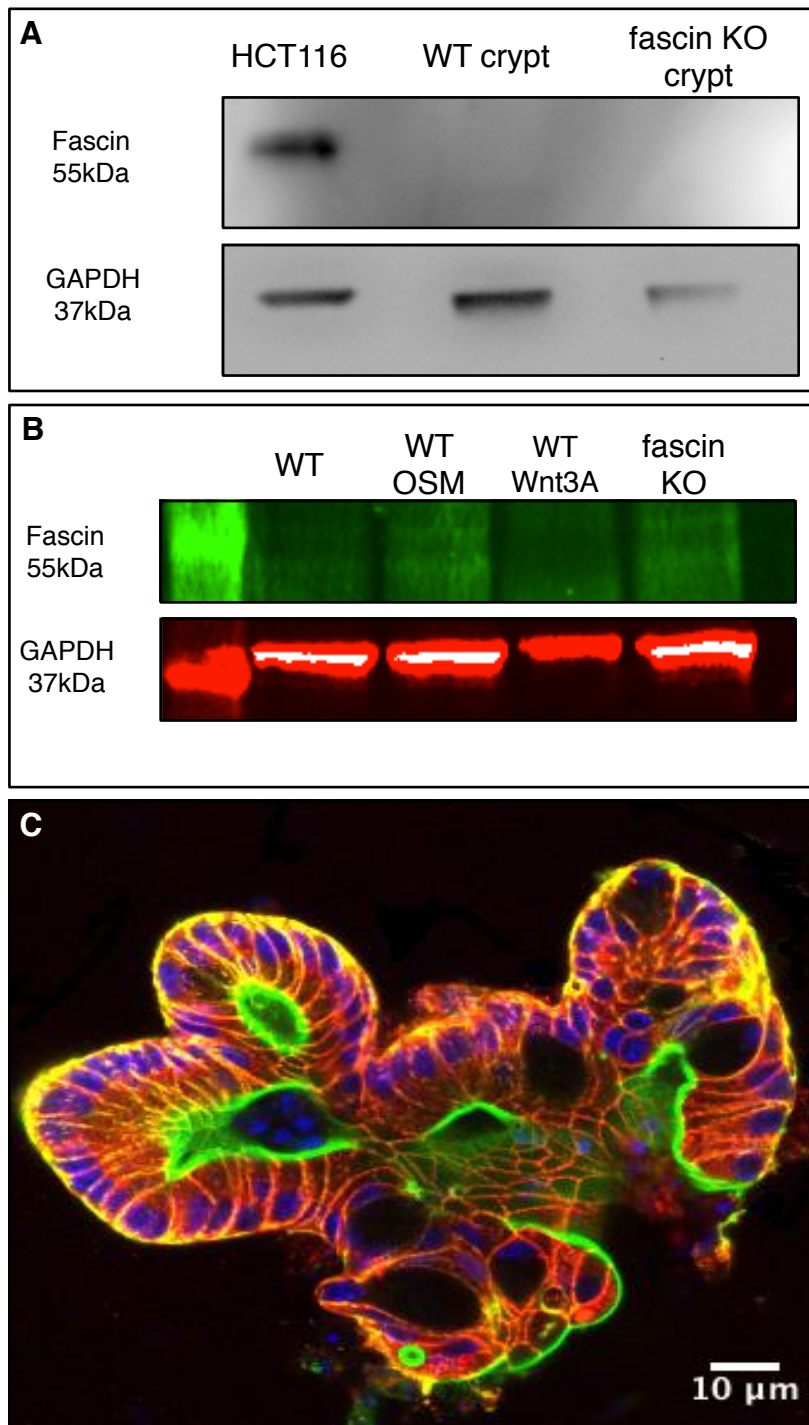


Figure 3-10 No detectable fascin expression in small intestinal crypts on WB

We found no detectable level of fascin on WB (HCT116 colon cancer cell line as positive control) in cultured small intestinal crypts (A), although the crypts had been in prolonged culture for several weeks and may have lost their expression or indeed may not express fascin at a detectable level on WB. We wished to determine whether Wnt3a or the cytokine Oncostatin M (OSM) could stimulate fascin, however we found no detectable band on WB (B). Images representative of 3 independent experiments Immunofluorescence micrograph of a WT small intestinal crypt grown in standard medium: green staining is phalloidin, the red is E-cadherin and the blue is nuclear (C).

3.3.8 Clonogenicity assay

In order to determine whether the enhanced proliferation seen in the regenerating fascin KO crypts was as a result of an increased number of stem cells, we quantified the number of WT and fascin KO crypt colonies which formed from single cells with and without the addition of Wnt3a (Fig. 3.11). There was no significant difference in the number of colonies formed in either assay, which suggests that proliferation, rather than an increase in the number of stem cells, is responsible for enhanced growth of the fascin KO crypts in response to Wnt3a.

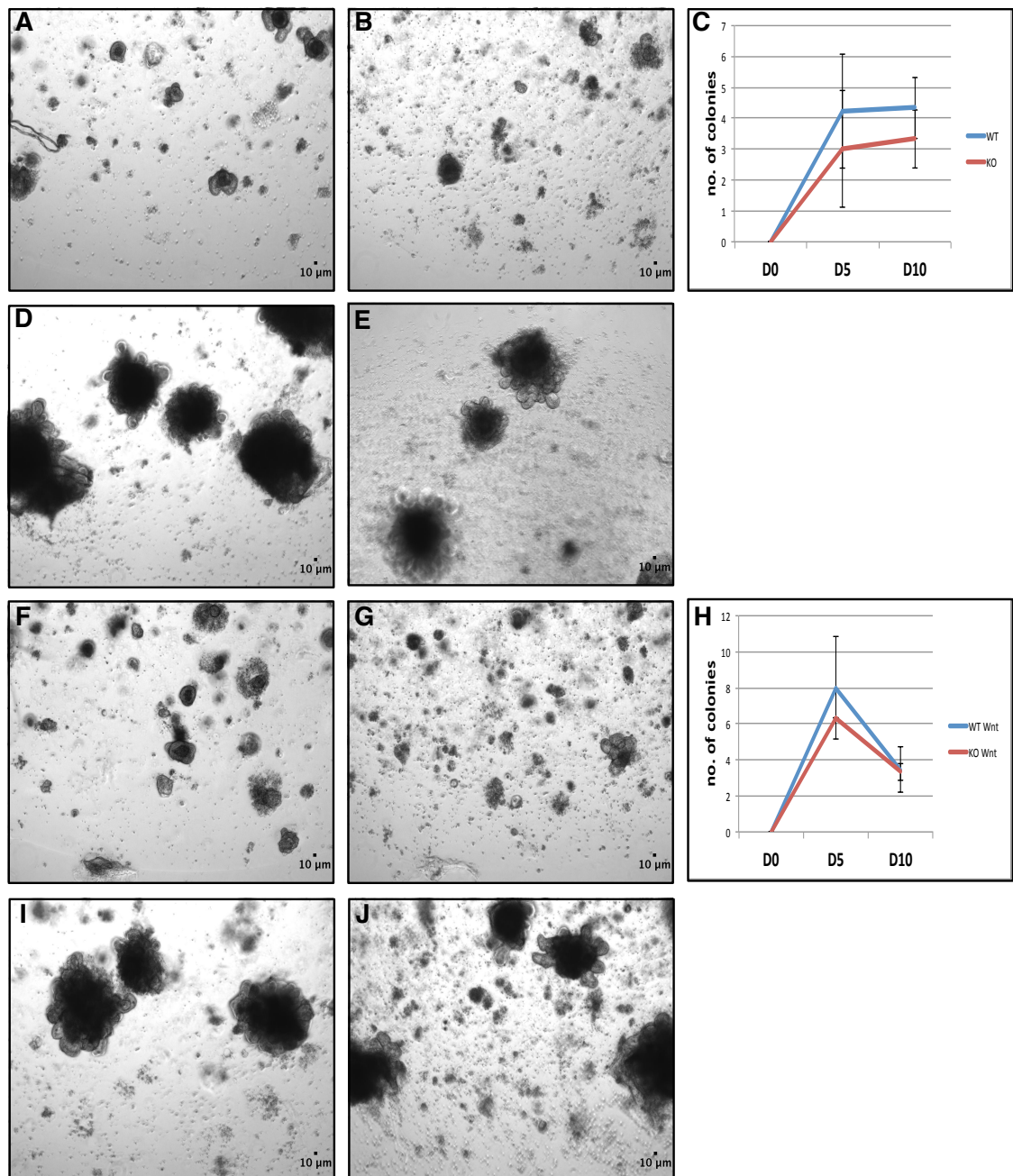


Figure 3-11 Clonogenicity assay

WT (A) and fascin KO (B) crypts after 5 days. Quantification (C) of the number of colonies formed from WT and fascin KO crypts after 5 and 10 days of culture (n=3). WT (D) and fascin KO (E) crypts after 10 days of culture in standard medium. WT (F) and KO (G) crypts in medium with exogenous Wnt3a after 5 days and 10 days (WT (I), fascin KO (J)) and quantification (H) of the number of colonies formed. n=3 per condition with all colonies counted per 6 well plate. Images representative of 3 independent experiments. Error bars represent SD.

3.3.9 Gene expression microarray WT vs. fascin KO crypts

Given the changes seen in the qRT-PCR data between the WT and fascin KO crypts we used an expression microarray analysis to profile the differences in genes and transcripts between the WT and fascin KO crypts in standard medium.

The top 10 genes with the highest significant ($p < 0.05$) fold change are demonstrated in Table 3.1 and significant networks involved detailed in Table 3.2. The network score is derived from a p-value indicating whether the genes involved in the network are found together by random chance. A score of 2 or more indicates a 99% confidence interval of not being as a result of random chance (Long, Liu et al. 2004).

It is interesting to note that Neuritin 1 (Nrn1) is significantly lower in the fascin KO which correlates with our own qRT-PCR data of crypts in standard medium. It would be important, in the next instance, to verify these targets, using qRT-PCR and then subsequently analyse these at the protein level to further determine their significance and role in the fascin KO crypts.

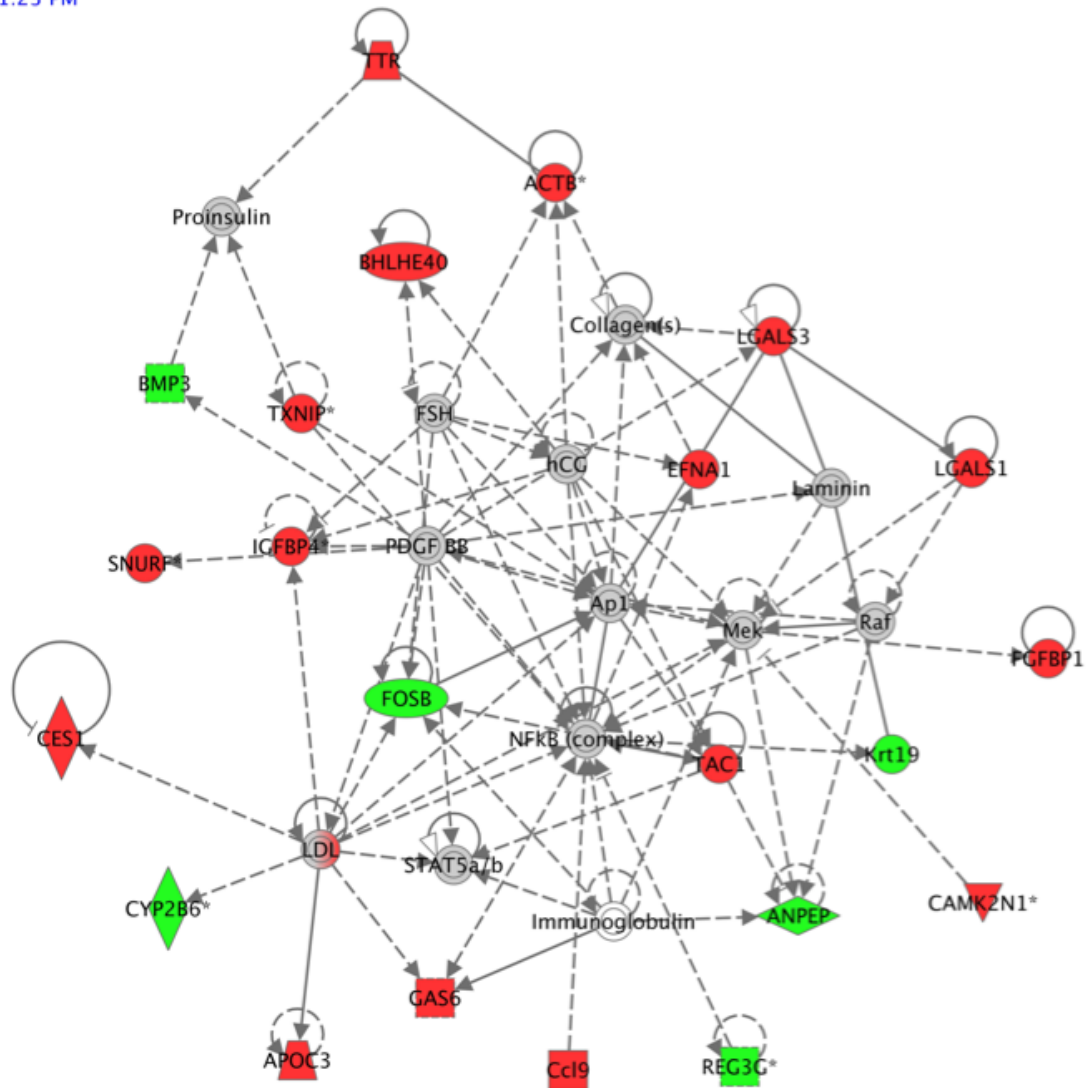
Gene	Fold change	direction	p-value
erythroid differentiation regulator 1	6.3932	down	<2e-16
eukaryotic translation initiation factor 2, subunit 3, structural gene Y-linked	3.687315634	up	<2e-16
erythroid differentiation regulator 1	2.9785	down	<2e-16
neuritin 1	2.7073	down	<2e-16
DNA segment, Chr 14, ERATO Doi 449, expressed	2.624671916	up	<2e-16
inactive X specific transcripts	2.4878	down	<2e-16
zinc finger protein 68	2.248	down	<2e-16
DEAD (Asp-Glu-Ala-Asp) box polypeptide 3, Y-linked	2.207992934	up	<2e-16
polyadenylate binding protein-interacting protein 1	1.833180568	up	<2e-16
lymphocyte antigen 6 complex, locus E	1.736412572	up	<2e-16

Table 3-1 Crypt gene expression microarray showing the top 10 genes with the highest fold change

Associated Network Functions	Score
Cell Death, Cell Cycle, Cellular Growth and Proliferation	47
Cellular Development, Cellular Growth and Proliferation, Reproductive System Development and Function	43
Gene expression, Organ Morphology, Vitamin and Mineral Metabolism	28
Inflammatory Response, Cellular compromise, Drug Metabolism	23
Amino Acid Metabolism, Endocrine System Development and Function, Molecular Transport	22

Table 3-2 Top 5 associated networks and network functions derived from small intestinal crypt gene expression array

Network 1 : RSkovRSwt_RP_fc1.25 - 2012-05-10 01:23 PM : RSkovRSwt_RP.xls : RSkovRSwt_RP_fc1.25 - 2012-05-10 01:23 PM



© 2000-2012 Ingenuity Systems, Inc. All rights reserved.

Figure 3-12 Cell Death, Cell Cycle, Cellular Growth and Proliferation

Pathway analysis of the gene expression microarray demonstrating the 1st associated network. Red symbols demonstrate genes which are higher in the fascin KO crypts, whilst green symbols demonstrate genes which are expressed at lower levels in the fascin KO. Grey symbols show no significant difference between WT and fascin KO.

Network 2 : RSkovRSwt_RP_fc1.25 - 2012-05-10 01:23 PM : RSkovRSwt_RP.xls : RSkovRSwt_RP_fc1.25 - 2012-05-10 01:23 PM

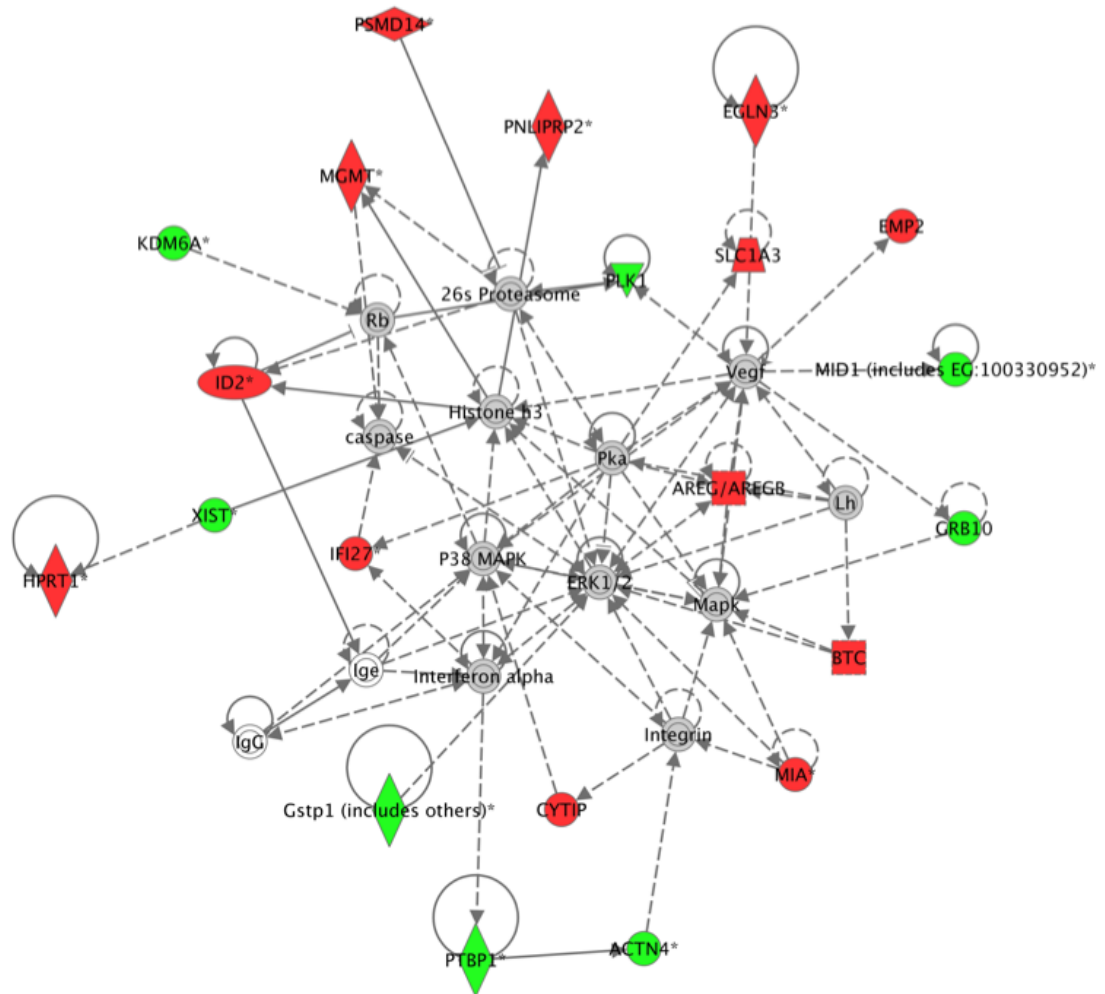


Figure 3-13 Cellular Development, Cellular Growth and Proliferation, Reproductive System Development and Function

Pathway analysis of the gene expression microarray demonstrating the 2nd most associated network. Red symbols demonstrate genes which are higher in the fascin KO crypts, whilst green symbols demonstrate genes which are expressed at lower levels in the fascin KO. Grey symbols show no significant difference between WT and fascin KO.

Network 3 : RSkovRSwt_RP_fc1.25 - 2012-05-10 01:23 PM : RSkovRSwt_RP.xls : RSkovRSwt_RP_fc1.25 - 2012-05-10 01:23 PM

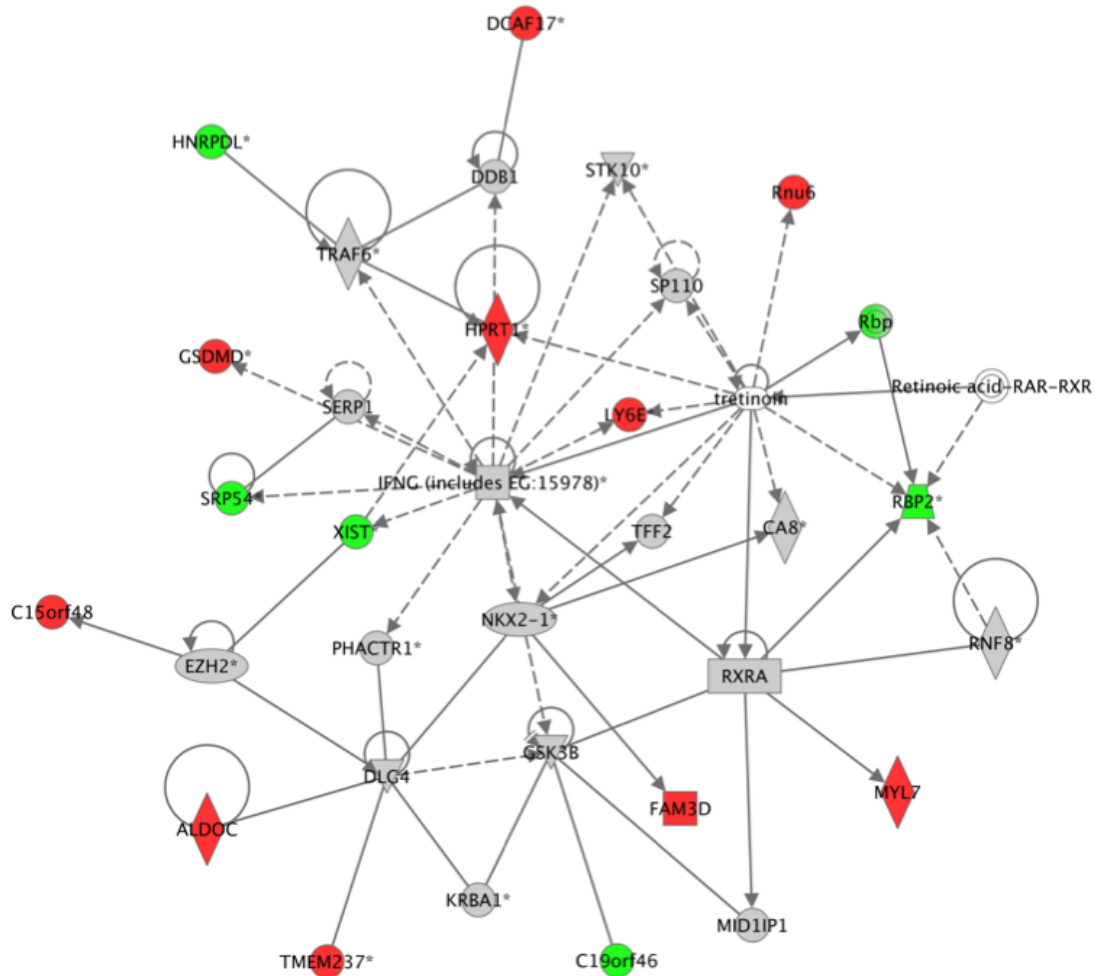


Figure 3-14 Gene expression, Organ Morphology, Vitamin and Mineral Metabolism

Pathway analysis of the gene expression microarray demonstrating the 3rd most associated network. Red symbols demonstrate genes which are higher in the fascin KO crypts, whilst green symbols demonstrate genes which are expressed at lower levels in the fascin KO. Grey symbols show no significant difference between WT and fascin KO.

Network 4 : RSkovRSwt_RP_fc1.25 - 2012-05-10 01:23 PM : RSkovRSwt_RP.xls : RSkovRSwt_RP_fc1.25 - 2012-05-10 01:23 PM

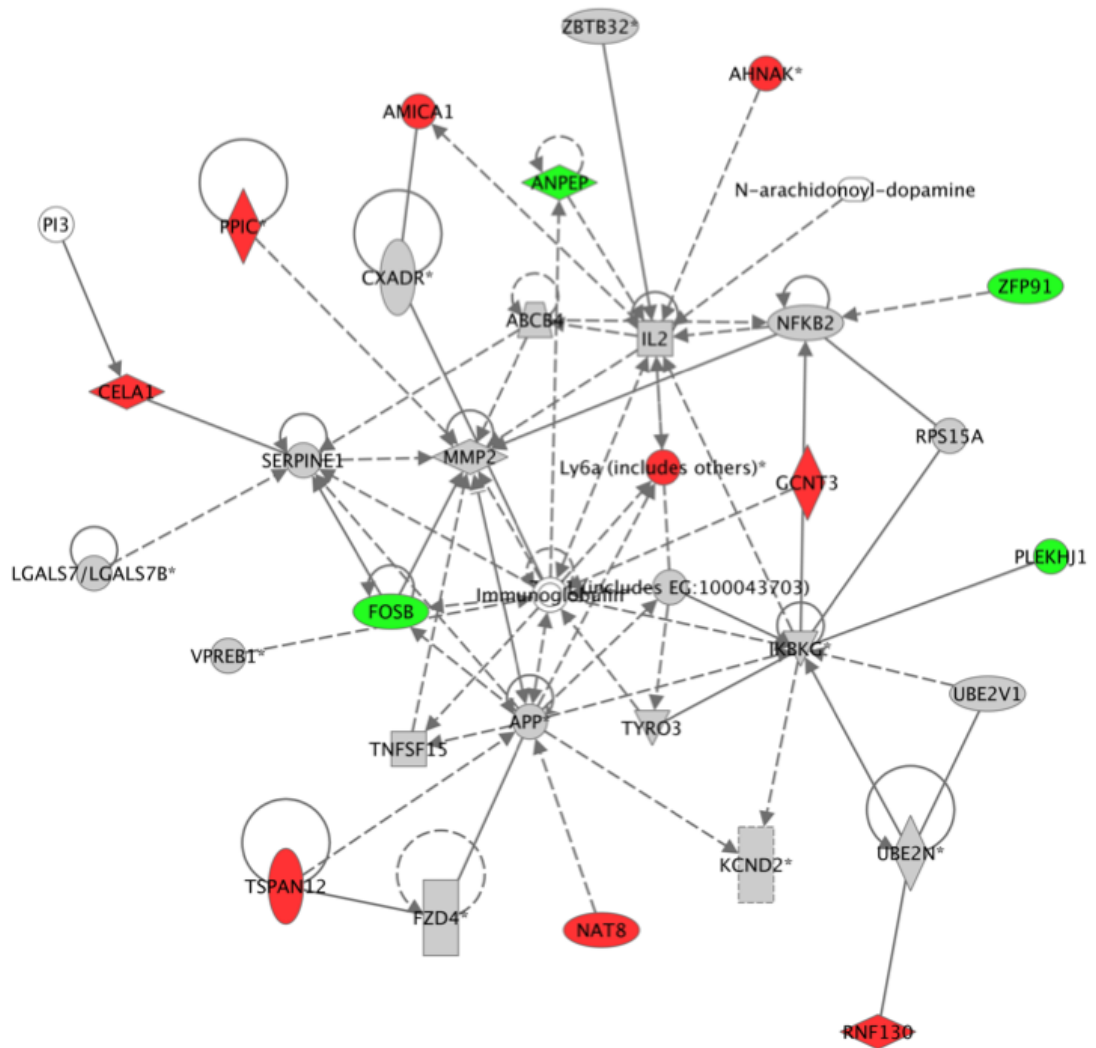


Figure 3-15 Inflammatory Response, Cellular compromise, Drug Metabolism

Pathway analysis of the gene expression microarray demonstrating the 4th most associated network. Red symbols demonstrate genes which are higher in the fascin KO crypts, whilst green symbols demonstrate genes which are expressed at lower levels in the fascin KO. Grey symbols show no significant difference between WT and fascin KO.

Network 5 : RSkovRSwt_RP_fc1.25 - 2012-05-10 01:23 PM : RSkovRSwt_RP.xls : RSkovRSwt_RP_fc1.25 - 2012-05-10 01:23 PM

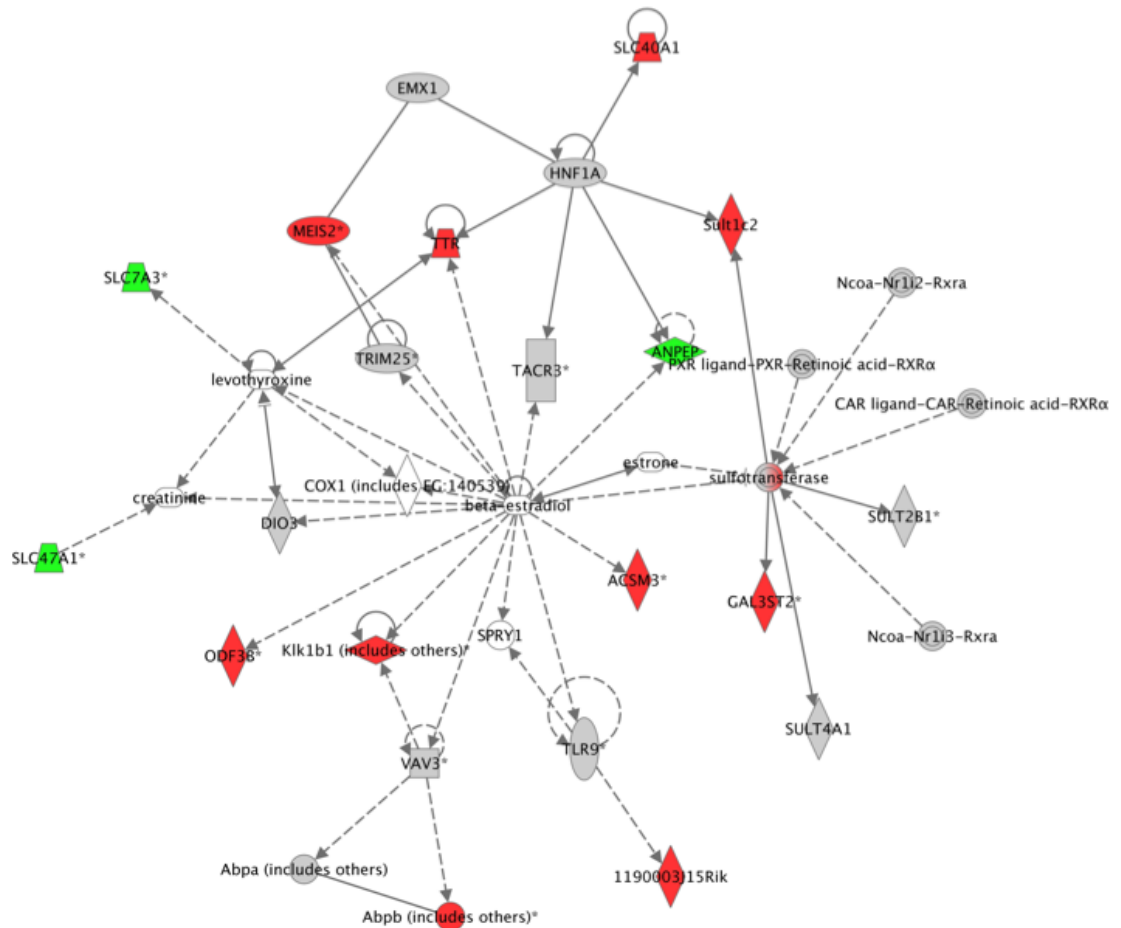


Figure 3-16 Amino Acid Metabolism, Endocrine System Development and Function, Molecular Transport

Pathway analysis of the gene expression microarray demonstrating the 5th most associated network. Red symbols demonstrate genes which are higher in the fascin KO crypts, whilst green symbols demonstrate genes which are expressed at lower levels in the fascin KO. Grey symbols show no significant difference between WT and fascin KO.

3.4 Discussion

3.4.1 Fascin is not required to maintain normal homeostatic small intestinal architecture

Our studies suggest that fascin is not required to maintain the normal small intestinal architecture under homeostatic conditions. Indeed, the presence of very low levels of fascin in the WT small intestine and the lack of statistical difference in the number of BrdU proliferating cells or paneth cells in the fascin KO indicates that fascin does not play an important role in the development or maintenance of the small intestinal architecture under normal homeostatic conditions. It is interesting that, at the gene mRNA level, there is a significant

reduction in the majority of recognised stem cell markers in the fascin KO compared with WT and that this does not manifest itself in a difference at the microscopic level. Both paneth cells and Lgr5 cells express fascin at low levels as shown in a gene expression microarray of these isolated cells (Sato, van Es et al. 2011) and available at

<http://www.ncbi.nlm.nih.gov/geo/query/acc.cgi?acc=GSE25109>. Therefore, absence of fascin in these cells in the fascin KO may result in an impairment of their function in situations of low Wnt levels during normal homeostasis resulting in reduced levels of stem cells, albeit to a level which does not result in a demonstrable difference at the microscopic level. It would be desirable to compare the position of Lgr5 cells and Ki67 cells in the WT and fascin KO mice using IHC.

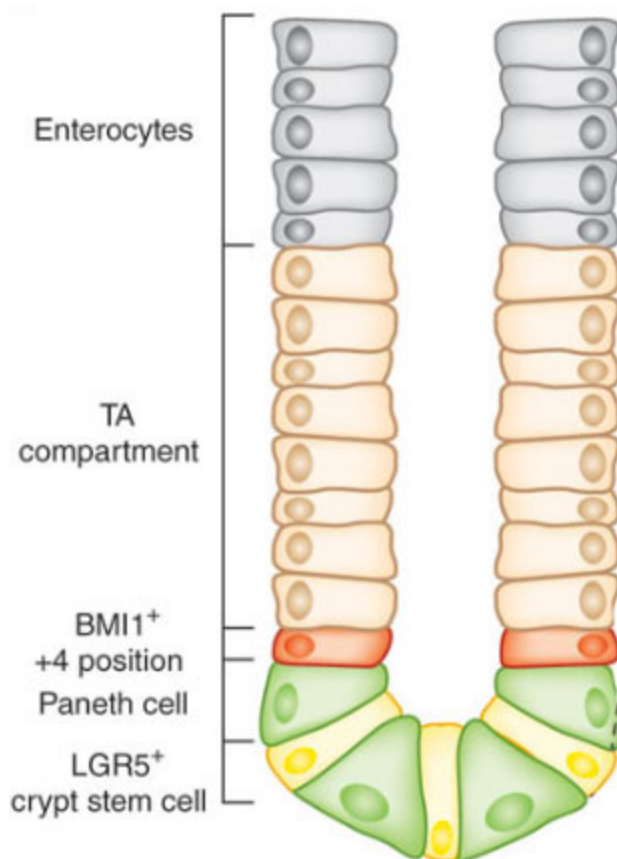


Figure 3-17 Schematic diagram demonstrating crypt architecture

Diagram adapted from (Abo and Clevers 2012) demonstrating the position of the Lgr5 (yellow) crypt based columnar (CBC) cells which mark the active ISCs and are located between the paneth cells (green) at the base of the crypt. The “label retaining cells” (LRCs), so called because they label retain BrdU for a significantly longer period than the rapid cycling stem cells, are defined by their slow cycling nature and are located above the paneth cells at the +4 position: BMI1⁺ (red) marks these quiescent cells (Yan, Chia et al. 2012). The transit amplifying (TA) progenitor cells are located further up the crypt axis and arise from the stem cells.

The higher level of NF- κ B in the WT, may contribute to increased levels of Lgr5.

NF- κ B has been shown to enhance Wnt signalling (Schwitalla, Fingerle et al.

2013) and this may in part explain the lower levels of generic Wnt members/targets seen in the fascin KO in physiological conditions in which there is moderate or low levels of Wnt ligand circulating. This further correlates with levels of TNF α , which is involved in the activation of NF- κ B (Malinin, Boldin et al. 1997) and again are shown to be lower in the fascin KO.

3.4.2 Loss of fascin results in a mild increase in histological damage in a small intestinal time course post irradiation

One of the key features of IBD is the histological damage caused by the inflammatory process. Given the structural importance of fascin as an actin bundling protein and in the formation of filopodia, the absence of fascin in cells subjected to irradiation and the subsequent inflammatory insult would, one would assume, result in enhanced damage as the intestinal epithelial cells (IEC) would be less able to maintain their cell structure or cell:cell adhesions. The irradiation time course seeks to identify any observed difference in the damage sustained following irradiation. Given the small sample size at each time point, it is difficult to draw definite conclusions, however our preliminary results indicate a slight increase in overall histological damage in the fascin KO small intestines at the 24 hour time point with a noted presence of vacuolated cells in 2 out of the 3 fascin KO samples whereas this appearance was not seen in any of the WT samples.

3.4.3 The absence of fascin allows enhanced small intestinal proliferation in the presence of high levels of Wnt ligand

In both *in-vivo* and *in-vitro* experiments, in the presence of high levels of Wnt ligand, there is enhanced proliferation and higher levels of stem cell markers in the fascin KO small intestines and crypts. This is in contrast to the situation in which there are low levels of Wnt circulating as is seen under physiological conditions in the untreated tissue or *in-vitro* when the crypts are cultured in standard medium. Lgr5 has recently been shown to be a target gene of NF- κ B (Schwitalla, Fingerle et al. 2013), which, in the same paper was shown to enhance Wnt signalling. Our data shows that in the presence of low Wnt levels, NF- κ B and Lgr5 are lower in the fascin KO, whilst in high Wnt levels they are

higher in the fascin KO. This would suggest that loss of fascin deregulates Wnt signalling and causes an exaggerated response. The mechanisms are unclear, but might involve membrane trafficking changes, changes in interaction of the cells with the microenvironment or involvement of the immune system. We can speculate that this is important in acutely inflamed tissue where the presence of fascin allows cells to maintain their architecture thereby minimising the cellular damage whilst also facilitating the recruitment of neutrophils through the function of chemokine release from dendritic cells. When the inflammation reduces, the level of fascin would also reduce thereby allowing enhanced Wnt signalling and subsequent regeneration. In the fascin KO mice this process is abolished thereby allowing hyperactive Wnt signalling in the acutely inflamed tissue.

The mechanism responsible for the enhanced proliferation is unlikely to be due to an increase in stemness given there was neither an increase in the number or height of the regenerating crypts *in-vivo*, nor an increase in the number of colonies formed by the dissociated crypts *in-vitro*. Rather, the phenotype we see is more likely a result of an increase in Wnt signalling driving the proliferative response. The mechanism behind the regulation of Wnt signalling may be through direct Wnt inhibition and/or indirectly through TNF α or NF- κ B regulation.

3.4.4 Fascin is required for optimal neutrophil recruitment

The significant reduction in recruited neutrophils in the fascin KO mice is likely to be multi-factorial. Dendritic cells express fascin and, whilst they are not known to directly interact with neutrophils they may have some involvement in the orchestration of the immune response to inflammation through the production of chemokines upon maturation (McColl 2002). Both CXCL1 and CXCL2 are known to be important mediators of neutrophil recruitment into areas of inflammation (Dhawan and Richmond 2002) (De Filippo, Dudeck et al. 2013). Indeed, dendritic cells have been specifically shown to express CXCL1 and CXCL2 (Zaharik, Nayar et al. 2007), the two chemokines we found to be significantly reduced in the fascin KO irradiated tissue. Loss of fascin by dendritic cells may result in impairment of their function and subsequent expression of these crucial chemokines with downstream effects of reduced neutrophil recruitment.

Neutrophils themselves are not reported to express fascin nor did we see expression when we ran a western blot on isolated murine neutrophils, although the expression level may be too low to detect on WB.

Lastly, fascin has been shown to be expressed by endothelial cells (Kureishy, Sapountzi et al. 2002) and therefore, a defect in the endothelial cytoskeleton could affect the transmigration of neutrophils.

Interestingly, despite the fascin KO having fewer neutrophils recruited to areas of inflammation, there is increased damage. One of the paradoxical effects of neutrophils is that, despite their primary role to destroy pathogens, through the release of proteases and increased reactive oxygen species (ROS), they also directly damage the tissue itself (Segel, Halterman et al. 2011). This may mask the true level of damage that loss of fascin has on the small intestinal architecture and we can speculate that, were the levels of neutrophils to be on a par with that of the WT, the degree of damage may be significantly more in the fascin KO.

3.4.5 Crypt gene expression microarray changes

While the data from our microarray analysis may hold some clues as to how loss of fascin affects normal growth of small intestinal cells, we actually saw rather few genes changed in the absence of fascin. This may in part be due to the fact the crypts had been in culture for several weeks prior to analysis and may have compensated for the lack of fascin. This longer term culturing was necessary to gain enough material to isolate mRNA from the cultures, so a method that used less material would be desirable for future studies on earlier cultures. Secondly, the crypts themselves were cultured in standard medium, but actually we see the largest difference in growth in fascin KO crypts in the presence of Wnt3a. We would therefore ideally like to repeat the microarray with the crypts having been incubated with Wnt3a.

The pathway analysis itself is interesting in that the top 2 pathways implicated involve cellular growth and proliferation. Whilst the pathway analysis must be interpreted with caution, it may point to the importance of fascin in these processes.

The top 10 genes which were found to have the greatest fold change difference are discussed here:

Erythroid differentiation regulator 1 (ERDR1) was found to be the gene which had the greatest fold change (6.39 fold lower in the fascin KO) from the expression array. It has been shown that, under stressful situations cells release ERDR1 which consequently enhances the survival of stromal cells (Dormer, Spitzer et al. 2004).

Eukaryotic translation initiation factor 2, subunit 3, structural gene Y-linked (Eif2s3y) was 3.69 fold higher in the fascin KO, however very little is known regarding this other than it is involved in translational initiation (reference: <http://rgd.mcw.edu/rgdweb/report/gene/main.html?id=2314438>).

Neuritin 1 (Nrn1) was 2.7 fold lower in the fascin KO and is a recognised receptor gene identified as part of the small intestine stem cell signature classification (Munoz, Stange et al. 2012).

DNA segment, Chr 14, ERATO Doi 449, expressed (D14Ert449e) was 2.62 fold higher in the fascin KO and is known to be a transmembrane protein (ncbi).

Inactive X specific transcripts (Xist) is an essential regulator of the x-inactivation process (ncbi).

Zinc finger protein 68 (Zfp68) was 2.25 fold lower in the fascin KO and forms part of the zinc finger family.

DEAD (Asp-Glu-Ala-Asp) box polypeptide 3, Y-linked (Ddx3y) is 2.21 fold higher in the fascin KO and is known to be a putative RNA helicase (ncbi) and is involved in a wide variety of cellular processes.

Polyadenylate binding protein-interacting protein 1 (Paip1) was 1.83 fold higher in the fascin KO and is known to be involved in translational initiation and protein biosynthesis (ncbi).

Lymphocyte antigen 6 complex, locus E (Ly6e) was 1.73 fold higher in the fascin KO, however very little is known regarding this gene.

References

- Abo, A. and H. Clevers (2012). "Modulating WNT receptor turnover for tissue repair." *Nat Biotechnol* **30**(9): 835-836.
- Banchereau, J. and R. M. Steinman (1998). "Dendritic cells and the control of immunity." *Nature* **392**(6673): 245-252.
- Barker, N., J. H. van Es, et al. (2007). "Identification of stem cells in small intestine and colon by marker gene Lgr5." *Nature* **449**(7165): 1003-1001.
- Bleich, A., M. Mahler, et al. (2004). "Refined histopathologic scoring system improves power to detect colitis QTL in mice." *Mamm Genome* **15**(11): 865-871.
- Brown, S. J. and L. Mayer (2007). "The immune response in inflammatory bowel disease." *Am J Gastroenterol* **102**(9): 2058-2069.
- De Filippo, K., A. Dudeck, et al. (2013). "Mast cell and macrophage chemokines CXCL1/CXCL2 control the early stage of neutrophil recruitment during tissue inflammation." *Blood* **121**(24): 4930-4937.
- Dhawan, P. and A. Richmond (2002). "Role of CXCL1 in tumorigenesis of melanoma." *J Leukoc Biol* **72**(1): 9-18.
- Dormer, P., E. Spitzer, et al. (2004). "EDR is a stress-related survival factor from stroma and other tissues acting on early haematopoietic progenitors (E-mix)." *Cytokine* **27**(2-3): 47-57.
- Fevr, T., S. Robine, et al. (2007). "Wnt/beta-catenin is essential for intestinal homeostasis and maintenance of intestinal stem cells." *Mol Cell Biol* **27**(21): 7551-7559.
- Khor, B., A. Gardet, et al. (2011). "Genetics and pathogenesis of inflammatory bowel disease." *Nature* **474**(7351): 307-317.
- Kureishy, N., V. Sapountzi, et al. (2002). "Fascin, and their roles in cell structure and function." *Bioessays* **24**(4): 350-361.
- Larmonier, C. B., M. T. Midura-Kiela, et al. (2011). "Modulation of neutrophil motility by curcumin: implications for inflammatory bowel disease." *Inflamm Bowel Dis* **17**(2): 503-515.
- Long, F., H. Liu, et al. (2004). "Genome-wide prediction and analysis of function-specific transcription factor binding sites." *In Silico Biol* **4**(4): 395-410.
- Malinin, N. L., M. P. Boldin, et al. (1997). "MAP3K-related kinase involved in NF-kappaB induction by TNF, CD95 and IL-1." *Nature* **385**(6616): 540-544.
- Mantovani, A., M. A. Cassatella, et al. (2011). "Neutrophils in the activation and regulation of innate and adaptive immunity." *Nat Rev Immunol* **11**(8): 519-531.
- McColl, S. R. (2002). "Chemokines and dendritic cells: a crucial alliance." *Immunol Cell Biol* **80**(5): 489-496.
- Munoz, J., D. E. Stange, et al. (2012). "The Lgr5 intestinal stem cell signature: robust expression of proposed quiescent '+4' cell markers." *EMBO J* **31**(14): 3079-3091.
- Pinkus, G. S., M. A. Lones, et al. (2002). "Langerhans cell histiocytosis immunohistochemical expression of fascin, a dendritic cell marker." *Am J Clin Pathol* **118**(3): 335-343.

- Pinkus, G. S., J. L. Pinkus, et al. (1997). "Fascin, a sensitive new marker for Reed-Sternberg cells of Hodgkin's disease. Evidence for a dendritic or B cell derivation?" Am J Pathol **150**(2): 543-562.
- Potten, C. S. and J. H. Hendry (1975). "Differential regeneration of intestinal proliferative cells and cryptogenic cells after irradiation." Int J Radiat Biol Relat Stud Phys Chem Med **27**(5): 413-424.
- Qualtrough, D., K. Smallwood, et al. (2011). "The actin-bundling protein fascin is overexpressed in inflammatory bowel disease and may be important in tissue repair." BMC Gastroenterol **11**: 14.
- Sato, T., J. H. van Es, et al. (2011). "Paneth cells constitute the niche for Lgr5 stem cells in intestinal crypts." Nature **469**(7330): 415-418.
- Sato, T., R. G. Vries, et al. (2009). "Single Lgr5 stem cells build crypt-villus structures in vitro without a mesenchymal niche." Nature **459**(7244): 262-265.
- Schwitalla, S., A. A. Fingerle, et al. (2013). "Intestinal tumorigenesis initiated by dedifferentiation and acquisition of stem-cell-like properties." Cell **152**(1-2): 25-38.
- Segel, G. B., M. W. Halterman, et al. (2011). "The paradox of the neutrophil's role in tissue injury." J Leukoc Biol **89**(3): 359-372.
- Snyder, M., X. Y. Huang, et al. (2011). "Signal Transducers and Activators of Transcription 3 (STAT3) Directly Regulates Cytokine-induced Fascin Expression and Is Required for Breast Cancer Cell Migration." Journal of Biological Chemistry **286**(45): 38886-38893.
- Tan, V. Y., S. J. Lewis, et al. (2013). "Association of fascin-1 with mortality, disease progression and metastasis in carcinomas: a systematic review and meta-analysis." BMC Med **11**: 52.
- Yamakita, Y., F. Matsumura, et al. (2009). "Fascin1 is dispensable for mouse development but is favorable for neonatal survival." Cell Motility and the Cytoskeleton **66**(8): 524-534.
- Yan, K. S., L. A. Chia, et al. (2012). "The intestinal stem cell markers Bmi1 and Lgr5 identify two functionally distinct populations." Proc Natl Acad Sci U S A **109**(2): 466-471.
- Zaharik, M. L., T. Nayar, et al. (2007). "Genetic profiling of dendritic cells exposed to live- or ultraviolet-irradiated *Chlamydia muridarum* reveals marked differences in CXC chemokine profiles." Immunology **120**(2): 160-172.
- Zhang, F. R., L. H. Tao, et al. (2008). "Fascin expression in human embryonic, fetal, and normal adult tissue." J Histochem Cytochem **56**(2): 193-199.

4 Chapter 4 – Fascin regulates colonic regeneration and neutrophil recruitment in response to injury

4.1 Summary

In Chapter 3, I presented data on a small intestinal mouse model of regeneration. The colon differs from the small intestine in a number of ways; both the healthy tissue function and the disease states can be different from the small intestine. We showed that fascin plays a key role in small intestinal regeneration and is involved in the inflammatory response through neutrophil recruitment. As such, we wished to investigate whether a similar role could be found for fascin in a colonic model of regeneration.

I demonstrate here that, under normal homeostatic conditions, loss of fascin from the colon has no effect on the architecture or cellular makeup of the colonic epithelial cells, however following the induction of colitis through the administration of Dextran Sodium Sulphate (DSS) we find, in a similar way to the small intestinal model, that loss of fascin results in mildly increased damage to the epithelium whilst simultaneously allowing enhanced proliferation. Furthermore, loss of fascin results in reduced numbers of circulating neutrophils and neutrophil recruitment to the inflamed colon, which may in part be chemokine dependent.

4.2 Introduction

As previously mentioned, fascin is largely absent from colonic epithelium under normal physiological conditions (Tan, Lewis et al. 2013), however a study published in 2011 demonstrated its expression in human histological samples of ulcerative colitis, Crohn's colitis and diverticulitis (Qualtrough, Smallwood et al. 2011). They demonstrated a correlation between expression of fascin and disease severity with strongest expression seen in the dysplastic pre-malignant cells. Furthermore, they demonstrated that fascin was expressed both at the edge of the ulcers and also in the crypt base of colonic samples with low-grade inflammation. Cells at the leading edge of the ulcers need to change their shape to enhance their motility in order to effectively complete the restitution phase of repair and it is likely that fascin plays an important role in this process given its actin bundling properties.

Fascin has previously been shown to have an important role in cell adhesion (Adams 2004) and this also could be a reason for the high expression in the inflamed tissue in order that cells maintain their architecture thereby minimising cellular damage.

In chapter 3, I demonstrated that loss of fascin results in impaired neutrophil recruitment. The small intestinal model uses irradiation to induce genotoxic stress, a complication of which is transient pancytopenia so we were unable to determine whether the reduction in the number of neutrophils was a consequence of impaired production, a failure in recruitment or both. In this chapter we again show reduced numbers of neutrophils in the fascin KO colitic tissue, but we further show that there are reduced circulating neutrophils in the fascin KO mice in response to colitis.

4.3 Results

4.3.1 Characterisation of untreated fascin KO colon with respect to WT

In order to establish a baseline, we initially quantified the number and height of the colonic crypts in untreated WT and fascin KO mice and found no difference (Fig. 4.1).

We next quantified the number and position of the final BrdU positive cell on the crypt axis of untreated WT and fascin KO colon crypts and again found no difference (Fig. 4.1).

Lastly we quantified the number of goblet cells using the alcian blue stain and found no difference between WT and fascin KO (Fig. 4.1).

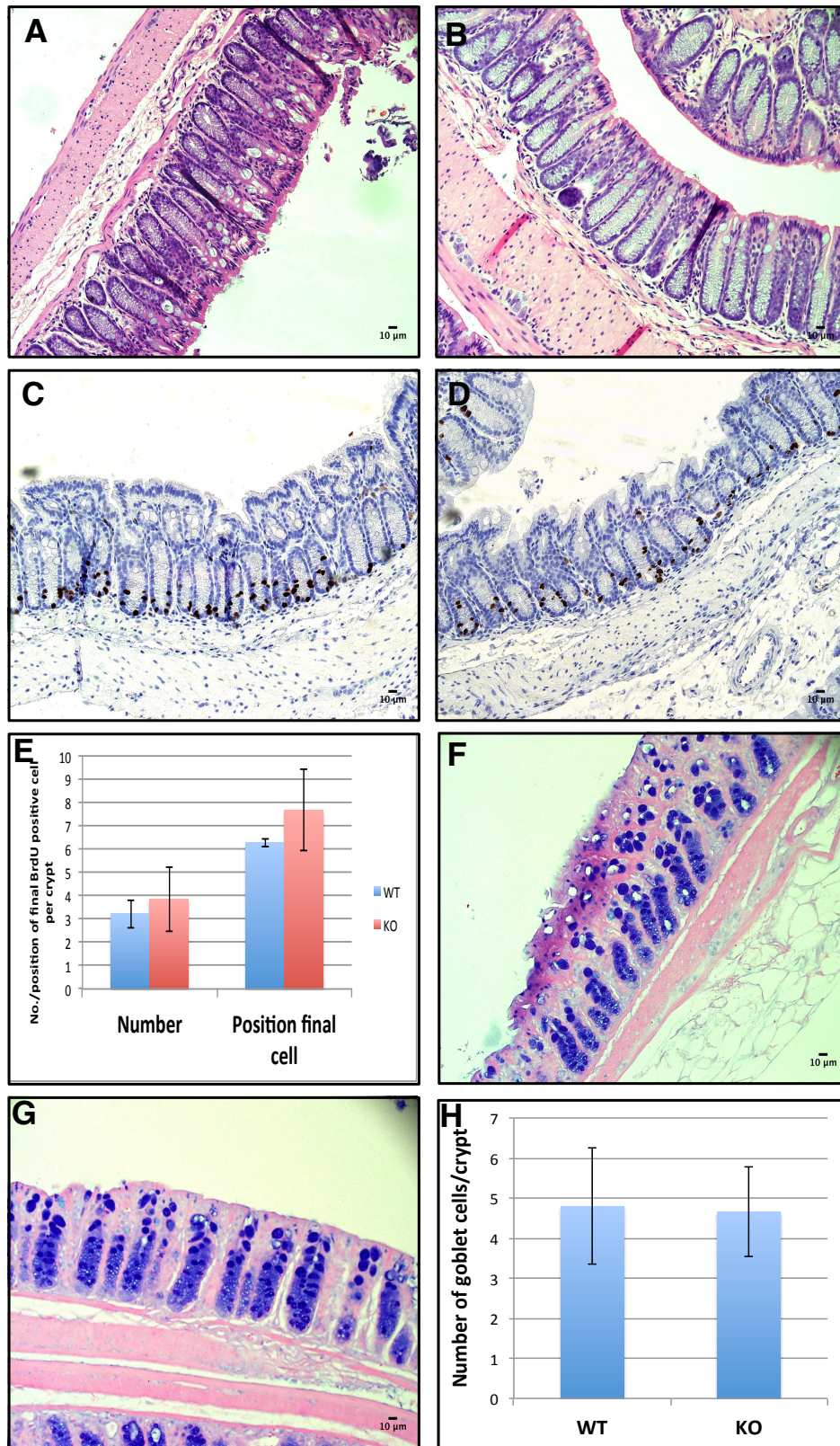


Figure 4-1 Characterisation of fascin KO colon with respect to WT

We found no statistical difference in the number or height of colonic crypts in untreated WT (A) and fascin KO (B) colons (mice were age matched 6-10 weeks old). Furthermore, we found no difference in the number or position of the final BrdU positive cell in WT (C) or fascin KO (D) on the crypt axis (E): $n=2$, error bars represent SD based on 25 crypts on each of 2 samples. Lastly, there was no difference in the number of goblet cells in WT (F) or fascin KO (G) untreated colons (H): $n=2$, error bars represent SD based on 25 crypts on each of 2 samples. Images representative of 2 independent experiments.

We then compared the gene expression profile using qRT-PCR of whole tissue extract in order to further compare untreated WT and fascin KO colons. As was the case in the small intestine, we found significantly lower levels of *Lgr5* ($p=0.000367$) in the fascin KO despite there being no microscopic difference in the crypt appearance (Fig. 4.2). There was no statistical difference in the levels of *Olfm4* ($p=0.346$) or *Nrn1* ($p=0.0760$) (Fig. 4.2). Given that *Lgr5* was higher in the WT, we wished to determine whether this was as a result of higher levels of Wnt signalling which would result in up regulation of other Wnt members and targets. There was no significant difference between the levels of Wnt ligand ($p=0.243$), *Axin2* ($p=0.310$) or β -catenin ($p=0.148$) although Wnt ligand was overall lower in the fascin KO (Fig. 4.2). Regarding Wnt targets, *c-Myc* ($p=0.0003$) and *Cyclin D1* ($p=0.0318$) were significantly lower in the fascin KO, whereas *Cyclin D2* ($p=0.00106$) was significantly higher in the fascin KO and there was no difference with *LEF1* ($p=0.445$) (Fig. 4.2). Levels of *TNF α* ($p=0.000151$) were significantly lower in the fascin KO, whereas there was no significant difference in *NF- κ B* ($p=0.271$) between WT and fascin KO (Fig. 4.2).

Lastly, we quantified the levels of the chemokines *CXCL1* ($p=0.239$), *CXCL2* ($p=0.232$) and *CXCL5* ($p=0.473$) and the chemokine receptor *CXCR2* ($p=0.312$), but found no significant difference between WT and fascin KO (Fig. 4.2).

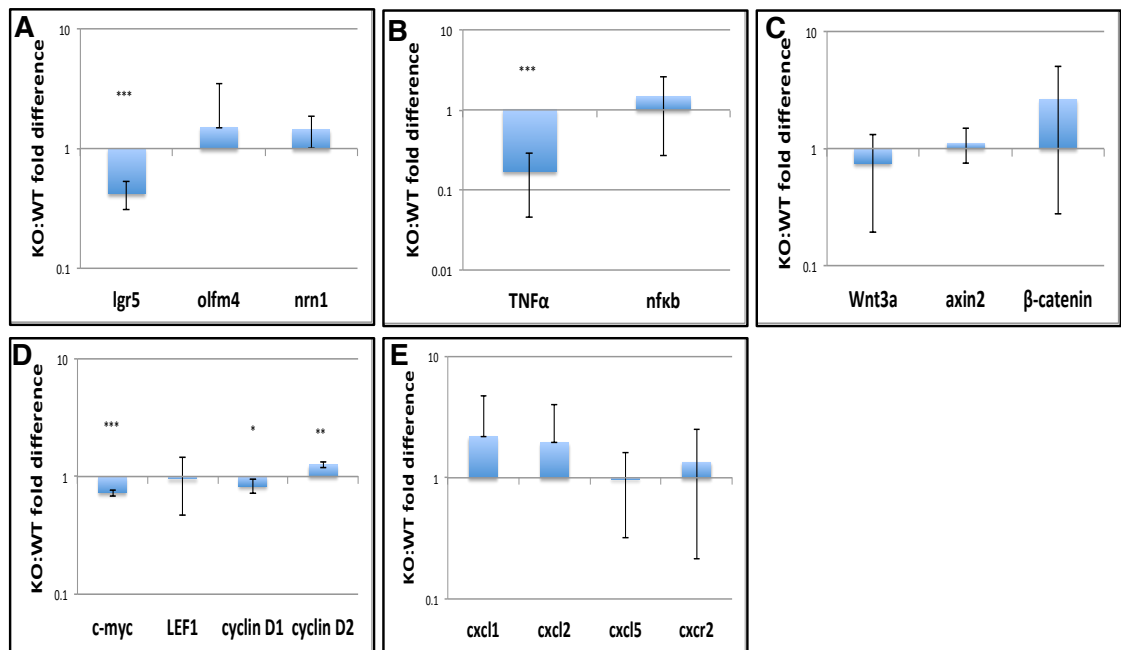


Figure 4-2 qRT-PCR data of untreated whole tissue extraction comparing WT and fascin KO colons

Logarithmic scale demonstrating significantly reduced levels of Lgr5 ($p=0.000367$) (A) TNF α ($p=0.000151$) (B), c-Myc ($p=0.000276$) and Cyclin D1 ($p=0.0318$) (D) in the fascin KO untreated colons. There was no significant difference in Olfm4 ($p=0.346$), Nrn1 ($p=0.0760$), NF- κ B ($p=0.271$), Wnt ligand ($p=0.243$), Axin2 ($p=0.310$), β -catenin ($p=0.148$) or LEF1 ($p=0.445$). Cyclin D2 was significantly higher in the fascin KO ($p=0.00106$). Analysis of various neutrophil related chemokines demonstrated no significant difference in CXCL1 ($p=0.239$), CXCL2 ($p=0.232$) or CXCL5 ($p=0.473$) and there was no significant difference in the chemokine receptor CXCR2 ($p=0.312$) (E). Statistical analysis using Student's t-test, $n=3$ for each sample. Error bars represent SD. Significance asterisks: * = <0.05 , ** = <0.01 , *** = <0.001 .

4.3.2 No difference in histological damage between WT and fascin KO colons in response to DSS

We initially compared the response of WT and fascin KO mice to a 5 day course of 3.5% DSS followed by 72 hours of normal drinking water. We used a modified clinical scoring method (Dohi, Borodovsky et al. 2009) (0-6, 0 being healthy, 6 being moribund), which incorporated the consistency of the stool, the presence of blood in the stool, the appearance of the mouse's coat and the mobility of the mouse. The fascin KO mice deteriorated to a significantly greater extent ($p=0.00270$) and also lost a higher percentage of their body weight following the treatment compared with WT (Fig. 4.3).

In order to determine the effect of loss of fascin on the damage to the colons we set up 3.5% DSS time course whereby we culled the mice on each of the first 3 days after starting treatment and again 72 hours after the 5 day DSS course had

completed. The histological damage was assessed, blind, by a pathology trainee using The Jackson Laboratory (TJL) scoring system developed at the Hannover Medical School (Bleich, Mahler et al. 2004). This incorporated four criteria which were subjectively used to assess and compare the histological damage notably (1) severity, (2) degree of hyperplasia, (3) degree of ulceration and (4) percentage of area involved in the proximal, mid and distal sections of the colon. A score of 0-3 was used (0 being no damage, 3 being maximal) for the four categories and an individual score out of 16 was calculated for each section of the colon and a combined overall score out of a maximum 48 was determined for the entire colon comprising proximal, mid and distal segments. Histological examination of colons sampled from a 3.5% DSS time course revealed no difference in histological damage between WT and fascin KO colons after 3 days of the DSS treatment (Fig. 4.3). We further quantified, using qRT-PCR of whole tissue extracted from the DSS treated colons the presence of the apoptotic marker caspase 8 and found there to be significantly higher levels of caspase 8 ($p=0.00208$) in the fascin KO compared with WT (Fig. 4.3).

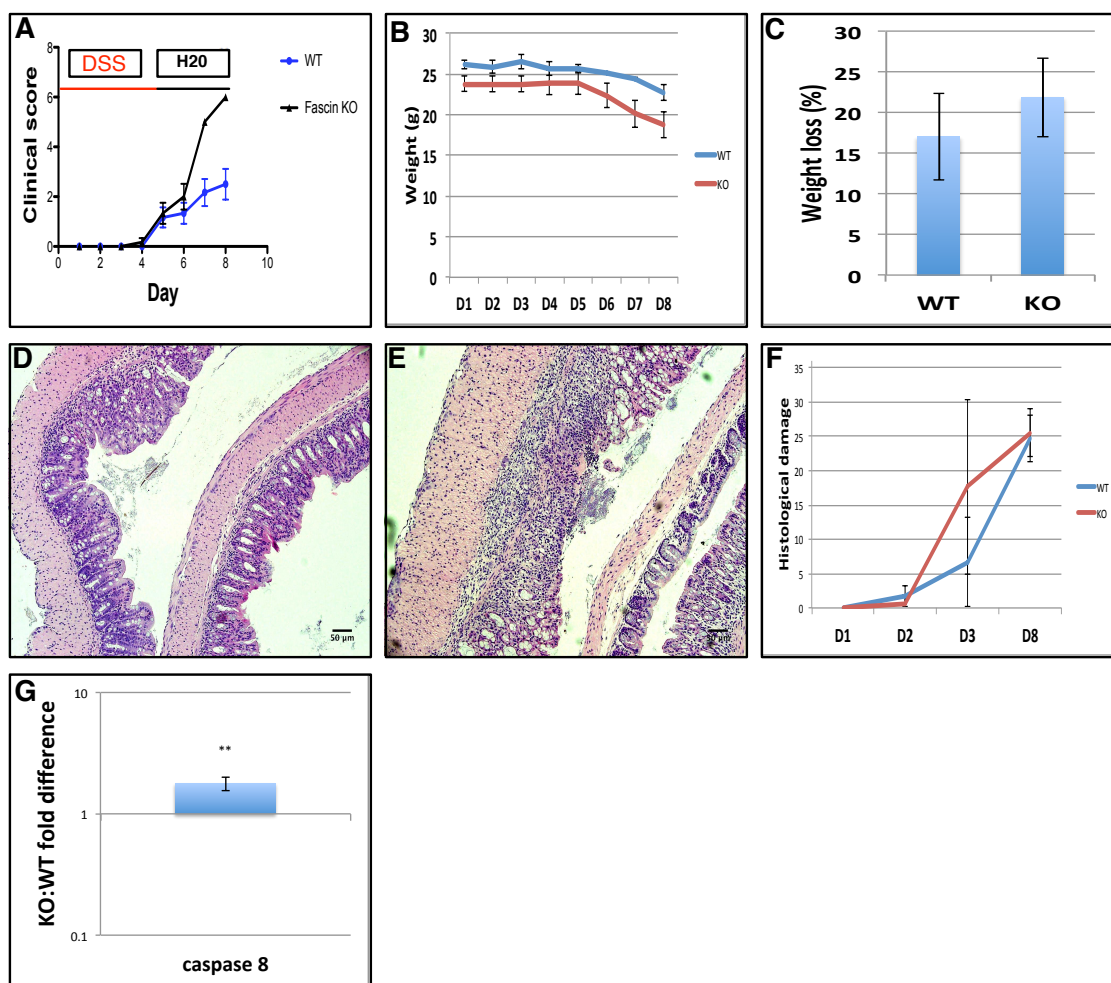


Figure 4-3 Fascin KO mice deteriorate clinically to a greater degree in response to DSS (compared with WT), however there is no difference in histological damage

Using a standardised clinical scoring method, fascin KO mice deteriorated clinically to a significantly greater extent ($p=0.00270$ at day 7, Mann Whitney) over the course of 5 days of 3.5% DSS followed by 72 hours of normal drinking water (A) and also lost a greater percentage of their body weight 72 hours after completing the DSS treatment (B,C): $n=6$ WT, $n=5$ fascin KO). H&E of WT (D) and fascin KO (E) colons after 5 days of 3.5% DSS treatment. Images representative of minimum of 5 independent experiments. Quantification of histological damage of WT and fascin KO colons over a 5 day course of 3.5% DSS followed by 72 hours of normal drinking water demonstrating no significant difference in histological damage between WT and fascin KO (F): $n=3$ mice/timepoint. qRT-PCR analysis of WT and fascin KO colons 72 hours after completing DSS treatment showing significantly greater expression of the apoptotic marker caspase 8 ($p=0.00208$) in the fascin KO colon indicating enhanced apoptosis in response to the DSS treatment. (G): statistical analysis using Student's t-test, $n=3$ for each sample. Error bars represent SD. Significance asterisks: * = <0.05 , ** = <0.01 , *** = <0.001 .

4.3.3 Loss of fascin results in enhanced crypt proliferation in regenerating colons

Given the enhanced levels of Wnt ligand, Lgr5 and certain Wnt members in the untreated WT colon we assumed there would be enhanced proliferation in the WT regenerating colon in response to the DSS. 72 hours after replacing the DSS

with normal drinking water we first quantified the number and height of regenerating crypts in the mice, but found no significant difference (not shown). We next quantified the number of and position of the highest BrdU positive cell in the crypt axis to examine any defect in proliferation in the fascin KO. Although not significant, there was a trend towards higher numbers ($p=0.155$) of BrdU positive cells in the fascin KO and also the position ($p=0.0660$) of the highest BrdU positive cell in the crypt axis that was higher in the fascin KO indicating enhanced proliferation in the absence of fascin (Fig. 4.4). FACS cell cycle analysis of crypt cells extracted from regenerating WT and fascin KO colons 72 hours after completing a 5 day 2% DSS course demonstrated no significant difference in the percentage of cells in each phase of the cell cycle (Fig. 4.4). It was necessary to pool crypt extracts from 3 mice and, despite this there were often less than the required optimal number of cells in each phase of the cell cycle thereby affecting the accuracy and reliability of the final analysis.

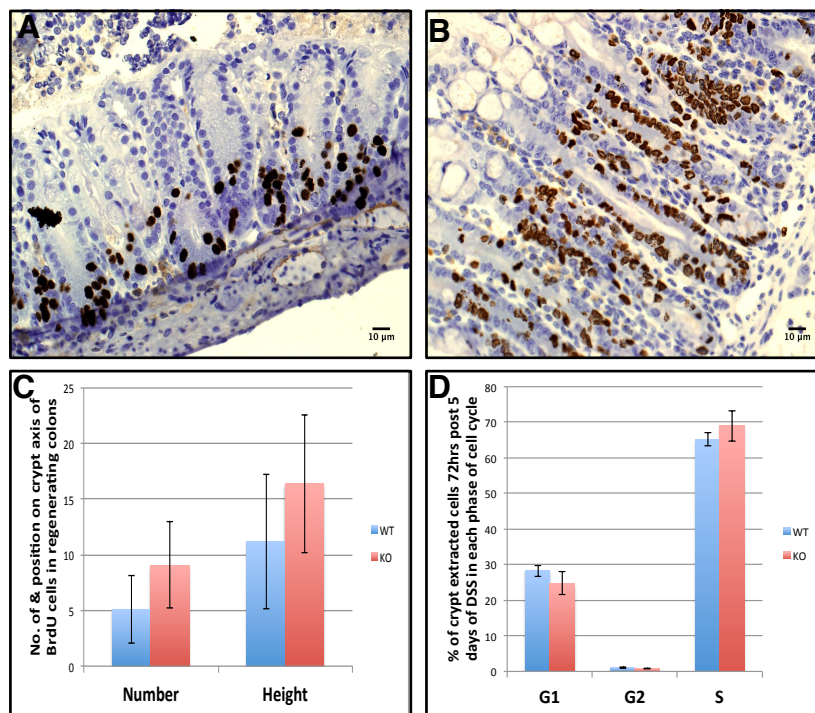


Figure 4-4 BrdU analysis shows that loss of fascin results in enhanced crypt proliferation in regenerating crypts

WT (A) and fascin KO (B) colons with BrdU staining 72 hours after completion of 5 day 2% DSS course and quantification (C) demonstrating a trend towards increased numbers ($p=0.155$, Mann Whitney) and higher position ($p=0.0660$) on the crypt axis of BrdU cells in the fascin KO colons: $n=6$ colons with 10-25 crypts independently counted/colon. Images representative of 6 independent experiments. FACS cell cycle analysis (D) demonstrating no significant difference in the percentage of WT and fascin KO colonic crypt cells in each phase of the cell cycle: $n=3$, each sample was made from 2 pooled epithelial extractions in age/sex matched mice. Error bars represent SD.

We next wished to determine whether there were any gene expression changes that could contribute to the observed phenotype. Using qRT-PCR of whole tissue extracted at the 72 hour time point from the colons we examined the same gene set as for the untreated colons and found that, in contrast to the untreated data (in which there were significantly lower levels of Lgr5 and other Wnt targets in the fascin KO), we found the opposite in that there were significantly higher levels of Lgr5 ($p=3.03E-05$), Nrn1 ($p=0.0161$) and other Wnt targets LEF1 ($p=0.00631$), Cyclin D1 ($p=0.0383$) and Cyclin D2 ($p=0.000368$) in the fascin KO (Fig. 4.5). The proliferative marker Ki67 was also higher in the fascin KO indicating enhanced proliferation in the absence of fascin (Fig. 4.5). There was no significant difference in the stem cell marker Olfm4 ($p=0.442$) (Fig. 4.5). The levels of Wnt3a ($p=0.280$) and Axin2 ($p=0.191$), although not significant showed a trend towards being higher in the fascin KO whilst β -catenin ($p=0.0465$) was significantly higher in the fascin KO (Fig. 4.5). We next examined the levels of TNF α and NF- κ B in the regenerating colons; there was no difference in TNF α ($p=0.343$), however NF- κ B ($p=0.0211$) was significantly higher in the fascin KO (Fig. 4.5). Thus, we conclude that, in regenerative conditions in the presence of high Wnt signalling loss of fascin results in higher levels of basal NF- κ B mRNA, which may account for the enhanced overall proliferative rate and higher Lgr5 mRNA levels also detected in the fascin KO.

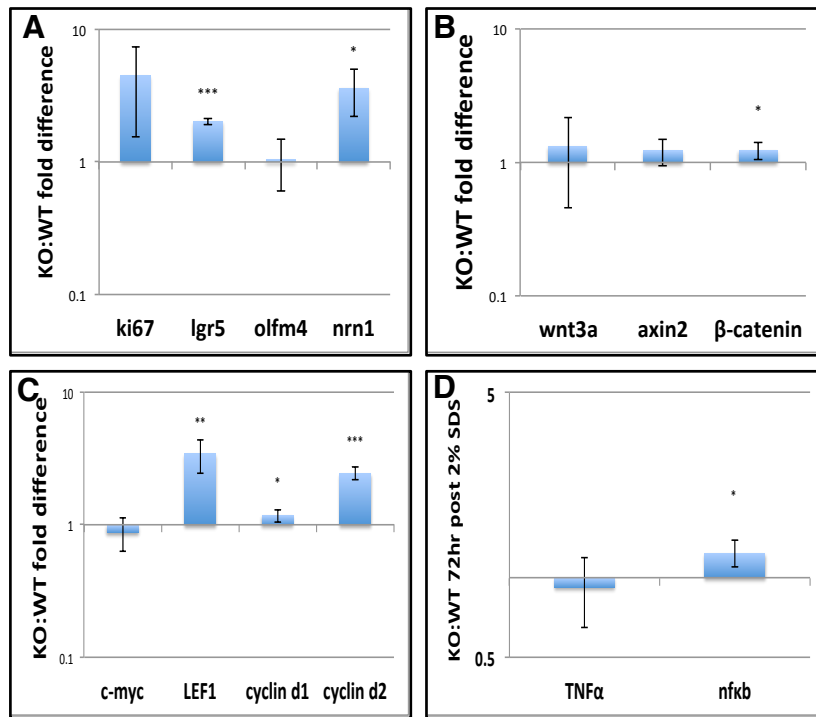


Figure 4-5 Enhanced levels of proliferation, stem cell and NF-κB markers in the fascin KO regenerating colons post DSS

Logarithmic scale of qRT-PCR data of whole tissue extracted from the regenerating WT and fascin KO colons post DSS treatment demonstrating a trend towards enhanced levels of Ki67 ($p=0.0543$) in the fascin KO. Significantly greater levels of Lgr5 ($p=3.03E-05$) and Nrn1 ($p=0.0161$) in the fascin KO with no difference in Olfm4 (A). There was a trend towards higher levels of the Wnt ligand and Axin 2 in the fascin KO, although not significant, and significantly higher levels of β -catenin ($p=0.0465$) in the fascin KO (B). Analysis of Wnt targets demonstrates no significant difference in c-Myc, however significantly higher levels of LEF1 ($p=0.00631$), Cyclin D1 ($p=0.0383$) and Cyclin D2 ($p=0.000368$) in the fascin KO (C). Analysis of the jak-stat markers in whole tissue extracted 72 hours following a 5 day course of 3.5% DSS demonstrates significantly higher levels of NF- κ B ($p=0.0211$) in the fascin KO, however there was no statistical difference in TNF α . Error bars represent SD. Significance asterisks: * = <0.05 , ** = <0.01 , *** = <0.001 .

Given the enhanced expression of NF- κ B and Lgr5 in the absence of fascin, we wished to further explore the possibility that fascin may act as a negative regulator, either directly or indirectly of either TNF α or Wnt ligand or conversely that TNF α or Wnt ligand regulate fascin expression. Consequently, we used a TNF α blocker, Etanercept (trade name Enbrel (Spencer-Green 2000)) on WT mice (daily intra-peritoneal injections one day prior and throughout a 5 day 3.5% DSS course followed by 72 hours of normal drinking water) to determine whether there was a resultant reduction in proliferation and change in fascin expression. The sections we stained showed no obvious difference in fascin expression (Fig. 4.6). We then wished to determine whether there was any effect on proliferation, however, again using IHC we found no difference in the number of Ki67 cells in either the control or the Etanercept treated group (Fig. 4.6). Lastly,

we examined for differences in neutrophils and macrophages, but again found no difference in the control or the Etanercept treated (Fig. 4.6). We used the anti-NIMP antibody to examine neutrophils, a feature common to this antibody is non-specific background epithelial staining which is also seen in negative controls - this is indicated by arrows in the Fig. 4.6.

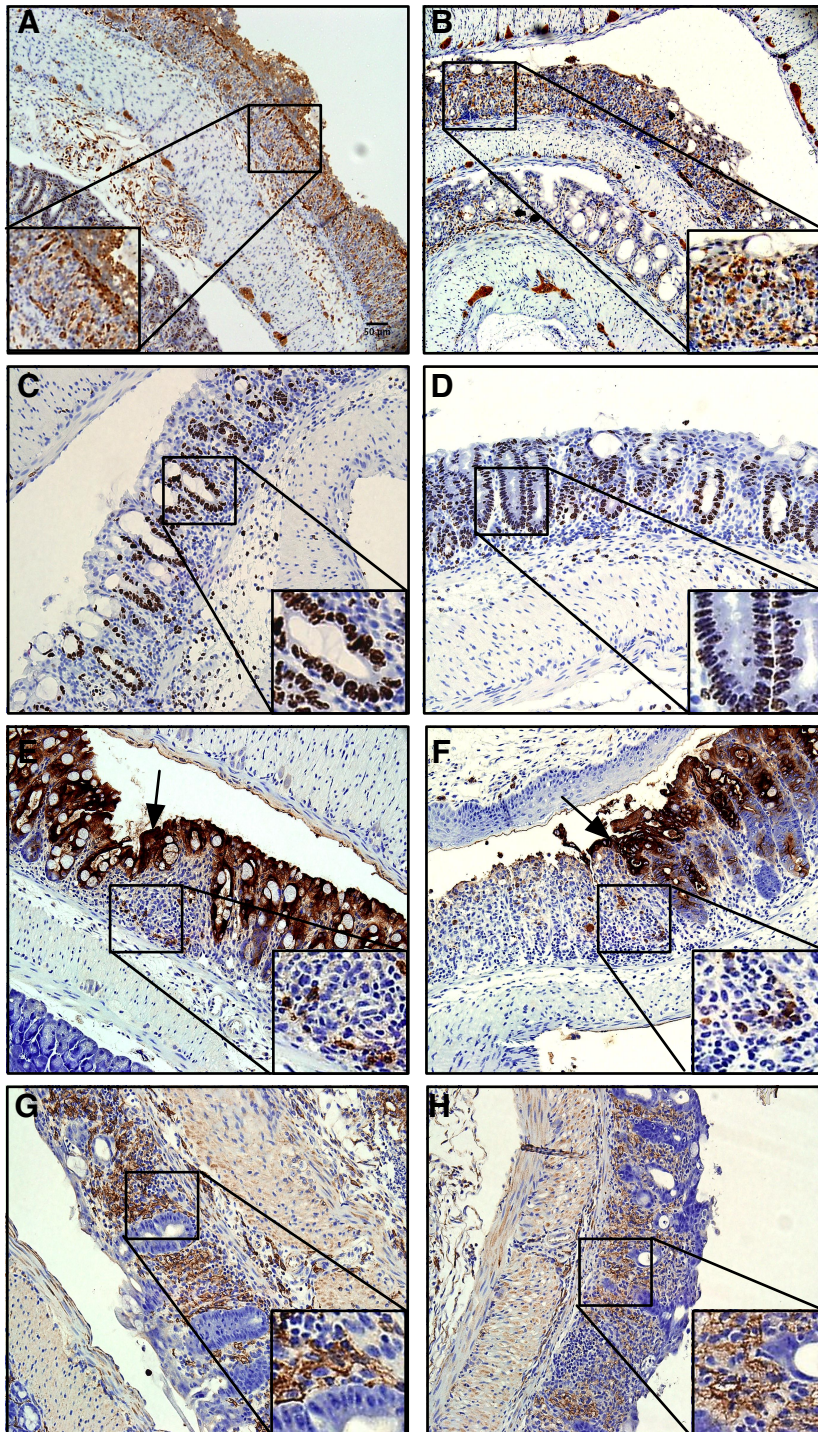


Figure 4-6 TNF α blocker has no demonstrable effect on the expression of fascin, proliferation of crypts or recruitment of neutrophils/macrophages in the colitis model

WT mice were subjected to daily IP injections of 3mg/ml Etanercept one day prior and throughout the duration of a 5 day 3.5% DSS course followed by 72 hours of normal drinking water. The control WT mice (A) and the WT mice treated with Etanercept (B) demonstrated no obvious difference in the expression of fascin (fascin antibody, brown, with haematoxylin counterstain, blue) seen in the regenerating colons. Furthermore, we found no difference in the number of Ki67 (using the anti-Ki67 antibody, brown with haematoxylin counterstain, blue) cells in either the control (C) or the Etanercept treated (D). We also examined for differences in neutrophils (using the anti-neutrophil NIMP antibody, brown with haematoxylin counterstain, blue) but found no difference between the control (E) or the Etanercept treated (F) group (non-specific background staining indicated with arrows). Lastly we found no difference in macrophages (using the anti-macrophage F4/80 antibody, brown with haematoxylin counterstain, blue) in the control (G) or the Etanercept treated (H). Images representative of 3 independent experiments.

4.3.4 Fascin expression in untreated and regenerating colons

We found low, but detectable levels of fascin in untreated WT colon, both on WB (again, using Femto substrate), IHC and using qRT-PCR (Fig. 4.7). We extracted tissue from the DSS time course to determine how the level of fascin in the treated colon varied with time. Using qRT-PCR of whole tissue extract, we found the level of fascin peaked 24 hours after cessation of a 5 day 2% DSS course and this level decreased following transition to normal drinking water and the regenerative phase (Fig. 4.7). We correlated this with the level of Wnt ligand and found that as the expression of fascin reduced from Day 5 onwards, so the level of Wnt ligand dramatically increased indicating potentially a regulatory role for fascin on Wnt expression (Fig. 4.7).

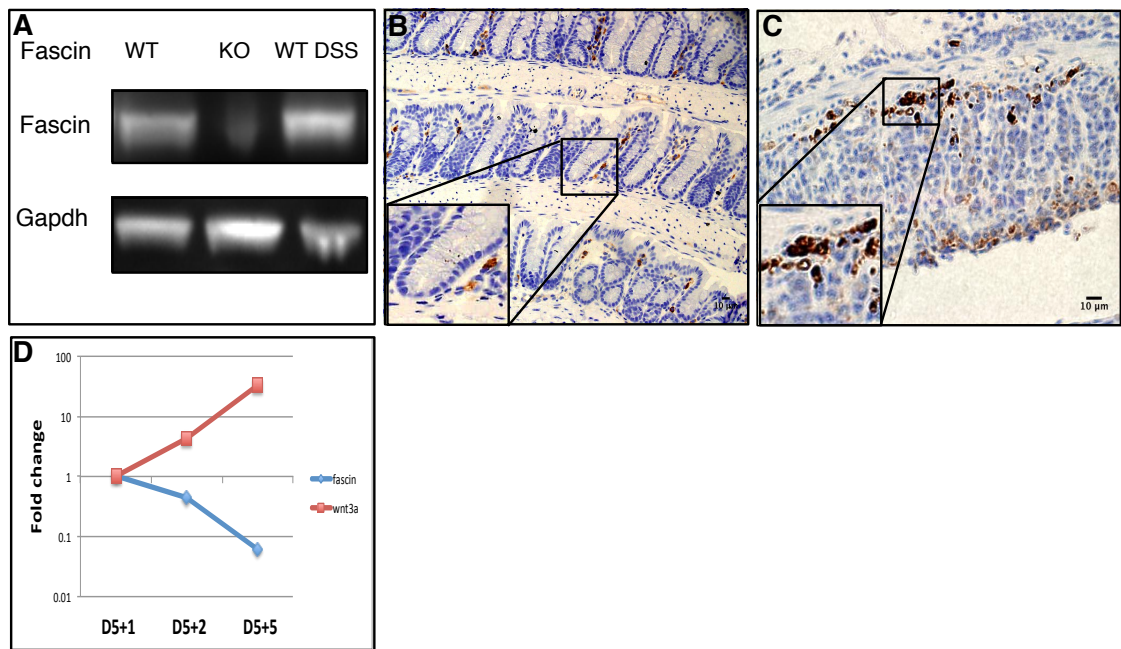


Figure 4-7 Fascin expression in untreated and regenerating colons

Western Blot using femto substrate demonstrating higher levels of fascin in whole tissue extracted from colons 5 days after commencing DSS treatment (WT DSS) compared with untreated (WT) (A): WB representative of 3 independent experiments. WT colons stained with fascin antibody (brown) demonstrating low levels of fascin in untreated (B) and DSS treated colons (C): images representative of 3 independent experiments. The staining of fascin is predominantly stromal, with some epithelial cells in the base of the crypt and also some blood vessels. Logarithmic scale showing the expression of fascin in WT colons decreasing as the levels of Wnt ligand increase in the regenerating colons (D): n=1 mouse/time point.

4.3.5 Loss of fascin results in impaired neutrophil production and recruitment in regenerating colons

In chapter 3, I demonstrated reduced numbers of neutrophils recruited in the fascin KO small intestine post irradiation and the associated reduction in chemokines in the fascin KO, which may in part explain the phenotype. As such, we wished to determine whether this would be replicated in our colitis model. We initially quantified the number of macrophages (using IHC with the anti-macrophage antibody F4/80) and neutrophils (using IHC with the anti-neutrophil antibody NIMP) in the regenerating colon 72 hours after completing a 5 day DSS course. There was no difference in macrophages, however we again demonstrated significantly reduced numbers of neutrophils in the fascin KO compared with WT ($p=0.00190$) (Fig. 4.8). We further wished to understand mechanistically the observed reduction in neutrophil recruitment in the fascin KO so, using qRT-PCR we quantified the levels of the CXCL ligands 1,2 and 5 and the chemokine receptor CXCR2 in whole tissue extracted from the DSS treated colons at the 72 hour time point. We found significantly reduced levels of CXCL2 ($p=7.99E-05$) in the fascin KO whereas there was no significant difference in the levels of CXCL1 ($p=0.228$) or CXCL5 ($p=0.140$) or the chemokine receptor CXCR2 ($p=0.475$) (Fig. 4.8).

There was no significant difference in the number of circulating neutrophils in the mice following irradiation: both WT and fascin KO had a significant pancytopenia as a consequence of the irradiation (Fig. 4.8). DSS, however does not affect haematopoiesis so we analysed the blood profile in both WT and fascin KO mice, before and following DSS treatment. In untreated mice there is no significant difference in the number of circulating white blood cells (WBCs) ($p=0.337$), neutrophils ($p=0.146$), lymphocytes ($p=0.419$), monocytes ($p=0.172$) or platelets ($p=0.388$) (Fig. 4.8). In blood collected from mice 72 hours after completing a 5 day DSS course we demonstrate here significantly reduced numbers of circulating WBCs ($p=0.00300$), neutrophils ($p=0.00500$) and lymphocytes ($p=0.00700$) in the fascin KO although there was no significant reduction in monocytes ($p=0.0570$) or platelets ($p=0.482$) (Fig. 4.8). We wished to further explore whether the expression of fascin correlated with neutrophil recruitment to the damaged colons. Using the CXCR2 mouse from Professor Owen Sansom's lab, we performed fascin staining on IHC sections from both

CXCR2 WT and CXCR2 KO mice following DSS treatment, however we found similar expression of fascin staining in both cohorts (Fig. 4.8). Collectively, these findings indicate the phenotype seen may be in part CXC chemokine mediated.

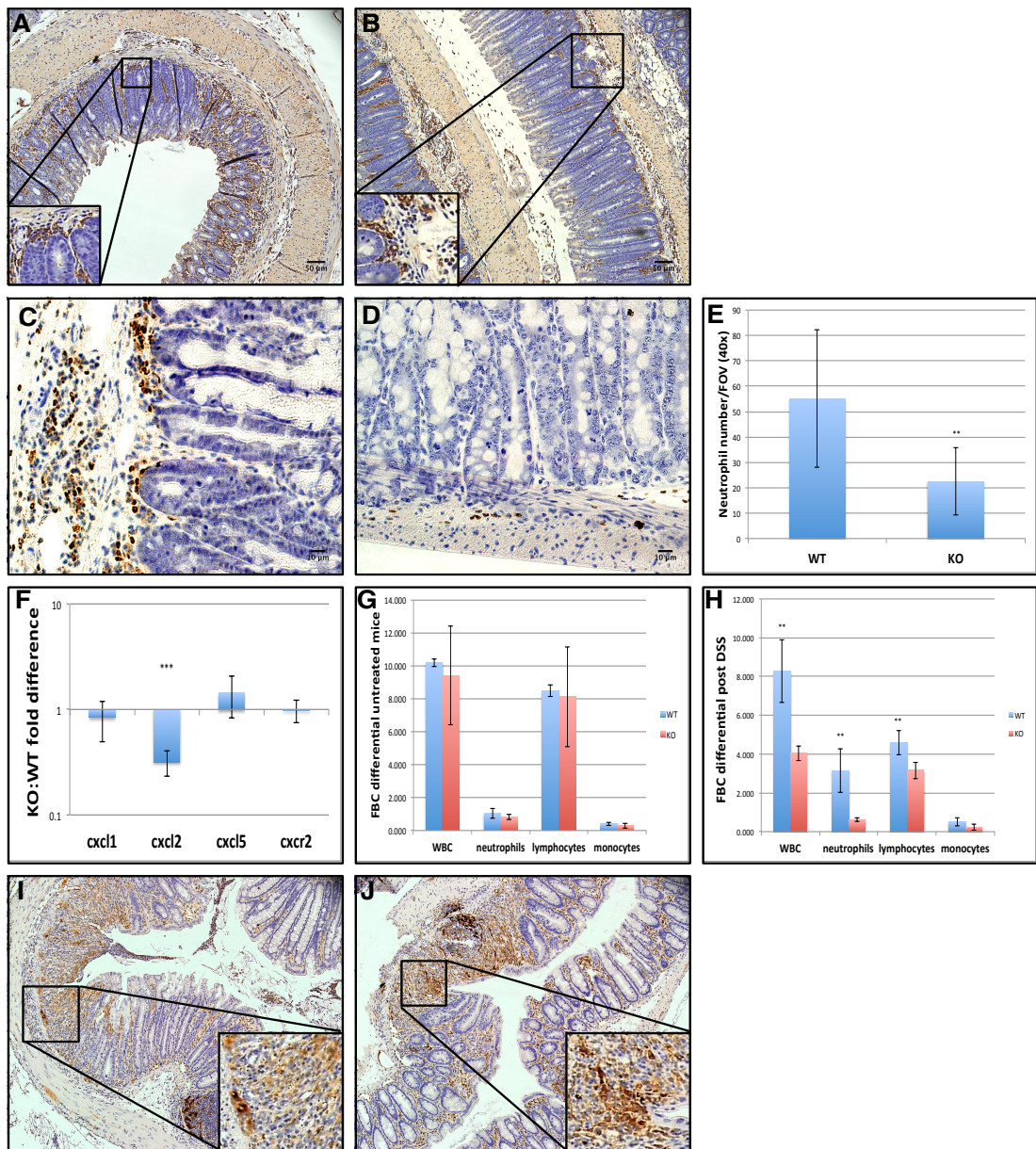


Figure 4-8 Loss of fascin results in impaired neutrophil production and recruitment in regenerating colons

There was no difference in the number of macrophages (F4/80 antibody, brown with haematoxylin counterstain, blue) in either WT (A) or fascin KO (B) colons following DSS damage. WT (C) and fascin KO (D) colons stained with MPO antibody (brown, with haematoxylin counterstain, blue) demonstrating significantly fewer recruited neutrophils to the fascin KO colons ($p=0.00910$, Mann Whitney) 72 hours after completing a 5 day 3.5% DSS course (E): $n=11$ WT, $n=6$ fascin KO with minimum of 5xFOVs per sample. Logarithmic scale of qRT-PCR data demonstrating significantly reduced levels of CXCL2 ($p=7.99E-05$) in the fascin KO colons, whilst no significant difference in levels of CXCL1 ($p=0.228$), CXCL5 ($p=0.140$) and CXCR2 ($p=0.475$) (F). FBC analysis of WT and fascin KO untreated mice (G) demonstrated no significant difference in WBCs ($p=0.337$), neutrophils ($p=0.146$), lymphocytes ($p=0.419$), monocytes ($p=0.172$) or platelets ($p=0.388$, not shown) whilst (H) shows significantly reduced levels of white blood cells ($p=0.00300$), neutrophils ($p=0.00500$) and lymphocytes ($p=0.00700$) in the fascin KO FBC 72 hours post 5 days of DSS. There was no significant difference in the number of monocytes ($p=0.0570$) or platelets ($p=0.482$, not shown). Statistical analysis using Student's t-test, $n=5$ WT, $n=3$ fascin KO. There was no difference in the level of fascin staining (fascin antibody brown, with haematoxylin counterstain, blue) in CXCR2 WT (I) and CXCR2 KO (J) colons following a 5 days 2% DSS course indicating there is no correlation between fascin expression and neutrophils. Images representative of 3 independent experiments. Error bars represent SD. Significance asterisks: * = <0.05 , ** = <0.01 , *** = <0.001 .

4.4 Discussion

4.4.1 Fascin is not required to maintain normal homeostatic colonic architecture

Our studies suggest that, as was the case with the small intestine, fascin is not required to maintain the normal colonic architecture under homeostatic conditions. The presence of low levels of fascin in the colon and lack of statistical difference in the crypt size, number of BrdU positive cells or goblet cells indicates that fascin does not play an important role in the maintenance of colonic architecture under normal homeostatic conditions.

In a similar pattern to the small intestinal model, at the mRNA level there is a significant reduction in the level of the stem cell marker Lgr5 with no apparent consequent reduction in crypt proliferation. Transcriptional profiling, using mass spectrometry of Lgr5 stem cells and their daughters revealed a multitude of unique genes (Munoz, Stange et al. 2012) including Olfm4 and Nrn1 which were not significantly different in the untreated colon. It would be interesting to determine the differences in the Lgr5 gene lineage between WT and fascin KO to further explore the differences seen; both in untreated tissue and also in the DSS treated colons.

As was the case in the small intestinal model, in physiological conditions, the level of basal TNF α mRNA was lower in the fascin KO and this may be an explanation for the reduced levels of Lgr5 in the fascin KO. There was no difference in the level of NF κ B, however it is the activation of NF κ B that is important and it would be interesting to look at this.

4.4.2 Fascin KO mice have greater clinical deterioration

Using the DSS time course, the fascin KO mice showed significantly greater clinical signs of colitis compared with WT, however histologically there was no difference.

The immune system plays a significant role in response to inflammation and this may be one explanation for the exaggerated deterioration in the fascin KO mice. We have demonstrated that there are significantly reduced levels of the

circulating immune cells in the fascin KO and reduced numbers of neutrophils recruited in the inflamed colons. A reduced ability to mount an adequate immune response to the colitis may result in an earlier clinical deterioration and enhanced histological damage, although the histological changes are likely to be multi-factorial. Furthermore, in the colitis associated carcinogenesis model, which I will discuss in chapter 5, there was a greater mortality in the fascin KO mice over the 70 days with the fascin KO mice not tolerating the milder 2% DSS as well as the WT. This reduced immunological response may result in more significant clinical signs of colitis and may in part, explain the phenotype seen with the fascin KO mice.

4.4.3 Fascin KO have enhanced crypt proliferation in the DSS model

As was seen in the small intestinal irradiation model, the level of Lgr5 (which in untreated colon is lower in the fascin KO) in the regenerating colon becomes significantly higher in the fascin KO resulting in a trend towards greater numbers of BrdU positive cells and indeed a higher position of the BrdU positive cells on the crypt axis indicating enhanced proliferation in the absence of fascin. Again, there is no difference in the number of regenerating crypts indicating a proliferative change as opposed to a mechanism dependant on stemness. As was the case in the Wnt3a conditioned crypt culture model, the levels of basal NFκB mRNA are significantly higher in the fascin KO regenerating colon, which may account for the enhanced overall proliferation rate and higher Lgr5 mRNA also detected in the fascin KO.

It would have been interesting to further compare isolated Lgr5 cells from both WT and fascin KO mice, using gene expression analysis to explore the observed differences. We attempted to do this by introducing the EGFP reporter of the IRES (internal ribosomal entry site) cassette to the Lgr5 cells of the fascin KO mice. We would then be able to isolate individual Lgr5 cells using FACS analysis for use in gene expression characterisation. This technique had been successfully used with the WT mice, however when we crossed the WT with the fascin KO, we failed to get sufficient numbers of homozygous mice carrying the EGFP

reporter despite multiple matings over a 6 month period. Further work is needed to understand the reason behind the reduced number. One potential explanation could be a conflict in the positioning of the reporters on the chromosomes overlapping with that of the fascin KO mouse.

The level of Wnt ligand is slightly higher in the fascin KO in the regenerating colon and it may be that fascin acts either as a direct or indirect regulator of Wnt signalling. In the time course we showed that as the level of fascin reduced following the cessation of DSS, the level of Wnt ligand increased by several magnitudes. In the fascin KO mouse, the absence of fascin permits higher levels of Wnt ligand and consequent higher levels of Wnt targets as was shown with the qRT-PCR data. Certainly, the role of fascin is not limited to the bundling of actin and it may be that the presence of fascin in the paneth cells (where Wnt ligand is secreted (Sato, van Es et al. 2011)) is important in the regulation of Wnt secretion.

4.4.4 Loss of fascin results in impaired neutrophil production and recruitment in regenerating colons

In the small intestinal model we demonstrated significantly reduced number of neutrophils recruited in the fascin KO regenerating small intestine, however it was not possible to determine whether this was a production or recruitment defect. Given there was no significant difference in the number of circulating neutrophils in the untreated mice, it was presumed to be recruitment related. DSS however does not impair haematopoiesis and it was interesting to note that, whilst again there were significantly fewer neutrophils recruited in the fascin KO colon, the full blood count analysis demonstrates significantly reduced numbers of circulating neutrophils and this may be solely responsible for the recruitment defect noted. In addition to the reduced circulating levels of neutrophils there was an overall reduction in the number of circulating white blood cells that may contribute to an ineffectual immune response to inflammation and consequent increased clinical susceptibility.

The mechanism behind the impaired neutrophil production is likely to be predominantly CXCL2 dependant. There were significantly reduced levels of CXCL1 and CXCL2 in the fascin KO regenerating small intestines, however in the regenerating colon it was solely CXCL2. It is reassuring to have consistently reduced levels of CXCL2 across the small intestinal and colonic model and, whilst other chemokines will likely play a part, it is possible to hypothesise that CXCL2 is the chemokine that is responsible for the phenotype seen. As previously mentioned, dendritic cells have been shown to express CXCL1 and CXCL2 (Zaharik, Nayar et al. 2007) and we hypothesise that there is some degree of dendritic cell impairment in the fascin KO mouse resulting in reduced levels of the aforementioned chemokines.

References

- Adams, J. C. (2004). "Roles of fascin in cell adhesion and motility." *Curr Opin Cell Biol* **16**(5): 590-596.
- Bleich, A., M. Mahler, et al. (2004). "Refined histopathologic scoring system improves power to detect colitis QTL in mice." *Mamm Genome* **15**(11): 865-871.
- Dohi, T., A. Borodovsky, et al. (2009). "TWEAK/Fn14 Pathway: A Nonredundant Role in Intestinal Damage in Mice Through a TWEAK/Intestinal Epithelial Cell Axis." *Gastroenterology* **136**(3): 912-923.
- Edwards, R. A. and J. Bryan (1995). "Fascin, a Family of Actin Bundling Proteins." *Cell Motility and the Cytoskeleton* **32**(1): 1-9.
- Munoz, J., D. E. Stange, et al. (2012). "The Lgr5 intestinal stem cell signature: robust expression of proposed quiescent '+4' cell markers." *EMBO J* **31**(14): 3079-3091.
- Qualtrough, D., K. Smallwood, et al. (2011). "The actin-bundling protein fascin is overexpressed in inflammatory bowel disease and may be important in tissue repair." *BMC Gastroenterol* **11**: 14.
- Sato, T., J. H. van Es, et al. (2011). "Paneth cells constitute the niche for Lgr5 stem cells in intestinal crypts." *Nature* **469**(7330): 415-+.
- Spencer-Green, G. (2000). "Etanercept (Enbrel): update on therapeutic use." *Annals of the Rheumatic Diseases* **59**: 46-49.
- Tan, V. Y., S. J. Lewis, et al. (2013). "Association of fascin-1 with mortality, disease progression and metastasis in carcinomas: a systematic review and meta-analysis." *BMC Med* **11**: 52.
- Zaharik, M. L., T. Nayar, et al. (2007). "Genetic profiling of dendritic cells exposed to live- or ultraviolet-irradiated *Chlamydia muridarum* reveals marked differences in CXC chemokine profiles." *Immunology* **120**(2): 160-172.

5 Chapter 5 – Loss of fascin results in an impaired inflammatory response and reduced tumourigenesis

5.1 Summary

Tumours arising within the GI tract may result from chronic inflammation (Coussens and Werb 2002) or sporadic genetic alterations (Kinzler and Vogelstein 1996). Sporadic tumours themselves will also have an inflammatory component and indeed have been shown to control aspects of the inflammatory response to enhance their progression (Coussens, Raymond et al. 1999). I demonstrate here that in both inflammatory and sporadic murine models of small intestinal and colonic tumourigenesis, loss of fascin profoundly suppresses tumour formation and size. Furthermore, we demonstrate significantly reduced numbers of neutrophils in inflammatory driven and sporadic tumours and hypothesise that the mechanism behind the reduced tumour burden in the fascin KO, is a consequence of a reduced inflammatory response secondary to impaired dendritic cell function resulting in reduced circulating and subsequent recruited neutrophils.

5.2 Introduction

We have shown the expression of fascin increases, in both the stroma and epithelial cells, at certain times in both inflammatory models of the small intestine and colon, albeit to a small extent. It was further shown, in human samples, to be strongly expressed in ulcerative colitis (UC), Crohn's colitis and diverticulitis human tissue samples with expression levels correlating with disease severity and strongest expression seen in the dysplastic pre-malignant cells (Qualtrough, Smallwood et al. 2011). Fascin is also highly expressed in tumours arising in the oesophagus (Hashimoto, Ito et al. 2005), stomach (Hashimoto, Shimada et al. 2004), small intestine (Ozcan, Karslioglu et al. 2011) and colon (Hashimoto, Skacel et al. 2006). Furthermore, high fascin expression has been shown to be an independent prognostic indicator of poor outcome in oesophageal, gastric and colon cancer (Tan, Lewis et al. 2013) (Kim, Kim et al. 2012) and is associated with metastasis in stomach and colon cancers (Tan, Lewis et al. 2013). In this chapter I will show significantly reduced circulating and recruited neutrophils in a fascin KO colitis associated carcinogenesis (CAC) model with consequent reduction in tumour number and burden. I further

demonstrate reduced numbers of neutrophils in inducible APC^{fl/fl} p53^{fl/fl} fascin KO and APC^{fl/fl} p53^{R172H} Ah-cre fascin KO models with consequent reduction in tumour size and burden. Surprisingly, in the inducible model there was no associated increase in survival in the fascin KO, despite the reduced tumour number and burden. In both normal and fascin KO models, tumours still invaded into the surrounding tissue and stroma indicating that the primary role of fascin may be one of early tumour formation and not progression.

5.3 Results

5.3.1 Colitis associated carcinogenesis (CAC) model

Following a single intra-peritoneal injection of Azoxymethane (AOM) and 3 rounds of 2% DSS the mice were culled at 70 days (Fig. 5.1).

5.3.1.1 Fascin KO mice have fewer colonic tumours and reduced tumour burden

The fascin KO mice had significantly fewer polyps per colon with a mean number of 1.9 polyps per colon with the WT mean being 7.3 ($p=0.000300$) (Fig. 5.1). The tumour burden was also reduced ($p=0.0550$), although not significant (Fig. 5.1). The WT polyps strongly expressed fascin, predominantly in the stroma, but also in some epithelial cells and blood vessels (Fig. 5.1). Preliminary qRT-PCR analysis of the polyps suggests there may be reduced levels of *Lgr5*, *Nrn1*, *Olfm4*, *Sox9*, *Ephb3* and *Slc14a1* in the fascin KO whilst *Ets2*, *Rgmb*, *Tnfrsf19*, *Ascl2* and *Bmi1* were higher in the fascin KO (Fig. 5.1) (although these results are not yet significant, as RNA was only successfully extracted from one polyp per mouse). Subsequent analysis of the jak-stat pathway demonstrated lower levels of TNF α , NF- κ B, IL-6, IL-11b, Jak1 and Jak2 in the fascin KO whereas IL-11, Jak3 and Stat3 were higher in the fascin KO (Fig. 5.1). Further analysis of the Wnt members showed lower levels of APC and β -catenin in the fascin KO, whilst Axin2 was higher (Fig. 5.1). Lastly, Wnt targets c-Myc and TCF1 were lower in the fascin KO whilst LEF1 was higher in the fascin KO (Fig. 5.1). Quantification of the number of BrdU positive cells per tumour demonstrated no significant difference ($p=0.393$) between WT and fascin KO (Fig.5.1).

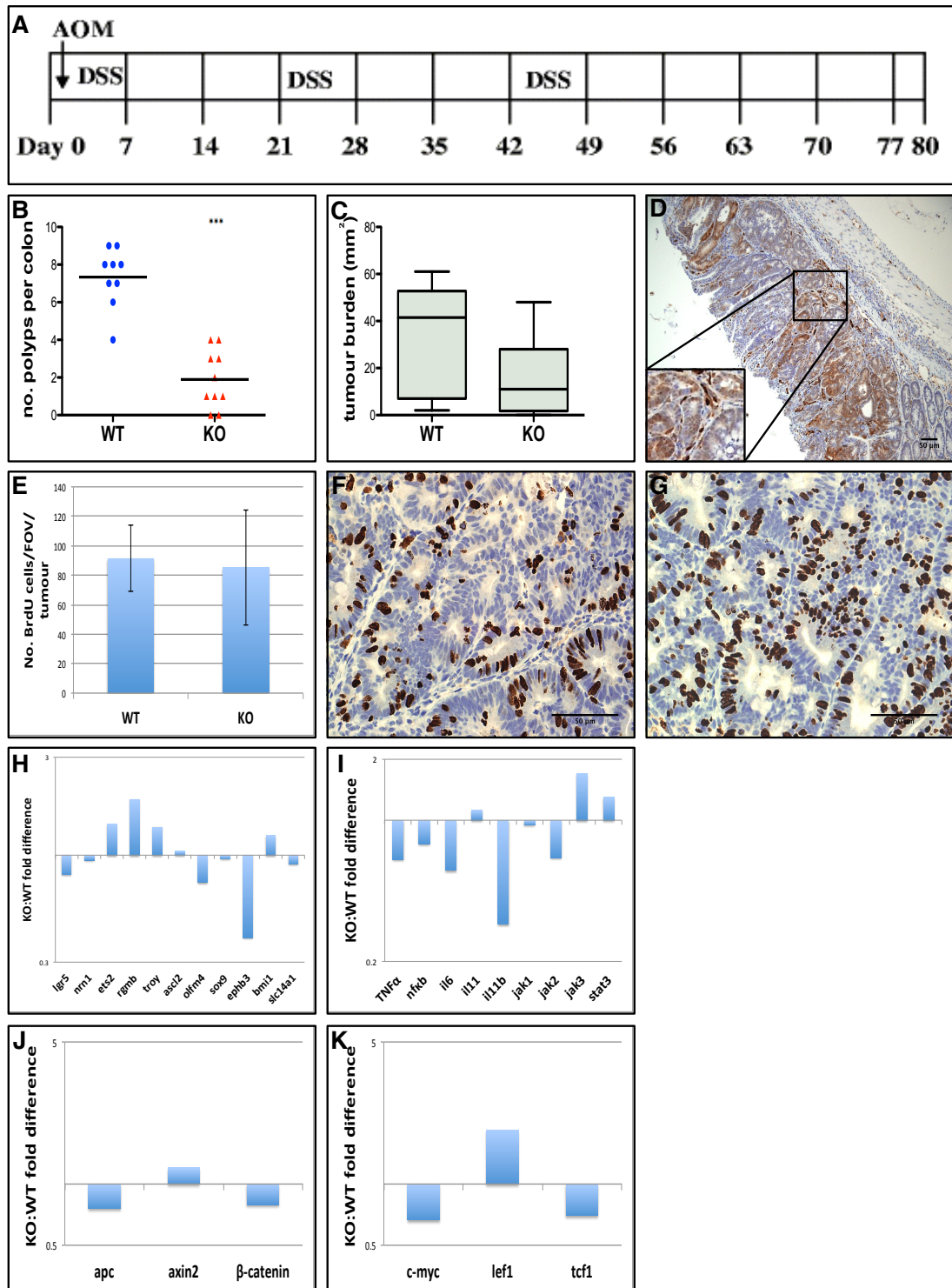


Figure 5-1 Fascin KO mice have reduced colonic tumour number and burden in the colitis associated carcinogenesis model

The CAC model (A): reproduced with kind permission from Springer (Tian, Ye et al. 2011)). The fascin KO mouse had significantly fewer tumours than the WT (B) (n=9 WT, n=10 fascin KO, p=0.000300, Mann Whitney) and reduced tumour burden (C) (p=0.0550, Mann Whitney). The WT tumours expressed fascin strongly (fascin antibody, brown, with haematoxylin counterstain, blue) (C) within the epithelial cells, stroma and blood vessels. There was no significant difference (p=0.393) in the number of BrdU positive cells (E) in either WT (F) or fascin KO (G) tumours. Images representative of a minimum of 9 independent experiments. qRT-PCR logarithmic scale analysis of a single WT and fascin KO tumour shows a mixed picture regarding stem cell markers (H), jak-stat markers (I), Wnt members (J) and targets (K). Error bars represent SD. Significance asterisks: * = <0.05, ** = <0.01, *** = <0.001.

5.3.1.2 Fascin KO mice have a reduced number of circulating leucocytes and recruited neutrophils to the tumour microenvironment

It was important to quantify the immunological response to the treatment, in particular because we found the fascin KO mice to have enhanced mortality compared with the WT (Fig 5.2). We initially quantified the number of circulating immune cells in the mice at the end of the treatment. The full blood count demonstrated significantly fewer circulating WBCs ($p=0.000440$) and platelets ($p=0.0340$) in the fascin KO (Fig 5.2). There is a trend towards fewer circulating neutrophils ($p=0.190$) and lymphocytes ($p=0.126$) in the fascin KO, however this was not yet significant (Fig 5.2). There were significantly more monocytes in the fascin KO ($p=0.019$). Given the reduced immunological response it is perhaps unsurprising that the fascin KO mice had a higher mortality (40%) compared with WT (20%) in the number of mice which had to be culled prior to the 70 day time point (Fig 5.2). We subsequently wished to determine whether the reduced number of circulating leucocytes translated into fewer neutrophils recruited to the fascin KO tumour microenvironment. Immunohistochemical (IHC) analysis (using the anti-neutrophil NIMP antibody) demonstrated significantly fewer recruited neutrophils ($p=0.000210$) in the fascin KO tumours with respect to the WT (Fig 5.2). We also looked at the number of macrophages recruited (using the anti-macrophage F4/80 antibody) and also the anti-von willebrand factor (vWF) antibody to detect differences in angiogenesis (Fig. 5.2). We did not quantify this analysis, but there was no obvious difference in the density of macrophages or blood vessels (Fig. 5.2). Regarding the vWF antibody, there was a considerable degree of non-specific background epithelial staining that was present in negative controls.

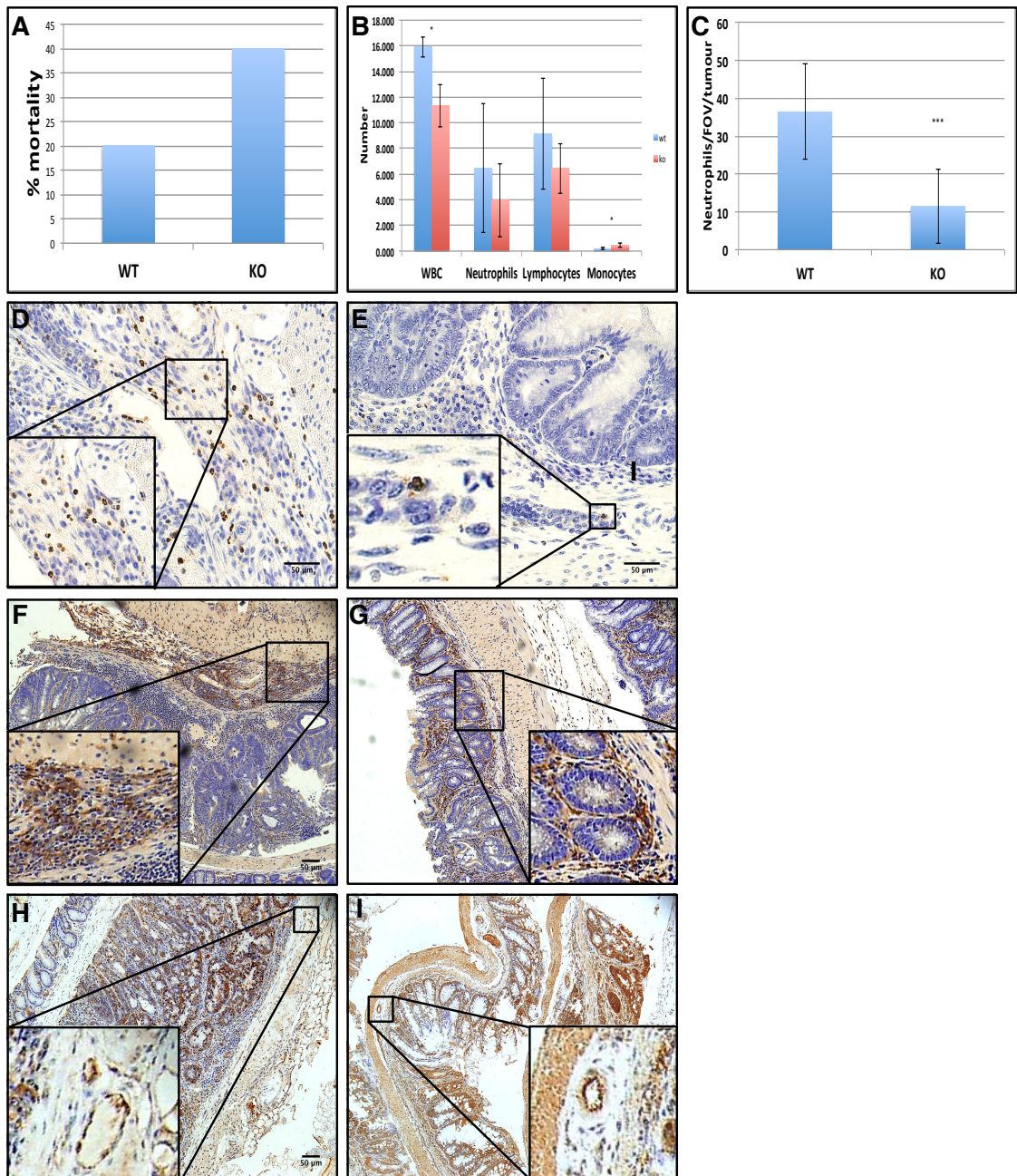


Figure 5-2 Fascin KO mice have reduced numbers of circulating leucocytes and recruited neutrophils to the tumour microenvironment

The fascin KO mice had an overall 40% mortality over the course of the treatment compared with WT having 20% (A) ($n=5$ WT, $n=20$ fascin KO). The full blood count analysis (B) of the mice at the end of the treatment course demonstrated significantly reduced numbers of circulating white blood cells ($p=0.000440$) and platelets ($p=0.0340$, not shown) in the fascin KO, with no significant difference in lymphocytes ($p=0.126$) or neutrophils ($p=0.190$). Significantly more monocytes in the fascin KO ($p=0.019$): $n=4$ WT, $n=5$ fascin KO. Given the reduced number of circulating leucocytes we next quantified the number of recruited neutrophils (using the NIMP antibody, brown, with haematoxylin counterstain, blue) to the WT (D) and fascin KO (E) tumour microenvironment. We found significantly reduced numbers of neutrophils in the fascin KO (tumour number $n=11$ (WT), 15 (fascin KO): $p=0.000210$, Mann Whitney): graph shows the mean number of neutrophils/FOV (under 40X lens) incorporating tumour and stroma with minimum of 4 FOVs/tumour. We found no difference in either the number of macrophages (F4/80 antibody, brown, with haematoxylin counterstain, blue) recruited in the WT (F) or fascin KO (G) or in angiogenesis (von Willebrand factor vWF, brown, with haematoxylin counterstain, blue) in the WT (H) or fascin KO (I) tumours: note the non-specific background epithelial staining which was also present in negative controls. Images representative of a minimum of 3 independent experiments. Error bars represent SD. Significance asterisks: * = <0.05 , ** = <0.01 , *** = <0.001 .

5.3.2 The role of fascin in sporadic and inducible tumourigenesis models

5.3.2.1 Fascin expression in sporadic and inducible murine intestinal tumourigenesis models

It has been well documented that fascin is expressed in human tumours arising from the GI tract (Hashimoto, Ito et al. 2005) (Hashimoto, Shimada et al. 2004) (Ozcan, Karslioglu et al. 2011) (Hashimoto, Skacel et al. 2006) so we initially wished to determine whether this was also true in our own murine models. Using the anti-fascin antibody on IHC sections of benign tumours arising from sporadic APC^{Min+} (Moser, Pitot et al. 1990) and APC^{1322t/+} (Pollard, Deheragoda et al. 2009) mice (bred in Professor Owen Sansom's lab), we demonstrated moderate expression of fascin within the stroma and epithelial cells of the tumours (Fig 5.3).

We next stained malignant tumours arising from an APC flox inducible mutant p53 flox mouse (APC^{fl/fl} p53^{fl/fl}) and an APC flox inducible P53 flox with mutant Kras G12D (APC^{fl/fl} p53^{fl/fl} Kras^{G12D}) mouse, and demonstrated strong fascin staining in both models with highest expression seen at the invasive front of the tumours (Fig. 5.3).

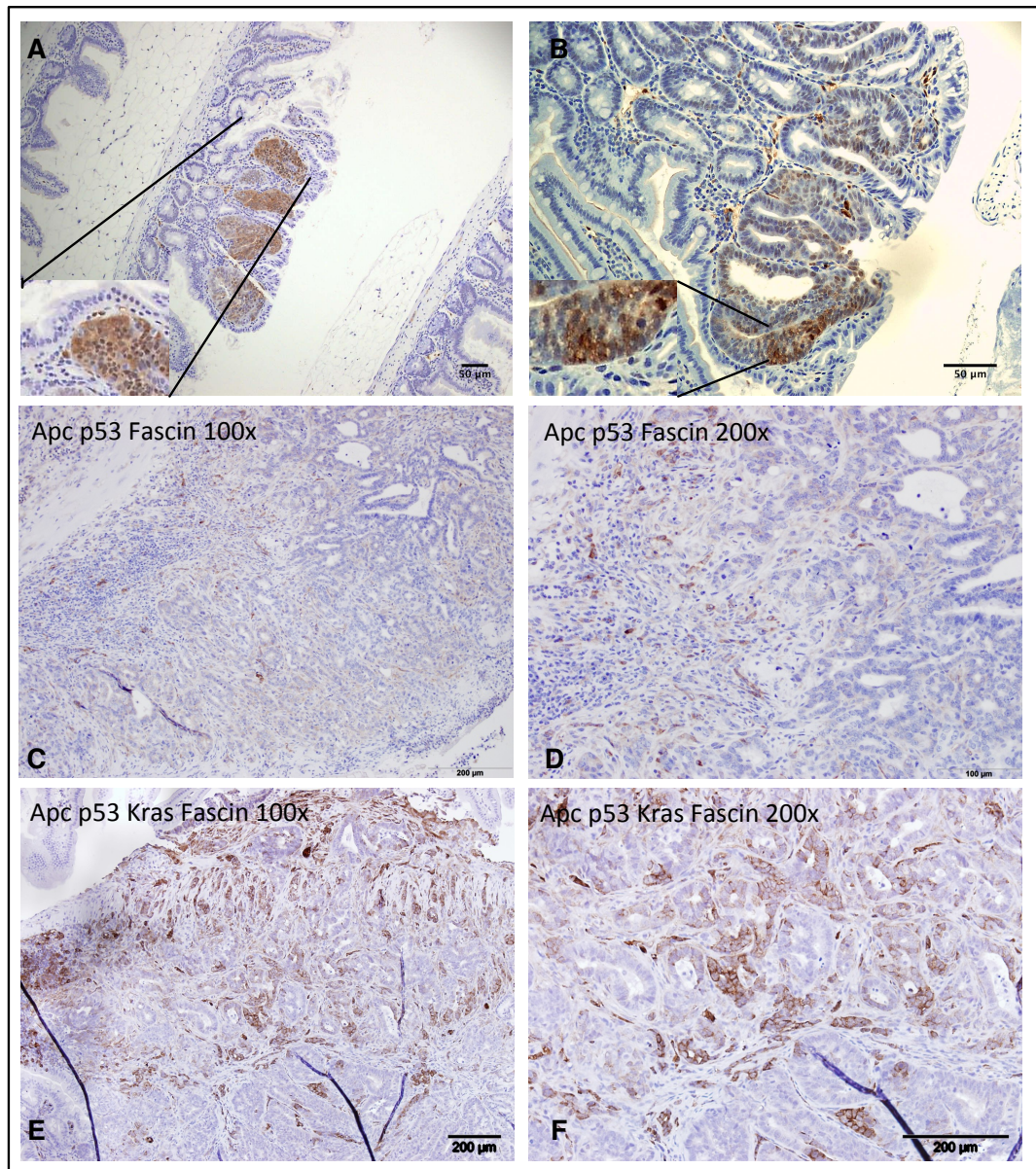


Figure 5-3 Fascin expression in sporadic and inducible murine intestinal tumourigenesis models

We found fascin (anti-fascin antibody, brown, with haematoxylin counterstain, blue) to be expressed moderately in the sporadic APC^{Min+} (A) and APC^{1322V+} (B) benign intestinal tumours. In the inducible malignant models we found fascin to be strongly expressed in the APC^{fl/fl} p53^{fl/fl} (C,D) and APC^{fl/fl} p53^{fl/fl} Kras^{G12D} (E,F) tumours with strongest expression seen at the invasive front. Images representative of a minimum of 3 independent experiments. Images C-F kindly donated by Dr. Ee Hong Tan.

Given the enhanced expression of fascin in these models, our initial thoughts were that fascin could be a Wnt target (Vignjevic, Schoumacher et al. 2007). We wished to explore this further in an inducible short-term model of proliferation using the AhCre⁺ APC^{fl/fl} mouse. The AhCre⁺ is regulated through transcriptional control of the Ah promoter and also through the binding of tamoxifen (Kemp, Ireland et al. 2004). Following induction, the loss of APC causes hyperactive Wnt

signalling and consequent hyper-proliferation. In collaboration with Professor Owen Sansom's lab, we stained sections of mouse small intestine 4 days following loss of APC, however there was no increase in fascin expression (Fig 5.4). This indicates that fascin is not a simple Wnt target in the small intestine in response to short-term APC deletion.

NF- κ B can directly interact with fascin in breast cancer cells in a stat3 dependent manner (Snyder, Huang et al. 2011). We thus explored the relationship between fascin with stat3 and NF- κ B in polyps and carcinomas, as both stat3 and NF- κ B have been heavily implicated in colon cancer and metastasis (Horst, Budczies et al. 2009) (Gavert, Ben-Shmuel et al. 2010). Again in collaboration with the Sansom lab, using IHC we stained sections of mouse small intestine which were either WT or homozygous for APC following a short term (4 day) treatment with the cytokine Il-11 in order to determine whether Il-11 and its subsequent up-regulation of Stat3 (Bollrath, Pheffe et al. 2009)) resulted in enhanced expression of fascin in the small intestines. There was, however no increase in the fascin expression (Fig 5.4).

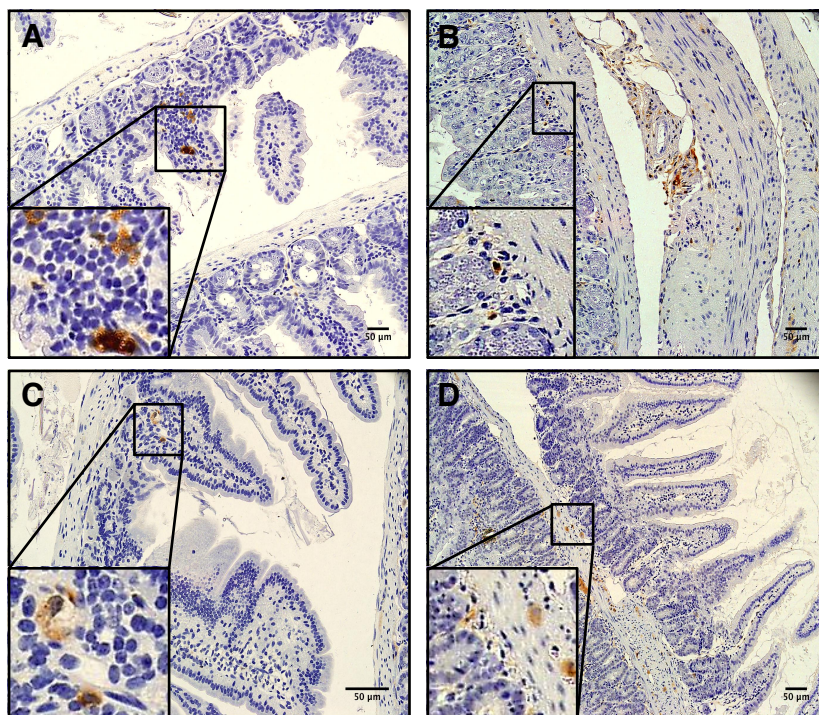


Figure 5-4 Fascin is not a Wnt target, nor is its expression regulated by Il-11 or Stat3

We obtained slides from Professor Owen Sansom's lab of mice which were either WT or homozygous for APC which had been induced to lose APC (or in the case of the WT to retain APC) in the presence or absence of the cytokine Il-11 in order to drive proliferation. We wished to determine whether the loss of APC (resulting in hyperactive Wnt signalling) induced fascin expression and furthermore, whether the addition of Il-11 (which in turn up regulates Stat3 in small intestinal epithelial cells) drove fascin expression. As can be seen in the APC WT (A) mouse, there is very low expression of fascin, similar to the levels seen in untreated, homeostatic WT small intestines. Upon addition of Il-11 in the APC WT small intestine (B) there is no increase in the expression of fascin indicating that il-11/stat3 does not regulate fascin expression. We next determined whether loss of APC resulted in enhanced fascin expression, however, as can be seen, in the APC hom (C) mouse, there is no increased expression relative to (A) or (B). The final slide demonstrates an APC hom mouse with the addition of Il-11 (D) and again there is no increase in the expression of fascin indicating the fascin is not regulated directly by the Wnt signalling pathway or Il-11/Stat3. Images representative of a minimum of 3 independent experiments.

5.3.2.2 Fascin^{-/-} APC^{fl/fl} p53^{fl/fl} Ah-cre and Fascin^{-/-} APC^{fl/fl} p53^{R172H} Ah-cre (FAPC) models

In collaboration with Professor Owen Sansom's lab, the APC^{fl/fl} p53^{fl/fl} Ah-cre and APC^{fl/fl} p53^{R172H} Ah-cre mice were crossed with our own fascin KO mouse (by Dr. Ee Hong Tan, post-doctoral researcher) to generate Fascin^{-/-} APC^{fl/fl} p53^{fl/fl} Ah-cre and Fascin^{-/-} APC^{fl/fl} p53^{R172H} Ah-cre (FAPC) inducible mice. The cre is induced with 3 intra-peritoneal injections of β -naphthoflavone in a single day on mice aged between 6-8 weeks. Whilst there was no difference in the survival ($p=0.207$) of the fascin KO and WT mice, the fascin KO had significantly fewer tumours ($p=0.0355$) and reduced tumour burden ($p=0.00980$) than the WT (Fig

5.5). Both WT and fascin KO tumours were invasive, although there was no evidence of metastasis in the organs we examined.

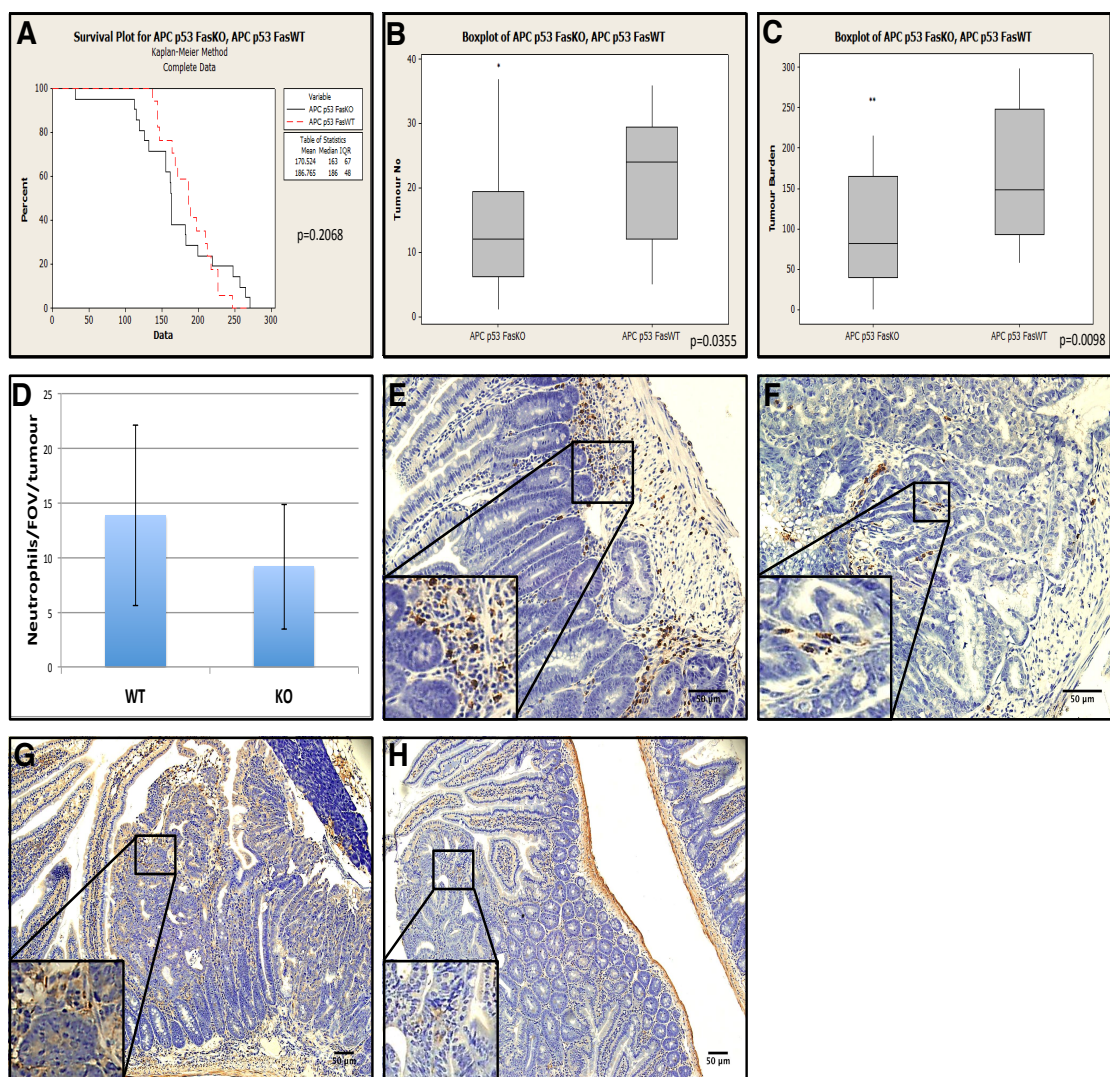


Figure 5-5 Reduced tumour number and burden in the inducible FAPC model

In collaboration with our own lab, Dr. Ee Hong Tan, post-doctoral researcher in Professor Owen Sansom's lab generated the FAPC mice. We initially compared the survival curve (A), but found no significant difference between WT and fascin KO ($n=17$ WT, fascin KO=21. Median survival WT=186 days, fascin KO 163 days. $p=0.207$, Wilcoxon). We next compared the tumour number (B) and found there to be significantly fewer tumours in the fascin KO ($n=17$ WT, fascin KO=20. Median tumour number WT=24, fascin KO=12. $p=0.0355$, Mann-Whitney). The tumour burden (C) was also significantly reduced in the fascin KO ($n=17$ WT, fascin KO=21. Median burden WT=148mm², fascin KO=82mm², $p=0.00980$, Mann-Whitney). We wished to determine whether, as was the case in the CAC model there were fewer neutrophils in the fascin KO. Using IHC, we stained the sections with the anti-neutrophil NIMP antibody (brown, with haematoxylin counterstain, blue) and found there was a trend towards fewer neutrophils in the fascin KO tumour microenvironment, although not significant (D) ($n=27$ WT tumours (E), 17 fascin KO tumours (F): $p=0.0775$, Mann-Whitney). We also stained the sections to look at macrophages with the anti-macrophage F4/80 antibody (brown, with haematoxylin counterstain, blue), but found no difference between the WT (G) and fascin KO (H). Images representative of minimum of 3 independent experiments. Error bars represent SD. Significance asterisks: * = <0.05, ** = <0.01, *** = <0.001. All scoring was done blind.

We next wished to determine whether, as was the case in the CAC model, there were fewer neutrophils in the fascin KO tumours. Using the anti-neutrophil NIMP antibody, we found a trend towards reduced numbers of neutrophils in the fascin KO tumour microenvironment, although this was not significant ($p=0.0775$) (Fig 5.5). We also looked at the number of macrophages recruited (using the anti-macrophage F4/80 antibody). We did not quantify this analysis, but there was no obvious difference in the density of macrophages or angiogenesis (Fig. 5.5).

5.3.2.3 Organotypic invasion model

We generated and cultured cell lines from tumours arising from the FAPC mice which were either WT or homozygous for fascin. Interestingly, following several passages of these cells we checked for expression of fascin using western blot (WB) in the WT line, however fascin was undetectable (Fig 5.6). Although both WT and fascin KO tumours were noted to be invasive *in-vivo*, we wished to determine whether there was any demonstrable difference *in-vitro*. Using the organotypic invasive model, the cell lines were seeded on a collagen matrix, the base of which lies in standard growth medium thereby creating an air/liquid interface which in turn creates a gradient through which cells may invade (Timpson, McGhee et al. 2011). Both fascin KO and WT cell lines invaded to similar depths (Fig 5.6). Interestingly, whilst the WT cell line lost expression of fascin when cultured in Matrigel with the standard medium, they re-expressed fascin in the organotypic model indicating that one of the constituents of the matrix (notably collagen and fibroblasts) or their secreted factors may be responsible for the expression of fascin by tumour cells (Fig. 5.6).

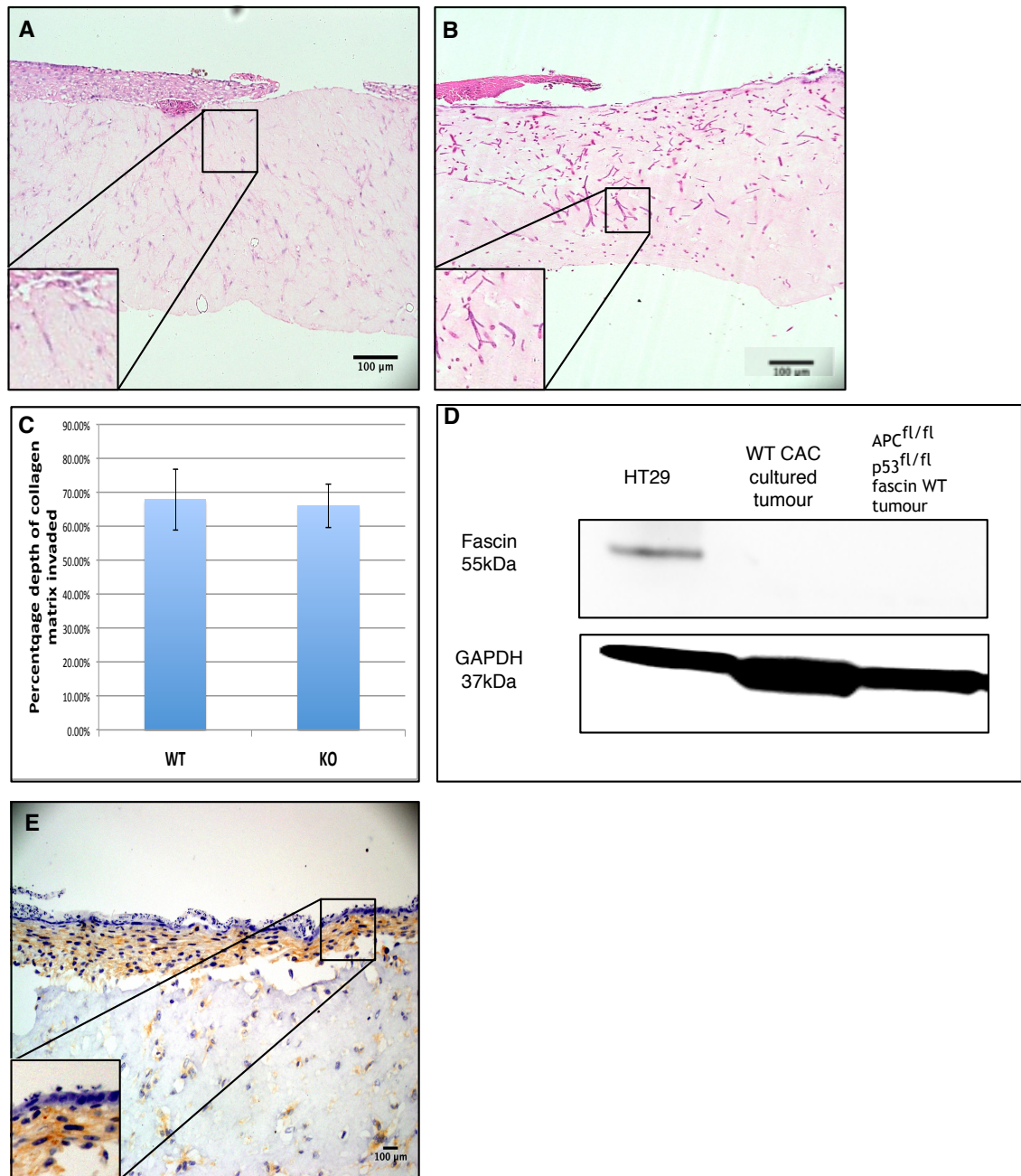


Figure 5-6 Organotypic invasion model

We wished to determine whether there was any difference in the invasive ability of the APC^{fl/fl} p53^{fl/fl} cells, isolated from the tumours from the mice which were either WT or fascin KO. Cells were plated on a collagen matrix with an air/medium interface and we demonstrated that the WT (A) and fascin KO (B) invaded to a similar depth (C) over a 14 day incubation period (n=3). Interestingly, despite cell lines cultured in Matrigel from both CAC and inducible APC^{fl/fl} p53^{fl/fl} tumours not expressing fascin in WB (D: WB representative of 3 independent experiments), upon plating on the collagen matrix the APC^{fl/fl} p53^{fl/fl} fascin WT cells expressed fascin using IHC (fascin antibody, brown with haemostoxilyn counterstain, blue) (E). Cell lines from CAC model were not used in the organotypic model. Images representative of minimum of 3 independent experiments. Error bars represent SD.

5.3.2.4 Orthotopic caecal model and cell adhesion assay

Given the reduced incidence of tumours in both the CAC and inducible intestinal models, we wished to determine, using an orthotopic caecal model of tumourigenesis (Tan, Holyoke et al. 1977) whether the phenotype was as a result of an impairment of the fascin KO cells to survive anoikis and establish initial contact with the matrix. We again used the established FAPC cell lines, which were either WT or KO for fascin, dissociated them to single cells and injected them into the caecum of nude mice. We initially set up a pilot experiment with 6 mice in each cohort. In the WT cohort, one of the 6 mice appeared to have a liver metastasis (or potentially it may have resulted from direct spread from the caecal tumour) and 50% of the mice survived less than 100 days (Fig 5.7). In contrast, none of the fascin KO mice developed metastasis and 80% of the mice survived greater than 100 days (Fig. 5.7). As such, we expanded the numbers, however, even though initially the nude mice with the WT tumours injected had enhanced mortality, only around 30% of the mice from both cohorts died with demonstrable tumours (Fig 5.7).

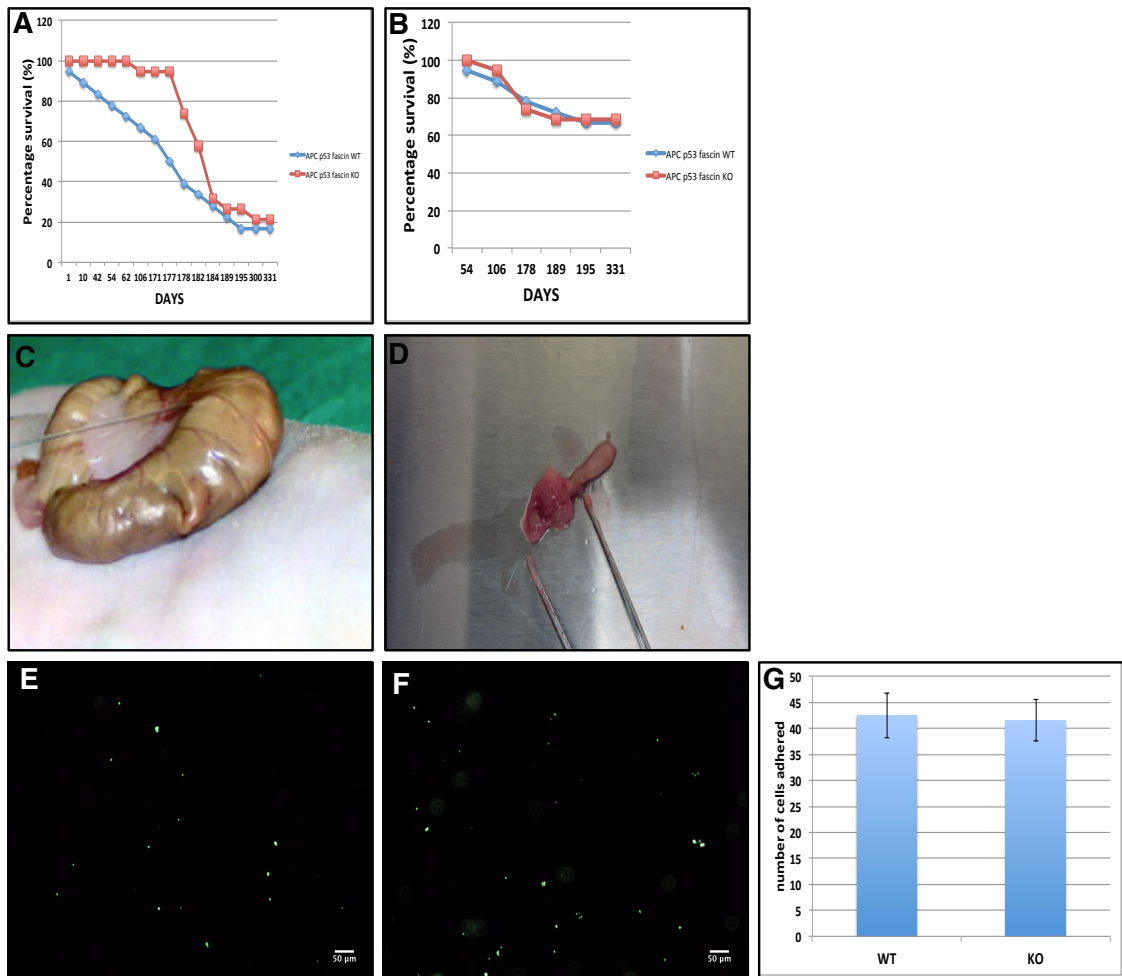


Figure 5-7 Orthotopic caecal model and cell adhesion assay

We wished to determine whether there was any difference in the ability of the APC^{fl/fl} p53^{fl/fl} cells, isolated from the tumours from the mice which were either WT or fascin KO and their ability to form tumours in nude mice. Overall, there was no significant difference in the percentage survival of the mice (A) and furthermore, only 27.8% of mice injected with WT tumours and 31.6% mice injected with fascin KO tumours had demonstrable tumours upon culling (B). n=12 WT, n=7 fascin KO, Photo, taken with permission from (Cespedes, Espina et al. 2007) demonstrating the injection of tumour cells into an exteriorised caecum in a nude mouse (C). Representative photograph of a WT caecal tumour after dissection (D). Using a cell adhesion assay we compared the ability of FAPC cell lines, which were either WT (E) or KO (F) for fascin to adhere to a fibronectin coated plate after dissociation to single cells (cells are green). There was no difference in the number of cells adhering to the plate (G) (n=3 plates per WT and fascin KO, 10 frames (10x magnification) counted per plate). Images representative of minimum of 3 independent experiments. Error bars represent SD.

We wished to further clarify, *in-vitro*, whether there was any difference in the ability of the APC^{fl/fl} p53^{fl/fl} cells, which were either WT or KO for fascin, to form adhesions. We thereby set up a cell adhesion assay whereby we trypsinised the adenomas to single cells, plated them on fibronectin covered plates for 30 minutes, washed them with PBS 3 times to wash off any non-adherent cells then stained the remaining adherent cells with calcein (a fluorescent cell permeable

dye) so that we could quantify the number of viable cells. We quantified both WT and fascin KO cells and there was no difference in either cohort (Fig. 5.7).

5.4 Discussion

5.4.1 Loss of fascin results in an impaired immune response and reduced tumourigenesis in the colitis associated carcinogenesis (CAC) model

Our studies suggest that, in response to the Azoxymethane and 3 rounds of 2% DSS, the fascin KO mice have globally reduced levels of circulating WBCs with consequent reduction in recruited neutrophils to the tumour microenvironment. It is unclear whether, in addition to a defect in the production of neutrophils in response to inflammation, there is also a defect in recruitment. Whilst we did not perform analysis of the chemokines or chemokine receptor in the CAC tissue, our data from the colitis model indicated that CXCL2 was significantly lower in the fascin KO in response to DSS and it is likely that the same mechanism is responsible in the CAC model. The reduced tumour number and burden in the fascin KO, may in part be related to the reduced neutrophil number as was seen in the CXCR2 KO mouse (Jamieson, Clarke et al. 2012), whereby reduced neutrophils in the colon resulted in profound suppression of tumours in the same CAC model. The relationship between inflammation and cancer initiation and maintenance has long been established with the infiltration of tumour promoting leucocytes thought to be of critical importance (Mantovani, Allavena et al. 2008). Ulcerative colitis is associated with a 20 fold increased lifetime risk of developing CRC (Xie and Itzkowitz 2008) so it is important to have a greater understanding of the pathways and mechanisms involved in modulating this. We have demonstrated that fascin is required for an adequate immunological response and leucocyte production to inflammation with consequent enhanced leucocyte infiltration into the inflamed tissue likely contributing to enhanced tumourigenesis. Measures to modulate this, for example inhibiting fascin, may prove useful, particularly for patients at high risk of developing inflammatory related tumours. Consequently, the drug development work, which I have contributed towards at the Beatson Institute, will be discussed in chapter 6. We

have also demonstrated the adverse immunosuppressive effects (in terms of increased clinical deterioration and mortality) of loss of fascin and these would obviously need to be taken into account. The reduced immunological response to inflammation is likely to have contributed to the enhanced clinical deterioration and mortality in both the short term 3.5% DSS course and the 70 day CAC model.

The presence of fascin in the stroma, epithelial cells and blood vessels of the WT CAC tumours is likely to be multi-factorial. The inflammatory nature of the tumours and the consequent damage the inflammation causes may necessitate the cells to express fascin in order to maintain the rigidity of their cytoskeleton to minimise apoptosis. The correlation we have demonstrated between fascin and circulating leucocytes may be a second reason, however as previously detailed fascin is likely to have multiple roles including cell adhesion and molecular signalling.

It was unfortunate not to have more RNA isolated from the CAC tumours (several of the processed samples were contaminated) to further establish any mechanism that may be responsible for the reduced tumourigenesis in the fascin KO mice. The preliminary data we do have indicated a mixed picture in that, with regard to the stem cell markers, jak-stat markers, Wnt members and targets we looked at there was no definitive trend. It may be that the cells which had mutated to form the tumours had, in essence, escaped the normal pathways involved and hence the variation.

5.4.2 Loss of fascin results in reduced tumourigenesis in the inducible Fascin^{-/-} APC^{fl/fl} p53^{fl/fl} and Fascin^{-/-} APC^{fl/fl} p53^{R172H} Ah-cre mice

It was surprising that, whilst the fascin KO mice had significantly reduced tumour number and burden, there was no difference in survival indicating that the mice were dying as a result of a non-tumour related cause. We have previously shown that the fascin KO mice have a reduced immunological response to inflammation and, whilst the FAPC inducible model is not an inflammatory model, tumours themselves have been shown to be pro-inflammatory (Coussens, Raymond et al. 1999) and we can hypothesise that the fascin KO mice are more susceptible to the immunological consequences of

tumourigenesis potentially resulting in enhanced susceptibility to opportunistic infections characteristic of an impaired immune state (Viget, Vernier-Massouille et al. 2008).

The mechanism behind the reduced tumour number and burden in the fascin KO may, in part, be as a consequence of reduced neutrophils resulting in a reduction in the initiation of tumours, as was seen in the CAC model, however further studies would be required to verify this given the lack of significance in the FAPC model. The lack of significance in the number of recruited neutrophils in the tumour microenvironment in the fascin KO FAPC mouse may reflect the reduced inflammatory nature of the inducible model as opposed to the CAC model, which is principally inflammatory driven. The effect of the reduced number of neutrophils would likely account for a reduction in tumour initiation, number and burden. It is unfortunate that we do not have data relating to the full blood count and chemokine tissue data in this model when the mice were culled, as this may have added important data as to the mechanism behind the number of recruited neutrophils, but also the immune state of the mice when they were culled. Given the data we have presented from the colitis regenerative and CAC models, however, it is possible to hypothesise that the mechanism is similar.

One point to note with regards the FAPC model is that the loss of p53 was mediated through either p53^{fl/fl} or the mutant p53^{R172H} model. Ideally, it would have been useful to use either one or the other, however, due to limited numbers the decision was made to combine the cohorts.

5.4.3 The regulation of fascin expression in benign and malignant tumours is unclear

We have demonstrated that fascin is expressed in murine models of both benign and malignant tumours with expression strongest at the invading edge. Given the high levels of Wnt signalling in the APC^{Min+}, APC^{1322t/+}, APC^{fl/fl} p53^{fl/fl} and APC^{fl/fl} p53^{fl/fl} Kras^{G12D} models it was important to determine whether fascin was a Wnt target. The short-term proliferative model whereby APC is inducibly knocked out using tamoxifen is a useful method to determine whether loss of APC resulting in high levels of Wnt signalling affects the level of fascin. We demonstrated the

loss of APC and resultant increase in Wnt signalling does not result in increased fascin expression. This correlates with our colitis data whereby fascin levels inversely correlated with Wnt levels indicating that fascin is potentially a negative Wnt regulator, either directly or indirectly. NF- κ B has previously been shown to bind fascin in breast cancer cells in a stat3 dependant manner (Snyder, Huang et al. 2011). We therefore wished to determine whether the expression of fascin increased in the short term APC proliferative model in response to treatment of the mice with the cytokine Il-11, which has previously been shown to up regulate Stat3 (Bollrath, Pheese et al. 2009). We did not, however see any increase in fascin in response to Il-11 which may indicate that the phenotype in breast cancer cells may be specific and not related to the small intestine.

It was of great interest to note, in the organotypic model that the APC^{fl/fl} p53^{fl/fl} cells, which when cultured in Matrigel in standard medium lost their expression of fascin, regained this expression when cultured on the collagen matrix in the organotypic model. In the organotypic model, the same medium was used as when cultured in Matrigel, the only difference being the collagen matrix, which consists of collagen extracted from rat tails and fibroblasts which contract the collagen. It is likely that either the fibroblasts or one of the factors which fibroblasts secrete induce the expression of fascin by the tumour cells and may be required for its maintenance. This is interesting in light of the fact that several colorectal cancer tissue culture cell lines, such as HT-29, express fascin. It may indicate that fascin expression has several thresholds during tumour progression and can be induced by external signals or can be stably switched on.

References

- Bollrath, J., T. J. Pheese, V. A. von Burstin, T. Putoczki, M. Bennecke, T. Bateman, T. Nebelsiek, T. Lundgren-May, O. Canli, S. Schwitalla, V. Matthews, R. M. Schmid, T. Kirchner, M. C. Arkan, M. Ernst and F. R. Greten (2009). "gp130-Mediated Stat3 Activation in Enterocytes Regulates Cell Survival and Cell-Cycle Progression during Colitis-Associated Tumorigenesis." *Cancer Cell* **15**(2): 91-102.
- Cespedes, M. V., C. Espina, M. A. Garcia-Cabezas, M. Trias, A. Boluda, M. T. G. del Pulgar, F. J. Sancho, M. Nistal, J. C. Lacal and R. Mangués (2007). "Orthotopic microinjection of human colon cancer cells in nude mice

- induces tumor foci in all clinically relevant metastatic sites." American Journal of Pathology **170**(3): 1077-1085.
- Coussens, L. M., W. W. Raymond, G. Bergers, M. Laig-Webster, O. Behrendtsen, Z. Werb, G. H. Caughey and D. Hanahan (1999). "Inflammatory mast cells up-regulate angiogenesis during squamous epithelial carcinogenesis." Genes & Development **13**(11): 1382-1397.
- Coussens, L. M. and Z. Werb (2002). "Inflammation and cancer." Nature **420**(6917): 860-867.
- Gavert, N., A. Ben-Shmuel, V. Lemmon, T. Brabletz and A. Ben-Ze'ev (2010). "Nuclear factor-kappa B signaling and ezrin are essential for L1-mediated metastasis of colon cancer cells." Journal of Cell Science **123**(12): 2134-2142.
- Hashimoto, Y., T. Ito, H. Inoue, T. Okumura, E. Tanaka, S. Tsunoda, M. Higashiyama, G. Watanabe, M. Imamura and Y. Shimada (2005). "Prognostic significance of fascin overexpression in human esophageal squamous cell carcinoma." Clinical Cancer Research **11**(7): 2597-2605.
- Hashimoto, Y., Y. Shimada, J. Kawamura, S. Yamasaki and M. Imamura (2004). "The prognostic relevance of fascin expression in human gastric carcinoma." Oncology **67**(3-4): 262-270.
- Hashimoto, Y., M. Skacel, I. C. Lavery, A. L. Mukherjee, G. Casey and J. C. Adams (2006). "Prognostic significance of fascin expression in advanced colorectal cancer: an immunohistochemical study of colorectal adenomas and adenocarcinomas." Bmc Cancer **6**.
- Horst, D., J. Budczies, T. Brabletz, T. Kirchner and F. Hlubek (2009). "Invasion Associated Up-Regulation of Nuclear Factor kappa B Target Genes in Colorectal Cancer." Cancer **115**(21): 4946-4958.
- Jamieson, T., M. Clarke, C. W. Steele, M. S. Samuel, J. Neumann, A. Jung, D. Huels, M. F. Olson, S. Das, R. J. Nibbs and O. J. Sansom (2012). "Inhibition of CXCR2 profoundly suppresses inflammation-driven and spontaneous tumorigenesis." J Clin Invest **122**(9): 3127-3144.
- Kemp, R., H. Ireland, E. Clayton, C. Houghton, L. Howard and D.J. Winton (2004). "Elimination of background recombination: somatic induction of Cre by combined transcriptional regulation and hormone binding affinity." Nucleic Acids Res **32**(11):e92
- Kim, S. J., D. C. Kim, M. C. Kim, G. J. Jung, K. H. Kim, J. S. Jang, H. C. Kwon, Y. M. Kim and J. S. Jeong (2012). "Fascin expression is related to poor survival in gastric cancer." Pathology International **62**(12): 777-784.
- Kinzler, K. W. and B. Vogelstein (1996). "Lessons from hereditary colorectal cancer." Cell **87**(2): 159-170.
- Mantovani, A., P. Allavena, A. Sica and F. Balkwill (2008). "Cancer-related inflammation." Nature **454**(7203): 436-444.
- Moser, A. R., H. C. Pitot and W. F. Dove (1990). "A Dominant Mutation That Predisposes to Multiple Intestinal Neoplasia in the Mouse." Science **247**(4940): 322-324.
- Ozcan, A., Y. Karlioglu, A. Gunal, A. H. Cermik, B. Kurt and O. Onguru (2011). "Fascin expression and its potential significance in gastrointestinal stromal tumors." Turkish Journal of Gastroenterology **22**(4): 363-368.
- Pollard, P., M. Deheragoda, S. Segditsas, A. Lewis, A. Rowan, K. Howarth, L. Willis, E. Nye, A. McCart, N. Mandir, A. Silver, R. Goodlad, G. Stamp, M. Cockman, P. East, B. Spencer-Dene, R. Poulson, N. Wright and I. Tomlinson (2009). "The Apc 1322T mouse develops severe polyposis

- associated with submaximal nuclear beta-catenin expression." Gastroenterology **136**(7): 2204-2213 e2201-2213.
- Qualtrough, D., K. Smallwood, D. Littlejohns and M. Pignatelli (2011). "The actin-bundling protein Fascin is overexpressed in inflammatory bowel disease and may be important in tissue repair." BMC Gastroenterol **11**.
- Snyder, M., X. Y. Huang and J. J. Zhang (2011). "Signal Transducers and Activators of Transcription 3 (STAT3) Directly Regulates Cytokine-induced Fascin Expression and Is Required for Breast Cancer Cell Migration." Journal of Biological Chemistry **286**(45): 38886-38893.
- Tan, M. H., E. D. Holyoke and M. H. Goldrosen (1977). "Murine Colon Adenocarcinoma - Syngeneic Orthotopic Transplantation and Subsequent Hepatic Metastases." Journal of the National Cancer Institute **59**(5): 1537-1544.
- Tan, V. Y., S. J. Lewis, J. C. Adams and R. M. Martin (2013). "Association of fascin-1 with mortality, disease progression and metastasis in carcinomas: a systematic review and meta-analysis." BMC Med **11**.
- Tian, Y., Y. Ye, W. Gao, H. Chen, T. Song, D. Wang, X. Mao and C. Ren (2011). "Aspirin promotes apoptosis in a murine model of colorectal cancer by mechanisms involving downregulation of IL-6-STAT3 signaling pathway." Int J Colorectal Dis **26**(1): 13-22.
- Timpson, P., E. J. McGhee, Z. Erami, M. Nobis, J. A. Quinn, M. Edward and K. I. Anderson (2011). "Organotypic collagen I assay: a malleable platform to assess cell behaviour in a 3-dimensional context." J Vis Exp(56): e3089.
- Viget, N., G. Vernier-Massouille, D. Salmon-Ceron, Y. Yazdanpanah and J. F. Colombel (2008). "Opportunistic infections in patients with inflammatory bowel disease: prevention and diagnosis." Gut **57**(4): 549-558.
- Vignjevic, D., M. Schoumacher, N. Gavert, K. P. Janssen, G. Jih, M. Lae, D. Louvard, A. Ben-Ze'ev and S. Robine (2007). "Fascin, a novel target of beta-Catenin-TCF signaling, is expressed at the invasive front of human colon cancer." Cancer Research **67**(14): 6844-6853.
- Xie, J. L. and S. H. Itzkowitz (2008). "Cancer in inflammatory bowel disease." World Journal of Gastroenterology **14**(3): 378-389.

6 Chapter 6 – Conclusions and Future Directions

6.1 Summary

A key aim of this thesis was to further our understanding of the role of fascin in IBD, particularly in the regeneration of the small intestine and the molecular mechanisms which underpin this.

In order to address this, in **Chapters 3 & 4** we used the fascin KO mouse in chemically induced models affecting both small intestine and colon thereby recapitulating the human diseases of UC and CD. Given the histological differences in the small intestine and colon, it was important to determine whether the role of fascin was similar in both tissues.

The data generated from the *in-vivo* work, and the realisation that the absence of fascin promotes an increase in stem cell marker levels resulting in greater crypt proliferation, was confirmed using the *in-vitro* crypt culture method. This was important, as the differences seen in the *in-vivo* data, whilst mostly significant, were small. This also suggested that fascin has an important role in the epithelial cells, as well as possibly in the stroma. The levels of fascin expression seen in the tissues, in particular in untreated conditions, are low and in many cases are only detectable at the gene level. We do know that fascin is expressed, albeit at low levels in both isolated paneth and Lgr5 cells, the expression being almost 3 times higher in the paneth cells compared to Lgr5 cells. We know that the two factors important for Lgr5 expressions are Wnt signalling and NF- κ B (Schwitalla, Fingerle et al. 2013). In conditions of homeostasis (with consequent low levels of circulating Wnt ligand (Haegebarth and Clevers. 2009)), crypt proliferation will be driven predominantly by NF- κ B pathways. Fascin is known to be a modifier of NF- κ B (Kress, Kalmer et al. 2011) and, consequently, in the absence of fascin this would result in reduced NF- κ B activation and downstream Lgr5 transcription. Conversely, during intestinal regeneration, crypt proliferation is driven predominantly by high circulating Wnt levels (Haegebarth and Clevers. 2009). We propose that fascin acts as a negative regulator of Wnt and, in these conditions, absence of fascin allows enhanced Wnt signalling and downstream Lgr5 transcription (Fig. 6.1). Thus, fascin plays an active role influencing gene expression changes as demonstrated by our data. It would be useful to further characterise the gene signature of isolated Lgr5 and paneth cells from the fascin KO mouse and compare them to their WT

counterpart, both in untreated and regenerative conditions. This would then potentially aid our understanding of the role fascin plays in influencing gene expression changes in the presence of differing levels of circulating Wnt ligand.

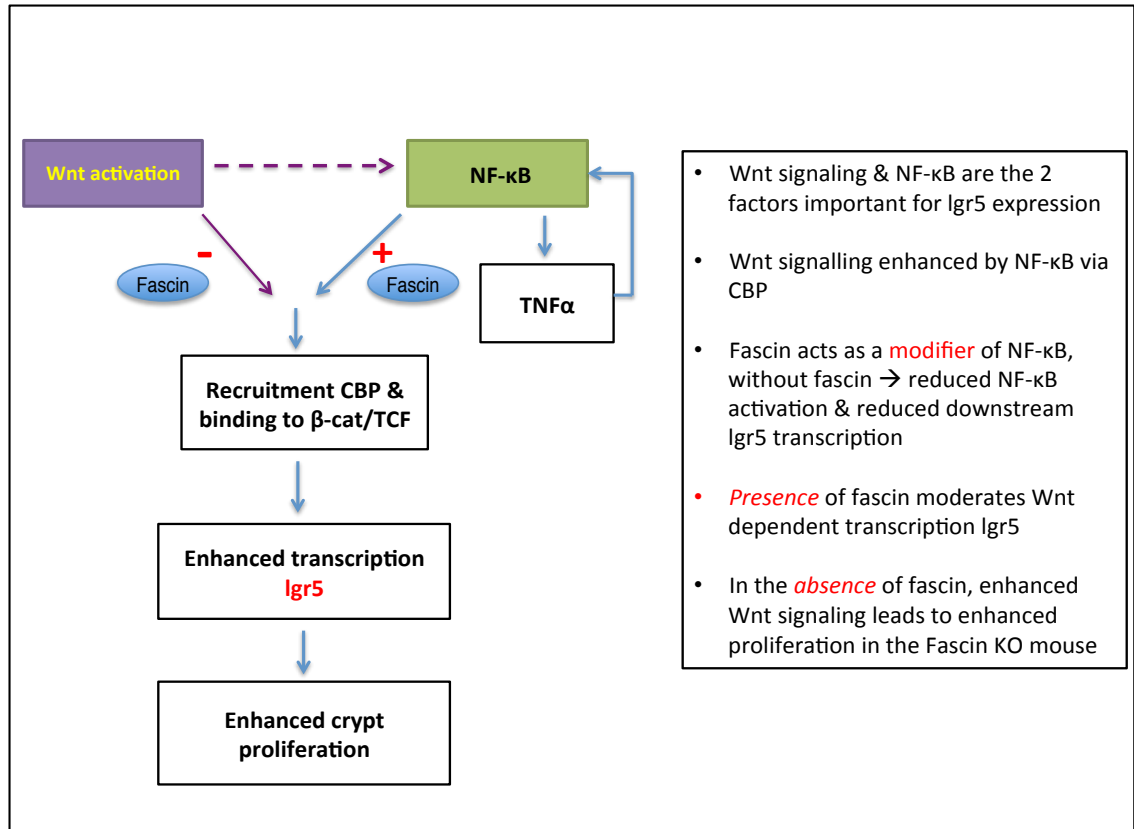


Figure 6-1 Proposed model of mechanism – the role of fascin in influencing gene expression changes

It was also apparent from the *in-vivo* work, that the fascin KO mice were clinically more sensitive to colitis-inducing treatments, both in the acute setting and the chronic colitis associated carcinogenesis (CAC) model. Analysis of the differential blood counts showed that, in response to inflammation, fascin plays a key role in the haematopoietic generation of circulating leucocytes, in particular neutrophils and this may be CXCL2 mediated. We observed a reduction in the number of recruited neutrophils to the inflamed tissues, but also from a clinical perspective, the effects of reduced numbers of circulating leucocytes could account for the morbidity and mortality experienced by the fascin KO mice. The role of fascin in the immunological response to inflammation has only been touched on in this thesis and it is likely that aiding leucocyte production is not the sole function of fascin in this regard. We

attempted to mechanistically understand how fascin enhanced haematopoiesis in response to inflammation through investigating chemokine signalling downstream of dendritic cells. Whilst it was encouraging to discover the observed phenotype may be in part CXCL2 mediated, it is likely that other immunological processes are also contributing and it would be interesting to explore this in greater depth.

It was interesting that, despite fewer inflammatory cells recruited to the fascin KO tissues there was no associated increase in the histological damage. Fascin plays a key role in actin dynamics and loss of this protein may predispose the fascin KO tissues to inherent structural weakness, which, in response to an inflammatory insult results in exaggerated damage. We can speculate that, were the number of inflammatory cells stimulated and recruited to the fascin KO tissues on a par with that of the WT, the histological damage would be significantly greater in the fascin KO. Other actin bundling proteins, such as villin, may in turn compensate for the absence of fascin, as has been seen in *Drosophila* (Cant, Knowles et al. 1998) which may ameliorate the loss, however this would need to be investigated and is beyond the scope of this thesis.

The second aim of this thesis was to explore the role of fascin in inflammatory driven and sporadic intestinal tumourigenesis, which was addressed in **Chapter 5**. Regarding the CAC model, the reduction in tumour number and burden in the fascin KO is likely, in part, to be as a consequence of the reduced leucocytes, in particular neutrophils, given the importance of tumour promoting leucocytes and cancer initiation (Jamieson, Clarke et al. 2012). Our proposed mechanism is a result of impaired dendritic cell function secondary to loss of fascin, which impairs the production of chemokines CXCL1 and CXCL2 by dendritic cells in response to inflammation. This results in a reduction in the number of circulating immune cells and their consequent recruitment to damaged areas. This would result in reduced levels of reactive oxygen species (ROS) and DNA damage which would result in the phenotype we have demonstrated, namely reduced numbers of tumours in the fascin KO (Fig. 6.2).

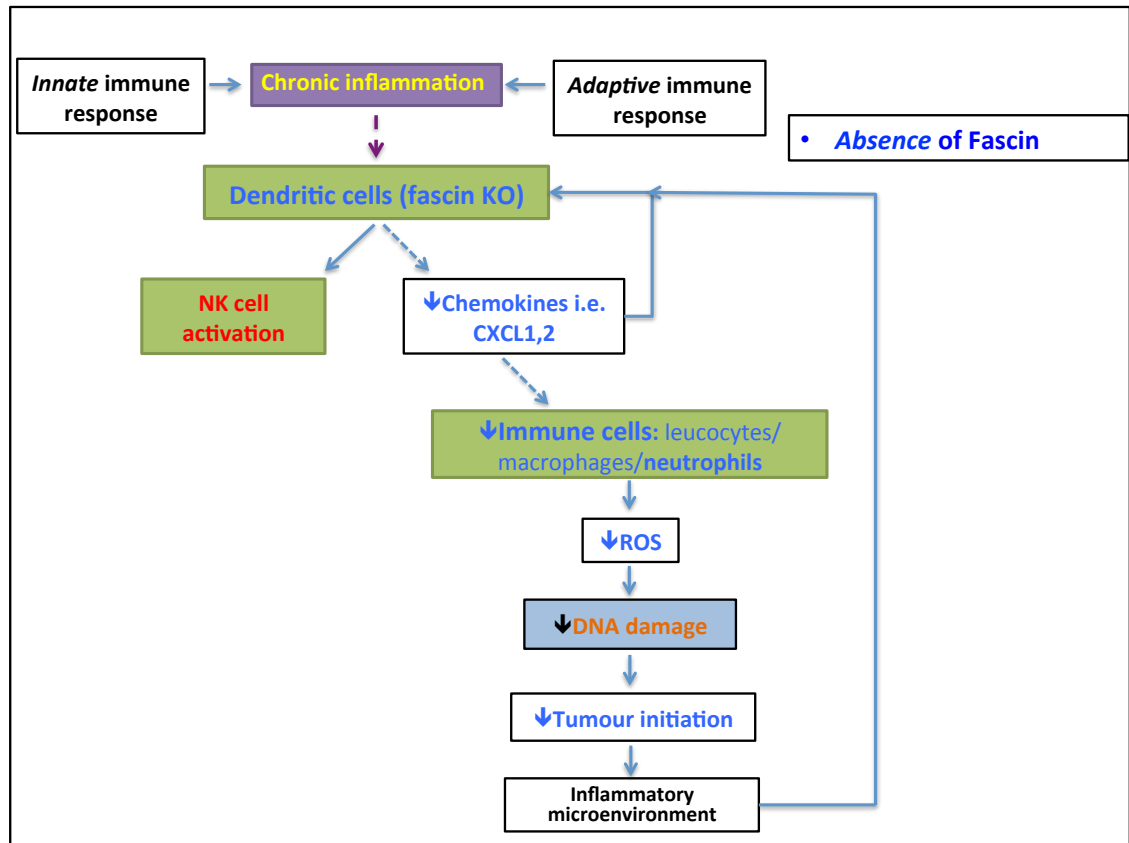


Figure 6-2 Proposed mechanism – reduced tumour initiation in CAC model

In the fascin KO mouse, we propose the reduced tumourigenesis is in part a consequence of impaired dendritic cell function, which in turn impairs chemokine production; the inflammatory response and downstream ROS production and DNA damage resulting in a reduction in tumour initiation.

In the FAPC mouse model we used, loss of APC and p53 are the most important triggers for tumour initiation, however leucocytes, in particular neutrophils may also contribute to the reduced tumour number and burden in the fascin KO mouse. Given the innate pro-inflammatory nature of tumours (Coussens, Raymond et al. 1999), loss of fascin would disrupt the inflammatory loop, created and driven by the tumour microenvironment thereby resulting in reduced tumourigenesis (Fig. 6.3).

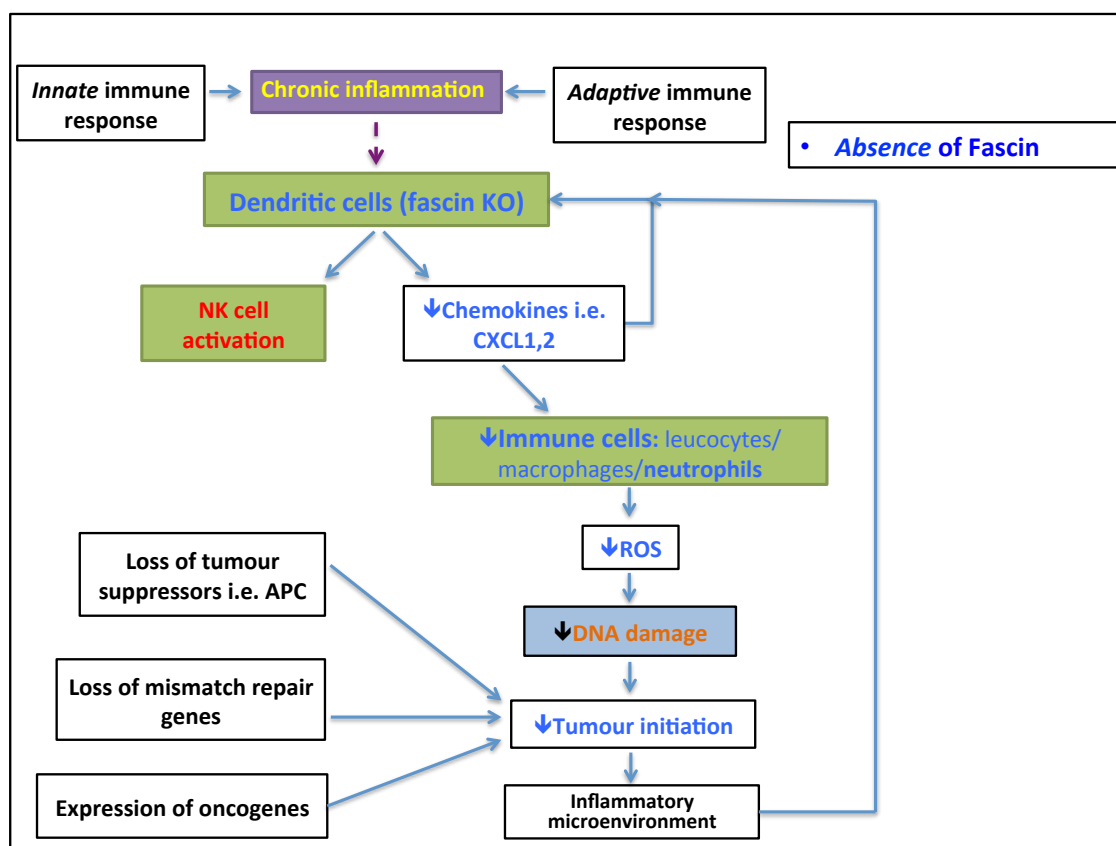


Figure 6-3 Proposed mechanism – reduced tumour initiation in FAPC mouse model

In the fascin KO mouse, we propose the reduced tumourigenesis is in part a consequence of impaired dendritic cell function, stimulated via the tumour inflammatory micro-environment, which in turn impairs chemokine production, the inflammatory response and downstream ROS production and DNA damage resulting in a reduction in overall tumourigenesis.

We are unable to ascertain whether, in addition to a role in leucocyte production, fascin is involved in the trafficking or recruitment of neutrophils to inflamed tissues or the tumour microenvironment. Further work in this area, for example the use of direct intravital imaging of the cremaster muscle would be useful to explore whether fascin plays a role in the recruitment of neutrophils in addition to gene expression analysis of isolated neutrophils from WT and fascin KO mice. It was interesting that the size of the tumours was comparable between WT and fascin KO indicating that, once the tumour had been initiated, fascin did not play an obvious role in the subsequent proliferation of the tumours. This was true for both the colitis associated carcinogenesis and FAPC models and it would be interesting to further explore whether there were additional processes underlying this phenotype in addition to our proposed tumour promoting leucocyte mechanism. Given the well-publicised importance of fascin in invadopodia (see chapter 1) formation (finger like protrusions used

by cancer cells to degrade the ECM and invade), it was surprising that a similar proportion of the fascin KO tumours invaded to that in the WT FAPC mice. Again, this may reflect other actin bundling proteins compensating for the absence of fascin and that the principal role of fascin in tumourigenesis is one of tumour initiation.

6.2 Future Directions

We have presented in this thesis *in-vivo* and *in-vitro* data indicating a novel role of fascin in regulating intestinal epithelial cell proliferation, however we have been unable to delineate the mechanism behind this. It appears that NF- κ B levels correlate with high Wnt signalling in the absence of fascin, whereas in the presence of low Wnt levels NF- κ B levels are higher in the presence of fascin. This relationship appears complex and further mechanistic work would need to be undertaken to further explore this area.

We have clearly demonstrated that loss of fascin compromises the initiation of tumours in inflammatory driven and sporadic mouse models. A goal of all cancer related research is ultimately one of patient benefit. Given the enhanced risk of patients with IBD developing inflammatory driven intestinal tumours, drugs that reduce fascin expression may be important in reducing the initiation of tumours in this high-risk group. One such drug commonly used as a treatment in IBD, 5-aminosalicylate (5-ASA), has been shown to reduce the expression of fascin in the colorectal epithelial cell line HT29 (Qualtrough, Smallwood et al. 2011). It may be that reducing the level of fascin modulates the inflammatory process and the subsequent damage caused by tumour promoting leucocytes. Reducing the expression of fascin in the tissues, in addition to reducing the level of inflammation, would potentially reduce the transformation from benign disease to a malignant process. Animal models may be key to investigate this further for example, using 5-ASA in the AOM/DSS model and also in the sporadic FAPC model may prove useful in testing this hypothesis.

Other actin bundling proteins, such as villin, have been shown to compensate for the loss of fascin in *Drosophila* (Cant, Knowles et al. 1998). As such, it would be useful to determine whether a similar phenomenon existed in the models used in

this thesis in particular, regarding restitution in the colitis model and tumour invasion in the FAPC model.

The correlation between fascin and neutrophils presented in this thesis could be further explored through correlating the expression of fascin and neutrophils in human tissue microarrays (TMAs) of IBD specimens, and also in inflammatory-driven and sporadic intestinal cancers. In order to understand the mechanism behind the correlation seen, it would be useful to analyse the CXCL chemokine makeup, using qRT-PCR, to determine whether the correlation is replicated in human data.

The on-going collaborative work with the Beatson drug discovery in the development of a fascin inhibitor is an exciting project and it would be useful to test potential inhibitors in the *in-vivo* and *in-vitro* models used in this thesis. Should these prove successful in reducing the incidence of tumours in the various models, it would be necessary to characterise any off-target effects (such as immunosuppression) before contemplating clinical trials in humans.

6.3 Conclusion

This thesis has further added to the knowledge of the role of fascin in the intestinal regeneration key to the pathogenesis of IBD and the development of tumours in inflammatory driven and sporadic intestinal tumourigenesis. I will hereby clarify the definite conclusions that have been generated by this work.

1. Loss of fascin in the presence of high Wnt levels, as seen in regenerating small intestines, results in enhanced proliferation of small intestinal epithelial cells.
2. Loss of fascin does not profoundly affect the histological damage to the small intestine or colon in response to chemical induced inflammation.
3. Fascin is required for the haematopoietic production of leucocytes in response to inflammation.

4. Loss of fascin impairs tumour initiation in inflammatory driven and sporadic intestinal tumourigenesis models.

References

- Cant, K., B. A. Knowles, et al. (1998). "Drosophila fascin mutants are rescued by overexpression of the villin-like protein, quail." Journal of Cell Science **111**: 213-221.
- Coussens, L. M., W. W. Raymond, et al. (1999). "Inflammatory mast cells up-regulate angiogenesis during squamous epithelial carcinogenesis." Genes & Development **13**(11): 1382-1397.
- Haegebarth, A. and H. Clevers. (2009). "Wnt Signaling, Lgr5, and Stem Cells in the Intestine and Skin." Am J Pathol **174**(3): 715-721
- Jamieson, T., M. Clarke, et al. (2012). "Inhibition of CXCR2 profoundly suppresses inflammation-driven and spontaneous tumorigenesis." J Clin Invest **122**(9): 3127-3144.
- Kress, A. K., M. Kalmer, et al. (2011). "The tumor marker Fascin is strongly induced by the Tax oncoprotein of HTLV-1 through NF-kappa B signals." Blood **117**(13): 3609-3612.
- Schwitalla, S., A. A. Fingerle, et al. (2013). "Intestinal tumorigenesis initiated by dedifferentiation and acquisition of stem-cell-like properties." Cell **152**(1-2): 25-38.
- Qualtrough, D., K. Smallwood, et al. (2011). "The actin-bundling protein Fascin is overexpressed in inflammatory bowel disease and may be important in tissue repair." BMC Gastroenterol **11**.

Appendices

Appendix A: Fascin1 is dispensable for developmental and tumour angiogenesis

Research Article

1

Fascin 1 is dispensable for developmental and tumour angiogenesis

Yafeng Ma¹, Louise E. Reynolds², Ang Li¹, Richard P. Stevenson¹, Kairbaan M. Hodivala-Dilke², Shigeko Yamashiro³ and Laura M. Machesky^{1,*}

¹Beatson Institute for Cancer Research, Gartcube Estate, Switchback Road, Bearsden, Glasgow G61 1BD, UK

²Adhesion and Angiogenesis Laboratory, Centre for Tumour Biology, Barts Cancer Institute – a CRUK Centre of Excellence, Queen Mary University of London, Charterhouse Square, London EC1M 6BQ, UK

³Department of Molecular Biology and Biochemistry, Rutgers University, Piscataway, NJ 08855, USA

*Author for correspondence (Laura.Machesky@glasgow.ac.uk)

Biology Open 0, 1–5
doi: 10.1242/bio.20136031
Received 3rd July 2013
Accepted 29th August 2013

Summary

The actin bundling protein fascin 1 is not expressed in adult epithelial tissues, but during development it is transiently expressed in many different cell types, and later in adults it is expressed in a subset of immune cells, nervous tissues, endothelial cells, smooth muscle cells and pericytes. In contrast to the wealth of knowledge about the role of fascin 1 in cancer cell migration and invasion, little is known about the involvement of fascin 1 in angiogenesis. We speculated that as angiogenesis involves migration and invasion of tissues by endothelial cells, fascin 1 might have a role in both normal and tumour angiogenesis. Here, we provide evidence that loss of fascin 1 causes relatively minor reductions to angiogenesis during embryonic, postnatal and cancerous development by examining E12.5 hindbrains, postnatal retinas and B16F0 tumour cell allografts in fascin 1-null mice. We also find that

in fascin 1 null tissues, endothelial cells display reduced filopodia formation during sprouting. We thus propose that fascin 1 expression promotes angiogenesis via filopodia formation, but is largely dispensable for both normal and tumour angiogenesis.

© 2013. Published by The Company of Biologists Ltd. This is an Open Access article distributed under the terms of the Creative Commons Attribution License (<http://creativecommons.org/licenses/by/3.0/>), which permits unrestricted use, distribution and reproduction in any medium provided that the original work is properly attributed.

Key words: fascin 1, Angiogenesis

Introduction

Angiogenesis, the formation of new capillaries from existing vessels, is a fundamental process in development and tumour growth. It involves multiple cell types in sequential controlled steps. Various growth factors such as vascular endothelial growth factors (VEGFs) (Ruhrberg et al., 2002; Gerhardt et al., 2003; Nakayama et al., 2013), Notch pathway components (Roca and Adams, 2007) and cell adhesion molecules (Reynolds et al., 2002; Silva et al., 2008) including integrins have been reported to play crucial roles in angiogenesis and vasculogenesis.

The actin bundling protein fascin 1 is associated with the formation of actin-based cell membrane protrusions such as filopodia (Vignjevic et al., 2006) and invadopodia (Li et al., 2010; Schoumacher et al., 2010). A high expression level of fascin 1 is positively correlated with cell motility and invasiveness (Anilkumar et al., 2003; Li et al., 2010). Besides its upregulated expression in some motile progenitor cells during embryogenesis (Hayashi et al., 2008; Chae et al., 2009; Zanet et al., 2009; Ma et al., 2013) and many epithelial cancers (Machesky and Li, 2010), fascin 1 is moderately or highly expressed in endothelial cells (ECs) and mural cells in normal adult tissue and primary cell culture (Jawhari et al., 2003; Zhang et al., 2008; Hoelzle and Svitkina, 2012).

Here, we demonstrate the effect of loss of fascin 1 on angiogenesis and endothelial cell morphology with various *in*

vivo angiogenesis models. Fascin 1 has been extensively studied in cancer cells and its role in promoting invasion and migration *in vitro* is well established, but its potential role in developmental angiogenesis or in tumour angiogenesis has not been explored. We suggest that fascin 1 facilitates angiogenesis via its well-known effects on filopodia formation and migration, but that overall the role of fascin 1 in angiogenesis is not greatly limiting for development or tumour formation.

Results and Discussion

Fascin 1-null C57BL/6 mice display partial neonatal death and retarded growth in early stages (Yamakita et al., 2009). Consistent with this previous observation, we also observed a lower survival rate in fascin 1-null mice (supplementary material Fig. S1A) and the surviving fascin 1-null pups showed retarded growth in their early life. The weight of fascin 1-null pups at day 7 and day 19 is approximately 60–90% of fascin 1^{+/+} or fascin 1^{+/-} pups (supplementary material Fig. S1B,C). Fascin 1 was reported previously to be expressed in endothelial cells, pericytes and smooth muscle cells and might be involved in the cardiovascular system (Adams, 2004). Immunofluorescence (IF) staining of tissue with isolectin B4 (BSI-B4) and fascin indicated that the endothelial layer and surrounding tissue (mural cells) in wild type aortas expressed fascin 1 whereas fascin 1-null mice

had a complete loss of fascin 1 (supplementary material Fig. S1D).

Fascin 1 loss delays embryonic brain angiogenesis

Mouse vascular morphogenesis starts in the yolk sac on E6.5 when endothelial cells differentiate from angioblasts. By E8.5, the dorsal aortae, cardinal veins and the surrounding primitive vasculature merge. Although fascin 1-null embryos were present at the normal Mendelian ratios (supplementary material Fig. S1A) and showed no apparent hemorrhage or prenatal death (data not shown), we wondered whether non-optimal angiogenesis might contribute to abnormal brain development and retarded growth (Yamakita et al., 2009). We examined the vascular patterns in the yolk sac, midbrain and hindbrain of the developing embryos (E11.5 or E12.5) on either fresh tissue or whole-mounts stained with FITC-conjugated BSI-lectin - an EC marker. Yolk sac blood vessels showed a similar vessel pattern and network at these stages (Fig. 1A–D; supplementary material Fig. S1E,F). For quantification of vascular complexity, embryonic hindbrains are ideal tools to study the potential role of fascin in angiogenic sprouting and vascular remodeling (Fantin et al., 2013). Expression of fascin in hindbrain endothelial cells is confirmed with immunofluorescence (supplementary material Fig. S2A). Reduced branching complexity was observed in hindbrains of fascin 1^{-/-} embryos, as measured by number of branch points per area (ventricular side facing up, Fig. 1E–G, E12.5). Together these results suggest that fascin 1 plays a positive role during embryonic brain angiogenesis, but are in agreement with a previous study showing that fascin 1 is dispensable for embryonic development (Yamakita et al., 2009).

Postnatal retinal angiogenesis is impaired in the absence of fascin 1

Next, we applied another widely used angiogenesis model, postnatal mouse retina, to visualize postnatal angiogenesis and vessel network patterning. Vessel sprouts emerge from the optic disc and spread perpendicularly along astrocytes and interact with macrophages (Fantin et al., 2010). We confirmed fascin expression in retina endothelial cells (supplementary material Fig. S2B). The retinal vessel network was examined for vascular sprouting at the periphery of the vessel plexus and remodeling at the center between arteries. Fascin 1^{-/-} retinas showed less radial vascular outgrowth at P6 (Fig. 2A,B). Fascin 1^{-/-} retinas also exhibited fewer branch points relative to fascin 1^{+/+} and ^{+/-} retinas (Fig. 2C,D).

Loss of fascin 1 reduces endothelial cell filopodia formation

Tip endothelial cells (ECs) guide sprouting angiogenesis by extending long filopodia extensions in response to angiogenic factors (Gerhardt et al., 2003). These numerous actin-rich filopodia mediate EC migration and fusion (Dorrell et al., 2002; Fantin et al., 2010; Fraccaroli et al., 2012; Villefranc et al., 2013). To further examine the potential role of fascin in sprouting angiogenesis and EC filopodia extension, we analysed hindbrain tip cells and stalk cells as well as tip cells in retina sprouting fronts. Fascin 1^{-/-} hindbrain vessels generally displayed fewer filopodia extensions (supplementary material Movies 1 and 2). Tip endothelial cells in fascin^{-/-} hindbrains also exhibit fewer filopodia (Fig. 3A,B). Also, a reduction of nearly 40% in filopodia numbers per vessel length was observed in fascin

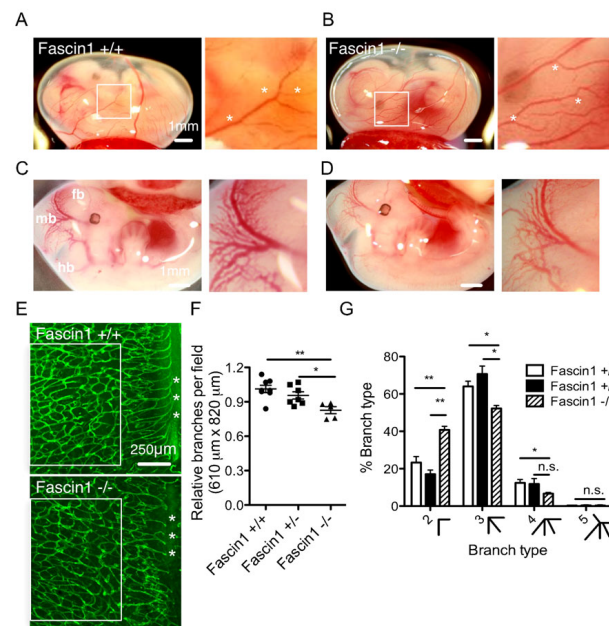


Fig. 1. Fascin 1 deficiency reduces brain angiogenesis. (A–B) Photographs of freshly isolated embryos in intact yolk sacs and magnified areas of vessel tips in yolk sacs (E12.5, A: fascin 1^{+/+} and B: fascin 1^{-/-}). White asterisks indicate vessel branch points in yolk sac. (C–D) Intact embryos and magnified midbrain area (E12.5, C: fascin 1^{+/+} or ^{+/-} and D: fascin 1^{-/-}). fb, forebrain; mb, midbrain; hb, hindbrain. (E) Representative IF pictures of FITC conjugated BSI-B4 stained hindbrains (E12.5). Flat mounting the hindbrain with the ventricular side up visualizes the subventricular vascular plexus (SVP). Asterisks indicate the midline of the hindbrain. (F) Relative branch point numbers per area (610 μm x 820 μm) as compared with littermate controls. 4 random areas are measured for each hindbrain. The white box in (E) is the cropped area for quantification. (G) Quantitation of branch types in fascin 1^{+/+}, ^{+/-} and ^{-/-} as measured with 4x objective. 100–400 branch knots per hindbrain were examined. Results are expressed as means ± s.e.m. Mann-Whitney test, *, P<0.05; **, P<0.01 and n.s., not significant (numbers of independent hindbrain samples- fascin 1^{+/+}, n=7; fascin 1^{+/-}, n=7 and fascin 1^{-/-}, n=5). Bars, 1 mm (A–D), 250 μm (E).

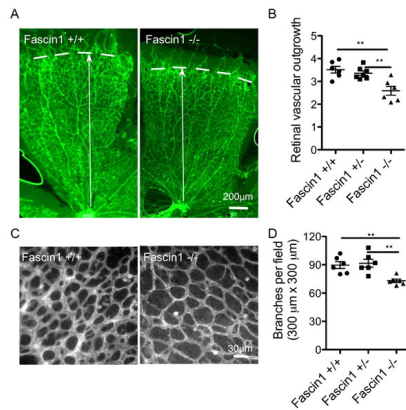


Fig. 2. Fascin 1 deficiency restricts postnatal retinal angiogenesis. (A, C) Visualization of blood vessels by FITC conjugated BSI-B4 IF staining in *fascin1*^{+/+} and *fascin1*^{-/-} littermate retinas at P6. Bars, 200 μm (A), 30 μm (C). (B, D) Quantitative analysis of the retinas shows relative vessel sprout length (B), numbers of vessel branching points (300 μm x 300 μm, D). 6 retinas per genotype. 2–4 fields were measured for sprout length for each retina in (B). 2–4 fields close to vessel fronts were randomly analysed for each littermate in (C and D). Results are expressed as means ± s.e.m. Mann-Whitney test, **, *P* < 0.01.

1^{-/-} hindbrains (Fig. 3C,D) as well as retinal angiogenic fronts (Fig. 3E,F). Fascin has been localized to endothelial cell filopodia (Hoelzle and Svitkina, 2012), but the role of fascin in endothelial cell filopodia extension *in vivo* has not been studied before to our knowledge. Our data agree with studies showing that dorsal root ganglion neurons and mouse embryo fibroblasts from fascin deficient mice have reduced filopodia numbers and length (Yamakita et al., 2009).

Fascin 1 deficiency in the host reduces tumour angiogenesis, but is not limiting for tumour growth

We next asked whether fascin 1 was important for the formation of the tumour vasculature by transplanting B16F0 melanoma cells into fascin 1-null and wild-type mice and examining subsequent tumour growth and vascularization (Reynolds et al., 2002). Fascin-1 expression in the host was not limiting for tumour growth, as tumour size and volume at 12 days after inoculation in *fascin1*^{-/-} mice showed no obvious difference to wild type mice (supplementary material Fig. S3A). Next, we quantified the vessel density in the tumour periphery (defined as the area 1 mm close to the tumour edge) or vessel density per entire tumour area. The number of blood vessels per cm² area in B16F0 allografts in *fascin1*^{-/-} mice were significantly reduced compared to that in *fascin1*^{+/+} and *fascin1*^{+/+} mice as measured by the endothelial cell marker PECAM-1 (Platelet endothelial cell adhesion molecule-1, CD31) (Fig. 4A,B), endomucin staining (Fig. 4C,D). Adult *fascin1*^{+/+} and *fascin1*^{-/-} mice show similar whole blood counts (supplementary material Fig. S3B) and recruitment of macrophages and CD3 positive cells in tumours (supplementary material Fig. S3C), indicating that loss of fascin 1 in the host has no detectable effect on immune cell

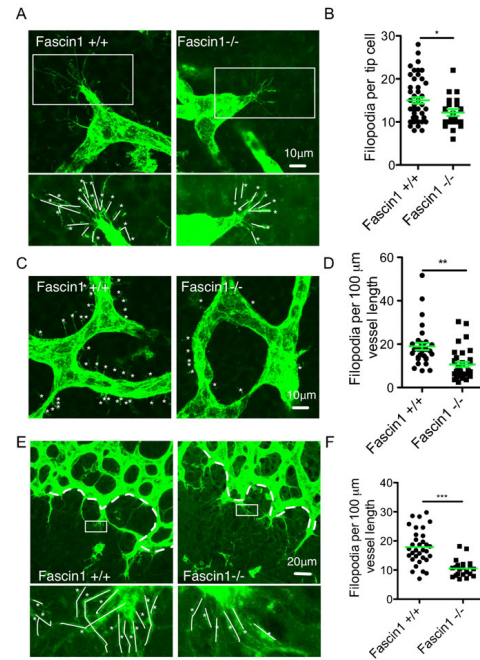


Fig. 3. Loss of fascin 1 reduces endothelial cell filopodia in hindbrain and retinal vessels. (A–D) Representative FITC conjugated BSI-B4 stained tip cells (A) and stalk cells (C) in E12.5 hindbrain. Bars, 10 μm. (B) Filopodia per tip cells. 20–50 tip cells from 4–5 hindbrains for each genotype. (D) Quantification of filopodia per 100 μm vessel length of stalk cells. Results are means ± s.e.m., 30–35 individual areas from 4 hindbrains for each genotype. (E) Representative FITC conjugated BSI-B4 stained vessel network in P6 retinas. Zoomed-in areas show filopodia of endothelial tip cells. Bars, 20 μm. White dashed lines show angiogenic front length for quantification. (F) Filopodia per 100 μm vessel length in retinas. 4–6 random pictures of vessel front for each littermate were counted. White asterisks mark filopodia. White lines indicate traces of filopodia. Mann-Whitney test, *, *P* < 0.05; **, *P* < 0.01; ***, *P* < 0.001.

recruitment during angiogenesis and tumour growth. We thus speculate that while fascin expression potentiates angiogenesis, it is not essential *in vivo* and these tumours can be sufficiently vascularized to support normal growth, just as mouse development can proceed in the absence of fascin.

In summary, we show several lines of evidence to suggest the involvement of fascin 1 in angiogenesis. Fascin 1 deficiency impairs prenatal and postnatal angiogenesis, which may contribute to early growth defects observed in fascin 1-null mice. Alternatively, growth defects could be caused by fascin deficiency in other cells and lead to impaired angiogenesis. Loss of fascin 1 likely retards filopodia formation and motility during sprouting angiogenesis. Fascin 1 is well-established to promote filopodia formation in many cell types in culture and *in vivo*, but has not been previously studied in the context of endothelial tip cells or angiogenesis *in vivo*. Our observations from allografts of B16F0 melanoma also reflect that fascin contributes to, but is not

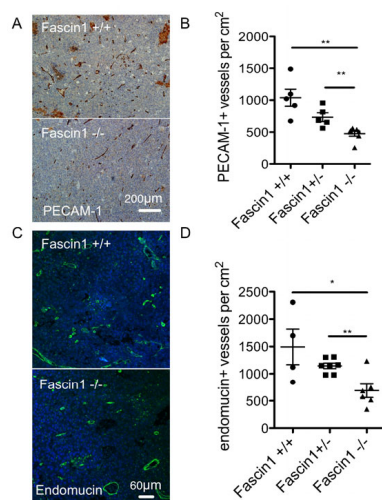


Fig. 4. Fascin 1 deficiency reduces tumour angiogenesis. (A) Representative PECAM-1 IHC pictures with hematoxylin counter staining of B16F0 tumour sections from fascin 1^{+/+} and fascin 1^{-/-} mice and (B) quantitation of PECAM-1 labeling vessel numbers per cm² tumour area. (C) Immunofluorescence staining with the blood vessel marker endomucin and (D) quantitation of endomucin labeling vessel numbers per cm² tumour area. Results are means \pm s.e.m., $n=4-7$; *, $P<0.05$; **, $P<0.01$. Bars, 200 μ m (A), 60 μ m (C).

limiting for tumour vascularization. As fascin inhibitors are developed with the eventual hope of targeting tumour metastasis, it is increasingly important to know what effects fascin inhibition would have on the host. We show that while fascin is abundantly expressed in endothelial and mural cells of blood vessels *in vivo*, its presence is not crucial for vasculature to form relatively normally, but can be limiting for branching and extent of vascularization. In addition to filopodia, fascin 1 also localizes in cell invasive structures, such as podosomes in endothelial cells and smooth muscle cells. Fascin 1 contributes to podosome formation, cell migration and basement membrane degradation both *in vitro* and *in vivo* in some specific organs and conditions (Varon et al., 2006; Rottiers et al., 2009; Quintavalle et al., 2010; Juin et al., 2013). Thus, the involvement of fascin 1 in the vasculature and angiogenesis is likely attributed to its function in filopodia and/or podosomes. To our knowledge, this is the first study to report that fascin 1 is required for optimal angiogenesis. Future studies could include the dissection of the role of fascin 1 in endothelial cells and mural cells and the involvement of fascin 1 in angiogenic pathways.

Materials and Methods

Mice

Fascin null (C57BL/6) mice (Yamakita et al., 2009) were maintained according to UK Home Office regulations. Embryonic day 0.5 was assessed at noon the day after mating and if a vaginal plug was observed, E11.5 or E12.5 embryos were isolated and judged according to their developmental stage and compared with their littermate control mice. The date of birth was regarded as postnatal day 0. To assess neonatal retinal angiogenesis, 6-day old pups from 3 litters were examined. 2-6 month old mice were used as previously described for *in vivo* tumour assays (Reynolds et al., 2002).

Immunohistochemistry (IHC) and immunofluorescence (IF) staining
5 μ m-depth sections were deparaffinised, rehydrated and treated in sodium citrate buffer (pH 6.0). After blocking with peroxidase blocking solution, samples were incubated with the following primary antibodies: rabbit anti-PECAM1 (CD31, Abcam, 1:100), mouse anti-fascin 1 (DAKO, clone 55K-2, 1:100), rabbit anti-CD3 (Vector Labs, VP-PM01, 1:75) for 1 hour. DAB-chromogenic detections were carried out using peroxidase labeled polymer (Envision kits) and detected with substrate-chromogen (Envision kits) followed with hematoxylin counterstain. For immunofluorescence staining, after deparaffinisation and rehydration, antigen retrieval using 20 μ g/ml proteinase K in TE buffer (pH 8.0) (15 minutes, 37°C) was performed. After blocking, sections were incubated with the following primary antibodies (overnight, 4°C): endomucin (Santa Cruz, 1:100), rat anti-mouse F4/80 antibody (AbD Serotec, 1:50) and respective species-specific secondary antibodies (RT, 1 hour, 1:100). After PBS washes, the sections were mounted with ProLong Gold Antifade reagent with DAPI (Invitrogen).

Hindbrain angiogenesis

E12.5 embryos were dissected as previously described (Fantin et al., 2013) and compared with their littermate control mice. For light microscopy, photographs of yolk sacs and whole embryos were taken with the same magnification at the same embryonic stage to visualize microvessel networks. The hindbrains were isolated and stained with FITC-conjugated isolectin B4 (BSI-B4, 40 μ g/ml, Sigma) after 4% paraformaldehyde (PFA) fixation (4°C, overnight) and PBS-1% Triton X-100 permeabilization. The hindbrains were gently mounted and visualised on Olympus OV1000 with 10 \times or 60 \times objective (1024 \times 1024). The branch type 2, 3, 4, 5 were defined by branch numbers and the percentages of branch types were expressed to measure the extent of angiogenesis (Stefater et al., 2011). The filopodia of the tip cells and stalk branches were analysed using z-stacked FITC-BSI-B4 positive cells and branches.

Retinal angiogenesis

The eyes of postnatal day 6 pups were fixed in 4% PFA in PBS and washed with PBS. Retinas were dissected as previously described (Pitulescu et al., 2010; Sawamiphak et al., 2010) and permeabilised in PBT (PBS, 1% BSA and 0.5% Triton X-100) and incubated with FITC-conjugated BSI-B4 at 4°C (overnight). Retinas were mounted with ProLong Gold Antifade reagent (Invitrogen). The vessel sprout length, branch points and filopodia were measured as before (Pitulescu et al., 2010; Sawamiphak et al., 2010). The pictures were taken with a 4 \times objective on a stereomicroscope (Olympus BX51 FL Microscope for sprout length). Pictures were taken of the areas close to the sprout front with 20 \times objective for quantification of branch points. The filopodia were visualised with a 60 \times objective on an Olympus OV1000.

In vivo tumour assays

13-16 C57BL/6 mice (2-6 month old) of fascin 1^{+/+}, fascin 1^{+/-}, fascin 1^{-/-} were injected subcutaneously into the scruff with 1×10^8 of mouse melanoma B16F0 cells in 100 μ l PBS. 12-days post-inoculation, the mice were sacrificed and the tumours were removed, weighed and photographed before fixation with 10% neutral formalin. Tumours were dissected and stained with hematoxylin and eosin. Size-matched tumours (6-8 per genotype) were immunostained with endothelial cell markers to quantify tumour blood vessel density. Tumour volume (v) was calculated as $v=0.5(l \times w^2)$, where l is tumour length (longest diameter) and w is tumour width (shortest diameter) (Reynolds et al., 2010).

Statistical analysis

Statistical significance was calculated using the Mann-Whitney test for comparison of two groups of large datasets (fascin 1^{+/+} vs. fascin 1^{-/-}) and one-way ANOVA followed by Mann-Whitney test for selected pairs of genotypes (fascin 1^{+/+}, fascin 1^{+/-} and fascin 1^{-/-}) (GraphPad Prism5). $P<0.05$ was considered statistically significant. *** denotes $P<0.001$, ** denotes $P<0.01$ and * denotes $P<0.05$.

Acknowledgements

The authors thank the Beatson Institute for Cancer Research Biological Services for animal maintenance, BAIR for imaging support, Colin Nixon and his staff for great assistance in histology. We thank Ayala King for her advice and fine dissection instruments.

Funding

Y.M., A.L. and L.M.M. are funded by a core CRUK grant.

Author Contributions

Y.M., L.M.M. and L.E.R. designed the study. S.Y. provided essential reagents. Y.M., L.E.R., R.P.S. and A.L. performed experiments,

Y.M. and L.M.M. wrote the manuscript with input from L.E.R., A.L. and K.M.H.-D.

Competing Interests

The authors have no competing interests to declare.

References

- Adams, J. C. (2004). Fascin protrusions in cell interactions. *Trends Cardiovasc. Med.* **14**, 221-226.
- Anilkumar, N., Parsons, M., Monk, R., Ng, T. and Adams, J. C. (2003). Interaction of fascin and protein kinase Calpha: a novel intersection in cell adhesion and motility. *EMBO J.* **22**, 5390-5402.
- Chae, J.-I., Kim, J., Woo, S.-M., Han, H.-W., Cho, Y. K., Oh, K.-B., Nam, K.-H. and Kang, Y.-K. (2009). Cytoskeleton-associated proteins are enriched in human embryonic-stem cell-derived neuroectodermal spheres. *Proteomics* **9**, 1128-1141.
- Dorrell, M. I., Aguilar, E. and Friedlander, M. (2002). Retinal vascular development is mediated by endothelial filopodia, a preexisting astrocytic template and specific R-cadherin adhesion. *Invest. Ophthalmol. Vis. Sci.* **43**, 3500-3510.
- Fantín, A., Vieira, J. M., Gestri, G., Dentí, L., Schwarz, Q., Prykhodzij, S., Peri, F., Wilson, S. W. and Ruhrberg, C. (2010). Tissue macrophages act as cellular chaperones for vascular anastomosis downstream of VEGF-mediated endothelial tip cell induction. *Blood* **116**, 829-840.
- Fantín, A., Vieira, J. M., Plein, A., Maden, C. H. and Ruhrberg, C. (2013). The embryonic mouse hindbrain as a qualitative and quantitative model for studying the molecular and cellular mechanisms of angiogenesis. *Nat. Protoc.* **8**, 418-429.
- Fraccaroli, A., Franco, C. A., Rognoni, E., Neto, F., Rehberg, M., Aszodi, A., Wedlich-Söldner, R., Pohl, U., Gerhardt, H. and Montanez, E. (2012). Visualization of endothelial actin cytoskeleton in the mouse retina. *PLoS ONE* **7**, e47488.
- Gerhardt, H., Golding, M., Fruttiger, M., Ruhrberg, C., Lundkvist, A., Abramsson, A., Jeltsch, M., Mitchell, C., Alitalo, K., Shima, D. et al. (2003). VEGF guides angiogenic sprouting utilizing endothelial tip cell filopodia. *J. Cell Biol.* **161**, 1163-1177.
- Hayashi, Y., Toda, K., Saibara, T., Okamoto, S., Osanai, M., Enzan, H. and Lee, G.-H. (2008). Expression of fascin-1, an actin-bundling protein, in migrating hepatoblasts during rat liver development. *Cell Tissue Res.* **334**, 219-226.
- Hoelzle, M. K. and Svitkina, T. (2012). The cytoskeletal mechanisms of cell-cell junction formation in endothelial cells. *Mol. Biol. Cell* **23**, 310-323.
- Jawhari, A. U., Buda, A., Jenkins, M., Shehzad, K., Sarraf, C., Noda, M., Farthing, M. J. G., Pignatelli, M. and Adams, J. C. (2003). Fascin, an actin-bundling protein, modulates colonic epithelial cell invasiveness and differentiation *in vitro*. *Am. J. Pathol.* **162**, 69-80.
- Juín, A., Planas, E., Guillemot, F., Horakova, P., Allbiges-Rizo, C., Génot, E., Rosenbaum, J., Moreau, V. and Saltel, F. (2013). Extracellular matrix rigidity controls podosome induction in microvascular endothelial cells. *Biol. Cell* **105**, 46-57.
- Li, A., Dawson, J. C., Forero-Vargas, M., Spence, H. J., Yu, X., König, I., Anderson, K. and Machesky, L. M. (2010). The actin-bundling protein fascin stabilizes actin in invadopodia and potentiates protrusive invasion. *Curr. Biol.* **20**, 339-345.
- Ma, Y., Li, A., Falter, W. J., Libertini, S., Fiorito, F., Gillespie, D. A., Sansom, O. J., Yamashiro, S. and Machesky, L. M. (2013). Fascin 1 is transiently expressed in mouse melanoblasts during development and promotes migration and proliferation. *Development* **140**, 2203-2211.
- Machesky, L. M. and Li, A. (2010). Fascin: Invasive filopodia promoting metastasis. *Commun. Integr. Biol.* **3**, 263-270.
- Nakayama, M., Nakayama, A., van Lessen, M., Yamamoto, H., Hoffmann, S., Drexlér, H. C. A., Itoh, N., Hirose, T., Breier, G., Vestweber, D. et al. (2013). Spatial regulation of VEGF receptor endocytosis in angiogenesis. *Nat. Cell Biol.* **15**, 249-260.
- Pitulescu, M. E., Schmidt, L., Benedito, R. and Adams, R. H. (2010). Inducible gene targeting in the neonatal vasculature and analysis of retinal angiogenesis in mice. *Nat. Protoc.* **5**, 1518-1534.
- Quintavalle, M., Elia, L., Condorelli, G. and Courtenidge, S. A. (2010). MicroRNA control of podosome formation in vascular smooth muscle cells *in vivo* and *in vitro*. *J. Cell Biol.* **189**, 13-22.
- Reynolds, L. E., Wyder, L., Lively, J. C., Taverna, D., Robinson, S. D., Huang, X., Sheppard, D., Hynes, R. O. and Hodivala-Dilke, K. M. (2002). Enhanced pathological angiogenesis in mice lacking beta3 integrin or beta3 and beta5 integrins. *Nat. Med.* **8**, 27-34.
- Reynolds, L. E., Watson, A. R., Baker, M., Jones, T. A., D'Amico, G., Robinson, S. D., Joffre, C., Garrido-Urbani, S., Rodriguez-Manzanique, J. C., Martino-Echarri, E. et al. (2010). Tumour angiogenesis is reduced in the Tc1 mouse model of Down's syndrome. *Nature* **465**, 813-817.
- Roca, C. and Adams, R. H. (2007). Regulation of vascular morphogenesis by Notch signaling. *Genes Dev.* **21**, 2511-2524.
- Rottiers, P., Saltel, F., Daubon, T., Chaigne-Delalande, B., Tridon, V., Billotet, C., Reuzeau, E. and Génot, E. (2009). TGFbeta-induced endothelial podosomes mediate basement membrane collagen degradation in arterial vessels. *J. Cell Sci.* **122**, 4311-4318.
- Ruhrberg, C., Gerhardt, H., Golding, M., Watson, R., Ioannidou, S., Fujisawa, H., Betsholtz, C. and Shima, D. T. (2002). Spatially restricted patterning cues provided by heparin-binding VEGF-A control blood vessel branching morphogenesis. *Genes Dev.* **16**, 2684-2698.
- Sawamiphak, S., Ritter, M. and Acker-Palmer, A. (2010). Preparation of retinal explant cultures to study ex vivo tip endothelial cell responses. *Nat. Protoc.* **5**, 1659-1665.
- Schoumacher, M., Goldman, R. D., Louvard, D. and Vignjevic, D. M. (2010). Actin, microtubules, and vimentin intermediate filaments cooperate for elongation of invadopodia. *J. Cell Biol.* **189**, 541-556.
- Silva, R., D'Amico, G., Hodivala-Dilke, K. M. and Reynolds, L. E. (2008). Integrins: the keys to unlocking angiogenesis. *Arterioscler. Thromb. Vasc. Biol.* **28**, 1703-1713.
- Stefater, J. A., I. I. L., Lewkowich, I., Rao, S., Marigeli, G., Carpenter, A. C., Burr, A. R., Fan, J., Ajima, R., Molkenin, J. D., Williams, B. O. et al. (2011). Regulation of angiogenesis by a non-canonical Wnt-Fhl1 pathway in myeloid cells. *Nature* **474**, 511-515.
- Varon, C., Tatin, F., Moreau, V., Van Obberghen-Schilling, E., Fernandez-Sauze, S., Reuzeau, E., Kramer, I. and Génot, E. (2006). Transforming growth factor beta induces rosettes of podosomes in primary aortic endothelial cells. *Mol. Cell Biol.* **26**, 3582-3594.
- Vignjevic, D., Kojima, S.-I., Aratyn, Y., Danciu, O., Svitkina, T. and Borisy, G. G. (2006). Role of fascin in filopodial protrusion. *J. Cell Biol.* **174**, 863-875.
- Villefranc, J. A., Nicoli, S., Bentley, K., Jeltsch, M., Zarkada, G., Moore, J. C., Gerhardt, H., Alitalo, K. and Lawson, N. D. (2013). A truncation allele in vascular endothelial growth factor c reveals distinct modes of signaling during lymphatic and vascular development. *Development* **140**, 1497-1506.
- Yamakita, Y., Matsumura, F. and Yamashiro, S. (2009). Fascin1 is dispensable for mouse development but is favorable for neonatal survival. *Cell Motil. Cytoskeleton* **66**, 524-534.
- Zanet, J., Stramer, B., Millard, T., Martin, P., Payre, F. and Plaza, S. (2009). Fascin is required for blood cell migration during *Drosophila* embryogenesis. *Development* **136**, 2557-2565.
- Zhang, F.-R., Tao, L.-H., Shen, Z.-Y., Lv, Z., Xu, L.-Y. and Li, E.-M. (2008). Fascin expression in human embryonic, fetal, and normal adult tissue. *J. Histochem. Cytochem.* **56**, 193-199.

Supplementary Material

Yafeng Ma et al. doi: 10.1242/bio.20136031

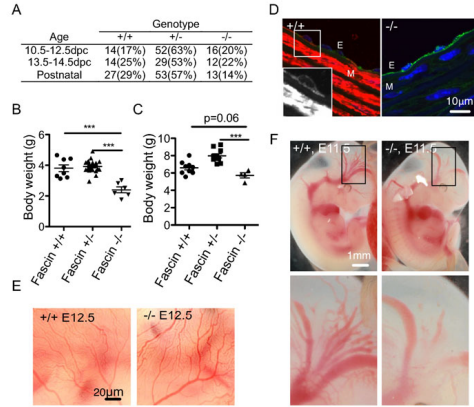


Fig. S1. (A) Genotypic analysis of progeny from fascin 1 heterozygous intercrosses (C57BL/6). Postnatal mice were scored 7 days after birth. Dpc = days postcoitum. (B-C) Body weight of fascin $1^{+/+}$, $1^{+/-}$, $1^{-/-}$ mice at postnatal day 7 and day 19. Results are expressed as means \pm s.e.m. Mann-Whitney test, ***, $P < 0.001$. (D) FITC conjugated BSI-B4 (green) and fascin 1 (red) IF stains of fascin $1^{+/+}$ and fascin $1^{-/-}$ aortas indicating a layer of endothelial cells surrounded by a few layers of mural cells. Immunostaining for fascin stains (white) in magnified area indicates that endothelial cells express lower levels of fascin compared to high level of fascin in mural cells. DAPI (blue), nuclear counterstain. E, endothelial cell layer; M, mural cell layers. (E) Representative pictures of E12.5 yolk sac showing normal vessel network in fascin $1^{-/-}$ embryos. (F) Representative pictures of E11.5 embryos showing less brain blood vessel in fascin $1^{-/-}$ embryos. Bars, 10 μ m (D), 20 μ m (E), 1 mm (F).

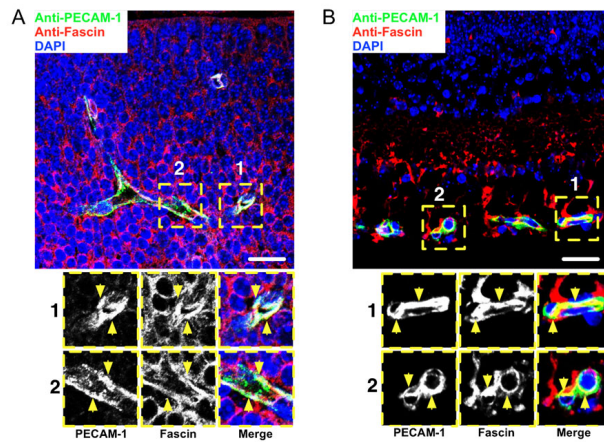


Fig. S2. (A, B) Immunostaining of hindbrain and retina tissue section with antibodies as labeled. Endothelial cells are identified with PECAM-1 staining. Insets show high-magnification views. Yellow arrows endothelial cells. Bars, 20 μ m.

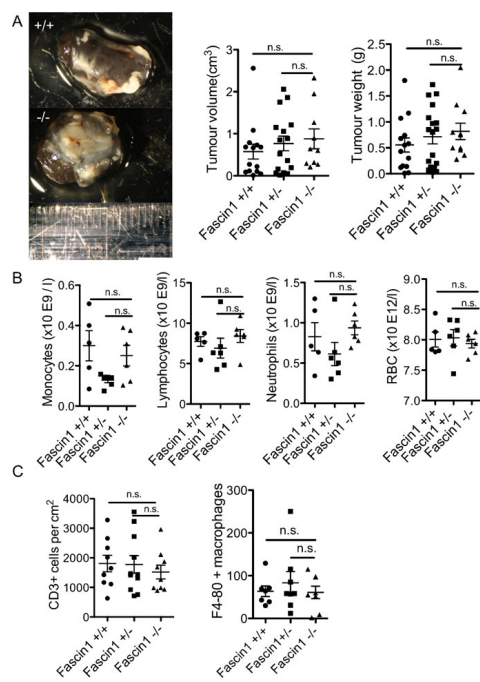
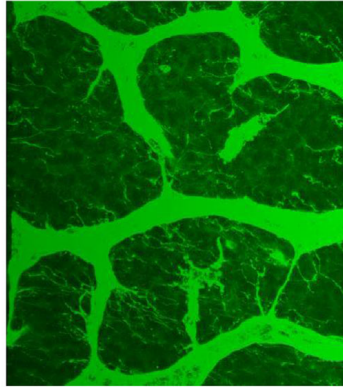
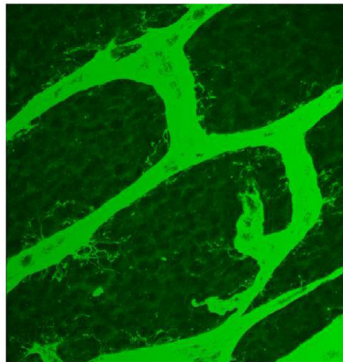


Fig. S3. (A) Representative images of B16F0 tumours from fascin 1^{+/+}, fascin 1^{+/-} and fascin 1^{-/-} mice, tumour volume and weight as calculated in Materials and Methods (fascin 1^{+/+}, 5; fascin 1^{+/-}, 7; fascin 1^{-/-}, 6). (B) Monocyte, neutrophil, lymphocyte and red blood cell (RBC) numbers of adult mice as measured by blood counts (fascin 1^{+/+}, 5; fascin 1^{+/-}, 6; fascin 1^{-/-}, 6) (C) CD3⁺ T cells and F4/80⁺ macrophages in B16F0 tumour sections ($n=7-9$). Results are expressed as means \pm s.e.m. Mann-Whitney test, n.s., not significant.



Movie 1. 3D-projected FITC conjugated BSI-B4 stained fascin 1^{+/+} hindbrain vessels (211.97 μm \times 211.97 μm , 1024 \times 1024, 60 \times objective).



Movie 2. 3D-projected FITC conjugated BSI-B4 stained fascin 1^{-/-} hindbrain vessels (211.97 μm \times 211.97 μm , 1024 \times 1024, 60 \times objective).

Appendix B: Fascin is regulated by Slug, promotes progression of pancreatic cancer in mice, and is associated with patient outcome

Accepted Manuscript

Fascin is Regulated by Slug, Promotes Progression of Pancreatic Cancer in Mice, and is Associated with Patient Outcome

Ang Li, Jennifer P. Morton, YaFeng Ma, Saadia A. Karim, Yan Zhou, William J. Faller, Emma F. Woodham, Hayley T. Morris, Richard P. Stevenson, Amelie Juin, Nigel B. Jamieson, Colin J. MacKay, C. Ross Carter, Hing Y. Leung, Shigeo Yamashiro, Karen Blyth, Owen J. Sansom, Laura M. Machesky

PII: S0016-5085(14)00105-X
DOI: [10.1053/j.gastro.2014.01.046](https://doi.org/10.1053/j.gastro.2014.01.046)
Reference: YGAST 58934

To appear in: *Gastroenterology*
Accepted Date: 17 January 2014

Please cite this article as: Li A, Morton JP, Ma Y, Karim SA, Zhou Y, Faller WJ, Woodham EF, Morris HT, Stevenson RP, Juin A, Jamieson NB, MacKay CJ, Carter CR, Leung HY, Yamashiro S, Blyth K, Sansom OJ, Machesky LM, Fascin is Regulated by Slug, Promotes Progression of Pancreatic Cancer in Mice, and is Associated with Patient Outcome, *Gastroenterology* (2014), doi: 10.1053/j.gastro.2014.01.046.

This is a PDF file of an unedited manuscript that has been accepted for publication. As a service to our customers we are providing this early version of the manuscript. The manuscript will undergo copyediting, typesetting, and review of the resulting proof before it is published in its final form. Please note that during the production process errors may be discovered which could affect the content, and all legal disclaimers that apply to the journal pertain.

All studies published in *Gastroenterology* are embargoed until 3PM ET of the day they are published as corrected proofs on-line. Studies cannot be publicized as accepted manuscripts or uncorrected proofs.



Fascin is Regulated by Slug, Promotes Progression of Pancreatic Cancer in Mice, and is Associated with Patient Outcome

Ang Li^{1,4}, Jennifer P. Morton¹, YaFeng Ma¹, Saadia A. Karim¹, Yan Zhou¹, William J. Faller¹, Emma F. Woodham¹, Hayley T. Morris¹, Richard P. Stevenson¹, Amelie Juin¹, Nigel B. Jamieson², Colin J. MacKay², C. Ross Carter², Hing Y. Leung¹, Shigeko Yamashiro³, Karen Blyth¹, Owen J. Sansom¹ and Laura M. Machesky^{1*}

*To whom correspondence should be addressed

l.machesky@beatson.gla.ac.uk

1 CRUK Beatson Institute for Cancer Research, College of Medical Veterinary and Life Sciences, University of Glasgow, Switchback Road, Garscube Estate, Glasgow, G61 1BD

2 Department of Surgery, West of Scotland Pancreatic Unit, Glasgow Royal Infirmary, Glasgow G4 0SF, UK

3 Department of Molecular Biology and Biochemistry, Rutgers University, Piscataway, NJ, 08855, USA.

4 Present Address: Laboratory of Mammalian Cell Biology and Development, The Rockefeller University, 1230 York Avenue, Box #300, New York, NY, 10065, USA

Study concept and design (A. L., J.P.M., K.B., O.J.S., L.M.M.); acquisition of data (A.L., Y.M., E.W., Y.Z., R.P.S.); analysis and interpretation of data (A.L., J.P.M., S.A.K., W.J.F., H.M., L.M.M.); drafting of the manuscript (A.L., L.M.); statistical analysis (S.K., W.J.F., J.P.M.); funding, technical or material support (K.B., N.B.J., C.J.M., C.R.C., S.Y., O.J.S., L.M.M.). The authors declare no conflicts of interest. This work was funded by CRUK core funding to K.B., O.J.S., H.Y.L. and L.M.M. and by MRC-UK funding to H.T.M.

The authors declare no known conflict of interest.

ACCEPTED MANUSCRIPT

Acknowledgements

We thank Joel Habener and Violeta Stanojevic of the Mass General Hospital, Boston, USA for their generous gift of slug antiserum. We also thank Colin Nixon of Beatson histology services, Matthew Neilson of Beatson Bioinformatics and all staff of BSU and the BAIR imaging facility.

ACCEPTED MANUSCRIPT

Abstract:

Background & Aims: Pancreatic ductal adenocarcinoma (PDAC) is often lethal because it is highly invasive and metastasizes rapidly. The actin-bundling protein fascin has been identified as a biomarker of invasive and advanced PDAC and regulates cell migration and invasion in vitro. We investigated fascin expression and its role in PDAC progression in mice.

Methods: We used KRas^{G12D} p53^{R172H} Pdx1-Cre (KPC) mice to investigate the effects of fascin deficiency (FKPC mice) on development of pancreatic intraepithelial neoplasia (PanIn), PDAC, and metastasis. We measured levels of fascin in PDAC cell lines and 122 human resected PDAC samples, along with normal ductal and acinar tissues; we associated levels with patient outcomes.

Results: Pancreatic ducts and acini from control mice, and early-stage PanINs from KPC mice, were negative for fascin, but approximately 6% of PanIN3 and 100% of PDAC expressed fascin. FKPC mice had longer survival times, delayed onset of PDAC, and a lower PDAC tumor burdens than KPC mice; loss of fascin did not affect invasion of PDAC into bowel or peritoneum in mice. Levels of slug and fascin correlated in PDAC cells; slug was found to regulate transcription of *Fascin* along with the epithelial–mesenchymal transition. In PDAC cell lines and cells from mice, fascin concentrated in filopodia, and was required for their assembly and turnover. Fascin promoted intercalation of filopodia into mesothelial cell layers and cell invasion. Nearly all human PDAC samples expressed fascin, and higher fascin histoscores correlated with poor outcome, vascular invasion, and time to recurrence.

Conclusions: The actin-bundling protein fascin is regulated by slug and involved in late-stage PanIN and PDAC formation in mice. Fascin appears to promote formation of filopodia and invasive activities of PDAC cells. Its levels in human PDAC correlate with outcome and time to recurrence, indicating it might be a marker or therapeutic target for pancreatic cancer.

KEYWORDS: pancreas, tumor progression, actin cytoskeleton, EMT

Introduction

Pancreatic ductal adenocarcinoma (PDAC) has a median survival of 6 months and a 5-year survival of <5%¹. 90% of patients have surgically unresectable disease at diagnosis and the majority of patients who undergo resection for localized lesions develop recurrent or metastatic disease². Consequently, the development of more effective strategies to combat metastasis is of paramount importance.

Human PDAC arises from PanINs frequently driven by activating mutations in KRas³, followed by loss or mutation of tumor suppressors, such as p53. Pdx1-Cre driven expression of KRas^{G12D} and Trp53^{R172H} in murine pancreas mimics the human disease and importantly the histopathology⁴. Disease progression and sites of metastases also mirror the human disease providing a good model for human PDAC⁵.

Slug is a snail family transcription factor that orchestrates the epithelial to mesenchymal transition (EMT) during developmental programs, including in the mouse pancreas⁶. The snail family transcription factors repress epithelial specific genes and enhance mesenchymal associated genes⁷. Snail proteins bind to specific E-box sequences in promoters or introns and thus regulate gene expression⁷. In the pancreas, slug (also called snail2) is expressed in a subset of pancreatic embryonic epithelial cells⁶ and is associated with endocrine cells delaminating from primitive ductal tubules and migrating into the parenchyma. Slug expression is highest in those cells of the embryonic pancreas that have lowest levels of E-cadherin, including developing islet cells⁶. Snail family transcription factors have also been implicated in tumor progression and metastatic dissemination⁸. EMT occurs in PDAC and is thought to be an important process in metastatic spread^{9,10}.

Expression of the actin bundling protein fascin is tightly regulated during development, with fascin present transiently in many embryonic tissues and later only in selected adult tissues^{11,12}. The fascin deficient mouse develops largely normally¹³. Fascin expression is low or absent from adult epithelia, but is often highly elevated in malignant tumors (reviewed in^{11,12}) and its

overexpression is associated with poor prognosis¹². Fascin is enriched in cancer cell filopodia (reviewed in¹¹) and in invadopodia^{14,15}. Fascin is also expressed by fibroblasts and dendritic cells and is thus associated with stroma^{11,12}. Fascin has also been associated with metastatic spread of breast cancer and tumor self-seeding¹⁶. However, the effect of loss or inhibition of fascin has not been previously tested in a spontaneous tumor model to determine whether fascin impacts on tumor progression, invasion or metastasis.

Results

Fascin expression correlates with poor survival and time to recurrence in human PDAC

Of 122 primary human resected PDAC, fascin was absent from normal ductal and acinar tissue but prominent in PDAC cytoplasm (Figure 1A). 95% of human PDAC expressed fascin and a high histoscore significantly correlated with decreased overall survival (Figure 1B), high tumor grade (Figure 1C; median histoscore 104.4 vs 72.8, $p < 0.05$) and vascular invasion (Figure 1D, median histoscore 94.5 vs 62.2) ($p < 0.04$). Fascin levels did not correlate with lymph node status, tumor stage, perineural invasion and lymphatic invasion (Data not shown). In a multivariate Cox proportional-hazards regression analysis, high fascin expression only reached borderline significance as an independent predictor of poor survival, with a hazard ratio of 0.663 (95% CI: 0.44-1; $p=0.05$) (Table S1). Importantly, fascin levels strongly correlated with time to recurrence, indicating potential importance as a predictor of tumor dissemination (Figure 1E; $p < 0.0005$).

To explore a functional role of fascin, we used a mouse model of pancreatic cancer ($KRas^{G12D}$ $p53^{R172H}$ Pdx1-Cre, KPC mice) recapitulating both pre-invasive PanIN (grade 1-3) and invasive, metastatic PDAC⁴. Wild-type ducts and acini and PanIN1-2 from 10w old KPC mice were negative for fascin (Figure 1F). Around 6% of PanIN3 and 100% of PDAC (both 10w and advanced tumors) (Table S2) were fascin positive (Figure 1F) and fascin was expressed in both well and poorly differentiated areas (Data not shown).

Fascin null mice had normal size pancreata with no apparent changes in tissue structure or proliferation (Figure S1). Although fascin is weakly expressed by a few cells in the islets of Langerhans (Figure 1F), fascin null mice had normal peripheral blood levels of several markers indicating normal pancreatic function (Table S3). Development of PanIN in $Kras^{G12D}$ or $Kras^{G12D}$ and $p53^{R172H}$ expressing pancreata was not changed by loss of fascin (Figure S2). Loss of fascin also did not affect progression, morphology or proliferation of cells in an acute model of pancreatitis using cerulein injection (Figure S3). However, by 21d of cerulein treatment, fascin was detected in stroma and epithelium of PanIN of KC animals (Figure S3). However, loss of fascin did not affect the numbers of monocytes, lymphocytes or neutrophils recruited to acute PanINs, revealing no gross abnormalities in the immune response to PanIN in the fascin null mice (Figure S3E, F). In summary, fascin expression was detected in a minority of PanIN3 and all PDAC and loss of fascin did not detectably affect pancreas development or PanIN.

Loss of fascin enhances survival and decreases early tumor burden

Fascin expression or function has not been studied before in the context of spontaneous tumor development, so we crossed the fascin knockout mouse with KPC to make FKPC (Figure 2A). Pdx1-Cre mediated recombination appeared normal in fascin deficient mice (Figure S4A), which showed a significant increase in survival (Figure 2B). Fascin was expressed in KPC and absent from FKPC tumors (Figure 2C). Fascin null mice displayed similar endpoint tumor histology and mass (Figure 2D), with no significant difference in the number of undifferentiated or sarcomatoid lesions in the cohorts (not shown). KPC and FKPC tumors showed identical proportions of cell proliferation and death (Figure 2E and S4B). There was no detectable difference in recruitment of T cells (CD3), B cells (CD45R) macrophages (F4/80), or neutrophils (NIMP) between KPC and FKPC tumors (Figure S4C, D) or difference in PECAM staining of vascularization (Figure S4E, F). Together, these data suggest that cell proliferation, cell death and fascin

deficient microenvironment do not contribute significantly to prolonged survival of FKPC mice.

We next examined mice at earlier timepoints during PDAC onset and progression. No differences were found at 6w (Figure 2F), but by 10w, 6/9 KPC vs 1/9 FKPC showed tumors (Figure 2F). By 15w, 9/10 KPC vs 3/6 FKPC showed tumors and FKPC showed smaller tumors (Figure 2F). Thus, loss of fascin significantly delays onset of PDAC and reduces early PDAC tumor burden, a surprising effect, which has not been previously described.

Slug drives fascin expression in PDAC

During the development of PDAC, ductal cells undergo epithelial to mesenchymal transition (EMT)¹⁰. Fascin is principally expressed in neural and mesenchymal derivatives during mammalian embryonic development^{17,18}, suggesting that fascin could be a potential EMT target. EMT involves three families of transcription factors, the snail, ZEB and bHLH families^{7,19}. We generated 10 independent KPC mouse PDAC cell lines that showed heterogeneous expression of E-cadherin, fascin and EMT transcription factors Tfs (Figure 3A), while normal primary ductal epithelial cells (PDEC) did not detectably express fascin or EMT Tfs (Figure S5A, B). Co-expression of E-cadherin and EMT Tfs indicate that most of our PDAC cell lines were in an intermediate stage of EMT (Figure 3A, S5C)¹⁰. Fascin deficient PDAC cells also showed a similar heterogeneous expression of E-cadherin, fascin and EMT Tfs (Figure S5D). Slug, zeb1 and zeb2 were expressed in all of our PDAC cell lines, while twist and snail were expressed in a subset (Figure 3A). Levels of fascin and slug correlated most closely (Figure 3A, B). Fascin and slug expression also correlated in a dataset of 23 human pancreatic cancer cell lines²⁰ (Figure S5E).

Epithelial-like 070669 PDAC cells expressed a low level of fascin (Figure 3A), which increased >2-fold upon Flag-slug or snail transfection (Figure 3C). Expressing snail or slug also suppressed E-cadherin but upregulated fascin (Figure 3D and S6A). Knockdown of slug reduced fascin expression (Figure S6B), whereas stable expression of twist (Figure 3C, D and S6A) or transient

knockdown of zeb1, zeb2, or E-cadherin did not change fascin levels (Figure S6C). Knockdown of fascin did not affect slug expression (Figure S6C). These observations were confirmed in 061843 PDAC cells (Figure S6D, E). Thus, slug mediates fascin expression in PDAC cells. Furthermore, expression of slug or snail in human pancreatic cancer cells PANC-1 and human colon cancer cells HT29 induced fascin expression (Figure S6F), suggesting a general effect of slug and snail on fascin expression in both mouse and human cancer cells.

Slug and fascin co-express during PDAC progression

We next investigated expression of fascin and slug during EMT changes in KPC PDAC tumors. Interestingly, fascin and slug were both absent from ductal and acinar cells in normal pancreas and PanIN1/2 lesions (Figure 4A). Slug was expressed in fascin positive (but not negative) PanIN3 lesions (Figure 4A), indicating a correlation between early markers of EMT and fascin expression during PDAC progression. Fascin and slug were present in all PDACs, regardless of E-cadherin staining or differentiation status (Figure 4B). In addition, fascin expression significantly correlated with slug expression in three independent cohorts of pancreatic cancer patients (Figure S7). We propose that slug induced EMT is an important regulator of fascin expression in pancreatic cancer.

Fascin is a direct slug target gene

Given the induction of fascin by slug and their tight association in human and mouse pancreatic cancer, we set out to determine whether fascin is a direct transcriptional target of slug. We screened the promoter and first intron region of mouse fascin for slug binding E-box sequences (CACCTG or CAGGTG)²¹. We found a potential E-box sequence CACCTG located within the first intron of the mouse fascin gene at +2,470 to +2,475 bp (Figure 5A). This consensus E-box sequence is highly conserved among mammalian fascins (Figure 5A). We designed three sets of primers around the putative E-box sequence: primer set 1 targets the identified E-box, while primer sets 2 and 3 target

adjacent regions (Figure 5A). Slug co-precipitated with the putative fascin E-box element (Figure 5B). Cotransfection of the +2,345 to +2,600 region of the fascin first intron in a luciferase reporter plasmid with a plasmid expressing slug into 070669 PDAC cells drove a significant increase in luciferase activity (Fig. 5C). Mutagenesis of the E-box sequence eliminated the ability of slug to induce luciferase activity. (Figures 5C). We propose that fascin is a direct transcriptional target of slug.

Fascin is required for local and distant metastasis but not invasion

We next explored the hypothesis that fascin was a driver of invasion and metastasis in PDAC. Invasive PDAC was present in around half of KPC mice and this was histologically similar in FKPC mice (Figure 6A,B). More than 80% of KPC mice, but only 30% of FKPC mice developed abdominal distension due to hemorrhagic ascites (Figure 6C). On average, KPC mice harbored 1.57ml ascitic fluid, while FKPC mice showed almost none (Figure 6C). Metastasis was dramatically reduced in FKPC mice (Figure 6B and Table S4). Around 95% of KPC mice and only 55% of FKPC had local metastasis to intestinal mesentery (Figure 6B, D, E). 44% of KPC mice, but only 13% of FKPC mice developed diaphragm metastasis (Figure 6B). Similar to local metastasis, 52% of KPC mice and only 13% of FKPC mice showed distant liver metastasis (Figure 6B, F). Both mesenteric and liver metastases of KPC mice were positive for fascin and p53 (Figure 6D,F). KPC mice had shorter survival overall than FKPC with liver metastases (Figure 6E). We conclude that loss of fascin significantly reduces ascites and metastasis to mesentery, diaphragm and liver.

Fascin mediates peritoneal metastasis via promotion of transmesothelial migration

To further investigate the mechanism by which fascin promotes metastasis, we first examined the actin dynamics of PDAC cells (105768) from the FKPC

mice compared with the same cell line rescued with GFP-fascin. GFP-fascin concentrated in filopodia (Figure 7A and Movie 1). Fascin rescue cells showed dynamic filopodia assembly and turnover (Figure S8A,B). Filopodia were significantly less frequent, shorter and shorter-lived in fascin-deficient cells than fascin-rescued cells (Figure S8B). Lamellipodial dynamics were greater in fascin-rescued cells (Figure S8C and Movie 2). Expression of fascin significantly enhanced protrusion frequency, distance protruded and protrusion rate and decreased protrusion persistence (Figure S8C). Fascin rescued PDAC cells migrated faster than fascin deficient cells (Figure S8D and Movie 3). Fascin expression status did not affect growth in 2D or 3D (Figure S8E), similar to PDAC in vivo. Moreover, fascin rescued cells behaved similarly to fascin deficient cells during anoikis (Figure S8E). Thus, fascin expression increases PDAC cell migration via lamellipodial and filopodial dynamics but doesn't affect growth and survival.

Formation of mesenteric and diaphragm metastasis involves transmigration of cancer cells through the mesothelial cell (MC) layer^{22,23}. We tested a potential role for fascin in mesothelial transmigration by plating PDAC cells (105768) atop a monolayer of human Met5a MCs. PDAC cells opened MC junctions and then inserted between MCs (Figure S9A). GFP-fascin localized intensively to the filopodia at the leading edge of transmigrating PDAC cells (Figure 7A and Movie 4). About 75% of fascin-rescued PDAC cells but only 35% of fascin deficient cells intercalated by 10 hr (Figure 7B, S9B and Movie 5). Fascin knockdown in KPC 070669 PDAC cells also significantly reduced intercalation (Figure S9 C-E). GFP-fascin rescued cells generated protrusions that more effectively transmigrated than fascin nulls (Figure 7C and Movie 6). Nude mice injected with fascin deficient PDAC cells developed significantly fewer mesenteric or diaphragm metastatic foci than with fascin-rescued cells (Figure 7E, F). These results are consistent with our spontaneous mouse model and suggest that targeting the interaction of PDAC cells with the mesothelium through fascin depletion is sufficient to reduce metastasis in vivo.

Discussion

Fascin is an EMT target in pancreatic cancer

Nearly all human PDAC expressed fascin, and a higher fascin histoscore correlated with poor outcome, vascular invasion and time to recurrence. Similar correlations have been reported for hepatocellular and extrahepatic bile duct carcinomas^{24,25}. Fascin expression in smaller cohorts of human PDAC and PanIN^{26,27} and also in pancreatobiliary adenocarcinomas²⁸ and pancreatic intraductal papillary mucinous carcinoma²⁹ correlated with shorter survival times and more advanced stages. Fascin expression contributes to progression of human PDAC, but is only of borderline significance as a prognostic indicator, indicating that other factors contribute to recurrence and spread.

Fascin is a wnt target in colorectal cancer, where it localises to tumor invasive fronts but is downregulated in metastases³⁰. However, in Kras^{G12D} and p53^{R172H} driven pancreatic cancer, fascin is evenly expressed in tumors and remains highly expressed in liver and peritoneal metastases. Unlike colorectal cancer, the role of wnt signalling in pancreatic cancer progression is less clear³¹ and we find that fascin is an EMT target of the transcription factor slug. Slug is expressed in pancreatic endocrine progenitor cells and effects EMT changes and migration during early embryonic development⁶. We speculate that PDAC cells may reacquire slug and fascin during a partial reversion to an embryonic migratory state.

Fascin contributes to PDAC progression

There is controversy about whether gene changes that confer metastatic dissemination of pancreatic cancer (or other cancers) occur early in tumor formation or late. A recent study provided compelling evidence based on lineage tracing of cells by tumor mutation analysis that metastasis could occur even before there was a recognisable tumor¹⁰. Our finding that fascin expression happens during late PanIN to PDAC transition suggests that EMT changes that promote metastasis start to happen early. EMT has been correlated with tumor initiating (stem) cell properties and thus as a part of an

EMT programme³². Fascin expression might allow tumor stem cells to thrive during initial tumor formation as well as later during metastasis. Perhaps primary tumors and metastases first arise from small nests of fascin-positive cells in PanIN3. In this case, expression of fascin in PanINs might be predictive of tumor formation and metastasis.

Fascin in invasion and metastatic colonisation

Fascin is not only expressed in PDAC tumor cells, but also in stroma of PDAC and of some PanIN. Since our fascin knockout is global and constitutive, loss of fascin in the stroma may have contributed to the phenotypes we observed. However, we could not detect any gross changes in the stromal immune cell component or blood vessel density of fascin knockout tumors and we recently reported that fascin loss is dispensible for growth of transplanted tumors³³.

Fascin has been implicated in migration and invasion in vitro, so it was surprising that fascin loss had no effect on invasion in vivo. We previously observed that only melanoma cell lines displaying elongated mesenchymal mechanisms of invasion were dependent on fascin¹⁴. Collective invasion into bowel or peritoneal wall is not limited by loss of fascin and thus may not be limited also by matrix remodelling or invadopodia formation. Collective PDAC invasion could occur in physiological clefts between tightly packed collagen bundles or muscle strands³⁴ and fascin-mediated protrusions may not be crucial.

We show that fascin null cells are less able to colonize the mesentery. ROCK and myosin-mediated contractility are required for transmesothelial migration of human multiple myeloma and ovarian cancer cells^{35,36}. We provide mechanistic evidence that fascin drives long filopodia that cross between the mesothelial cells and make initial contact with the substratum to aid transmigration. Our study suggests that at least for PDAC, it is not invasion of the primary tumor, but rather colonization of the new site that is most affected by fascin loss.

Materials and Methods

Genetically Modified Mice- All experiments were performed according to UK Home Office regulations. Mouse models are described in Supplementary Materials.

Immunoblotting and Quantitative PCR- Immunoblotting and quantitative PCR were carried out by standard protocols (details in Supplementary materials). N= 3 independent experiments in triplicate.

Human Tissue Analysis-The human pancreatobiliary tissue microarray was previously described^{37,38} (See Supplementary Information). All statistical analyses were performed using SPSS version 15.0 (SPSS Inc., Chicago, IL). We used OncoPrint to examine fascin and slug expression in Jimeno Pancreas³⁹, Pei Pancreas⁴⁰, Badea Pancreas⁴¹ and Wagner CellLine²⁰.

Cell Culture and expression of siRNA or constructs-PDAC cell lines were generated from primary pancreatic tumors from KPC or FKPC mice (see Supplementary information). All experiments used cells < 6 passages. Standard methods for siRNA were described previously¹⁴.

Tissue Immunofluorescence-For staining fascin, slug, snail and twist, cells were fixed with -20°C methanol for 10 min. For all other staining, cells were fixed in 4% formaldehyde as previously described¹⁴. Primary antibodies were detected with Alexa488, Alexa594 and Alexa647-conjugated secondary antibodies. Samples were examined using Olympus FV1000 or Nikon A1 inverted laser scanning confocal microscope.

Immunohistochemistry, live cell imaging and cell growth assays- Standard methods were used. See Supplementary Information for details.

In vivo PDAC transplant studies- For mesenteric and diaphragm seeding experiments, 1×10^6 PDAC cells in 100 μ l PBS were introduced into each nude mouse (CD-1 nude females 6w old, Charles River Lab, Wilmington, MA) by intraperitoneal injection and tumor nodules were quantified after 2w.

Figure Legends:**Figure 1 High fascin histoscore predicts poor survival and recurrence in human PDAC**

(A) Representative images of fascin staining in human PDAC. (B) Kaplan-Meier analysis showing cases with high histoscore have poorer outcomes compared with low expression ($p=0.011$ by log-rank test). (C) Boxplot of fascin histoscore versus tumor grade. (D) Boxplot of fascin histoscore versus vascular invasion (E) Boxplot of fascin histoscore versus time to recur. (F) Representative fascin staining in KPC mice as indicated. Yellow dashes outline the tumor. Insets show high-magnification views of ductal cells. Yellow arrows- fascin positive cells in normal islets. Fascin positive cells in PanIN3 are yellow arrowed. Scale Bars: (F) 50 μ m for normal and PanINs, 200 μ m for early PDAC.

Figure 2 Fascin is required for early PDAC formation

(A) Gene targeting strategy for generating *fascin*^{-/-}, *KRas*^{G12D} *p53*^{R172H} *Pdx1-Cre* (FKPC) mice. (B) Kaplan-Meier curves. (C) Top: Western blot analyses of tumor tissue. Bottom: Histology of PDAC H&E (top), IHC for fascin (middle) and p53 (bottom). (D) Dot plot of primary tumor-to-body weight ratios at sacrifice (mean \pm SEM). (E) 2h BrdU, Ki67+, phospho-histone H3+ (PHH3) and cleaved caspase3+ (CC3) cells in PDACs from KPC and FKPC mice. N \geq 16 fields from n \geq 4 mice (mean \pm SEM). (F) Left: Number of PDAC positive KPC and FKPC mice at indicated times. * $p<0.05$ by chi-square test. Middle: Primary pancreas-to-body weight ratios (mean \pm SEM) * $p<0.05$, ** $p<0.01$ by Mann Whitney U-test. Right: Relative tumor size, Lower quartile, median, and upper quartile are shown. * $p<0.05$ by Mann Whitney U-test. Scale bars: (C)100 μ m.

Figure 3 Fascin is a target of slug in PDAC

(A) Expression of EMT markers in a representative panel of 10 independent KPC PDAC cell lines. (B) Spearman correlation analysis of fascin and slug protein expression in mouse PDAC cell lines. Fascin and slug expression level in PDAC cell lines was plotted as relative expression to 070669 PDAC cell line, with other cell lines

ACCEPTED MANUSCRIPT

numbered as in (A). (C) Left: Western blot analysis with control, Flag-slug, Flag-snail and twist expressing 070669 PDAC cells for proteins as indicated. Bar graphs: Relative protein levels of fascin or qPCR analysis mRNA in 070669 PDAC cells expressing EMT Tfs as indicated (mean±SEM, n=3). *p<0.05, **p<0.01 Student's t-test. (D) Phase and immunofluorescence microscopy of 070669 PDAC cells expressing EMT Tfs as indicated. Low E-cadherin and high fascin expressing cells are yellow arrowed. Scale Bars: (D) 10µm for immunofluorescence, 50µm for phase. GAPDH loading control in A&C.

Figure 4 Slug drives fascin expression in KRas^{G12D} p53^{R172H} Pdx1-Cre (KPC) driven PDAC (A) Fluorescent images of sections from normal pancreas and PanINs co-stained for E-cadherin (w= white), fascin (green), slug (red) and DNA (DAPI, blue). Insets show high-magnification views of ductal cells. (B) Well (top) and poorly differentiated (bottom) PDACs from KPC mice co-stained for E-cadherin, fascin and slug. Insets higher magnification. Scale bars: (A, B) 20µm.

Figure 5 Fascin is a slug target gene

(A) Schematic showing the potential E-box element in intron 1 of the fascin gene and regions targeted by three primer pairs (#1-3, red lines). Primer pair #1 targets the putative E-box while primer pair #2 and #3 target downstream regions. The number in parentheses indicates distance downstream of transcription start site. (B) Chromatin from 070669 PDAC cells expressing Flag-slug was immunoprecipitated using Flag antibody and PCR was performed on the ChIP product using three primer pairs. Primers for an E-cadherin promoter E-box element were used as positive control. (Mean± SEM). **p<0.01 by Student's t-test. (C) Top: the putative E-box on the mouse fascin gene and mutations. Bottom: Relative luciferase activities of 070669 PDAC cells transfected as indicated. n=3 experiments. (Mean± SEM). **p<0.01 * p<0.05 by Student's t-test.

Figure 6 Fascin is required for efficient metastasis in KRas^{G12D} p53^{R172H} Pdx1-Cre (KPC) mice. (A) H&E staining of (left) bowel and (right) peritoneal invasion by cells from KPC and FKPC tumors. Insets show zoom of invasion area. Black arrows indicate direction of invasion. (B) Table shows incidence of invasion (top) and metastasis (bottom) in KPC and FKPC mice with PDAC. (*p<0.05, **p < 0.01, chi-square test) (C) Incidence and volume of ascites in PDAC bearing KPC and FKPC mice (left **p < 0.01, chi-square test; right mean± SEM. **p<0.01 by Mann Whitney U-test.) (D) Top: Representative pictures of metastatic nodules (red arrows) on intestinal mesentery of KPC and FKPC mice. Bottom: Mesenteric metastasis from KPC mice H&E (left), fascin (middle) and p53 (right). (E) Left: Number of mesenteric metastases **p<0.01 by Mann Whitney U-test. Right: Survival of mice with liver metastases. Blue and red dotted lines indicate median survival for KPC and FKPC mice respectively. (F) Liver metastasis from KPC mice for H&E (left), fascin (middle) and p53 (right). Scale bar: (A, D) 100µm (F) 50µm.

Figure 7 Fascin mediates peritoneal metastasis via promotion of transmesothelial intercalation. (A) Still image of live GFP-fascin in PDAC cells transmigrating through a red CMTPIX CellTracker (CT) labeled confluent Met5A monolayer. Yellow stars indicate fascin-positive filopodia. (B) Intercalation for individual cells during 10hr. (n=100 cells, 8 fields, mean±SEM, n=3) **p<0.01 by Student's t-test. (C) Time lapse movie stills of PDAC cells intercalating between MCs. Protrusions are yellow arrowed. (D) PDAC cells as indicated were injected intraperitoneally into nude mice. Yellow arrows indicate tumor nodules. (E) Mesenteric tumor nodules from GFP-fascin rescued cells express fascin and p53. Insets show high magnification. (F) Number of mesenteric and diaphragm metastases. N=10 mice per condition. *p<0.05, **p<0.01 by Mann Whitney U-test. Scale bars: (B, C, D) 10µm. (E) 100µm.

References

ACCEPTED MANUSCRIPT

1. Warshaw, AL, Fernandez-del Castillo, C. Pancreatic carcinoma. *N Engl J Med.* 1992;326:455-465.
2. Onkendi, EO, Boostrom, SY, Sarr, MG et al. 15-year experience with surgical treatment of duodenal carcinoma: a comparison of periampullary and extra-ampullary duodenal carcinomas. *J Gastrointest Surg.* 2012;16:682-691.
3. Almoguera, C, Shibata, D, Forrester, K et al. Most human carcinomas of the exocrine pancreas contain mutant c-K-ras genes. *Cell.* 1988;53:549-554.
4. Hingorani, SR, Wang, L, Multani, AS et al. Trp53R172H and KrasG12D cooperate to promote chromosomal instability and widely metastatic pancreatic ductal adenocarcinoma in mice. *Cancer Cell.* 2005;7:469-483.
5. Olive, KP, Tuveson, DA. The use of targeted mouse models for preclinical testing of novel cancer therapeutics. *Clin Cancer Res.* 2006;12:5277-5287.
6. Rukstalis, JM, Habener, JF. *snail2*, a mediator of epithelial-mesenchymal transitions, expressed in progenitor cells of the developing endocrine pancreas. *Gene Expr Patterns.* 2007;7:471-479.
7. Peinado, H, Olmeda, D, Cano, A. *snail*, *Zeb* and *bHLH* factors in tumor progression: an alliance against the epithelial phenotype? *Nat Rev Cancer.* 2007;7:415-428.
8. Polyak, K, Weinberg, RA. Transitions between epithelial and mesenchymal states: acquisition of malignant and stem cell traits. *Nat Rev Cancer.* 2009;9:265-273.
9. Hotz, B, Arndt, M, Dullat, S et al. Epithelial to mesenchymal transition: expression of the regulators *snail*, *slug*, and *twist* in pancreatic cancer. *Clin Cancer Res.* 2007;13:4769-4776.
10. Rhim, AD, Mirek, ET, Aiello, NM et al. EMT and dissemination precede pancreatic tumor formation. *Cell.* 2012;148:349-361.
11. Hashimoto, Y, Kim, DJ, Adams, JC. The roles of fascins in health and disease. *J Pathol.* 2011;224:289-300.
12. Machesky, LM, Li, A. Fascin: Invasive filopodia promoting metastasis. *Commun Integr Biol.* 2010;3:263-270.
13. Yamakita, Y, Matsumura, F, Yamashiro, S. Fascin1 is dispensable for mouse development but is favorable for neonatal survival. *Cell Motil Cytoskeleton.* 2009;66:524-534.

ACCEPTED MANUSCRIPT

14. Li, A, Dawson, JC, Forero-Vargas, M et al. The actin-bundling protein fascin stabilizes actin in invadopodia and potentiates protrusive invasion. *Curr Biol*. 2010;20:339-345.
15. Schoumacher, M, Louvard, D, Vignjevic, D. Cytoskeleton networks in basement membrane transmigration. *Eur J Cell Biol*. 2011;90:93-99.
16. Kim, MY, Oskarsson, T, Acharyya, S et al. Tumor self-seeding by circulating cancer cells. *Cell*. 2009;139:1315-1326.
17. De Arcangelis, A, Georges-Labouesse, E, Adams, JC. Expression of fascin-1, the gene encoding the actin-bundling protein fascin-1, during mouse embryogenesis. *Gene Expr Patterns*. 2004;4:637-643.
18. Zhang, FR, Tao, LH, Shen, ZY et al. Fascin expression in human embryonic, fetal, and normal adult tissue. *J Histochem Cytochem*. 2008;56:193-199.
19. Massague, J. TGFbeta in Cancer. *Cell*. 2008;134:215-230.
20. **Wagner, KW, Punnoose, EA, Januario, T et al.** Death-receptor O-glycosylation controls tumor-cell sensitivity to the proapoptotic ligand Apo2L/TRAIL. *Nat Med*. 2007;13:1070-1077.
21. Batlle, E, Sancho, E, Franci, C et al. The transcription factor snail is a repressor of E-cadherin gene expression in epithelial tumor cells. *Nat Cell Biol*. 2000;2:84-89.
22. Burleson, KM, Casey, RC, Skubitz, KM et al. Ovarian carcinoma ascites spheroids adhere to extracellular matrix components and mesothelial cell monolayers. *Gynecol Oncol*. 2004;93:170-181.
23. Burleson, KM, Hansen, LK, Skubitz, AP. Ovarian carcinoma spheroids disaggregate on type I collagen and invade live human mesothelial cell monolayers. *Clin Exp Metastasis*. 2004;21:685-697.
24. Iguchi, T, Aishima, S, Umeda, K et al. Fascin expression in progression and prognosis of hepatocellular carcinoma. *J Surg Oncol*. 2009;100:575-579.
25. Okada, K, Shimura, T, Asakawa, K et al. Fascin expression is correlated with tumor progression of extrahepatic bile duct cancer. *Hepatogastroenterology*. 2007;54:17-21.
26. Maitra, A, Iacobuzio-Donahue, C, Rahman, A et al. Immunohistochemical validation of a novel epithelial and a novel stromal marker of pancreatic ductal adenocarcinoma identified by global expression microarrays: sea urchin fascin homolog and heat shock protein 47. *Am J Clin Pathol*. 2002;118:52-59.

ACCEPTED MANUSCRIPT

27. Maitra, A, Adsay, NV, Argani, P et al. Multicomponent analysis of the pancreatic adenocarcinoma progression model using a pancreatic intraepithelial neoplasia tissue microarray. *Mod Pathol.* 2003;16:902-912.
28. Tsai, WC, Chao, YC, Sheu, LF et al. EMMPRIN and fascin overexpression associated with clinicopathologic parameters of pancreatobiliary adenocarcinoma in Chinese people. *APMIS.* 2007;115:929-938.
29. Yamaguchi, H, Inoue, T, Eguchi, T et al. Fascin overexpression in intraductal papillary mucinous neoplasms (adenomas, borderline neoplasms, and carcinomas) of the pancreas, correlated with increased histological grade. *Mod Pathol.* 2007;20:552-561.
30. Vignjevic, D, Schoumacher, M, Gavert, N et al. Fascin, a novel target of beta-catenin-TCF signaling, is expressed at the invasive front of human colon cancer. *Cancer Res.* 2007;67:6844-6853.
31. White, BD, Chien, AJ, Dawson, DW. Dysregulation of Wnt/beta-catenin signaling in gastrointestinal cancers. *Gastroenterology.* 2012;142:219-232.
32. Mani, SA, Guo, W, Liao, MJ et al. The epithelial-mesenchymal transition generates cells with properties of stem cells. *Cell.* 2008;133:704-715.
33. Ma, Y, Reynolds, LE, Li, A et al. Fascin 1 is dispensable for developmental and tumor angiogenesis. *Biol Open.* 2013;2:1187-1191.
34. Alexander, S, Koehl, GE, Hirschberg, M et al. Dynamic imaging of cancer growth and invasion: a modified skin-fold chamber model. *Histochem Cell Biol.* 2008;130:1147-1154.
35. Itoh, K, Yoshioka, K, Akedo, H et al. An essential part for Rho-associated kinase in the transcellular invasion of tumor cells. *Nat Med.* 1999;5:221-225.
36. Iwanicki, MP, Davidowitz, RA, Ng, MR et al. Ovarian cancer spheroids use myosin-generated force to clear the mesothelium. *Cancer Discov.* 2011;1:144-157.
37. Morton, JP, Jamieson, NB, Karim, SA et al. LKB1 haploinsufficiency cooperates with Kras to promote pancreatic cancer through suppression of p21-dependent growth arrest. *Gastroenterology.* 2010;139:586-97, 597.e1-6.
38. Morton, JP, Karim, SA, Graham, K et al. Dasatinib inhibits the development of metastases in a mouse model of pancreatic ductal adenocarcinoma. *Gastroenterology.* 2010;139:292-303.

ACCEPTED MANUSCRIPT

39. Jimeno, A, Tan, AC, Coffa, J et al. Coordinated epidermal growth factor receptor pathway gene overexpression predicts epidermal growth factor receptor inhibitor sensitivity in pancreatic cancer. *Cancer Res.* 2008;68:2841-2849.
40. Pei, H, Li, L, Fridley, BL et al. FKBP51 affects cancer cell response to chemotherapy by negatively regulating Akt. *Cancer Cell.* 2009;16:259-266.
41. Badea, L, Herlea, V, Dima, SO et al. Combined gene expression analysis of whole-tissue and microdissected pancreatic ductal adenocarcinoma identifies genes specifically overexpressed in tumor epithelia. *Hepatogastroenterology.* 2008;55:2016-2027.

*Author names in bold designate shared co-first authorship

Figure 1

[Click here to download high resolution image](#) ACCEPTED MANUSCRIPT

Li_Figure 1

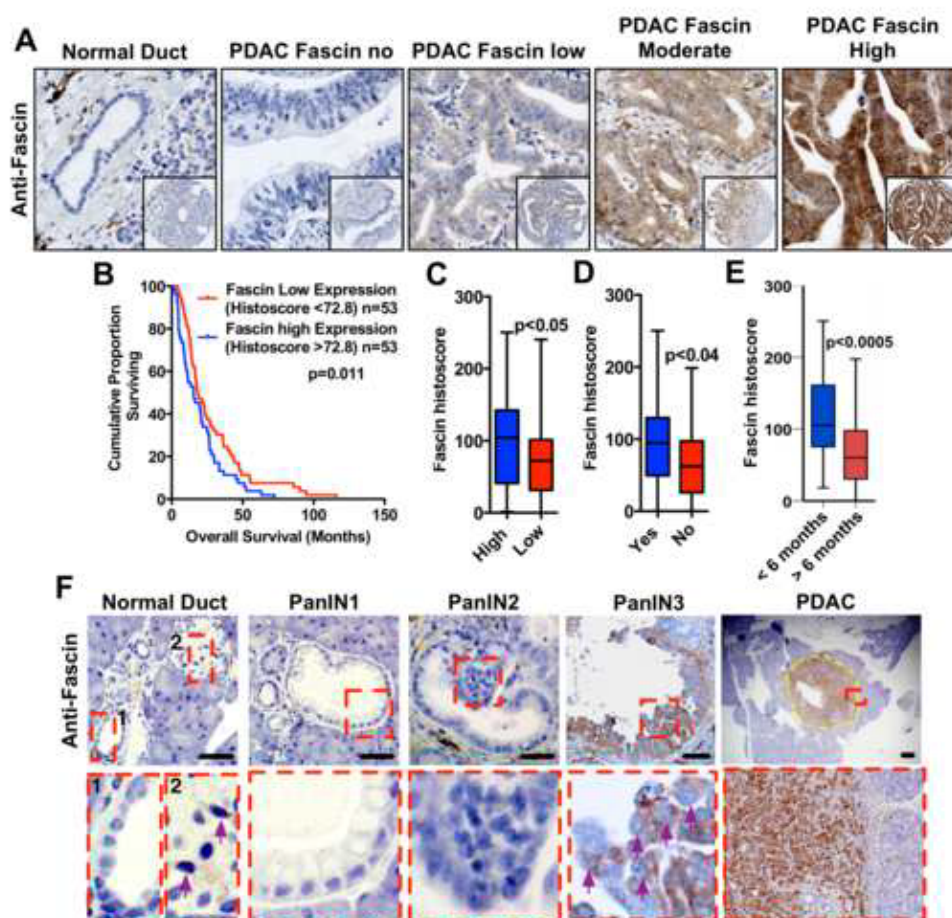


Figure 2

[Click here to download high resolution image](#)

ACCEPTED MANUSCRIPT

LI_Figure 2

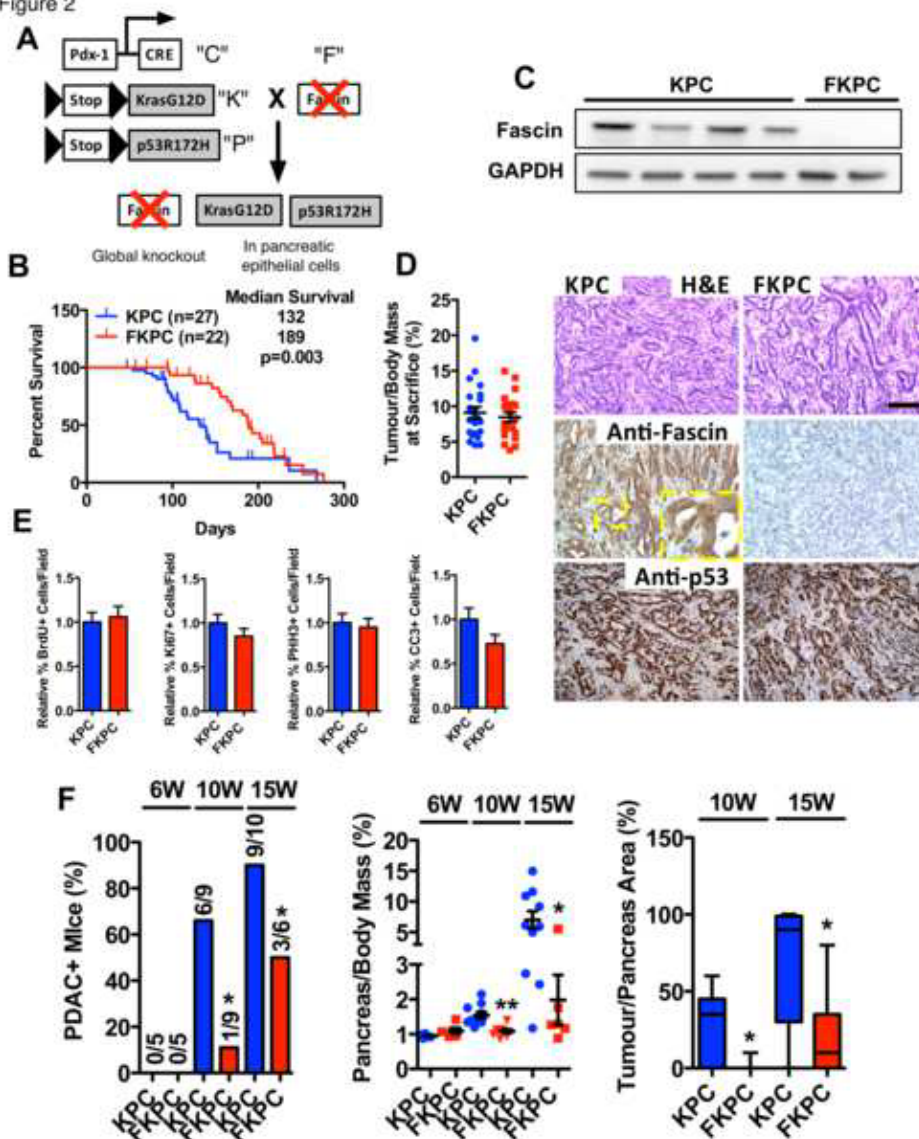


Figure 3

[Click here to download high resolution image](#)

ACCEPTED MANUSCRIPT

Li_Figure 3

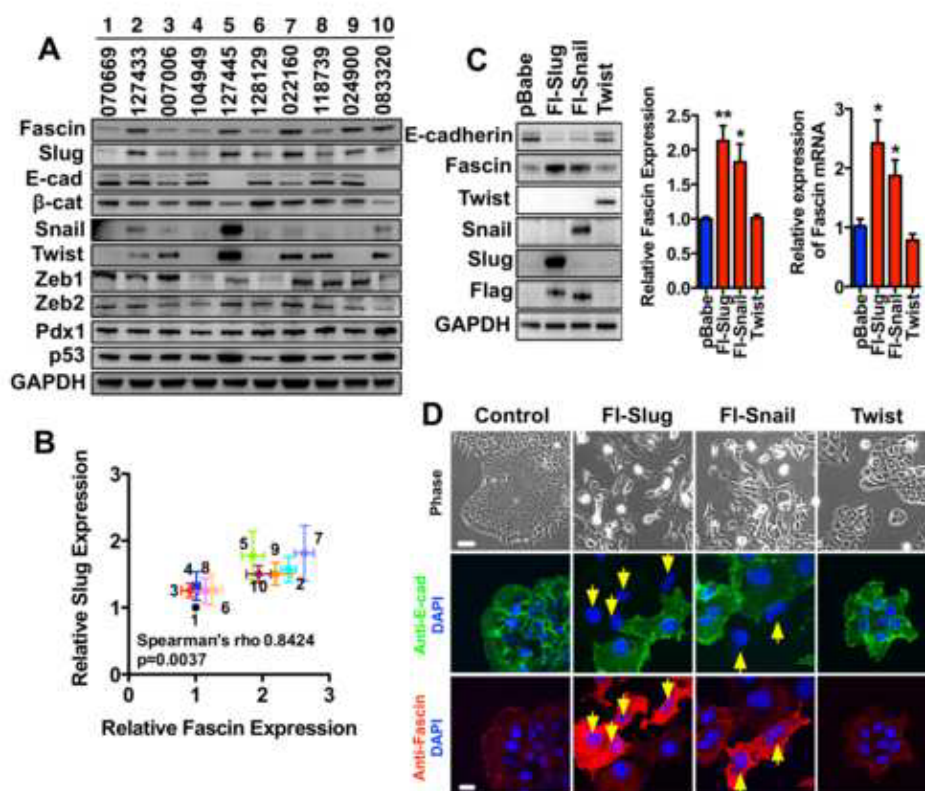


Figure 4

[Click here to download high resolution image](#)

ACCEPTED MANUSCRIPT

LI_Figure 4

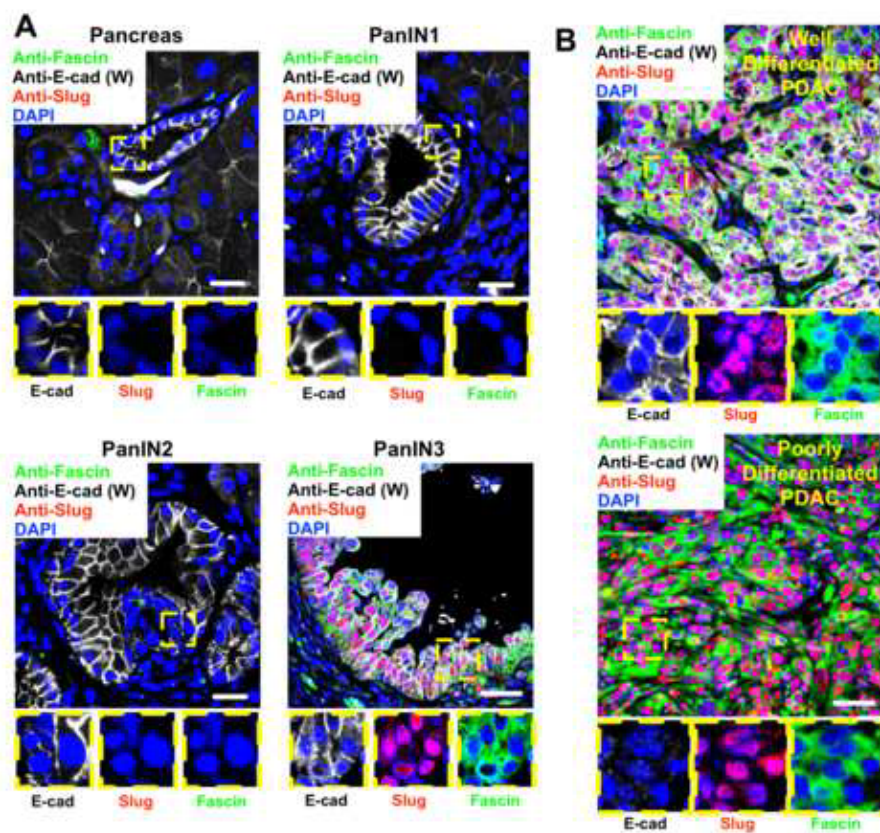


Figure 5

[Click here to download high resolution image](#) ACCEPTED MANUSCRIPT

LI_Figure 5

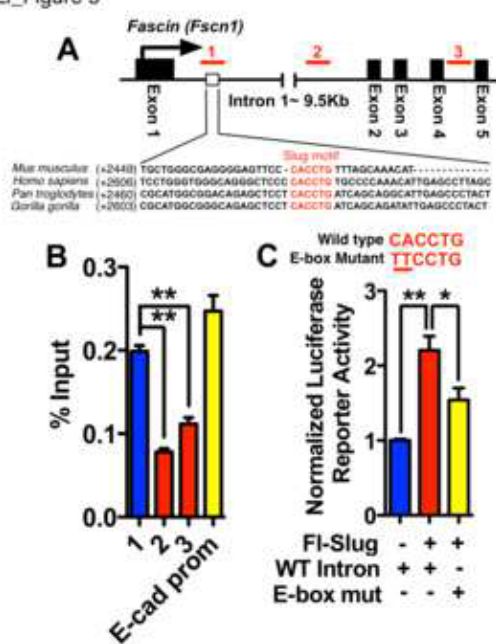


Figure 6
[Click here to download high resolution image](#) ACCEPTED MANUSCRIPT

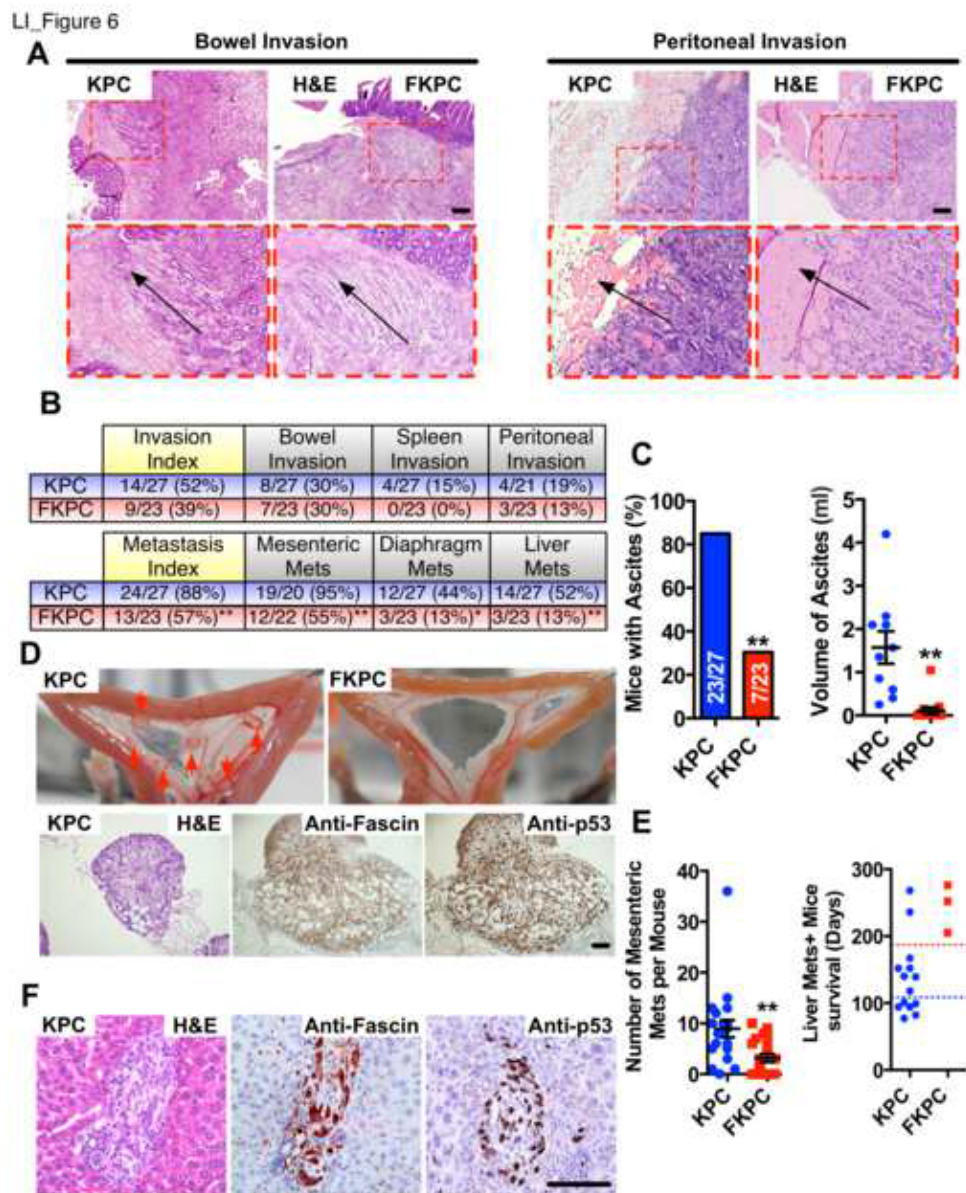


Figure 7

[Click here to download high resolution image](#)

ACCEPTED MANUSCRIPT

Li_Figure 7

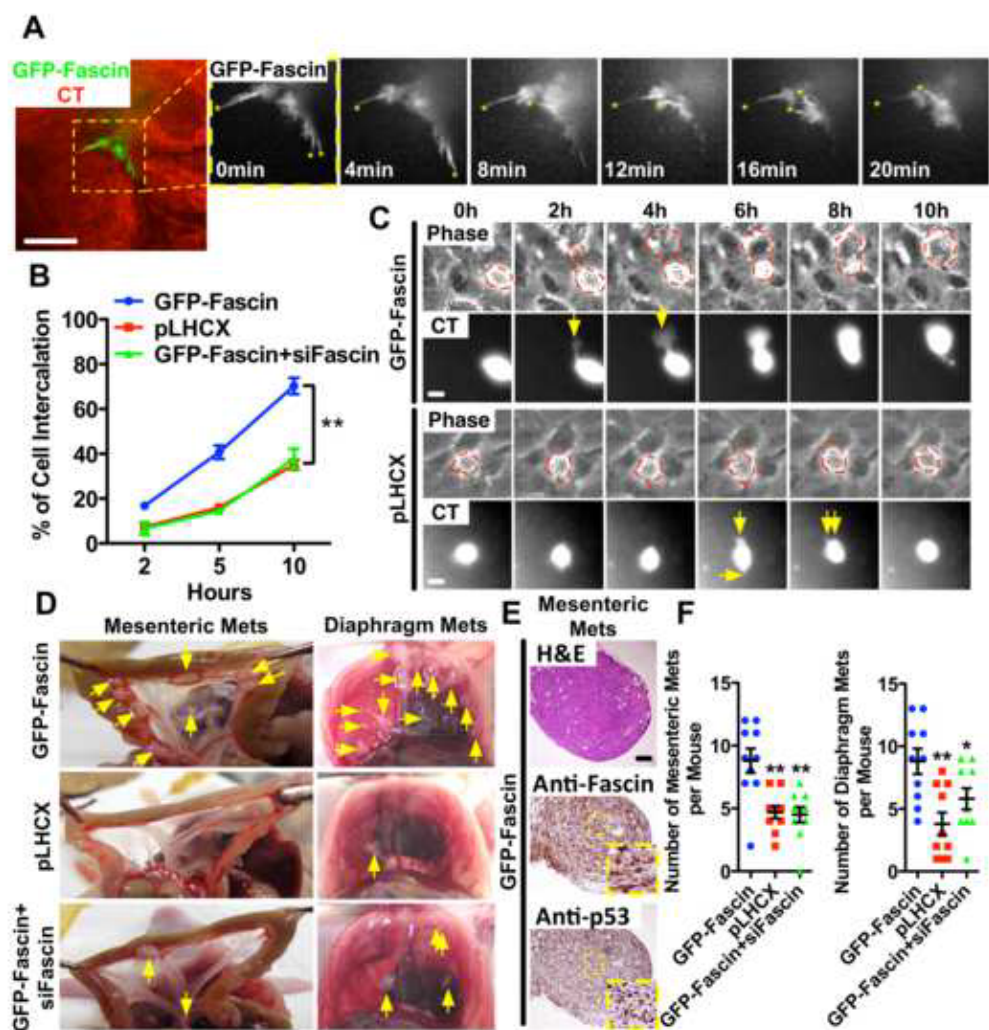
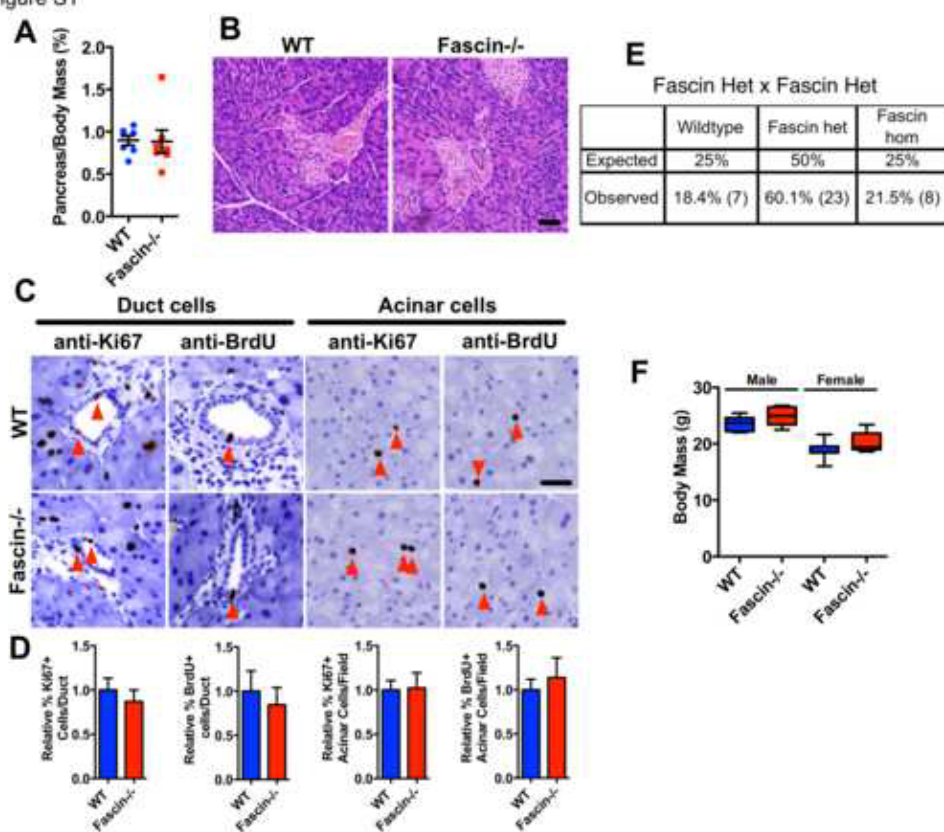


Figure S1

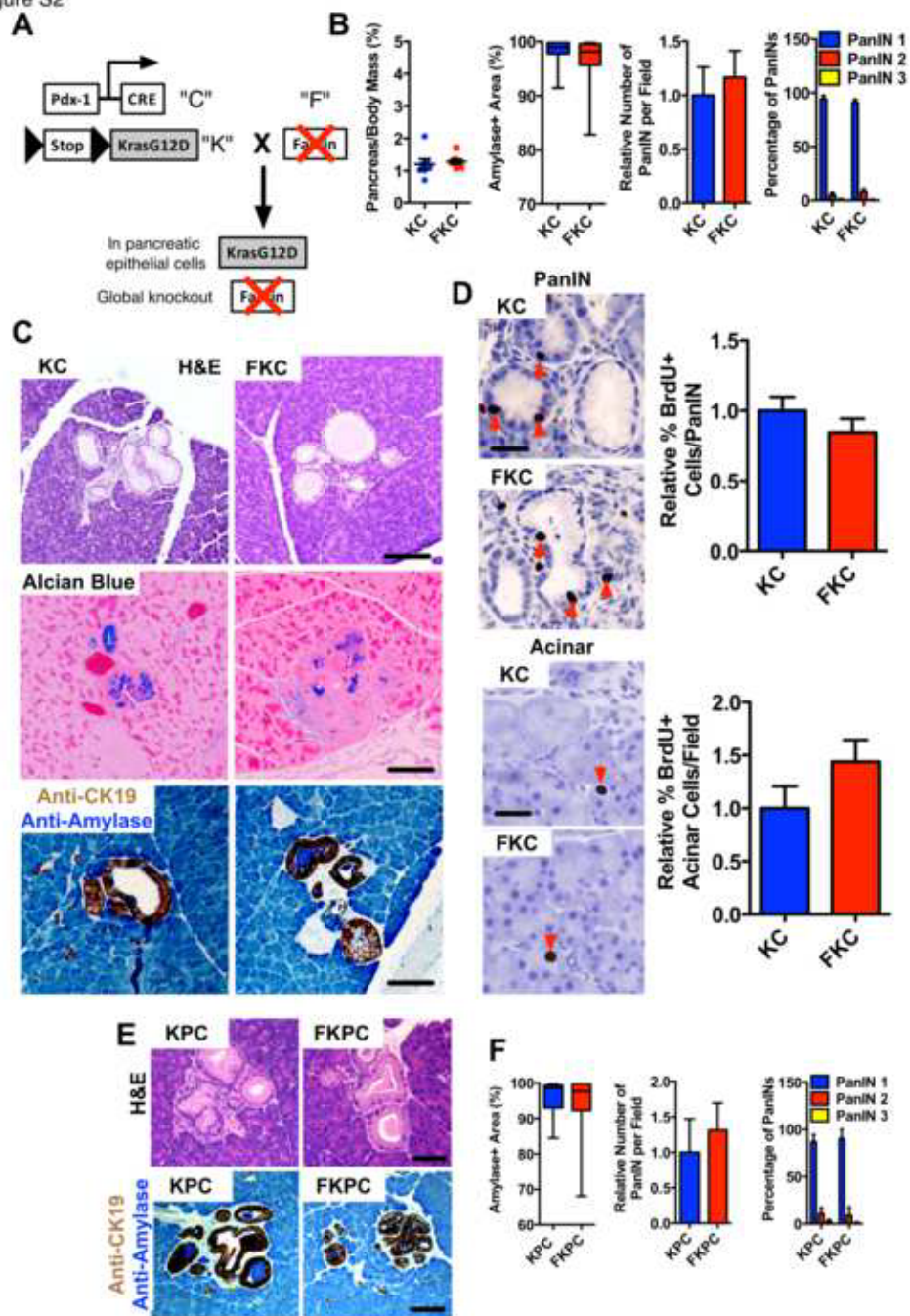


Supplementary Figure 2

[Click here to download high resolution image](#)

ACCEPTED MANUSCRIPT

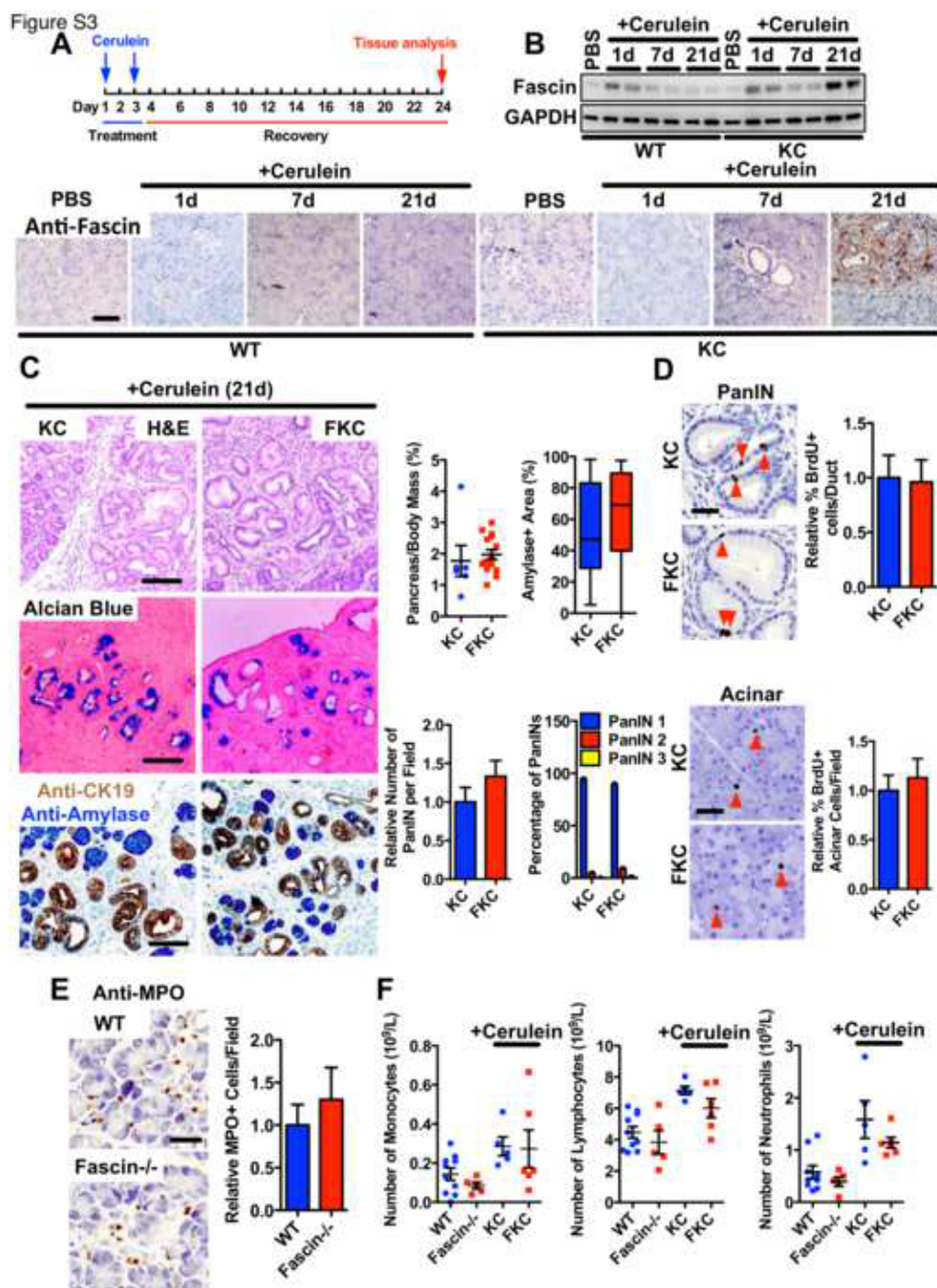
Figure S2



Supplementary Figure 3

[Click here to download high resolution image](#)

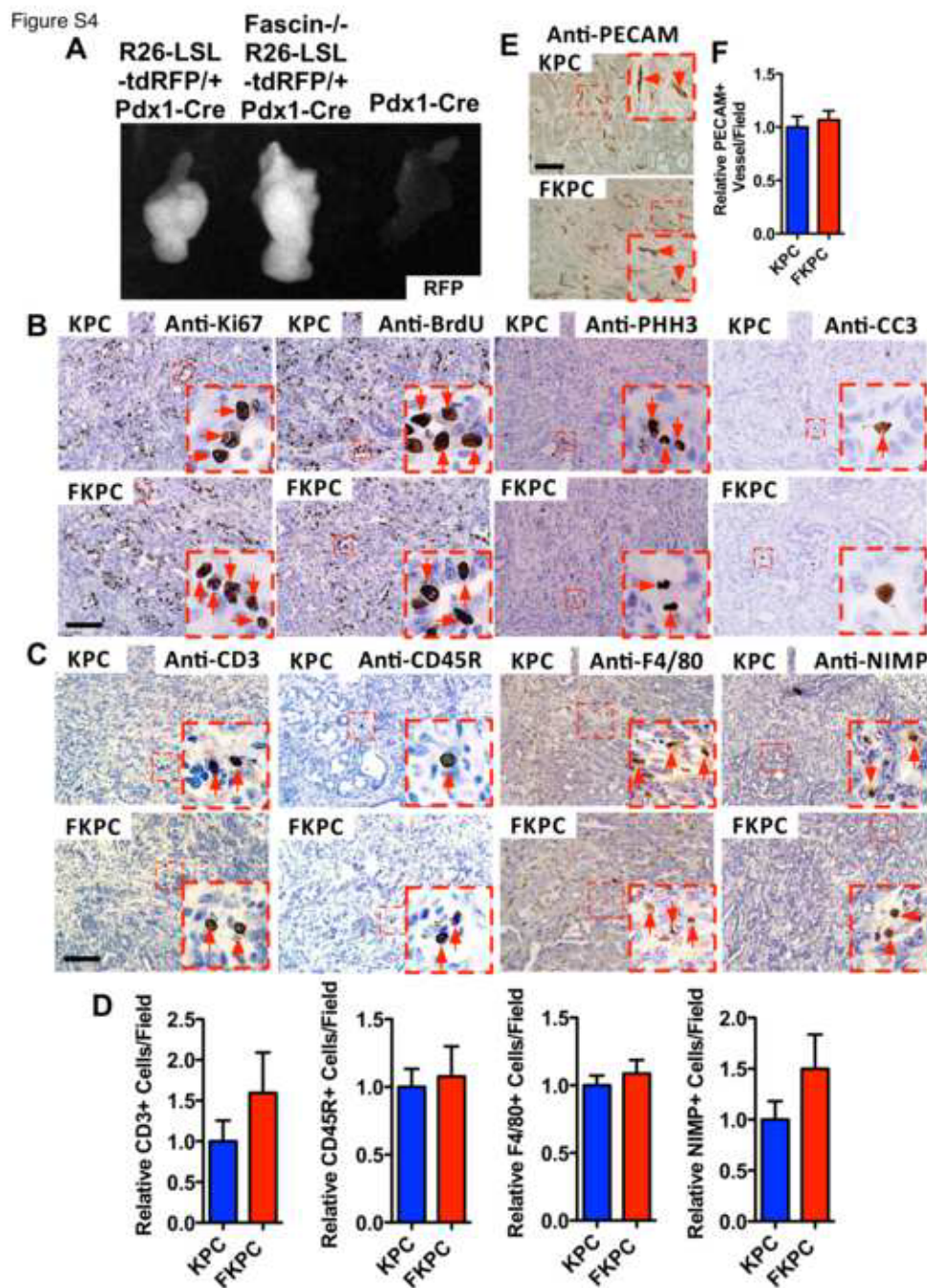
ACCEPTED MANUSCRIPT



Supplementary Figure 4

[Click here to download high resolution image](#)

ACCEPTED MANUSCRIPT

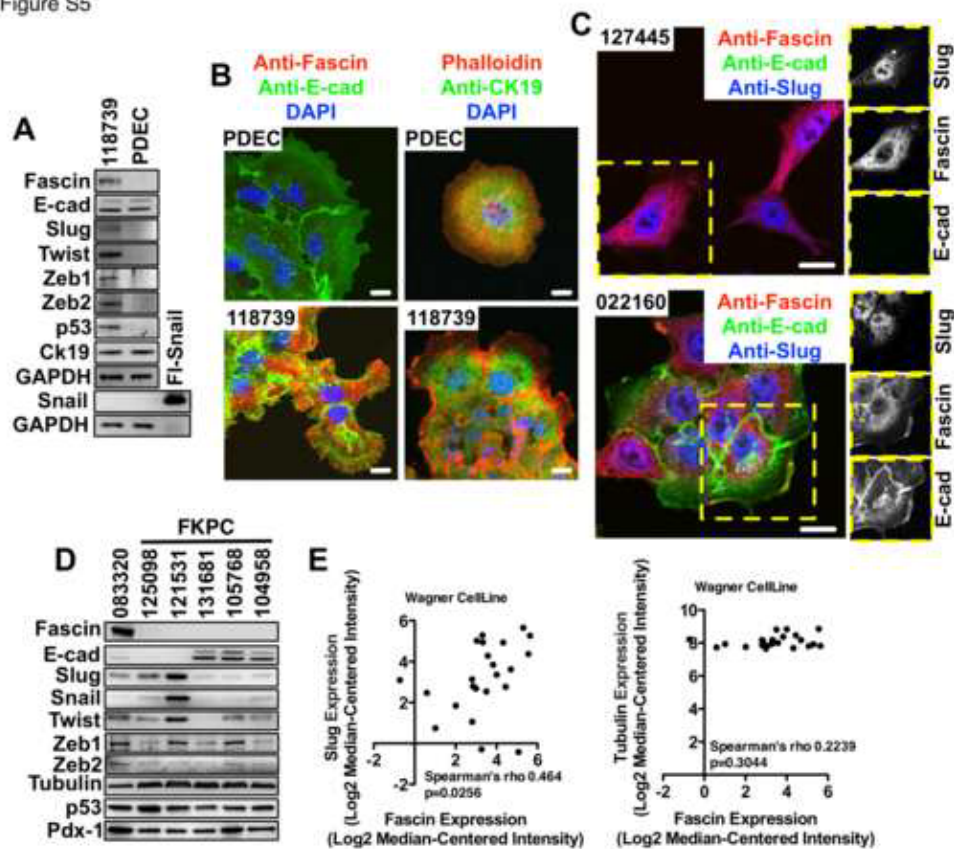


Supplementary Figure 5

[Click here to download high resolution image](#)

ACCEPTED MANUSCRIPT

Figure S5

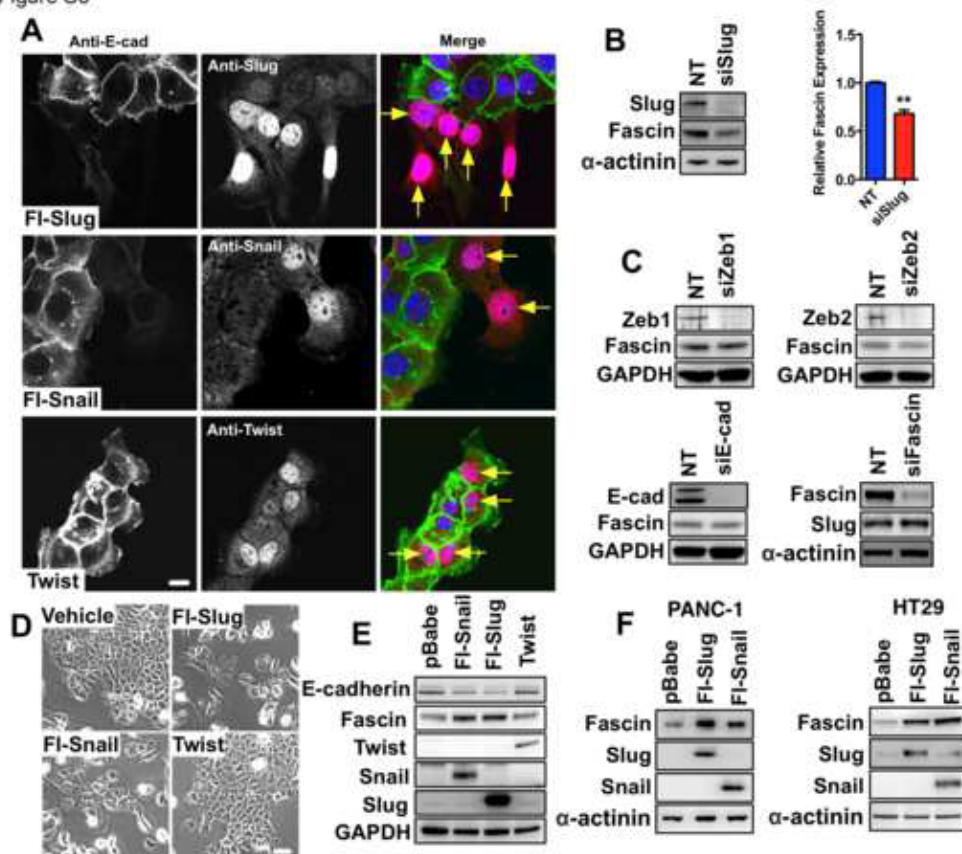


Supplementary Figure 6

[Click here to download high resolution image](#)

ACCEPTED MANUSCRIPT

Figure S6

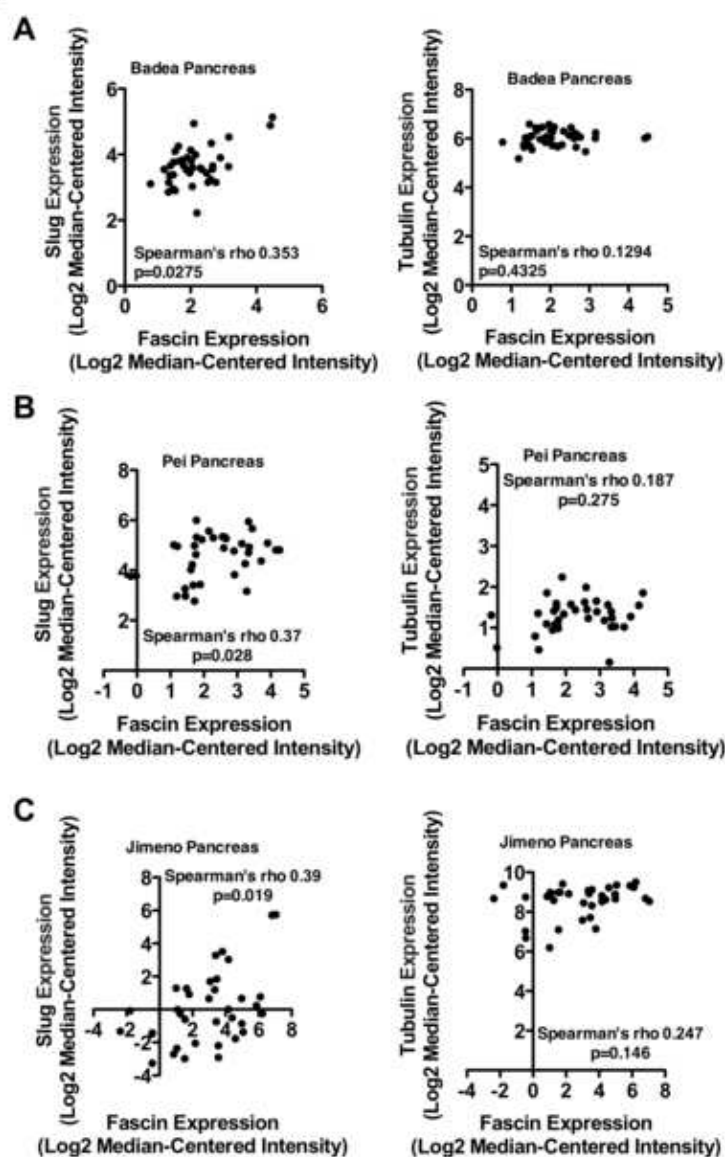


Supplementary Figure 7

[Click here to download high resolution image](#)

ACCEPTED MANUSCRIPT

Figure S7



Supplementary Figure 8

[Click here to download high resolution image](#)

ACCEPTED MANUSCRIPT

Figure S8

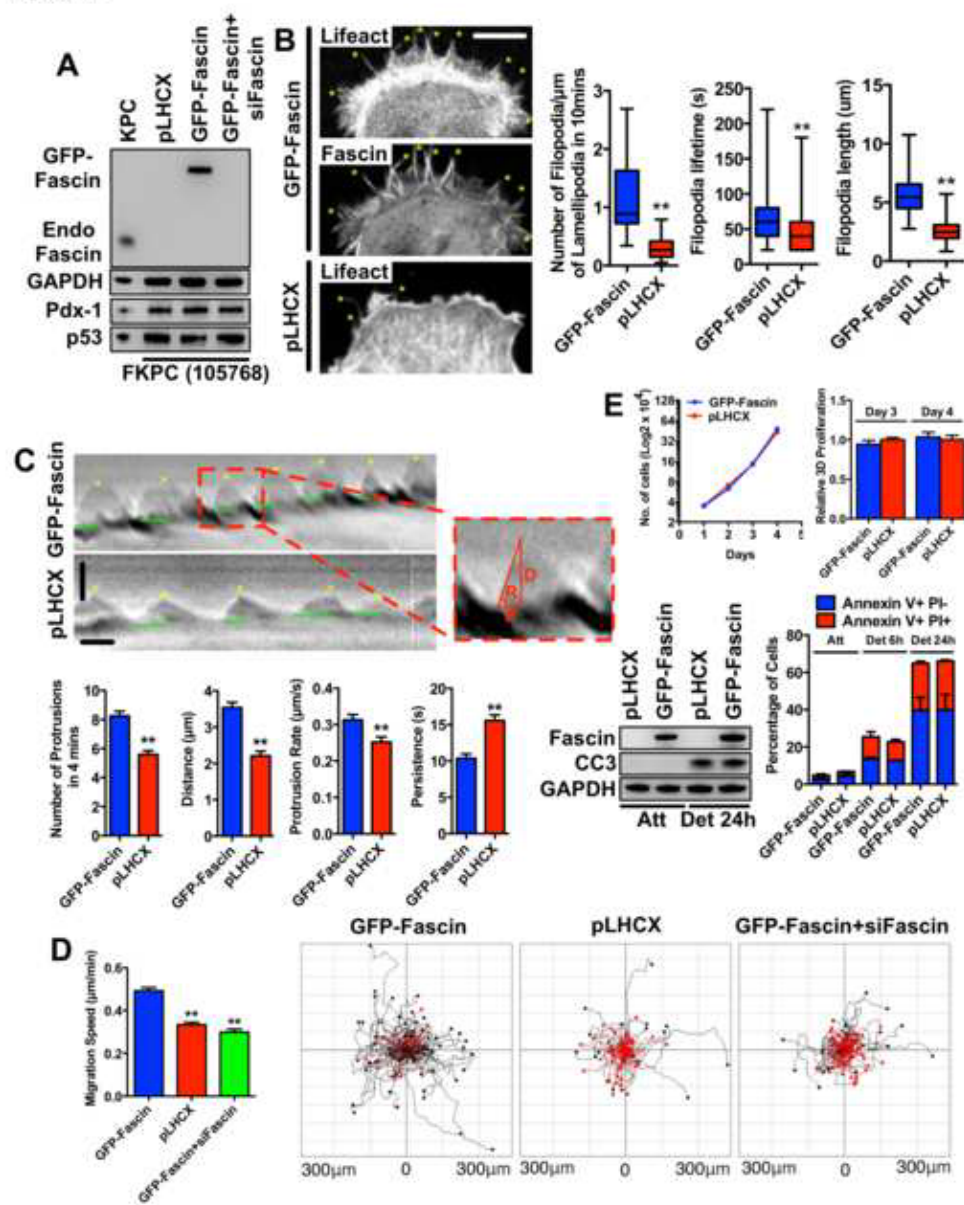
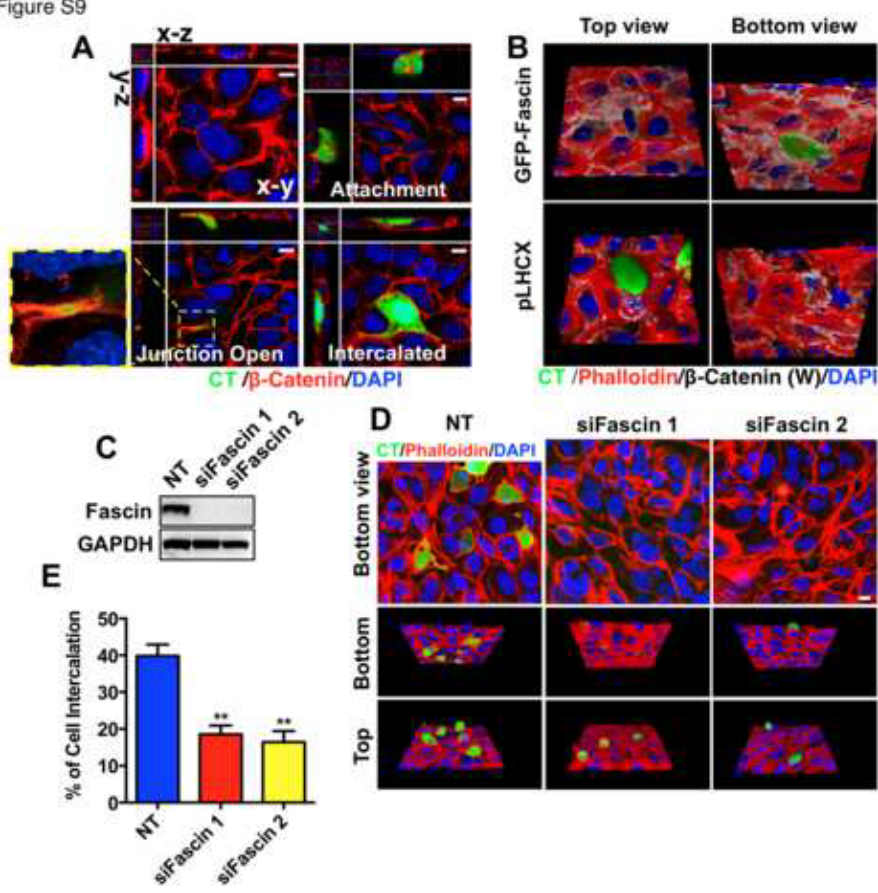


Figure S9



Supplementary Table 1

[Click here to download Supporting Document: Supplementary Table 1.doc](#)

ACCEPTED MANUSCRIPT

Table 1. Multivariate Cox Regression Analysis of Association of Fascin and Clinicopathological Parameters with Overall Survival

	Hazard Ratio	95% CI	p-value
Fascin (below v above median histoscore)	0.663	0.440 – 1.000	0.05
T-stage (T2 v T3)	0.572	0.309 – 1.059	0.076
Grade (low v high)	0.574	0.374 – 0.882	0.011
Resection margin status (negative v positive)	0.634	0.398 – 1.010	0.055
Lymphnode status (negative v positive)	0.588	0.349 – 0.992	0.046

CI, confidence interval.

Supplementary Table 2

[Click here to download Supporting Document: Supplementary Table 2.doc](#)**Supplementary Table 2. Percentage of Fascin Positive Lesions in KPC Mice**

Grade	Fascin⁺ Lesions (%)	Total
PanIN 1	0	100
PanIN 2	0	70
PanIN 3	4 (6%)	65
PDAC	20 (100%)	20

Percentage of each type of lesion from KPC mice having at least one fascin positive cell. Data were collected from eight 10w old KPC mice for PanINs and twenty KPC mice with tumours for PDACs

Supplementary Table 3

[Click here to download Supporting Document: Supplementary Table 3.pdf](#)

ACCEPTED MANUSCRIPT

Supplementary Table 3. Results of whole blood pancreatic function tests on normal and fascin knockout mice.

	WT				Fascin ^{-/-}				
Mouse ID	101500	110147	110148	101494	107636	114542	114544	101495	110145
Sex	F	M	M	M	M	M	M	M	M
Age (days)	115	73	73	115	90	54	54	115	73
Weight (g)	21.65	25.58	23.39	25.78	25.74	23.1	16.25	27.05	22.81
Glucose (mmol/l)	12.9	12.9	13.8	10.9	12.7	14	12.4	11.6	11.4
Pancreatic Profile									
Urea (mmol/l)	7.3	7.7	7	7.9	8.1	6.6	7.2	10.4	8.9
Creatinine(umol/l)	31	32	31	30	31	32	28	29	30
Triglyceride (mmol/l)	1.11	1.16	1.18	1.04	2.6	1.24	1.08	0.91	0.92
Amylase (U/l)	1028	2766	2415	2534	2629	2599	2047	2381	2543
Lipase (U/l)	78	158	72	74	75	190	71	79	90

Supplementary Information

[Click here to download Supporting Document: Supplementary Material Li 2ndRev v1.doc](#)

ACCEPTED MANUSCRIPT

Supplementary Material Li et al.**Fascin is Regulated by Slug, Promotes Progression of Pancreatic Cancer in Mice, and is Associated with Patient Outcome****Supplemental Data**

Figure S1: Fascin deficient mice have normal pancreas morphology and normal survival rate. (A) Dot plot of pancreas-to-body weight ratios in wild type and fascin deficient mice at 5w. (B) Histology analysis of H&E stained sections from pancreas of 5w control or fascin deficient mice. Representative Images (C) and quantification (D) of BrdU+ or Ki67+ duct cells (left) and acinar cells (right) in pancreata from 5w control and fascin deficient mice measured by IHC. Red arrows indicate BrdU or Ki67 positive nuclei. (n=4 mice per genotype). (E) Mendelian segregation of pups at weaning (3w). 6 litters from crosses between fascin heterozygous males and females in a mixed background were recorded. (F) Body mass of control and fascin deficient mice in a mixed background at 8w. At least 5 mice were measured for each genotype and gender. Scale Bars: (B, C) 50µm.

Figure S2 Fascin is not required for PanIN formation (A) Gene targeting strategy for generating *fascin*^{-/-}, *KRas*^{G12D} *Pdx1-Cre* (FKC). (B) Quantitation of spontaneous (4m) PanIN formation in KC and FKC mice. (left) Dot plot of measurements of pancreas-to-body weight ratios. (middle) Box plot of amylase-positive area (Lower quartile, median, and upper quartile are shown). (right two bar graphs) Relative number and percentage of PanINs of grade 1-3 per histopathological section of pancreas (Data are shown as mean±SEM) (n=6 mice per genotype). (C) Panels show tissue sections with spontaneous PanIN in FKC compared to KC mice- H&E (top), alcian blue (middle) and dual IHC for CK19 (brown) and amylase (blue) (bottom). (D) Images and quantification of BrdU incorporation assay measured by IHC in duct cells (Top) and acinar cells (bottom) in 4 months KC and FKC pancreas. Red arrows indicate BrdU positive nuclei (n=4 mice per genotype). (E) Panels show spontaneous PanIN formation in 6w FKPC or KPC mice, with H&E (top) and dual IHC for CK19 (brown) and amylase (blue) (bottom). (F) Quantitation of spontaneous (6w) PanIN formation in KPC and FKPC mice. (left) Box plot

of amylase-positive area (Lower quartile, median, and upper quartile are shown). (right two bar graphs) Number and percentage of PanINs of grade 1-3 per histopathological section of pancreas (Data are shown as mean \pm SEM) (n=5 mice per genotype). Scale bars: (C, E) 100 μ m, (D) 50 μ m.

Figure S3: Fascin is not required for acute pancreatitis induced PanIN formation. (A) Protocol used for cerulein-induced PanIN formation in KC and FKC mice. (B) Western blot (top) and IHC analysis (bottom) of fascin expression in control and KC mice after PBS or cerulein treatments (1d, 7d and 21d post-cerulein). (C) Left: Panels show cerulein-induced (21d post-cerulein) PanIN formation in FKC compared to KC mice, shown by H&E (top), Alcian Blue (middle) and dual IHC for CK19 (brown) and amylase (blue) (bottom). Right: Quantitation of cerulein-induced (21d post-cerulein) PanIN formation in KC and FKC mice. Graphs describe the following as indicated: Dot plot of pancreas-to-body mass ratios (n=6 for KC, n=15 for FKC mice); Box plot of amylase-positive area (Lower quartile, median, and upper quartile are shown); Relative number of PanIN per field and percentage of PanINs of grade 1-3 per histopathological section of pancreas (Data are shown as mean \pm SEM) (n=6 mice per genotype). (D) Images and quantification of BrdU incorporation assay measured by IHC in duct cells (top) and acinar cells (bottom) in KC and FKC pancreas 21d post-cerulein injection. BrdU positive nuclei are red arrowed (n=4 mice per genotype). (E) Quantification of neutrophil (anti-myeloperoxidase (MPO)) recruitment to normal and fascin deficient pancreas 1 day after cerulein injection. (Data are shown as mean \pm SEM, n=4 mice per genotype). (F) Dot plots of whole blood counts from 6w control and fascin deficient mice 21d post cerulein injection. (left) Monocytes, (middle) Lymphocytes and (right) Neutrophils are shown. (Data are shown as mean \pm SEM). Scale Bars: (B, C) 100 μ m, (D, E) 50 μ m.

Figure S4: Tumor-intrinsic action of fascin. (A) Pancreata from Rosa26-LSL-tdRFP/+ Pdx1-Cre, fascin^{-/-} Rosa26-LSL-tdRFP/+ Pdx1-Cre and Pdx1-

ACCEPTED MANUSCRIPT

Cre mice were analyzed using an OV100 in vivo imaging system. RFP signaling is detected in whole pancreata from Rosa26-LSL-tdRFP/+ Pdx1-Cre and fascin^{-/-} Rosa26-LSL-tdRFP/+ Pdx1-Cre mice, but not in pancreata from mice only expressing Pdx1-Cre. (B) Representative images of immunohistochemical staining for Ki67, 2h BrdU pulse, phospho-histone H3 (PHH3) and cleaved caspase-3 (CC3). Quantitations were shown in Figure 3F-I. Images (C) and quantifications (D) of infiltration of B cells (CD45R), T cells (CD3), macrophages (F4/80) and neutrophils (NIMP) into tumors. At least 16 medium-powered fields from four KPC and FKPC PDACs were analyzed (Data are shown as mean \pm SEM.) (E) Immunohistochemical visualization of PECAM (CD31) in tumors in KPC and FKPC mice. (F) Quantification of D, no significant difference in vascularization. (Data are shown as mean \pm SEM. N=4 mice from each genotype). Scale bars: 100 μ m.

Figure S5: Slug signaling regulates fascin expression in PDAC cells. (A) Western blot analysis of fascin and EMT markers in primary ductal epithelial cells (PDEC) isolated from the pancreas of a wild type mouse and a PDAC cell line 118739 harvested from a KPC mouse. Expression of CK-19 in the cell lines confirms their ductal origin and p53 in 118739 cell line confirms its PDAC origin. Flag-snail was used as positive control for snail antibody. GAPDH, loading control. (B) Immunofluorescence microscopy analysis of PDEC and 118739 PDAC cells stained for the indicated proteins. (C) Representative images of example of E-cadherin negative (127445) and E-cadherin positive (022160) PDAC cells stained for fascin, E-cadherin and Slug. Co-expression of slug and E-cadherin in 022160 PDAC cells suggest partial EMT. Inserts show individual channels (D) Expression of EMT markers in a representative panel of 5 independent FKPC PDAC cell lines. 083320 PKC PDAC cell line was used as positive control for fascin. (E) Spearman correlation analysis of (left) fascin and slug and (right) fascin and tubulin gene expression in human pancreatic cancer cell lines using Wagner Cell Line data set. As a control, fascin does not correlate with tubulin expression. Scale Bars: (B, C) 10 μ m.

Figure S6: Slug is an important regulator of fascin expression. (A) Immunofluorescence microscopy analysis of 070669 PDAC cells transduced with vector (control), Flag-slug, Flag-snail and twist and stained for the proteins as indicated. Slug, snail and twist overexpressing cells are yellow arrowed. (B) Western blots (left) and quantitation (right) of proteins as indicated with 070669 PDAC cells treated with slug siRNA (Data are shown as mean \pm SEM). ** $p < 0.01$ by Student's t-test. Loading control: α -actinin. (C) Western blot analysis of proteins as indicated with 070669 PDAC cells treated with Zeb1 (top left), Zeb2 (top right), E-cadherin (bottom left) and fascin (bottom right) siRNA. GAPDH and α -actinin, loading controls as indicated. (D) Phase contrast images of 061843 PDAC cells transduced with vector (control), Flag-slug, Flag-snail and twist as indicated. (E) Western blot analysis with control, Flag-slug, Flag-snail and twist expressing 061843 PDAC cells for proteins as indicated. α -actinin, loading control. (F) Western blot analysis with control, Flag-slug, Flag-snail expressing PANC-1 (left) and HT29 (right) human pancreatic and colon cancer cells for proteins as indicated. Loading control: α -actinin Scale Bars: (A) 10 μ m (D) 50 μ m.

Figure S7: Slug correlates with fascin in human pancreatic cancer Spearman correlation analysis of fascin and slug (left) or tubulin (right) gene expression in human pancreatic cancer using the Badea data set (A), Pei data set (B) and Jimeno data set (C). Fascin correlation with tubulin was used as a control.

Figure S8: Fascin regulates lamellipodia dynamics and migration but not cell proliferation. (A) Western blots of 105768 FKPC mouse PDAC cells expressing control vector (pLHCX), human GFP-fascin and fascin siRNA treated rescue cells. GAPDH loading control. (B) Left: Control vector and GFP-fascin expressing FKPC 105768 cells expressing RFP or GFP-lifeact. Yellow stars indicate filopodia. Bar graphs show box plots of quantifications as indicated. ** $p < 0.01$ by Student's t-test. (C) Top: Representative kymograph

pictures of GFP-fascin rescued and fascin deficient PDAC cells (Derived from Movie 2). Green lines indicate persistence time for each protrusion, yellow stars indicate each protrusion. Pixel intensities along a 1-pixel wide line were used to generate the kymograph from the corresponding Movie 2; a magnified region (outlined in red) is displayed on the top. Red lines indicate the parameters for one protrusion. Abbreviations are as follows: D, protrusion distance; P, protrusion persistence; and R, protrusion rate. Bottom Bar Graphs: Frequency of lamellipodial protrusion events, distance, protrusion rate and persistence of individual lamellipodial protrusions. Values are averages of means from at least 30 cells (Data are shown as mean \pm SEM). **p<0.01 by Student's t-test. (D) Left: Migration speed of 105768 cells expressing **vectors/siRNA as indicated**. More than 300 cells from three experiments were randomly selected and mean migration speed over 6hr was plotted according to frequency in the population. **p < 0.01 by t test. Right: 6 hr tracks of individual cell migration, black tracks migrated faster than 0.5 μ m/min, red indicates slower. (E) Top left: 2D proliferation assay, no difference between control vector and GFP-fascin expressing FKPC 105768 cells. (n=3). Top right: 3D collagen I cell proliferation assay, no difference between control vector and GFP-fascin expressing FKPC 105768 cells. (Data are shown as mean \pm SEM, n=3). Bottom left: Western blot analysis of the effects on the viability of control vector and GFP-fascin expressing FKPC 105768 cells grown in normal culture plates and Ultra low attachment plate for 24 h to induce anoikis with cleaved-caspase3 antibody. Bottom right: FACS analysis using annexin V and propidium iodide for cells undergoing anoikis with control vector and GFP-fascin expressing FKPC 105768 cells cultured in ultra-low attachment plate for 6 and 24 hours, attached cells were used as negative control. (Data are shown as mean \pm SEM, n=3).

Figure S9: fascin regulates transmesothelial migration (A) Representative image of PDAC cell transmesothelial migration. Met5A cells on fibronectin coated glass bottom dish stained with β -catenin and DAPI (top left). Green CMFDA labeled fascin-expressing PDAC 070669 cells were added to MCs for 2 hr (**attachment**, top right), 5hr (**junction open**, bottom left) and 10hr (**intercalated**, bottom right). Insert shows the junction opening of Met5A cells

by PDAC cells. (B) Green CMFDA-labeled 070669 PDAC cells (green) were added to confluent MCs (labeled with β -catenin (white) and phalloidin (red)) grown on a fibronectin coated glass bottom dish. Cells were fixed after 10 hr and their localization was analyzed by confocal microscopy. Top and bottom views of the MC monolayers are shown. (C) Western blots analysis of transient fascin knockdown in 070669 PDAC cells. Loading control: GAPDH. (D) Representative image of Green CMFDA labeled NT or fascin siRNA expressing 070669 PDAC cells added to MCs for 5hr. Top images show the MC monolayer. Middle and bottom images show the 3D top and bottom view of the MC monolayers. (E) Quantification of intercalation for NT and fascin siRNA treated 070669 cells **5hr after seeding on** MC monolayers. (Data are shown as mean \pm SEM, n=3), **p < 0.01 by t test, Scale bars: (A, D) 10 μ m.

Movie Legends

Movie 1 Fascin promotes the formation of filopodia. Fascin deficient 105768 PDAC cells expressing human GFP-fascin and empty vector (pLHCX) were transfected with GFP/RFP-lifeact and spread on collagen I coated glass-bottomed dishes overnight. Cells were filmed every 20 sec Individual filopodia are yellow arrowed.

Movie 2 Fascin promotes lamellipodia dynamics. Fascin deficient 105768 PDAC cells expressing human GFP-fascin and empty vector (pLHCX) were plated on 6 well plastic dishes overnight. Cells were filmed at 1 sec intervals.

Movie 3 Fascin promotes 2D random migration. Fascin deficient 105768 PDAC cells expressing human GFP-fascin and empty vector (pLHCX) and human GFP-fascin treated with fascin siRNA were plated on 6 well plastic dishes overnight. Cells were filmed at 10 min intervals.

Movie 4 Fascin localizes to leading edges of transmigrating protrusions. For live imaging of protrusion dynamics of transmigrating PDAC cells, GFP-

fascin expressing PDAC cells were added to red CMTPX labeled confluent MC monolayer for 3 hr. The leading protrusion from PDAC cells within the junction between MCs was imaged at 2 min intervals. Individual fascin filopodia are yellow arrowed. Notably, some fascin positive filopodia also protrude from cell body through the MC cell junctions (red arrowed)

Movie 5 Fascin promotes efficient transmesothelial migration. Green CMFDA labeled GFP-fascin rescued cells and red CMTPX labeled PDAC fascin deficient cells were added to a confluent MC monolayer. Cells were monitored by time-lapse microscopy at 10 min intervals for 10 hr.

Movie 6 Fascin promotes efficient protrusion for transmesothelial migration. CellTracker labeled fascin deficient (pLHCX) and GFP-fascin rescued PDAC cells were added to confluent MC monolayer. Cells were monitored by time-lapse microscopy at 10 min intervals. Phase (Left), CellTracker (Middle) and merged images (Right) are shown, Individual protrusions are yellow arrowed

Supplementary Table 1. Multivariate Cox Regression Analysis of Association of Fascin and Clinicopathological Parameters with Overall Survival

Supplementary Table 2. Percentage of Fascin positive Lesions in KPC Mice

Supplementary Table 3. Results of whole blood pancreatic function tests on normal and fascin knockout mice.

Supplementary Table 4. Clinical spectrum of disease in LSL-KRasG12D/+;LSL-Trp53R172H/+;Pdx1Cre (KPC) and Fascin-/- LSL-KRasG12D/+;LSL-Trp53R172H/+;Pdx1Cre (FKPC) mice.

Supplemental Experimental Procedures

Antibodies and Inhibitors- Goat anti-Zeb2 (L-20), rabbit anti-Zeb1(H-102) (Santa Cruz); Rabbit anti-T-plastin (ab137585), Rabbit Ck19 for western blots (ab15463) Rabbit anti-Pdx1 (ab47267), mouse anti-Twist (ab50887), rat anti-Neutrophil antibody (NIMP-R14) (ab2557), rat anti-CD45R (RA3-6B2) (ab64100), rabbit Anti-Pecam (CD31) (ab28364), Rabbit Anti-Myeloperoxidase (MPO) (ab9535) and rat anti-F4/80 (Cl:A3-1) (ab6640) (Abcam); rabbit anti-Ki67 (SP6) (Neomarkers); mouse anti- β -catenin, mouse anti-E-cadherin for western blots and mouse anti-BrdU (BD bioscience); rabbit Phospho Histone H3 (Ser10) (#9701), rabbit anti-Cleaved Caspase-3 (Asp175) (#9664), rabbit anti-slug for western blots (C19G7) (#9585), rabbit anti-Snail (C15D3) (#3879) and rabbit anti-GAPDH (14C10) (#2118) (Cell signaling); Rat anti-E-cadherin for IF (clone DECMA-1), mouse anti- α -actinin (clone BM-75.2) and rabbit anti-Amylase (A8273) (Sigma); Mouse anti-Fascin1 and Mouse anti-S100A4 (Dako); Rabbit anti-p53 (CM-5) and Rabbit anti-CD3 (VP-RM01) (Vector Labs); Rat anti-Ck19 for IHC and IF (TROMA III, Developmental Studies Hybridoma Bank, Iowa). Rabbit anti-Slug¹ for immunofluorescence was a kind gift from Joel Habener. Monoclonal biotinylated goat anti-rabbit or mouse IgG secondary antibody was obtained from (Dako). Alexa594 phalloidin, anti-mouse IgG, anti-rabbit IgG and anti-rat IgG AlexaFluor secondary antibodies were obtained from Invitrogen. Horseradish peroxidase-conjugated secondary antibodies were obtained from Jackson ImmunoResearch Laboratories.

Immunoblotting and Quantitative PCR- For Western blot analysis, Cells or tissue were lysed in RIPA buffer (50 mM Tris-HCl, 150 mM NaCl, 1% NP-40, 0.25% Na-deoxycholate and 0.1% SDS) with Halt protease inhibitor cocktail (Pierce) and Halt phosphatase inhibitor cocktail (Pierce) for 10 min on ice. Tissue samples were then homogenized with electronic homogenizer (Precellys 24, Stretton Scientific Ltd) and lysates were separated by SDS-PAGE and transferred to PVDF membranes. Western blotting was performed with the ECL chemiluminescence detection kits (Pierce) with appropriate species-specific horseradish peroxidase-conjugated secondary antibodies.

The images were recorded and processed using GeneSnap software and Bio-imaging system. (Syngene). Western blots are representative of typical results obtained on multiple (>3) occasions for each experiment shown.

Quantification of western blots for siRNA or overexpression experiments was done using ImageJ to outline the bands on the blots and calculate the pixel density, the pixel density was then divided by pixel density for loading control and then results were compared with the non-targeted control. For quantitative PCR, total RNA was extracted from cells with the RNAeasy kit (Qiagen) and cDNA and qPCR was done with DyNAmo SYBR Green 2-Step qRT-PCR Kit (Thermo Scientific) according to the manufacturer's instruction using specific oligos for mouse Fascin (QT00165907) (Qiagen). The mRNA levels of the targets were normalized using primers for GAPDH (QT01658692) (Qiagen) as a housekeeping gene. Analysis was completed with Opticon 3 software (Biorad, UK). Three independent experiments in triplicate for each sample were carried out.

Tissue Microarray Analysis-The human pancreatico-biliary tissue microarray was previously described^{2,3}. Briefly, a TMA was created within the West of Scotland Pancreatic Unit, University Department of Surgery, Glasgow Royal Infirmary. All patients gave written, informed consent for the collection of tissue samples, and the local Research Ethics Committee approved collection. All cases had undergone a standardized pancreaticoduodenectomy. A total of 1500 cores from a total of 224 cases with pancreatico-biliary cancer (including 114 pancreatic ductal adenocarcinomas) with a full spectrum of clinical and pathological features were arrayed in slides. At least 6 tissue cores (0.6 mm diameter) from tumor and 2 from adjacent normal tissue were sampled. Complete follow-up data was available for all cases within the tissue microarray analysis. Fascin expression levels were scored based on staining intensity and area of tumor cells using a weighted histoscore calculated from the sum of (1 x % weak staining) + (2 x % moderate staining) + (3 x % strong staining), providing a semi-quantitative classification of staining intensity. The cutoff for high and low expression of fascin was a histoscore of 72.8. Kaplan-Meier survival analysis was used to analyze the overall survival from the time of surgery.

ACCEPTED MANUSCRIPT

Patients alive at the time of follow-up point were censored. To compare length of survival between curves, a log-rank test was performed. All statistical analyses were performed using SPSS version 15.0 (SPSS Inc., Chicago, IL).

Cell Culture-PDAC cell lines were generated from primary pancreatic tumors taken from Fascin^{-/-} or Fascin^{+/+} KRas^{G12D} Trp53^{R172H/+} Pdx1-Cre mice and then passaged in growth media (Dulbecco's modified Eagle medium containing 10% fetal bovine serum and 2 mM L-glutamine), PDAC origin for these cell lines are confirmed with antibody against Pdx-1 and p53 using western blots. Primary pancreatic ductal epithelial cells (PDECs) were isolated from control animals and then cultured and passaged on collagen-coated plates in fully supplemented medium, as described previously⁴. Briefly, the pancreata of 3–4-month-old WT mice were dissected, minced, and digested at 37°C in a Hank's balanced salt solution (Hank's balanced salt solution + 5 mmol/L glucose + 0.05 mmol/L CaCl₂) containing 2 mg/mL type V collagenase (Sigma) with agitation by a magnetic stir bar. After 20 minutes, the digested material was filtered through a 40µm cell strainer (BD Falcon). Fragments trapped on the mesh were digested further in 0.05% trypsin– 0.53 mmol/L EDTA (Life Technologies) for 2 minutes, and then proteases were inactivated by the addition of Dulbecco's modified Eagle medium/F12 (Invitrogen, Carlsbad, CA) supplemented with 10% fetal bovine serum. The tissue then was washed 3 times in Hank's balanced salt solution wash to remove collagenase completely. The ductal fragments were plated on 2.31 mg/mL rat tail collagen type I (BD Biosciences) precoated plastic dishes for growth in monolayer, PDECs were cultured for 4 days and then harvested for immunoblotting or immunofluorescence. MET5A human pleural mesothelial cells were obtained from American Type Culture Collection (ATCC). MET5A Cells were cultured in a 1:1 ratio of Medium 199 (GIBCO) and MCDB105 (Sigma) supplemented with 10% fetal bovine serum (GIBCO). All experiments were done with cells of fewer than 6 passages. PANC-1 human pancreatic carcinoma and HT29 human colon adenocarcinoma grade II cell lines were cultured in medium as mentioned above for PDAC cell lines.

Stable gene expression, siRNA treatments and GFP-Fascin constructs- pPGS-hFlag-Snail (Plasmid 25695), pPGS-hFlag-Slug (Plasmid 25696) and pBABE-puro-mTwist (Plasmid 1783) were obtained from Addgene. mRFP-Lifeact and GFP-Lifeact were kind gifts from Dr Roland Wedlich-Soldner, Max Planck Institute, Martinsreid, Germany. Mouse PDAC cells expressing Flag-Snail, Flag-Slug, Twist or GFP tagged human fascin were generated by retroviral infection using the modified Retro-X retroviral expression system (Clontech). To subclone human GFP-fascin into *HindIII* and *Clal* sites of the pLHCX retroviral expression vector, an *HindIII* restriction site, followed by Kozak consensus translation initiation site was introduced to the 5' end of the coding sequence of GFP-fascin⁵, by PCR (5'-AGA AAG CTT ATG GTG AGC AAG GGC GAG GAG CTG TTC -3'), with a *Clal* restriction site introduced to the 3' end in the same reaction (5'-AGA ATC GAT A CTA GTA CTC CCA GAG CGA GGC GGG GTC-3'), GFP-fascin was used as template. High-titre, replication-in-competent retroviral particles were produced in Phoenix Eco packaging cell line (Orbigen). Subsequent infection of target lines resulted in transfer of the coding region of interest, along with a selectable marker. Pooled cell lines stably expressing the construct of interest were isolated by selection with hygromycin-B (500µg/ml) for GFP-fascin. Control lines were infected with retroviral particles expressing an empty pLHCX control vector transcript, and subjected to an identical selection procedure. For siRNA experiment, Nontargeting (NT) control was from Dharmacon; siRNAs against human fascin (siFascin, target sequence: CAC GGG CAC CCT GGA CGC CAA). siRNA against mouse fascin, siFascin 1, target sequence: CTCAGTCAACTCTGAGCCTTA; siFascin 2 target sequence: CCCCATGATAGTAAGCTTTGAA; sets of four siRNAs target mouse fascin (GS14086), slug (GS20583), Zeb1 (GS21417), Zeb2 (GS24136) and E-cadherin (GS12550) were obtained from Qiagen. For transient knockdown of mouse fascin, slug, Zeb1, Zeb2 and E-cadherin, four siRNAs targeting each gene were mixed and diluted to 20µM and used at 100nM for transfection. Procedures used to transfect cells with siRNA were described previously⁵.

Immunohistochemistry- Formalin-fixed paraffin-embedded sections were deparaffinized and rehydrated by passage through xylene and a grade alcohol

series. For Alcian blue staining, rehydrated paraffin sections were stained for 30 minutes at room temperature in a 3% solution of Alcian blue diluted in acetic acid and counterstained with eosin. For antibody staining, antigen retrieval was performed by incubation of sections in microwave-heated citrate buffer (Dako) in a pressure cooker, except for anti-F4/80 and anti-NIMP, for which 10 minute proteinase K retrieval (Dako) was used. Sections were blocked with peroxidase blocking reagent (Dako) for 5 mins. Sections were then blocked in 10% serum for 1 hr and then incubated with primary antibody for 2 hr at RT. Sections were incubated with horseradish peroxidase labelled secondary antibody (Dako) for 1 hr and staining was visualized with DAB substrate chromogen and hematoxylin was used as the nuclear counterstain. For amylase/Ck19 dual IHC, after primary antibody, sections were incubated with anti-rabbit alkaline phosphatase labeled and anti-rat horseradish peroxidase labelled secondary antibody for 30 mins, staining was visualized with DAB substrate chromogen and blue alkaline phosphatase substrate kit (Vector lab) and mounted with Prolong Gold Antifade reagent (Invitrogen). For immunofluorescence on tissue sections, after antigen retrieval, sections were blocked with 10% donkey serum for 1 hr and incubated with primary antibody overnight at 4 °C. Sections were then washed in PBS and incubated with fluorescent conjugated secondary antibodies for 1 hr and mounted with Prolong Gold Antifade reagent (Invitrogen).

Live cell imaging-For live imaging of filopodia, 105768 PDAC cells expressing control vector or GFP-fascin were transfected with GFP or RFP-lifeact using Lipofectamine 2000 according to the manufacturer's instructions. Cells were then plated on glass-bottomed dishes pre-coated with 20ug collagen I (BD Bioscience) overnight. Timelapse images were captured every 20 sec for 10 mins using an Nikon A1 inverted laser scanning confocal microscope in a 37°C chamber with 5% CO₂. For live imaging of lamellipodia dynamics, 300 images were captured at 1-second intervals on Nikon TE 2000 Timelapse microscope systems with PFS (20× objective, ×1.5). Lamellipodial kymographs show pixel densities over time (*x*-axis) on a single pixel-wide straight line (*y*-axis) in the direction of lamellipodial protrusion (Image J plug-in multiple kymograph). Distance extended (*D*) was measured against

lamellipodial persistence (P), defined as the amount of time that the cell spends persistently extending a lamellipod before pausing or entering a retraction phase. Rate of protrusion (R) is shown as a broken line in Fig. S8B and represents the distance protruded (D) divided by the time of protrusion (P). For live imaging of random cell migration, cells on plastic dish were captured on Nikon TE 2000 Timelapse microscope (10× objective) at 10-minute intervals for 6 hours. Cell speed was measured with Image J plug-in manual tracking and chemotaxis tool. 300 cells from 3 experiments were tracked. For live imaging of transmesothelial migration, green CMFDA or red CMTPX CellTracker (Molecular Probes) labeled PDAC cells (1.5×10^5) were added to confluent Met5A monolayer on 35mm glass bottomed dish pre-coat with $10 \mu\text{g/ml}$ fibronectin. Cells were monitored by time-lapse microscopy at 10-minute intervals for up to 15 hr in a humidified chamber at 37°C and 5% CO_2 with an inverted microscope (TE2000; Nikon), with a 20x objective lens and using MetaMorph software (Molecular Devices). To quantify intercalation, a cell was considered as intercalated when its shape was not round, when it was no longer phase-bright, and when it was clearly part of the MC monolayer. For live imaging of protrusion dynamics of transmigrating PDAC cells, GFP-fascin expressing PDAC cells were added to red CMTPX labeled confluent Met5A monolayer for 3 hr. The leading protrusion from PDAC cells within the junction between Met5A cells were imaged using a spinning disk confocal scan head (Yokogawa CSU-10) attached to an Nikon A1 inverted microscope.

Cell growth assay- For 2D growth assay, 2×10^4 cells were plated in each well of 6 well plates at day 0, and number of cells were trypsinized and counted every day from one well of 6 well plates for 4 days using CASY cell counter (Roche Innovats). Each point (mean \pm SEM) is derived from the mean of hemocytometer count of cells from three replicate dishes from three independent experiments. 3D proliferation assay in collagen I was performed using Culturex 3D culture cell proliferation assay kit (Culturex instructions), Briefly, 5×10^3 cells in $100 \mu\text{l}$ cell culture medium supplemented with 2%

ACCEPTED MANUSCRIPT

collagen I were cultured on the top of the gel plug of 1 mg/ml collagen I in cell culture medium (pH7) in 96 well plate for 3 or 4 days and 8µl of cell proliferation reagent were added to each well and incubated at 37°C chamber with 5% CO₂ for 2 hours and the absorbance was read at 450 nm. For the anoikis assay, 2x10⁵ cells were plated on 6 wells ultra low attachment plates for 6 and 24 hrs. Cells were collected, washed once with PBS and stained with Alexa Fluor 647 Conjugate annexin V according to the manufacturer's instructions. After washing with PBS, cells were stained with propidium iodide (1 mg/ml) and RNaseA (250 µg/ml) for 30 min before processing on BD FACS-Calibur (BD Bioscience).

Blood analysis - Whole Blood Counts: Mice were humanely sacrificed with a rising concentration of carbon dioxide and then bled from the hepatic portal vein into a syringe containing 50µl of Acid Citrate Dextrose (ACD). Blood was then either emptied into a blood tube containing EDTA for blood cell analysis. Blood cell analysis was completed using both Advia 120 (Siemens, Camberley, UK) and by examination of a blood smear. **Pancreatic Function:** Mice were humanely sacrificed with a rising concentration of carbon dioxide and then bled by cardiac puncture. Blood was then emptied into a tube containing lithium heparin (LH/0.5) and centrifuged to separate the plasma into a new tube. Samples were analysed by the Clinical Pathology Laboratory at the University of Glasgow School of Veterinary Medicine.

Caerulein Treatment and BrdU Assay-Acute pancreatitis was induced by intraperitoneal (i.p.) cerulein injections (50 mg/kg; Sigma): one injection per hour for six injections and repeated 2 days later. Mice were sacrificed at 1, 7 or 21 days after last injection. For BrdU assay, mice were injected intraperitoneally with 2.5 mg BrdU (BD bioscience) for 2 hr before sacrifice.

PanIN and amylase positive area Quantification- Quantitation of amylase positive area was performed on DAB stained sections with amylase antibody. Amylase positive area/pancreas area was measured manually with ImageJ using the freehand selection tool. PanINs were defined according to previously published guidelines for reporting of these lesions in genetically

ACCEPTED MANUSCRIPT

engineered mouse models⁶. Briefly, to be defined as PanIN, a lesion must arise in native pancreatic ducts measuring less than 1mm and should not arise on a background of acinar-ductal metaplasia. PanIN lesions are then graded as PanIN-1, 2 or 3, according to the severity of cytological and architectural abnormalities, as detailed in the consensus guidelines published by Hruban et al⁷. Quantitation of number of PanINs was performed on DAB stained sections with CK19 antibody. Final quantitation represents the average of 20 of 20X fields of view from 4 mice. PanIN lesions were independently graded by one of the investigators (A.L.) and confirmed by a trainee pathology resident (H.T.M.) and another investigator with extensive experience in mouse pancreatic histopathology (J.M.).

Luciferase Reporter assay-A region of the first intron from the mouse fascin gene (+2189 to +2,735) was subcloned into into *SacI* and *XmaI* sites of pGL3-prom vector (Promega), by PCR, an *SacI* restriction site was introduced to the 5' end (5'-AGA GAG CTC ATG CAG AGG GCA AAG CCT TGG GTG GGG CC-3'), and a *XmaI* restriction site was introduced to the 3' end in the same reaction (5'-AGA CCC GGG ATA GCT ATG CAG GGC TTC TCT ATT TGC AAC T-3'), mouse genomic DNA was used as template. Mutation to the E-box was generated using QuikChange II Site Directed Mutagenesis kit (Agilent, UK) according to manufacture's protocol with primer pairs: forward: GGG TCA GAG TTC CTT CCT GTT TAG CAA ACA TTG and reverse: CAA TGT TTG CTA AAC AGG AAG GAA CTC TGA CCC. Luciferase activity was assayed using dual-luciferase assay kit (Promega). The firefly luciferase activity was normalized to that of Renilla luciferase to control transfection efficiency between samples.

Chromatin Immunoprecipitation (ChIP) quantitative-PCR-ChIP from 070669 PDAC cell line expressing flag-tagged Slug was performed as described previously⁸ using 10 µg of monoclonal anti-flag M2, Clone M2 (Sigma, F1804) per assay. ChIP enrichment levels were determined by SyBr green PCR. The sequence for primer pairs: #1: Forward: ACCATGGCCTCTCTTGTTC; Reverse: ACATTCCCAAGAGACGTTTACC;

ACCEPTED MANUSCRIPT

#2: Forward: AGGTGGGTCTCTGAGTTCTT; Reverse: TTTGAGACAGGGTTTCTCTGC; #3: Forward: CTGGCCTCGAACTCAGAAAT; Reverse: GCATGACCACCAGTTCAAGAC; primer pair for E-box on mouse E-cadherin promoter was used as positive control⁹: Forward: GGGTGGAGGAAGTTGAGG; Reverse: CTCCCACACCAGTGAGC.

Supplementary References:

1. Rukstalis, J. M. & Habener, J. F. Snail2, a mediator of epithelial-mesenchymal transitions, expressed in progenitor cells of the developing endocrine pancreas. *Gene Expr Patterns* **7**, 471-479 (2007).
2. Morton, J. P. et al. LKB1 haploinsufficiency cooperates with Kras to promote pancreatic cancer through suppression of p21-dependent growth arrest. *Gastroenterology* **139**, 586-97, 597.e1 (2010).
3. Morton, J. P. et al. Dasatinib inhibits the development of metastases in a mouse model of pancreatic ductal adenocarcinoma. *Gastroenterology* **139**, 292-303 (2010).
4. Schreiber, F. S. et al. Successful growth and characterization of mouse pancreatic ductal cells: functional properties of the Ki-RAS(G12V) oncogene. *Gastroenterology* **127**, 250-260 (2004).
5. Li, A. et al. The actin-bundling protein fascin stabilizes actin in invadopodia and potentiates protrusive invasion. *Curr Biol* **20**, 339-345 (2010).
6. Hruban, R. H. et al. Pathology of genetically engineered mouse models of pancreatic exocrine cancer: consensus report and recommendations. *Cancer Res* **66**, 95-106 (2006).
7. Hruban, R. H. et al. Pancreatic intraepithelial neoplasia: a new nomenclature and classification system for pancreatic duct lesions. *Am J Surg Pathol* **25**, 579-586 (2001).
8. Forsberg, E. C. et al. Developmentally dynamic histone acetylation pattern of a tissue-specific chromatin domain. *Proc Natl Acad Sci U S A* **97**, 14494-14499 (2000).
9. Peinado, H., Ballestar, E., Esteller, M. & Cano, A. Snail mediates E-cadherin repression by the recruitment of the Sin3A/histone deacetylase 1 (HDAC1)/HDAC2 complex. *Mol Cell Biol* **24**, 306-319 (2004).

Supplementary Material Li et al.**Fascin is Regulated by Slug, Promotes Progression of Pancreatic Cancer in Mice, and is Associated with Patient Outcome****Supplemental Data**

Figure S1: Fascin deficient mice have normal pancreas morphology and normal survival rate. (A) Dot plot of pancreas-to-body weight ratios in wild type and fascin deficient mice at 5w. (B) Histology analysis of H&E stained sections from pancreas of 5w control or fascin deficient mice. Representative Images (C) and quantification (D) of BrdU+ or Ki67+ duct cells (left) and acinar cells (right) in pancreata from 5w control and fascin deficient mice measured by IHC. Red arrows indicate BrdU or Ki67 positive nuclei. (n=4 mice per genotype). (E) Mendelian segregation of pups at weaning (3w). 6 litters from crosses between fascin heterozygous males and females in a mixed background were recorded. (F) Body mass of control and fascin deficient mice in a mixed background at 8w. At least 5 mice were measured for each genotype and gender. Scale Bars: (B, C) 50 μ m.

Figure S2 Fascin is not required for PanIN formation (A) Gene targeting strategy for generating *fascin*^{-/-}, *KRas*^{G12D} *Pdx1-Cre* (FKC). (B) Quantitation of spontaneous (4m) PanIN formation in KC and FKC mice. (left) Dot plot of measurements of pancreas-to-body weight ratios. (middle) Box plot of amylase-positive area (Lower quartile, median, and upper quartile are shown). (right two bar graphs) Relative number and percentage of PanINs of grade 1-3 per histopathological section of pancreas (Data are shown as mean \pm SEM) (n=6 mice per genotype). (C) Panels show tissue sections with spontaneous PanIN in FKC compared to KC mice- H&E (top), alcian blue (middle) and dual IHC for CK19 (brown) and amylase (blue) (bottom). (D) Images and quantification of BrdU incorporation assay measured by IHC in duct cells (Top) and acinar cells (bottom) in 4 months KC and FKC pancreas. Red arrows indicate BrdU positive nuclei (n=4 mice per genotype). (E) Panels show spontaneous PanIN formation in 6w FKPC or KPC mice, with H&E (top) and dual IHC for CK19 (brown) and amylase (blue) (bottom). (F) Quantitation of spontaneous (6w) PanIN formation in KPC and FKPC mice. (left) Box plot

of amylase-positive area (Lower quartile, median, and upper quartile are shown). (right two bar graphs) Number and percentage of PanINs of grade 1-3 per histopathological section of pancreas (Data are shown as mean \pm SEM) (n=5 mice per genotype). Scale bars: (C, E) 100 μ m, (D) 50 μ m.

Figure S3: Fascin is not required for acute pancreatitis induced PanIN formation. (A) Protocol used for cerulein-induced PanIN formation in KC and FKC mice. (B) Western blot (top) and IHC analysis (bottom) of fascin expression in control and KC mice after PBS or cerulein treatments (1d, 7d and 21d post-cerulein). (C) Left: Panels show cerulein-induced (21d post-cerulein) PanIN formation in FKC compared to KC mice, shown by H&E (top), Alcian Blue (middle) and dual IHC for CK19 (brown) and amylase (blue) (bottom). Right: Quantitation of cerulein-induced (21d post-cerulein) PanIN formation in KC and FKC mice. Graphs describe the following as indicated: Dot plot of pancreas-to-body mass ratios (n=6 for KC, n=15 for FKC mice); Box plot of amylase-positive area (Lower quartile, median, and upper quartile are shown); Relative number of PanIN per field and percentage of PanINs of grade 1-3 per histopathological section of pancreas (Data are shown as mean \pm SEM) (n=6 mice per genotype). (D) Images and quantification of BrdU incorporation assay measured by IHC in duct cells (top) and acinar cells (bottom) in KC and FKC pancreas 21d post-cerulein injection. BrdU positive nuclei are red arrowed (n=4 mice per genotype). (E) Quantification of neutrophil (anti-myeloperoxidase (MPO)) recruitment to normal and fascin deficient pancreas 1 day after cerulein injection. (Data are shown as mean \pm SEM, n=4 mice per genotype). (F) Dot plots of whole blood counts from 6w control and fascin deficient mice 21d post cerulein injection. (left) Monocytes, (middle) Lymphocytes and (right) Neutrophils are shown. (Data are shown as mean \pm SEM). Scale Bars: (B, C) 100 μ m, (D, E) 50 μ m.

Figure S4: Tumor-intrinsic action of fascin. (A) Pancreata from Rosa26-LSL-tdRFP/+ Pdx1-Cre, fascin^{-/-} Rosa26-LSL-tdRFP/+ Pdx1-Cre and Pdx1-

Cre mice were analyzed using an OV100 in vivo imaging system. RFP signaling is detected in whole pancreata from Rosa26-LSL-tdRFP/+ Pdx1-Cre and fascin^{-/-} Rosa26-LSL-tdRFP/+ Pdx1-Cre mice, but not in pancreata from mice only expressing Pdx1-Cre. (B) Representative images of immunohistochemical staining for Ki67, 2h BrdU pulse, phospho-histone H3 (PHH3) and cleaved caspase-3 (CC3). Quantitations were shown in Figure 3F-I. Images (C) and quantifications (D) of infiltration of B cells (CD45R), T cells (CD3), macrophages (F4/80) and neutrophils (NIMP) into tumors. At least 16 medium-powered fields from four KPC and FKPC PDACs were analyzed (Data are shown as mean \pm SEM.) (E) Immunohistochemical visualization of PECAM (CD31) in tumors in KPC and FKPC mice. (F) Quantification of D, no significant difference in vascularization. (Data are shown as mean \pm SEM. N=4 mice from each genotype). Scale bars: 100 μ m.

Figure S5: Slug signaling regulates fascin expression in PDAC cells. (A) Western blot analysis of fascin and EMT markers in primary ductal epithelial cells (PDEC) isolated from the pancreas of a wild type mouse and a PDAC cell line 118739 harvested from a KPC mouse. Expression of CK-19 in the cell lines confirms their ductal origin and p53 in 118739 cell line confirms its PDAC origin. Flag-snail was used as positive control for snail antibody. GAPDH, loading control. (B) Immunofluorescence microscopy analysis of PDEC and 118739 PDAC cells stained for the indicated proteins. (C) Representative images of example of E-cadherin negative (127445) and E-cadherin positive (022160) PDAC cells stained for fascin, E-cadherin and Slug. Co-expression of slug and E-cadherin in 022160 PDAC cells suggest partial EMT. Inserts show individual channels (D) Expression of EMT markers in a representative panel of 5 independent FKPC PDAC cell lines. 083320 PKC PDAC cell line was used as positive control for fascin. (E) Spearman correlation analysis of (left) fascin and slug and (right) fascin and tubulin gene expression in human pancreatic cancer cell lines using Wagner Cell Line data set. As a control, fascin does not correlate with tubulin expression. Scale Bars: (B, C) 10 μ m.

Figure S6: Slug is an important regulator of fascin expression. (A) Immunofluorescence microscopy analysis of 070669 PDAC cells transduced with vector (control), Flag-slug, Flag-snail and twist and stained for the proteins as indicated. Slug, snail and twist overexpressing cells are yellow arrowed. (B) Western blots (left) and quantitation (right) of proteins as indicated with 070669 PDAC cells treated with slug siRNA (Data are shown as mean \pm SEM). ** $p < 0.01$ by Student's t-test. Loading control: α -actinin. (C) Western blot analysis of proteins as indicated with 070669 PDAC cells treated with Zeb1 (top left), Zeb2 (top right), E-cadherin (bottom left) and fascin (bottom right) siRNA. GAPDH and α -actinin, loading controls as indicated. (D) Phase contrast images of 061843 PDAC cells transduced with vector (control), Flag-slug, Flag-snail and twist as indicated. (E) Western blot analysis with control, Flag-slug, Flag-snail and twist expressing 061843 PDAC cells for proteins as indicated. α -actinin, loading control. (F) Western blot analysis with control, Flag-slug, Flag-snail expressing PANC-1 (left) and HT29 (right) human pancreatic and colon cancer cells for proteins as indicated. Loading control: α -actinin Scale Bars: (A) 10 μ m (D) 50 μ m.

Figure S7: Slug correlates with fascin in human pancreatic cancer Spearman correlation analysis of fascin and slug (left) or tubulin (right) gene expression in human pancreatic cancer using the Badea data set (A), Pei data set (B) and Jimeno data set (C). Fascin correlation with tubulin was used as a control.

Figure S8: Fascin regulates lamellipodia dynamics and migration but not cell proliferation. (A) Western blots of 105768 FKPC mouse PDAC cells expressing control vector (pLHCX), human GFP-fascin and fascin siRNA treated rescue cells. GAPDH loading control. (B) Left: Control vector and GFP-fascin expressing FKPC 105768 cells expressing RFP or GFP-lifeact. Yellow stars indicate filopodia. Bar graphs show box plots of quantifications as indicated. ** $p < 0.01$ by Student's t-test. (C) Top: Representative kymograph

ACCEPTED MANUSCRIPT

pictures of GFP-fascin rescued and fascin deficient PDAC cells (Derived from Movie 2). Green lines indicate persistence time for each protrusion, yellow stars indicate each protrusion. Pixel intensities along a 1-pixel wide line were used to generate the kymograph from the corresponding Movie 2; a magnified region (outlined in red) is displayed on the top. Red lines indicate the parameters for one protrusion. Abbreviations are as follows: D, protrusion distance; P, protrusion persistence; and R, protrusion rate. Bottom Bar Graphs: Frequency of lamellipodial protrusion events, distance, protrusion rate and persistence of individual lamellipodial protrusions. Values are averages of means from at least 30 cells (Data are shown as mean \pm SEM). **p<0.01 by Student's t-test. (D) Left: Migration speed of 105768 cells expressing vectors/siRNA as indicated. More than 300 cells from three experiments were randomly selected and mean migration speed over 6hr was plotted according to frequency in the population. **p < 0.01 by t test. Right: 6 hr tracks of individual cell migration, black tracks migrated faster than 0.5um/min, red indicates slower. (E) Top left: 2D proliferation assay, no difference between control vector and GFP-fascin expressing FKPC 105768 cells. (n=3). Top right: 3D collagen I cell proliferation assay, no difference between control vector and GFP-fascin expressing FKPC 105768 cells. (Data are shown as mean \pm SEM, n=3). Bottom left: Western blot analysis of the effects on the viability of control vector and GFP-fascin expressing FKPC 105768 cells grown in normal culture plates and Ultra low attachment plate for 24 h to induce anoikis with cleaved-caspase3 antibody. Bottom right: FACS analysis using annexin V and propidium iodide for cells undergoing anoikis with control vector and GFP-fascin expressing FKPC 105768 cells cultured in ultra-low attachment plate for 6 and 24 hours, attached cells were used as negative control. (Data are shown as mean \pm SEM, n=3).

Figure S9: fascin regulates transmesothelial migration (A) Representative image of PDAC cell transmesothelial migration. Met5A cells on fibronectin coated glass bottom dish stained with β -catenin and DAPI (top left). Green CMFDA labeled fascin-expressing PDAC 070669 cells were added to MCs for 2 hr (attachment, top right), 5hr (junction open, bottom left) and 10hr (intercalated, bottom right). Insert shows the junction opening of Met5A cells

ACCEPTED MANUSCRIPT

by PDAC cells. (B) Green CMFDA-labeled 070669 PDAC cells (green) were added to confluent MCs (labeled with β -catenin (white) and phalloidin (red)) grown on a fibronectin coated glass bottom dish. Cells were fixed after 10 hr and their localization was analyzed by confocal microscopy. Top and bottom views of the MC monolayers are shown. (C) Western blots analysis of transient fascin knockdown in 070669 PDAC cells. Loading control: GAPDH. (D) Representative image of Green CMFDA labeled NT or fascin siRNA expressing 070669 PDAC cells added to MCs for 5hr. Top images show the MC monolayer. Middle and bottom images show the 3D top and bottom view of the MC monolayers. (E) Quantification of intercalation for NT and fascin siRNA treated 070669 cells 5hr after seeding on MC monolayers. (Data are shown as mean \pm SEM, n=3), **p < 0.01 by t test, Scale bars: (A, D) 10 μ m.

Movie Legends

Movie 1 Fascin promotes the formation of filopodia. Fascin deficient 105768 PDAC cells expressing human GFP-fascin and empty vector (pLHCX) were transfected with GFP/RFP-lifeact and spread on collagen I coated glass-bottomed dishes overnight. Cells were filmed every 20 sec Individual filopodia are yellow arrowed.

Movie 2 Fascin promotes lamellipodia dynamics. Fascin deficient 105768 PDAC cells expressing human GFP-fascin and empty vector (pLHCX) were plated on 6 well plastic dishes overnight. Cells were filmed at 1 sec intervals.

Movie 3 Fascin promotes 2D random migration. Fascin deficient 105768 PDAC cells expressing human GFP-fascin and empty vector (pLHCX) and human GFP-fascin treated with fascin siRNA were plated on 6 well plastic dishes overnight. Cells were filmed at 10 min intervals.

Movie 4 Fascin localizes to leading edges of transmigrating protrusions. For live imaging of protrusion dynamics of transmigrating PDAC cells, GFP-

fascin expressing PDAC cells were added to red CMTPIX labeled confluent MC monolayer for 3 hr. The leading protrusion from PDAC cells within the junction between MCs was imaged at 2 min intervals. Individual fascin filopodia are yellow arrowed. Notably, some fascin positive filopodia also protrude from cell body through the MC cell junctions (red arrowed)

Movie 5 Fascin promotes efficient transmesothelial migration. Green CMFDA labeled GFP-fascin rescued cells and red CMTPIX labeled PDAC fascin deficient cells were added to a confluent MC monolayer. Cells were monitored by time-lapse microscopy at 10 min intervals for 10 hr.

Movie 6 Fascin promotes efficient protrusion for transmesothelial migration. CellTracker labeled fascin deficient (pLHCX) and GFP-fascin rescued PDAC cells were added to confluent MC monolayer. Cells were monitored by time-lapse microscopy at 10 min intervals. Phase (Left), CellTracker (Middle) and merged images (Right) are shown, Individual protrusions are yellow arrowed

Supplementary Table 1. Multivariate Cox Regression Analysis of Association of Fascin and Clinicopathological Parameters with Overall Survival

Supplementary Table 2. Percentage of Fascin positive Lesions in KPC Mice

Supplementary Table 3. Results of whole blood pancreatic function tests on normal and fascin knockout mice.

Supplementary Table 4. Clinical spectrum of disease in LSL-KRas^{G12D/+};LSL-Trp53^{R172H/+};Pdx1Cre (KPC) and Fascin^{-/-} LSL-KRas^{G12D/+};LSL-Trp53^{R172H/+};Pdx1Cre (FKPC) mice.

Supplemental Experimental Procedures

Antibodies and Inhibitors- Goat anti-Zeb2 (L-20), rabbit anti-Zeb1(H-102) (Santa Cruz); Rabbit anti-T-plastin (ab137585), Rabbit Ck19 for western blots (ab15463) Rabbit anti-Pdx1 (ab47267), mouse anti-Twist (ab50887), rat anti-Neutrophil antibody (NIMP-R14) (ab2557), rat anti-CD45R (RA3-6B2) (ab64100), rabbit Anti-Pecam (CD31) (ab28364), Rabbit Anti-Myeloperoxidase (MPO) (ab9535) and rat anti-F4/80 (Cl:A3-1) (ab6640) (Abcam); rabbit anti-Ki67 (SP6) (Neomarkers); mouse anti- β -catenin, mouse anti-E-cadherin for western blots and mouse anti-BrdU (BD bioscience); rabbit Phospho Histone H3 (Ser10) (#9701), rabbit anti-Cleaved Caspase-3 (Asp175) (#9664), rabbit anti-slug for western blots (C19G7) (#9585), rabbit anti-Snail (C15D3) (#3879) and rabbit anti-GAPDH (14C10) (#2118) (Cell signaling); Rat anti-E-cadherin for IF (clone DECMA-1), mouse anti- α -actinin (clone BM-75.2) and rabbit anti-Amylase (A8273) (Sigma); Mouse anti-Fascin1 and Mouse anti-S100A4 (Dako); Rabbit anti-p53 (CM-5) and Rabbit anti-CD3 (VP-RM01) (Vector Labs); Rat anti-Ck19 for IHC and IF (TROMA III, Developmental Studies Hybridoma Bank, Iowa). Rabbit anti-Slug¹ for immunofluorescence was a kind gift from Joel Habener. Monoclonal biotinylated goat anti-rabbit or mouse IgG secondary antibody was obtained from (Dako). Alexa594 phalloidin, anti-mouse IgG, anti-rabbit IgG and anti-rat IgG AlexaFluor secondary antibodies were obtained from Invitrogen. Horseradish peroxidase-conjugated secondary antibodies were obtained from Jackson ImmunoResearch Laboratories.

Immunoblotting and Quantitative PCR- For Western blot analysis, Cells or tissue were lysed in RIPA buffer (50 mM Tris-HCl, 150 mM NaCl, 1% NP-40, 0.25% Na-deoxycholate and 0.1% SDS) with Halt protease inhibitor cocktail (Pierce) and Halt phosphatase inhibitor cocktail (Pierce) for 10 min on ice. Tissue samples were then homogenized with electronic homogenizer (Precellys 24, Stretton Scientific Ltd) and lysates were separated by SDS-PAGE and transferred to PVDF membranes. Western blotting was performed with the ECL chemiluminescence detection kits (Pierce) with appropriate species-specific horseradish peroxidase-conjugated secondary antibodies.

The images were recorded and processed using GeneSnap software and Bio-imaging system. (Syngene). Western blots are representative of typical results obtained on multiple (>3) occasions for each experiment shown.

Quantification of western blots for siRNA or overexpression experiments was done using ImageJ to outline the bands on the blots and calculate the pixel density, the pixel density was then divided by pixel density for loading control and then results were compared with the non-targeted control. For quantitative PCR, total RNA was extracted from cells with the RNAeasy kit (Qiagen) and cDNA and qPCR was done with DyNAmo SYBR Green 2-Step qRT-PCR Kit (Thermo Scientific) according to the manufacturer's instruction using specific oligos for mouse Fascin (QT00165907) (Qiagen). The mRNA levels of the targets were normalized using primers for GAPDH (QT01658692) (Qiagen) as a housekeeping gene. Analysis was completed with Opticon 3 software (Biorad, UK). Three independent experiments in triplicate for each sample were carried out.

Tissue Microarray Analysis-The human pancreatico-biliary tissue microarray was previously described^{2,3}. Briefly, a TMA was created within the West of Scotland Pancreatic Unit, University Department of Surgery, Glasgow Royal Infirmary. All patients gave written, informed consent for the collection of tissue samples, and the local Research Ethics Committee approved collection. All cases had undergone a standardized pancreaticoduodenectomy. A total of 1500 cores from a total of 224 cases with pancreatico-biliary cancer (including 114 pancreatic ductal adenocarcinomas) with a full spectrum of clinical and pathological features were arrayed in slides. At least 6 tissue cores (0.6 mm diameter) from tumor and 2 from adjacent normal tissue were sampled. Complete follow-up data was available for all cases within the tissue microarray analysis. Fascin expression levels were scored based on staining intensity and area of tumor cells using a weighted histoscore calculated from the sum of (1 x % weak staining) + (2 x % moderate staining) + (3 x % strong staining), providing a semi-quantitative classification of staining intensity. The cutoff for high and low expression of fascin was a histoscore of 72.8. Kaplan-Meier survival analysis was used to analyze the overall survival from the time of surgery.

ACCEPTED MANUSCRIPT

Patients alive at the time of follow-up point were censored. To compare length of survival between curves, a log-rank test was performed. All statistical analyses were performed using SPSS version 15.0 (SPSS Inc., Chicago, IL).

Cell Culture-PDAC cell lines were generated from primary pancreatic tumors taken from Fascin^{-/-} or Fascin^{+/+} KRas^{G12D} Trp53^{R172H/+} Pdx1-Cre mice and then passaged in growth media (Dulbecco's modified Eagle medium containing 10% fetal bovine serum and 2 mM L-glutamine), PDAC origin for these cell lines are confirmed with antibody against Pdx-1 and p53 using western blots. Primary pancreatic ductal epithelial cells (PDECs) were isolated from control animals and then cultured and passaged on collagen-coated plates in fully supplemented medium, as described previously⁴.

Briefly, the pancreata of 3–4-month-old WT mice were dissected, minced, and digested at 37°C in a Hank's balanced salt solution (Hank's balanced salt solution + 5 mmol/L glucose + 0.05 mmol/L CaCl₂) containing 2 mg/mL type V collagenase (Sigma) with agitation by a magnetic stir bar. After 20 minutes, the digested material was filtered through a 40µm cell strainer (BD Falcon). Fragments trapped on the mesh were digested further in 0.05% trypsin– 0.53 mmol/L EDTA (Life Technologies) for 2 minutes, and then proteases were inactivated by the addition of Dulbecco's modified Eagle medium/F12 (Invitrogen, Carlsbad, CA) supplemented with 10% fetal bovine serum. The tissue then was washed 3 times in Hank's balanced salt solution wash to remove collagenase completely. The ductal fragments were plated on 2.31 mg/mL rat tail collagen type I (BD Biosciences) precoated plastic dishes for growth in monolayer, PDECs were cultured for 4 days and then harvested for immunoblotting or immunofluorescence. MET5A human pleural mesothelial cells were obtained from American Type Culture Collection (ATCC). MET5A Cells were cultured in a 1:1 ratio of Medium 199 (GIBCO) and MCDB105 (Sigma) supplemented with 10% fetal bovine serum (GIBCO). All experiments were done with cells of fewer than 6 passages. PANC-1 human pancreatic carcinoma and HT29 human colon adenocarcinoma grade II cell lines were cultured in medium as mentioned above for PDAC cell lines.

Stable gene expression, siRNA treatments and GFP-Fascin constructs- pPGS-hFlag-Snail (Plasmid 25695), pPGS-hFlag-Slug (Plasmid 25696) and pBAGE-puro-mTwist (Plasmid 1783) were obtained from Addgene. mRFP-Lifeact and GFP-Lifeact were kind gifts from Dr Roland Wedlich-Soldner, Max Planck Institute, Martinsreid, Germany. Mouse PDAC cells expressing Flag-Snail, Flag-Slug, Twist or GFP tagged human fascin were generated by retroviral infection using the modified Retro-X retroviral expression system (Clontech). To subclone human GFP-fascin into *HindIII* and *Clal* sites of the pLHCX retroviral expression vector, an *HindIII* restriction site, followed by Kozak consensus translation initiation site was introduced to the 5' end of the coding sequence of GFP-fascin⁵, by PCR (5'-AGA AAG CTT ATG GTG AGC AAG GGC GAG GAG CTG TTC -3'), with a *Clal* restriction site introduced to the 3' end in the same reaction (5'-AGA ATC GAT A CTA GTA CTC CCA GAG CGA GGC GGG GTC-3'), GFP-fascin was used as template. High-titre, replication-in-competent retroviral particles were produced in Phoenix Eco packaging cell line (Orbigen). Subsequent infection of target lines resulted in transfer of the coding region of interest, along with a selectable marker. Pooled cell lines stably expressing the construct of interest were isolated by selection with hygromycin-B (500µg/ml) for GFP-fascin. Control lines were infected with retroviral particles expressing an empty pLHCX control vector transcript, and subjected to an identical selection procedure. For siRNA experiment, Nontargeting (NT) control was from Dharmacon; siRNAs against human fascin (siFascin, target sequence: CAC GGG CAC CCT GGA CGC CAA). siRNA against mouse fascin, siFascin 1, target sequence: CTCAGTCAACTCTGAGCCTTA; siFascin 2 target sequence: CCCCATGATAGTAAGCTTTGAA; sets of four siRNAs target mouse fascin (GS14086), slug (GS20583), Zeb1 (GS21417), Zeb2 (GS24136) and E-cadherin (GS12550) were obtained from Qiagen. For transient knockdown of mouse fascin, slug, Zeb1, Zeb2 and E-cadherin, four siRNAs targeting each gene were mixed and diluted to 20µM and used at 100nM for transfection. Procedures used to transfect cells with siRNA were described previously⁵.

Immunohistochemistry- Formalin-fixed paraffin-embedded sections were deparaffinized and rehydrated by passage through xylene and a grade alcohol

series. For Alcian blue staining, rehydrated paraffin sections were stained for 30 minutes at room temperature in a 3% solution of Alcian blue diluted in acetic acid and counterstained with eosin. For antibody staining, antigen retrieval was performed by incubation of sections in microwave-heated citrate buffer (Dako) in a pressure cooker, except for anti-F4/80 and anti-NIMP, for which 10 minute proteinase K retrieval (Dako) was used. Sections were blocked with peroxidase blocking reagent (Dako) for 5 mins. Sections were then blocked in 10% serum for 1 hr and then incubated with primary antibody for 2 hr at RT. Sections were incubated with horseradish peroxidase labelled secondary antibody (Dako) for 1 hr and staining was visualized with DAB substrate chromogen and hematoxylin was used as the nuclear counterstain. For amylase/Ck19 dual IHC, after primary antibody, sections were incubated with anti-rabbit alkaline phosphatase labeled and anti-rat horseradish peroxidase labelled secondary antibody for 30 mins, staining was visualized with DAB substrate chromogen and blue alkaline phosphatase substrate kit (Vector lab) and mounted with Prolong Gold Antifade reagent (Invitrogen). For immunofluorescence on tissue sections, after antigen retrieval, sections were blocked with 10% donkey serum for 1 hr and incubated with primary antibody overnight at 4 °C. Sections were then washed in PBS and incubated with fluorescent conjugated secondary antibodies for 1 hr and mounted with Prolong Gold Antifade reagent (Invitrogen).

Live cell imaging-For live imaging of filopodia, 105768 PDAC cells expressing control vector or GFP-fascin were transfected with GFP or RFP-lifeact using Lipofectamine 2000 according to the manufacturer's instructions. Cells were then plated on glass-bottomed dishes pre-coated with 20ug collagen I (BD Bioscience) overnight. Timelapse images were captured every 20 sec for 10 mins using an Nikon A1 inverted laser scanning confocal microscope in a 37°C chamber with 5% CO₂. For live imaging of lamellipodia dynamics, 300 images were captured at 1-second intervals on Nikon TE 2000 Timelapse microscope systems with PFS (20× objective, ×1.5). Lamellipodial kymographs show pixel densities over time (*x*-axis) on a single pixel-wide straight line (*y*-axis) in the direction of lamellipodial protrusion (Image J plug-in multiple kymograph). Distance extended (*D*) was measured against

lamellipodial persistence (P), defined as the amount of time that the cell spends persistently extending a lamellipod before pausing or entering a retraction phase. Rate of protrusion (R) is shown as a broken line in Fig. S8B and represents the distance protruded (D) divided by the time of protrusion (P). For live imaging of random cell migration, cells on plastic dish were captured on Nikon TE 2000 Timelapse microscope (10× objective) at 10-minute intervals for 6 hours. Cell speed was measured with Image J plug-in manual tracking and chemotaxis tool. 300 cells from 3 experiments were tracked. For live imaging of transmesothelial migration, green CMFDA or red CMTPIX CellTracker (Molecular Probes) labeled PDAC cells (1.5×10^5) were added to confluent Met5A monolayer on 35mm glass bottomed dish pre-coat with 10 μ g/ml fibronectin. Cells were monitored by time-lapse microscopy at 10-minute intervals for up to 15 hr in a humidified chamber at 37°C and 5% CO₂ with an inverted microscope (TE2000; Nikon), with a 20x objective lens and using MetaMorph software (Molecular Devices). To quantify intercalation, a cell was considered as intercalated when its shape was not round, when it was no longer phase-bright, and when it was clearly part of the MC monolayer. For live imaging of protrusion dynamics of transmigrating PDAC cells, GFP-fascin expressing PDAC cells were added to red CMTPIX labeled confluent Met5A monolayer for 3 hr. The leading protrusion from PDAC cells within the junction between Met5A cells were imaged using a spinning disk confocal scan head (Yokogawa CSU-10) attached to an Nikon A1 inverted microscope.

Cell growth assay- For 2D growth assay, 2×10^4 cells were plated in each well of 6 well plates at day 0, and number of cells were trypsinized and counted every day from one well of 6 well plates for 4 days using CASY cell counter (Roche Innovats). Each point (mean \pm SEM) is derived from the mean of hemocytometer count of cells from three replicate dishes from three independent experiments. 3D proliferation assay in collagen I was performed using Culturex 3D culture cell proliferation assay kit (Culturex instructions), Briefly, 5×10^3 cells in 100 μ l cell culture medium supplemented with 2%

ACCEPTED MANUSCRIPT

collagen I were cultured on the top of the gel plug of 1 mg/ml collagen I in cell culture medium (pH7) in 96 well plate for 3 or 4 days and 8µl of cell proliferation reagent were added to each well and incubated at 37°C chamber with 5% CO₂ for 2 hours and the absorbance was read at 450 nm. For the anoikis assay, 2x10⁵ cells were plated on 6 wells ultra low attachment plates for 6 and 24 hrs. Cells were collected, washed once with PBS and stained with Alexa Fluor 647 Conjugate annexin V according to the manufacturer's instructions. After washing with PBS, cells were stained with propidium iodide (1 mg/ml) and RNaseA (250 µg/ml) for 30 min before processing on BD FACS-Calibur (BD Bioscience).

Blood analysis - Whole Blood Counts: Mice were humanely sacrificed with a rising concentration of carbon dioxide and then bled from the hepatic portal vein into a syringe containing 50µl of Acid Citrate Dextrose (ACD). Blood was then either emptied into a blood tube containing EDTA for blood cell analysis. Blood cell analysis was completed using both Advia 120 (Siemens, Camberley, UK) and by examination of a blood smear. **Pancreatic Function:** Mice were humanely sacrificed with a rising concentration of carbon dioxide and then bled by cardiac puncture. Blood was then emptied into a tube containing lithium heparin (LH/0.5) and centrifuged to separate the plasma into a new tube. Samples were analysed by the Clinical Pathology Laboratory at the University of Glasgow School of Veterinary Medicine.

Caerulein Treatment and BrdU Assay-Acute pancreatitis was induced by intraperitoneal (i.p.) cerulein injections (50 mg/kg; Sigma): one injection per hour for six injections and repeated 2 days later. Mice were sacrificed at 1, 7 or 21 days after last injection. For BrdU assay, mice were injected intraperitoneally with 2.5 mg BrdU (BD bioscience) for 2 hr before sacrifice.

PanIN and amylase positive area Quantification- Quantitation of amylase positive area was performed on DAB stained sections with amylase antibody. Amylase positive area/pancreas area was measured manually with ImageJ using the freehand selection tool. PanINs were defined according to previously published guidelines for reporting of these lesions in genetically

ACCEPTED MANUSCRIPT

engineered mouse models⁶. Briefly, to be defined as PanIN, a lesion must arise in native pancreatic ducts measuring less than 1mm and should not arise on a background of acinar-ductal metaplasia. PanIN lesions are then graded as PanIN-1, 2 or 3, according to the severity of cytological and architectural abnormalities, as detailed in the consensus guidelines published by Hruban et al⁷. Quantitation of number of PanINs was performed on DAB stained sections with CK19 antibody. Final quantitation represents the average of 20 of 20X fields of view from 4 mice. PanIN lesions were independently graded by one of the investigators (A.L.) and confirmed by a trainee pathology resident (H.T.M.) and another investigator with extensive experience in mouse pancreatic histopathology (J.M.).

Luciferase Reporter assay-A region of the first intron from the mouse fascin gene (+2189 to +2,735) was subcloned into into *SacI* and *XmaI* sites of pGL3-prom vector (Promega), by PCR, an *SacI* restriction site was introduced to the 5' end (5'-AGA GAG CTC ATG CAG AGG GCA AAG CCT TGG GTG GGG CC-3'), and a *XmaI* restriction site was introduced to the 3' end in the same reaction (5'-AGA CCC GGG ATA GCT ATG CAG GGC TTC TCT ATT TGC AAC T-3'), mouse genomic DNA was used as template. Mutation to the E-box was generated using QuikChange II Site Directed Mutagenesis kit (Agilent, UK) according to manufacture's protocol with primer pairs: forward: GGG TCA GAG TTC CTT CCT GTT TAG CAA ACA TTG and reverse: CAA TGT TTG CTA AAC AGG AAG GAA CTC TGA CCC. Luciferase activity was assayed using dual-luciferase assay kit (Promega). The firefly luciferase activity was normalized to that of Renilla luciferase to control transfection efficiency between samples.

Chromatin Immunoprecipitation (ChIP) quantitative-PCR-ChIP from 070669 PDAC cell line expressing flag-tagged Slug was performed as described previously⁸ using 10 µg of monoclonal anti-flag M2, Clone M2 (Sigma, F1804) per assay. ChIP enrichment levels were determined by SyBr green PCR. The sequence for primer pairs: #1: Forward: ACCATGGCCTCTCTTGTTC; Reverse: ACATTCCCAAGAGACGTTTACC;

ACCEPTED MANUSCRIPT

#2: Forward: AGGTGGGTCTCTGAGTTCTT; Reverse: TTTGAGACAGGGTTTCTCTGC; #3: Forward: CTGGCCTCGAACTCAGAAAT; Reverse: GCATGACCACCAGTTCAAGAC; primer pair for E-box on mouse E-cadherin promoter was used as positive control⁹: Forward: GGGTGGAGGAAGTTGAGG; Reverse: CTCCCACACCAGTGAGC.

Supplementary References:

1. Rukstalis, J. M. & Habener, J. F. Snail2, a mediator of epithelial-mesenchymal transitions, expressed in progenitor cells of the developing endocrine pancreas. *Gene Expr Patterns* **7**, 471-479 (2007).
2. Morton, J. P. et al. LKB1 haploinsufficiency cooperates with Kras to promote pancreatic cancer through suppression of p21-dependent growth arrest. *Gastroenterology* **139**, 586-97, 597.e1 (2010).
3. Morton, J. P. et al. Dasatinib inhibits the development of metastases in a mouse model of pancreatic ductal adenocarcinoma. *Gastroenterology* **139**, 292-303 (2010).
4. Schreiber, F. S. et al. Successful growth and characterization of mouse pancreatic ductal cells: functional properties of the Ki-RAS(G12V) oncogene. *Gastroenterology* **127**, 250-260 (2004).
5. Li, A. et al. The actin-bundling protein fascin stabilizes actin in invadopodia and potentiates protrusive invasion. *Curr Biol* **20**, 339-345 (2010).
6. Hruban, R. H. et al. Pathology of genetically engineered mouse models of pancreatic exocrine cancer: consensus report and recommendations. *Cancer Res* **66**, 95-106 (2006).
7. Hruban, R. H. et al. Pancreatic intraepithelial neoplasia: a new nomenclature and classification system for pancreatic duct lesions. *Am J Surg Pathol* **25**, 579-586 (2001).
8. Forsberg, E. C. et al. Developmentally dynamic histone acetylation pattern of a tissue-specific chromatin domain. *Proc Natl Acad Sci U S A* **97**, 14494-14499 (2000).
9. Peinado, H., Ballestar, E., Esteller, M. & Cano, A. Snail mediates E-cadherin repression by the recruitment of the Sin3A/histone deacetylase 1 (HDAC1)/HDAC2 complex. *Mol Cell Biol* **24**, 306-319 (2004).